Traffic-Driven Energy Efficient Operational Mechanisms in Cellular Access Networks

Md. Farhad Hossain

A thesis submitted in fulfilment of
the requirements for the degree of Doctor of Philosophy
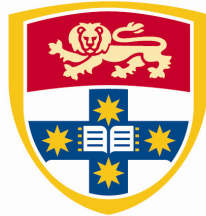
Faculty of Engineering & Information Technologies
University of Sydney

March 2014

Statement of Originality

This is to certify that to the best of my knowledge and belief, all material presented in this thesis is the original work of the author, unless otherwise stated. The content of this thesis has not been previously submitted as a part of any academic qualification to any other university or institution.

_____

Md. Farhad Hossain
March 2014

Abstract

Emerging smart user terminals and diverse multimedia applications that have driven recent explosive growth in mobile data traffic are increasing energy consumption in cellular networks at an incredible rate. Constituting a significant portion of network operating expenditure and in a context of global warming, rising energy utilization has become a key concern from both economic and environmental perspectives. Consequently, in recent time, the issue of designing energy efficient cellular networks has drawn significant attention, which is also the foremost motivation behind this research. This thesis presents various novel operation mechanisms for single-tier cellular networks designed to enhance the energy efficiency.

In a cellular system, base stations (BSs) in the radio access network (RAN) are the most dominant energy consuming equipment estimated between 60%-80%. Therefore, most recently, the idea of attaining a "green cellular network" by reducing energy consumption in BSs has become the spotlight of many researchers. Contemporary BSs consume a considerable amount of energy even at no traffic load. Correspondingly, conventional cellular networks, which are provisioned based on peak-traffic load without accounting for inherent high-degree temporal-spatial traffic diversity, are wasting a significant amount of electrical energy, especially during low-traffic periods.

Considering these facts, the proposed research is focused on the design of traffic-sensitive dynamic network reconfiguring mechanisms for energy efficiency in cellular systems. Under the proposed techniques, RANs are adaptively reconfigured using less equipment leading to reduced energy utilization. At the same time, quality of service (QoS) is guaranteed within the target limits. The proposed mechanisms work in a self-organizing fashion requiring no operator assistance. The main contributions of this thesis can be summarized as below:

• An energy efficient cellular network framework by employing distributed inter-BS cooperation in a RAN is proposed. Under this framework, based on the instantaneous traffic demand, BSs mutually cooperate for dynamically switching between active and sleep modes by redistributing traffic among themselves and thus, energy savings is achieved. The focus is then extended to exploiting the availability of multiple cellular networks for extracting energy savings through inter-RAN cooperation. Two alternative mutual cooperation mechanisms among BSs belonging

to different RANs are developed for dynamically sharing each other's traffic and switching their operating modes. Mathematical models for analytically evaluating the switching dynamics of BSs under both of these single-RAN and multi-RAN cooperation mechanisms are also formulated.

- A centralized dynamic BS switching mechanism for energy efficiency in cellular networks is also proposed. Various user association techniques as well as BS selection policies are also explored for redistributing traffic load. For avoiding the high computational complexities of the optimal exhaustive search based energy saving optimization techniques, a heuristically guided greedy style low complexity algorithm is presented.

- An alternative energy saving technique using dynamic sectorization under which some of the sectors in the underutilized BSs are turned into sleep mode is also proposed. Heuristic algorithms for both the distributed and the centralized implementations are developed. Finally, a two-dimensional network provisioning mechanism is proposed by jointly applying both the dynamic sectorization and the dynamic BS switching.

- Utilization of the instantaneous traffic load for switching BSs and sectors under the proposed mechanisms may impose a lot of signaling and computational load. Focusing to minimize this overhead, an exponentially weighted moving average (EWMA)-based novel technique is proposed for forecasting the traffic load envelope of an entire day in advance from the past traffic data, which is then integrated into the proposed energy saving mechanisms.

- In this thesis, a novel eco-inspired network design approach is also introduced by developing the aforementioned distributed inter-BS cooperation based on the principle of ecological self-organization. For demonstrating the applicability of ecological principles in cellular systems, an ecological multi-species multi-resource competition based resource management scheme is proposed, which shows its capability in allocating resources in a sustainable way.

Extensive simulations are carried out for evaluating the system performance, which demonstrate the capability of all the proposed mechanisms in substantially enhancing the energy efficiency of cellular networks. Effectiveness of the proposed EWMA-based predictor in reducing the system overhead without sacrificing any energy saving performance is also identified.

Dedication

my respected parents

my beloved wife, Jannat and sweet son, Faysal

my lovely sisters, Lizo, Nadia and Nahida

Acknowledgements

Related Publications

Journal Papers

[J1] M. F. Hossain, K. S. Munasinghe and A. Jamalipour, "Traffic-Aware Two-Dimensional Dynamic Network Provisioning for Energy-Efficient Cellular Systems," *Transactions on Emerging Telecommunications Technologies (under review)*, pp. 1-13, Feb 2014.

[J2] M. F. Hossain, K. S. Munasinghe and A. Jamalipour, "Distributed Inter-BS Co-operation Aided Energy Efficient Load Balancing for Cellular Networks," *IEEE Transactions on Wireless Communications*, vol. 12, no. 11, pp. 5929-5939, Nov 2013.

[J3] M. F. Hossain, K. S. Munasinghe and A. Jamalipour, "Energy-Aware Dynamic Sectorization of Base Stations in Multi-Cell OFDMA Networks," *IEEE Wireless Communications Letter*, vol. 2, no. 6, pp. 587-590, Dec 2013.

[J4] M. F. Hossain, K. S. Munasinghe and A. Jamalipour, "On the eNB-based Energy-Saving Cooperation Techniques for LTE Access Networks," *Wireless Communications and Mobile Computing, (early view available in online)*, pp. 1-20, Jan 2013.

Conference Papers

[C1] M. F. Hossain, K. S. Munasinghe and A. Jamalipour, "Toward Self-organizing Sectorization of LTE eNBs for Energy Efficient Network Operation Under QoS Constraints," in *Proc. IEEE WCNC*, Shanghai, China, pp. 1279-1284, Apr 2013. (1 citations [†])

[†]Source: Google Scholar© of 17/02/2014.

[C2] M. F. Hossain, K. S. Munasinghe and A. Jamalipour, "On the Energy Efficiency of Self-Organizing LTE Cellular Access Networks," in *Proc. IEEE GLOBECOM*, Anaheim, California, USA, pp. 5536-5541, Dec 2012. (3 citations[†])

[C3] M. F. Hossain, K. S. Munasinghe and A. Jamalipour, "A Self-Organizing Cooperative Heterogeneous Cellular Access Network for Energy Conservation," in *Proc. IEEE ICC*, Ottawa, Canada, pp. 6838-6842, Jun 2012.

[C4] M. F. Hossain, K. S. Munasinghe and A. Jamalipour, "Two Level Cooperation for Energy Efficiency in Multi-RAN Cellular Network Environment," in *Proc. IEEE WCNC*, Paris, France, pp. 2493-2497, Apr 2012. (3 citations[†])

[C5] M. F. Hossain, K. S. Munasinghe and A. Jamalipour, "Ecological Competition based Resource Control for Sustainable Heterogeneous Wireless Networks," in *Proc. IEEE PIMRC*, Toronto, Canada, pp. 1336-1370, Sep 2011.

[C6] M. F. Hossain, K. S. Munasinghe and A. Jamalipour, "An Eco-Inspired Energy Efficient Access Network Architecture for Next Generation Cellular Systems," in *Proc. IEEE WCNC*, Cancun, Mexico, pp. 992-997, Mar 2011. (19 citations[†])

[C7] M. F. Hossain, K. S. Munasinghe and A. Jamalipour, "A Protocooperation-based Sleep-Wake Architecture for Next Generation Green Cellular Access Networks," in *Proc. IEEE ICSPCS*, Gold Coast, Australia, pp. 1-8, Dec 2010. (7 citations[†])

Conference Presentations

[P1] "On the Energy Efficiency of Self-Organizing LTE Cellular Access Networks," *IEEE GLOBECOM*, Anaheim, California, USA, Dec 2012.

[P2] "Two Level Cooperation for Energy Efficiency in Multi-RAN Cellular Network Environment," *IEEE WCNC*, Paris, France, Apr 2012.

[P3] "A Protocooperation-based Sleep-Wake Architecture for Next Generation Green Cellular Access Networks," *IEEE ICSPCS*, Gold Coast, Australia, Dec 2010.

Contents

List of Figures

xvi

List of Tables

List of Acronyms

2G	Second Generation
3G	Third Generation
3GPP	3rd Generation Partnership Project
AMC	Adaptive Modulation and Coding
AP	Access Point
AWGN	Additive White Gaussian Noise
BS	Base Station
BSC	Base Station Controller
BTS	Base Transceiver Station
BW	Bandwidth
CB	Coordinated Beamforming
CBR	Constant Bit Rate
CC	Component Carrier
cdf	cumulative distribution function
CEC	Constant Energy Consumption
CoMP	Coordinated Multi-Point Transmission
CS	Coordinated Scheduling
CSI	Channel State Information
CUE	Capacity Utilization Efficiency
CUG	Capacity Utilization Gain
DPD	Digital Predistortion
DS	Dynamic Sectorization
DSBS	Dynamic Switching of Base Station
DTX	Discontinuous Transmission
E^{3}F	Energy Efficiency Evaluation Framework
EARTH	Energy Aware Radio and Network Technologies

EB	Exabyte
EDGE	Enhanced Data for Global Evolution
ELF	Expected Load Factor
ELPC	Energy-Load Proportionality Constant
eNB	Evolved Node B
EPC	Evolved Packet Core
EU	European Union
E-UTRAN	Evolved Universal Terrestrial Radio Access Network
EWMA	Exponentially Weighted Moving Average
FDD	Frequency Division Duplexing
FEP	Fully Energy Proportional
FFR	Fractional Frequency Reuse
GBR	Guaranteed Bit Rate
GeSI	Global e-Sustainability Initiative
GPRS	General Packet Radio Service
GSM	Global System for Mobile Communications
HetNet	Heterogeneous Network
HL	Higher-to-Lower
HSPA	High Speed Packet Access
HWN	Heterogeneous Wireless Network
HWNE	Heterogeneous Wireless Network Ecosystem
ICIC	Inter-Cell Interference Coordination
ICT	Information and Communication Technology
IP	Internet Protocol
IRC	Interference Rejection Combining
JDSBS	Joint Dynamic Switching of Base Station
JT	Joint Transmission
LF	Load Factor
LH	Lower-to-Higher
LTE	Long Term Evolution
LTE-A	Long Term Evolution - Advanced
MCS	Modulation and Coding Scheme
MIMO	Multiple-Input Multiple-Output
MME	Mobility Management Entity

MR	Multipoint Reception
MSMRC	Multi-Species Multi-Resource Competition
NEP	Non-Energy Proportional
NF	Noise Figure
NGMN	Next Generation Mobile Network
NLOS	Non-Line-of-Sight
OFDMA	Orthogonal Frequency Division Multiple Access
PA	Power Amplifier
PC	Personal Computer
PDCCH	Physical Downlink Control Channel
pdf	Probability Distribution Function
PLMN	Public Land Mobile Network
P-SCH	Primary Synchronization Channel
PSTN	Public Service Telephone Network
QAM	Quadrature Amplitude Modulation
QoS	Quality of Service
RAN	Radio Access Network
RB	Resource Block
RF	Radio Frequency
RNC	Radio Network Controller
RRM	Radio Resource Management
RV	Random Variable
SAC	Session Admission Control
SBS	Sequential-to-Better-Signal
SE	Spectral Efficiency
SFR	Soft Frequency Reuse
SGW	Serving Gateway
SINR	Signal-to-Interference-plus-Noise-Ratio
SNR	Signal-to-Noise-Ratio
SON	Self-Organizing Network
SS	Sequential-Sequential
S-SCH	Secondary Synchronization Channel
SWM	Sleep-Wake Module
TP	Transmit Power

TRX	Transceiver
TTI	Transmission Time Interval
UE	User Equipment
UMTS	Universal Mobile Telecommunications System
WCDMA	Wideband Code Division Multiple Access
WiMAX	Worldwide Interoperability for Microwave Access
WLAN	Wireless Local Area Network

Chapter 1

Introduction

This chapter describes the background and motivation for this research work by briefly introducing the field and explaining the principal research problem. A brief summary of the contributions of this thesis is also presented. Finally, a concise outline of the thesis is provided at the end of the chapter.

1.1 Energy Efficiency in Cellular Networks

The steady rise in popularity of emerging new generation user terminals (e.g., smart phones), the ubiquitous availability of Internet access and the diverse multimedia applications are currently driving an explosive growth in cellular network data traffic. Correspondingly, energy consumption as well as CO_2 footprint of cellular networks is increasing at an incredible rate leading to a higher network operating cost and a not inconsiderable contribution to the worsening global warming phenomenon respectively. Cellular network operators and vendors as well are immensely concerned about the ever increasing cost of energy [1], [2]. For instance, it has been estimated that the information and communication technology (ICT) industry emitted approximately 2% of the worldwide CO_2 emissions in 2007 [3], [4], [5]. This amount is equivalent to the world-wide CO_2 emissions by airplanes or one quarter of the world-wide CO_2 emissions by cars [6], [7]. Recent studies have predicted that although the overall carbon footprint of ICT is expected to less than double from 2007 to 2020, it can triple for cellular networks within the same

time frame [8], [9]. However, existing cellular architectures are designed for optimizing network coverage and throughput with virtually no real emphasis on the energy efficiency aspect. Therefore, it has now become essential to include energy efficiency as a major performance indicator in both the planning and the operation stages of cellular networks.

In a cellular system, the base stations (BSs) in its radio access network (RAN) are the most dominant energy consuming equipment adding up to 60% - 80% of the total utilization [10], [11], [12], [13], whereas the accumulated energy requirement for user equipments (UEs) lies in the range of 1% - 10% [12], [14], [15]. Therefore, reduction of energy consumption in BSs may considerably enhance the energy efficiency of cellular networks. Remarkably, contemporary BSs have a high-degree non-load-proportional energy consumption characteristic and thus draw a significant amount of energy even at no-load condition [16], [17], [18], [19].

On the other hand, modern day cellular network traffic generation exhibits a high-degree temporal-spatial diversity, i.e., traffic demand varies both in time and space [12], [20], [21]. This variation is directly related to the population density of the neighborhood, and the random call making behaviour and mobility pattern of the users. From recently released traffic data by various network operators, it has been clearly identified that for a large portion over a day, traffic intensity is much lower than that of the peak-traffic periods and many BSs remain significantly under-utilized.

However, under the conventional static-type network operation approach, all BSs are kept powered irrespective of traffic load. This traditional network operation and the aforementioned non-load-proportional energy utilization in BSs are the major causes behind the substantial amount of energy wastage in existing cellular networks, especially in the low-traffic periods. Thus, there is a genuine prospect for exploiting these aspects in devising operation techniques for managing cellular networks in a much more energy efficient way than the existing ones.

1.2   Self-Organizing Networks

Despite the unprecedented increase in cellular data, operators revenue has failed to grow in the same proportion [22]. Therefore, self-organizing networks (SONs) with autonomous operation, control and maintenance have been identified as the key way to run networks

with minimal human intervention leading to reduced cost and complexity [23], [24], [25], [26]. Such automation in networks has great potential for attaining lower energy requirements, improved mobility management, better load balancing, efficient resource utilization and so on. Correspondingly, the demand for SONs is increasingly becoming stronger, especially among service providers. In light of this, 3rd generation partnership project (3GPP) long term evolution - advanced (LTE-A), worldwide interoperability for microwave access (WiMAX) and next generation mobile network (NGMN) alliance have adopted SON architectures in their respective standards [27], [28], [29]. Therefore, most recently, researchers are putting significant emphasis on the self-organizing feature of any new mechanism designed for cellular networks.

1.3 Research Objectives

Given the nature of energy wastage, natural traffic diversity and the predicted traffic growth trends, it is crucial to bring fundamental changes in network operation for enhancing the energy efficiency in cellular networks. The objective of this thesis is to develop dynamic operation mechanisms for cellular access networks, which can reduce the energy wastage resulting in lower energy requirement and higher load-proportional energy consumption.

The main focus is to leverage the inherent temporal-spatial traffic diversity for managing cellular networks in an energy efficient way. Thus, the proposed mechanisms adaptively reconfigure cellular RANs by dynamically switching the access network equipment between a high power active mode and a low power sleep mode, while satisfying the instantaneous traffic demand. More precisely, under the proposed schemes, BSs and the sectors in each BS are the RAN equipment subject to the dynamic switching. Through this dynamic switching, RANs are provisioned to utilize a reduced the number of active equipment and thus, energy savings is achieved.

It is also aimed to develop frameworks for both the distributed and the centralized implementations of the proposed mechanisms. An additional target is to exploit single-RAN as well as multi-RAN scenarios for capitalizing any potential energy savings. Moreover, from the motivation gained by the expected benefits of SONs, all the proposed mechanisms are aimed to operate in a self-organizing fashion requiring no human assistance.

1.4   Research Motivations

As the concern on the energy efficiency of cellular networks intensifies among the operators as well as the environmentalists, various proposals have emerged in recent years for minimizing the energy consumption at RAN level by switching network equipment on/off [5], [10], [30]. For instance, LTE proposed turning off under loaded BSs at low-traffic times for saving energy [31], while refrained to specify any particular BS switching scheme and thus, the issue is left open for thorough investigations [31].

Several early works, such as [32], [33], [34] and [35] introduced the concept of manual switching of BSs, which are not suitable for SONs. In contrast, [9], [11], [12], [36], [37], [38], [39] and other recent works proposed dynamic BS switching for energy savings. However, most of these works are based on simple system models or failed to present complete framework and necessary algorithms for implementations. For example, the proposals in [9], [36], [37] and [38] are developed on the unrealistic assumption of constant power consumption in BSs. In addition, the algorithms presented [9], [37] and [38] completely ignored the data rate demand and the actual locations of users. Furthermore, none of these systems are designed under the guidelines of next generation OFDMA-based LTE and WiMAX systems.

An alternative approach of reducing energy utilization in cellular RANs by turning off the redundant sectors of the under-utilized BSs is investigated in few works, such as [40], [41] and [42]. The works in [40] and [41] investigated switching off sectors, while ignored the impact of change in antenna patterns on energy savings. On the other hand, although the impact of antenna pattern is included in the scheme presented in [42], this work as well as [40] and [41] have not accounted other crucial factors, namely, the change in antenna gain with the beamwidth and the load-dependent power consumption in BSs.

Although many schemes have been proposed for energy efficiency of RANs, research in this field is still in its infancy. Existing schemes have their own limitations, such as the use of simplified system models, inadequate analysis, incompatibility with the future SONs and unsuitability with the OFDMA-based cellular systems. This field thus deserves a lot more attention from the leading research community for developing effective energy saving techniques, which has worked as the foremost motivation to carry out this proposed research.

1.5   Thesis Contributions

Although the notion of energy efficient green cellular networks has gained much attention from the telecommunication industries as well as from the academics, investigation in this field is still in the early stage requiring extensive efforts from the research communities. The contribution of this thesis can be considered as a significant move toward the realization of the so called green cellular networks. This thesis proposes and investigates several traffic-dependent energy efficient dynamic operation mechanisms for single-tier cellular networks. System performance is evaluated using extensive simulations as well as the formulated analytical models. A brief summary of the contributions of this thesis is presented below.

• Switching off some of the BSs during low-traffic times is currently considered the most prospective approach in substantially reducing energy utilization in cellular networks [5], [10]. Similarly, switched off BSs have to be switched on during high-traffic times for reducing the traffic load on the other BSs. Therefore, it is essential to develop autonomous mechanisms, which can achieve this dynamic switching of BSs with traffic changes without involving any operator assistance. In light of this, distributed inter-BS cooperation assisted various frameworks are proposed in this thesis for realizing this traffic-aware energy saving dynamic BS switching. Frameworks are developed for both the single-network and the multi-network scenarios.

Under a single-network scenario, intra-network intelligent mutual cooperation among the neighboring BSs belonging to the same RAN is employed for sharing each other's traffic and thus, some of these BSs are switched to sleep mode for saving energy. Various selection schemes are explored for deciding on the best neighbors for offloading the traffic of a BS. Implemented distributed cooperation is developed based on the ecological principle of self-organization, where each BS directly cooperates only with its neighboring BSs without being aware of the overall network behavior. This kind of local cooperation among BSs ultimately generates the global dynamic network behavior. On the other hand, for multi-network scenarios, two alternative distributed-type cooperation mechanisms for dynamic traffic sharing among the geographically colocated RANs for saving energy are proposed. The first mechanism, named inter-network cooperation, implements cooperation among the co-located BSs belonging to different RANs. Under the second technique,

named joint cooperation, both the intra-network cooperation and the inter-network cooperation are applied together. Analytical models for estimating the switching dynamics under all three of these cooperative mechanisms are also formulated. Extensive simulations are carried out for demonstrating the capability of these techniques in achieving a substantial amount of energy savings, while the joint cooperation offers the maximum. Energy saving performance under various traffic scenarios, selection schemes, design parameters, user data rates, user distributions, BS power profiles and number of cooperating networks is thoroughly investigated. Impact of this dynamic switching on the other system parameters, such as resource utilization, switching in BSs and sleeping period of BSs is also analyzed.

• For a single-RAN scenario, a centralized dynamic BS switching mechanism involving no direct interaction among BSs is also proposed. In this case, based on the instantaneous network traffic demand, a central network controller selects an optimal subset of BSs, which are left in active mode switching the remaining into sleep mode. A generalized energy saving optimization problem is formulated, which is extremely challenging for a solution using optimal exhaustive search technique due to its exponential complexity, especially under a large number of BSs. Therefore, a greedy style heuristically guided algorithm with much lower complexity is developed. Furthermore, various user association techniques are explored. In addition to the standard signal-to-interference-plus-noise-ratio (SINR)-based UE association policy, predefined BS sequence-based and BS energy efficiency level-based (assuming that a network can have BSs of various degrees of energy efficiency) policies are proposed and investigated. Along with the energy saving performance, the impact on the achievable spectral efficiency (SE) and the resource requirement per UE is also analyzed.

• Although developing BS switching based schemes is the main focus for most of the green cellular network researchers, many challenging issues have to be overcome before its actual practical implementation [5], [36], [43]. Some of the greatest obstacles are frequent switching in BSs requiring extremely fast hardware, managing potential coverage holes created from on/off BSs, reduced battery life of UEs for increased uplink transmit power and highly dynamic interference from coverage adjustments and so on. In light of this, this thesis also proposes a much simpler dynamic sectorization scheme under which instead of switching an entire BS to sleep mode, each BS is dynamically reconfigured with a smaller number of sectors. Once again, considering the high complexity

of the optimal exhaustive search method, heuristically guided greedy style algorithms for both the centralized and the distributed implementations are developed. Various sector switching patterns including the regular configurations (e.g., single-sector, three-sector and six-sector cells) are thoroughly investigated. Impacts of various network parameters on the system performance, such as single-cell and multi-cell scenarios, user data rates, uniform and non-uniform user distributions and the number of original sectors in each BS are evaluated. Energy saving performance is also compared with that of the semi-dynamic sector switching schemes, optimal exhaustive search technique and the popular BS switching-based schemes. Remarkably, due to better granularity, the proposed dynamic sectorization is found to achieve higher energy savings than that achieved by a BS switching-based scheme.

- The last energy saving mechanism proposed in this thesis reconfigures cellular access networks in two different dimensions by switching some selected BSs as well as some of the sectors in the active BSs into sleep mode. For reducing the complexity in implementations, dynamic sectorization and BS switching problems are decoupled into time domain and sequentially applied. Two variants of this joint mechanism are investigated demonstrating a large volume of energy savings. It is also found that the two variants outperform each other in low-traffic and high-traffic regions respectively. Furthermore, the proposed joint mechanism is identified to have a superior energy saving performance than that of individual applications of dynamic sectorization and BS switching-based schemes.

- In all of the proposed schemes, a dynamic switching operation is carried out periodically, which is triggered by the central controller based on the aggregate network load factor (LF). Triggering by instantaneous LF requires the controller to have accessibility to all the network parameters resulting in highly signaling intensive systems. Therefore, for reducing the network reconfiguring instances, an exponentially weighted moving average (EWMA)-based technique for predicting the LF envelope of an entire day in advance from the historical data is proposed. From the predicted LF, a subset of instances is selected at which network reconfiguring operations are carried out leading to a reduced signaling and computational burden. Performance of the proposed dynamic network reconfiguring mechanisms by integrating this EWMA-based estimator is also evaluated, which demonstrates its capability in substantially reducing equipment switching operations without trading off any energy saving performance.

• As stated above, the distributed cooperation among neighboring BSs is developed based on the ecological self-organization principle. For establishing the rationality of applying ecological principles in the cellular network domain, at first, a comprehensive analogy between a heterogeneous wireless network (HWN) and the ecosystem on Earth is established. Thereafter, an ecological multi-species multi-resource competition (MSMRC)-based model is developed for characterizing the unfairness in resource distribution and the potential competitive exclusion of certain classes of services in the absence of any radio resource management (RRM) scheme. A RRM technique is then proposed for eliminating any chance of competitive exclusion even under extremely intense competition scenarios. Results demonstrate the capability of the proposed eco-inspired RRM scheme for ensuring the coexistence of all service classes having widely varying quality of service (QoS) requirements. More importantly, this opens up a new design paradigm of integrating ecological principles when developing and analyzing future generation cellular network operation mechanisms.

In summary, the proposed research explores various alternative energy efficient dynamic network equipment switching mechanisms. Thorough investigations carried out in this thesis provide us with the essential understandings of the network characteristics, degree of energy savings and the impact on the other system parameters under dynamic equipment switching mechanisms. The presented system performance can be used by cellular network operators as a design guideline for achieving the envisioned real green cellular networks. Furthermore, these results can also be used by other researchers as a performance guideline and a benchmark for evaluating similar scenarios.

1.6   Organization of the Thesis

This thesis consists of eight chapters presenting the background material, reviews of the relevant literature, proposed energy saving mechanisms with thorough investigations and insightful analysis, summary of the key findings and potential future research opportunities.

Chapter 1 establishes the motivation behind the proposed research by briefly pointing out the energy efficiency aspect in today's cellular networks as well as the prospects of future SONs. The research goal and the outcome of the thesis, as well as the organization of the thesis are also briefly summarized in this chapter.

Chapter 2 provides an essential background to a basic cellular system including a detailed discussion of energy consumption in the existing as well as the future cellular networks. A comprehensive study of the fundamental approaches and the related publications by classifying them into different approaches is also presented. Finally, this chapter identifies the key enabling technologies for implementing the dynamic equipment switching schemes.

Chapter 3 aims to establish the rationality of integrating ecological principles in cellular network operations. Therefore, by briefly reviewing the analogy between HWNs and the ecosystem on Earth, this chapter introduces a novel eco-inspired network design approach for integrating ecological principles in network operations. An ecological MSMRC-based RRM scheme is then proposed for demonstrating the prospect of this new design paradigm.

Chapter 4 proposes an ecological self-organization inspired distributed inter-BS cooperation assisted traffic-aware load-balancing framework for energy efficient dynamic BS switching under a single-RAN scenario. An estimated aggregated LF of the network is used for triggering the network reconfiguring events. Therefore, an EWMA-based technique for estimating the LF of an entire day in advance from past LF data is also proposed in this chapter.

Chapter 5 then extends the focus for developing distributed energy efficient BS switching techniques for a multi-RAN scenario. In light of this, two alternative cooperation mechanisms among the co-located networks, named as inter-network cooperation and joint cooperation, are proposed and investigated.

Chapter 6 presents dynamic sectorization techniques, both centralized and distributed types, for achieving energy efficiency in cellular networks. In addition, a centralized scheme for dynamic BS switching is also proposed in this chapter.

Chapter 7 proposes a two-dimensional dynamic network reconfiguring mechanism by applying dynamic sectorization and dynamic switching of BSs jointly. Two different variants of this scheme are outlined and thoroughly investigated.

Chapter 8 concludes the thesis by summarizing the major findings, as well as identifying several potential research opportunities for the improvements and extensions of the

proposed mechanisms.

1.7   Chapter Summary

This chapter has formulated the principal research objective by exposing the highly inefficient energy utilization in contemporary cellular networks and the statistically evident exceptionally growing energy expenditure. A concise overview of the contributions of this thesis is then provided. Finally, for the ease of readers in following the contents, a chapter-wise outline of the thesis is briefly presented.

Chapter 2

Energy Efficient Cellular Networks: Background and Research Trends

This chapter first presents the basic concepts of a typical cellular system. Cellular traffic characteristics as well as global trends in traffic growth are also discussed. Furthermore, a detailed account of the energy utilization in different functional entities of a cellular network is presented. In particular, a component-wise breakdown of energy consumption in BSs is further examined. This chapter also discusses the fundamental approaches for realizing the envisaged energy efficient green cellular networks. The focus is then turned onto the energy saving RAN equipment (more precisely, BSs and sectors) switching based approach, and a comprehensive study of the existing related schemes is presented. This chapter finally concludes by identifying some of the major technological issues for enabling practical implementations of such dynamic switching mechanisms.

2.1 Basic Concept of a Cellular Network

A basic cellular system architecture consists of two network domains - an access network and a core network. They together form the cellular network infrastructure. A cellular network can also be interconnected with other public land mobile networks (PLMNs), public service telephone networks (PSTNs) and/or Internet through the core network. A simple view of a typical cellular network is shown in Fig. 2.1.

Figure 2.1: A simple view of typical 2G/3G based cellular networks.

The access network mainly consists of several cell sites and cell site controllers. Each cell site covers a certain geographical area providing access for the users to be connected to the core network, while a controller controls a group of cell sites. The cell site is known as a base transceiver station (BTS), Node B and evolved node B (eNB) in second generation (2G) global system for mobile communications (GSM)/general packet radio service (GPRS)/enhanced data for global evolution (EDGE), third generation (3G) universal mobile telecommunications system (UMTS) and beyond 3G long term evolution (LTE) systems respectively[1]. On the other hand, the controller is termed base station controller (BSC) and radio network controller (RNC) in GSM/GPRS/EDGE and UMTS respectively. In traditional 2G/3G cellular systems, the cell site controller is responsible for RRM and some of the mobility management functions over multiple cell sites. However, in LTE, these functions are moved to the intelligent eNBs leading to the removal of the controller. Thus, LTE has a flatter and much more distributed architecture.

---

[1]Throughout the thesis, the term base station (BS) is used for referring all kinds of cell sites.

Figure 2.2: A single-tier cellular network with macrocells only.

2.1.1 Single-Tier Network

A single-tier cellular network, also known as an homogeneous network, is deployed using only a single type of BS. Conventional cellular networks are of this type utilizing only macrocells. A simple demonstration of a single-tier cellular network is presneted in Fig. 2.2. Each macrocell can provide coverage for a large geographical area. Cell ranges usually vary among the deployment areas (e.g., smaller cells for urban areas and larger cells for rural areas), which can be upto several kilometers.

A single-tier macro cell network suffers from many limitations [44]. Poor indoor penetration and the presence of dead spots leading to reduced indoor coverage is one of the major bottlenecks. Moreover, as the users move to cell edges, inter-cell interference increases significantly resulting in drastic reduction in user throughput. At the same time, due to the requirement of higher transmit power, edge users run out of power very quickly. Furthermore, with the rapid rise of traffic demand, it is essential to install new BSs. In many areas, adding further macrocells is not very effective due to higher cost and the lack of feasible cell sites [45].
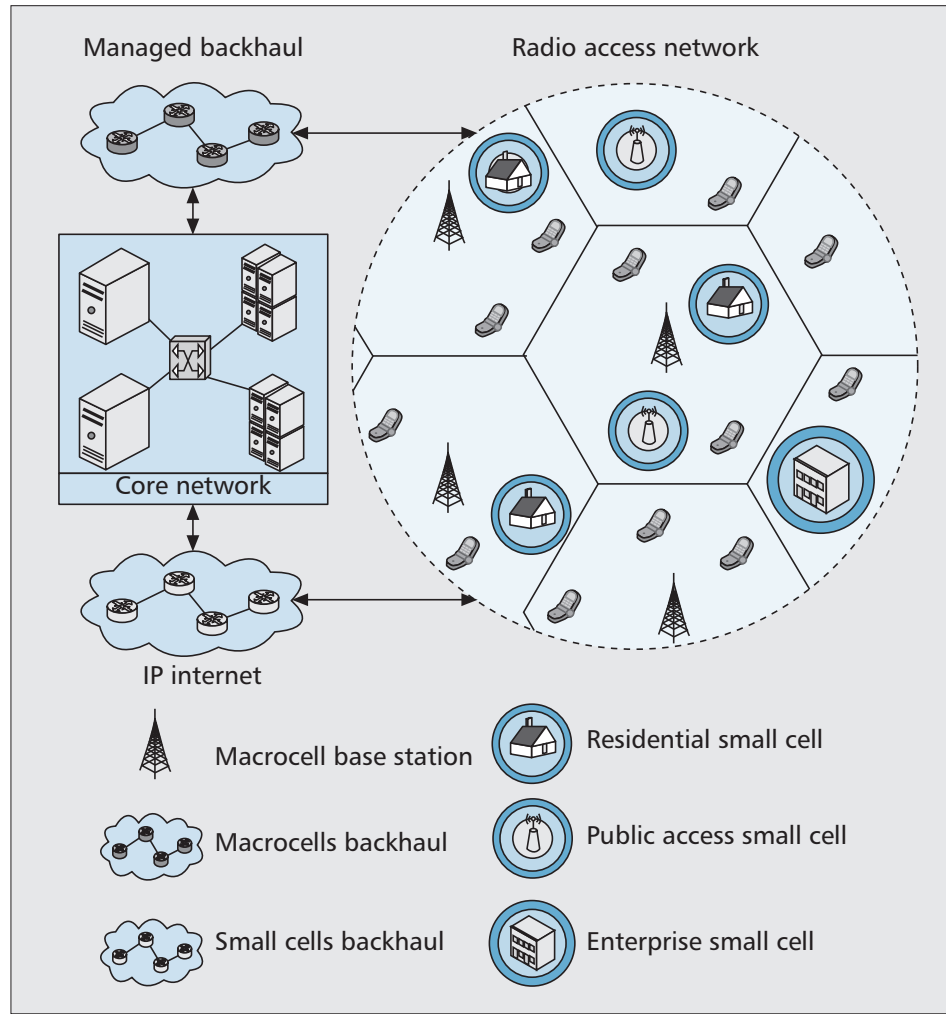
Figure 2.3: Illustration of a multi-tier cellular network with a combination of macrocells and small cells [46].

2.1.2 Multi-Tier Network

In order to lessen the degree of the aforementioned drawbacks of single-tier networks and meet the unprecedented growth in traffic demand, next generation cellular network architectures, such as LTE-A, have embraced the concept of a multi-tier network. A multi-tier cellular network is deployed using a mix of macrocells and small cells. Small cells include microcells, picocells, femtocells and metrocells, which are overlaid on macrocells for forming multi-tier networks as illustrated in Fig. 2.3 [46]. A multi-tier network has a huge potential in substantially improving network coverage, capacity and energy efficiency with fast and flexible installation. Many researchers also refer to a multi-tier

network as a heterogeneous network (HetNet), though HetNet carries a broader meaning including heterogeneous cell sizes, radio technologies, services, frequency bands and user terminals.

Introduction of multiple tiers has brought a total paradigm shift from the conventional deterministic hexagonal cell layout to a near random topology. Therefore, the techniques for network modeling, planning and optimization can significantly differ from those of legacy networks. Furthermore, all the algorithms and the protocols for various network functions, such as admission control, mobility management, resource management, BS and UE sleep strategies, interference mitigations and power control have to be either developed starting from scratch or upgraded for adapting to the complex multi-tier scenarios [45].

2.2   Cellular Network Traffic Diversity

Since the emergence of cellular networks, many studies have been carried out for characterizing the traffic generation of individual BSs as well as that of the aggregate network. In recent times, several network operators have also come forward to disclose their normalized daily traffic patterns. Most of the studies have clearly identified strong diurnal patterns of aggregated traffic. That means, the traffic volume significantly varies over a day having both peak-times and off-peak times, which can be termed temporal diversity. It has also been identified that the peak-time traffic load can be over twenty times higher than that of at off-peak times [12], [47], [48]. This diurnal pattern can also vary from network to network.

Furthermore, although slow changes in traffic generation on consecutive weekdays (or weekends) are identified, significant variation from weekdays to weekends is clearly exhibited. This temporal variation is strongly related to the natural life styles, daily activities, random call making behavior and unpredictable mobility patterns of subscribers; diverse applications with heterogeneous characteristics (e.g., session durations, bit rates and file sizes); density of subscribers; network size and so on. For instance, in a commercial area, day time is the usual peak-traffic time with almost no traffic during the night time. Fig. 2.4 shows the recorded traffic behavior in two different real cellular networks demonstrating temporal diversity. As seen for a large fraction of a day ($8 \sim 10$ hours), traffic load remains much lower than the network capacity indicating the underutilization

(a) Normalized aggregated traffic over one week [21].
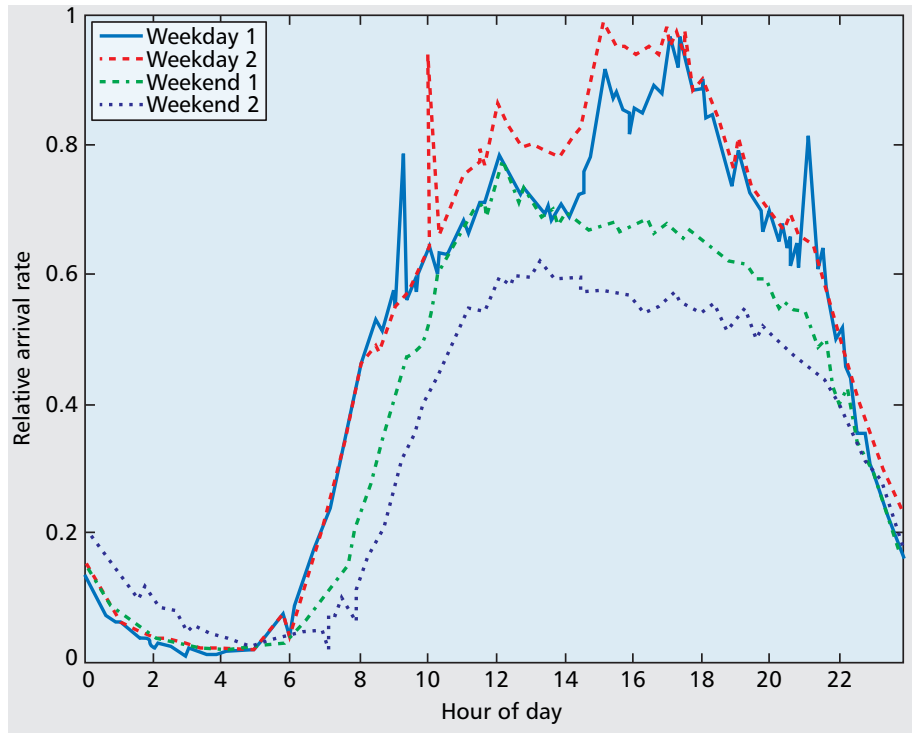
(b) Normalized aggregated call arrival rate in various days [47].

Figure 2.4: Temporal traffic diversity in two different real cellular networks.
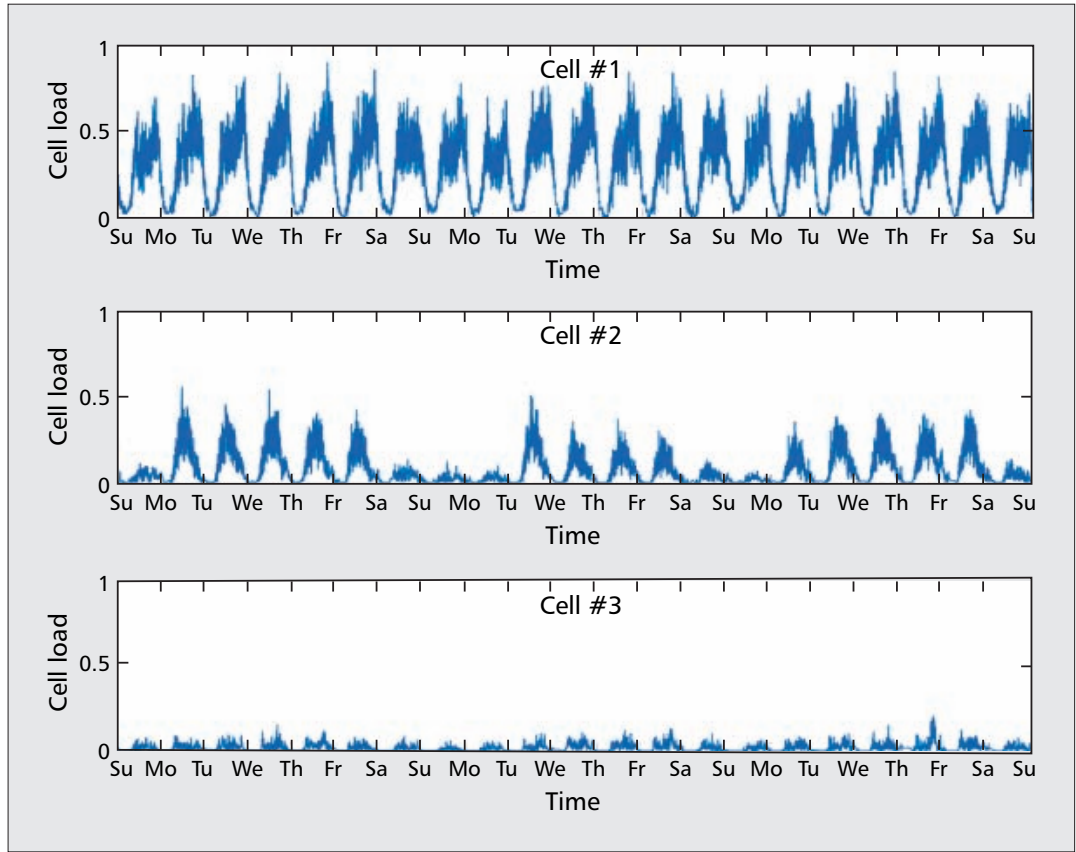
Figure 2.5: Demonstration of spatial traffic diversity [47]. Presented normalized traffic in three different cells over three weeks illustrates a substantial variation of traffic in space.

of the network resources.

On the other hand, traffic intensity as well as peak-time and off-peak time can substantially differ over the network coverage, even between neighboring BSs, resulting in spatial diversity. The degree of this kind of diversity can be dependent on the distribution of different classes of subscribers, population density in the neighborhood, BS deployment density, location of special event venues and so on. In one study, for example, it is figured out that only 5% of devices generate approximately 90% of network traffic, while 99% of sessions are generated by 10% of applications contributing to the spatial diversity [21]. Another study has pointed out that only 10% of BSs carry 50-60% of traffic load indicating a high-degree spatial diversity [20]. Spatial diversity can become even more evident during peak-traffic times [12]. Normalized traffic over three consecutive weeks taken from three different cells of the same network is plotted in Fig. 2.5 [47], which clearly

Figure 2.6: A forecast of mobile data traffic growth [50].

demonstrates the spatial diversity. As seen, at any particular time, traffic generation is much lower in cell 3 compared to the other two.

2.3   Trends in Global Mobile Traffic

The exceptional success of cellular networks, the dramatic rise in popularity of smart phones and other emerging mobile terminals, and the prevalent demand for new diverse applications are leading the recent explosive growth in mobile traffic. Data traffic has long crossed voice traffic manyfold [49]. From various surveys, it is clearly evident that with the continuing advent of UE features and the high speed network technologies, this trend will continue globally over the next decade. For instance, a recent report released by CISCO estimated that average smart phone usage increased from 189MB in 2011 to 342MB 2012, a total of 81% increment in one year [50]. Fig. 2.6 taken from the same report presents a forecast showing exponential growth in global mobile data traffic [50]. Other studies also have identified similar trends and predicted that total traffic may double every 4-5 years [49], [51].

Figure 2.7: Power consumption in a typical cellular network [13].

2.4   Energy Usage in Cellular Systems

To meet the ever-growing demand for mobile data traffic, network operators are continually expanding and upgrading their infrastructure. To the end of 2011, it was estimated that approximately 4 million BSs were operating across the world [5]. Correspondingly, energy utilization in cellular networks is rising at an incredible rate. The Global e-Sustainability Initiative (GeSI) report suggested that by 2020, cellular network infrastructure may represent more than 50% of the total energy utilization in communication networks [6], [10].

However, conventional cellular networks are designed paying virtually negligible focus on the energy efficiency aspect. For instance, although cellular network traffic exhibits significant temporal diversity, cellular networks are provisioned based on the *worst-case* peak-traffic situation [19]. Thus, considering that all BSs will be required for satisfying the users at peak-traffic times, all of them are kept on for 24 hours a day ignoring the time-varying traffic demand. This would not be a matter of concern from the energy efficiency point of view if BSs were not consuming energy in a non-load-proportional fashion [11], [12], [18], [19]. More downside is that BSs are the dominant energy hungry equipment in a cellular network amounting to around 60%-80% of the total consumption [10], [11], [12], [13]. A representative detailed breakdown of power consumption in

different components of a typical cellular network is illustrated in Fig. 2.7 [13]. Conse-
quently, by keeping all BSs in active mode all the time, existing networks are wasting a
substantial amount of energy, which eventually adds to the operating expenditure of the
network operators. Thus, current cellular networks have turned out to be highly energy
inefficient.

2.5 Architecture and Power Consumption in Macrocell Base Stations

A reference architecture of a macrocell BS having three sectors and four transmit antennas
per sector is presented in Fig. 2.8 [13]. For simplicity and clarity, only one transceiver
(TRX) chain is shown. A TRX chain mainly consists of an antenna, a switch/duplexer, a
power amplifier (PA), a radio frequency (RF) small-signal module, a base-band module
for both uplink and downlink, a power supply unit, a cooling system and an antenna
feeder. Usually, a single power supply unit as well as a single cooling system is shared by
all the TRXs of a BS. It is worth mentioning that a microcell BS covering a much smaller
area generally supports only one sector having the same set of equipment corresponding
to one TRX chain of macrocell BSs (cooling system is an optional item) [16].

A comprehensive breakdown of the total power consumption in different components
of a macrocell BS is shown in Fig. 2.9 [17]. As shown in the figure, the PA and the
cooling system are the two major energy consuming equipment in a BS. The PA is one of
the most energy inefficient elements incurring more than 50% power loss at high traffic
load [17], [52]. Furthermore, under medium and low-traffic times, its efficiency goes as
low as 5% [5], [17]. On the other hand, although the energy consumption in a cooling
system scales with the BS load, it consumes a significant amount of power even at no
traffic load. Thus, the PA and the cooling system are the two major contributors to the
non-load-proportional energy consumption in BSs.

2.6 Power Profiles of Macrocell Base Stations

Majority of the existing studies on energy efficiency of cellular networks consider the
BS transmit power for evaluating the performance measures [17]. However, such perfor-
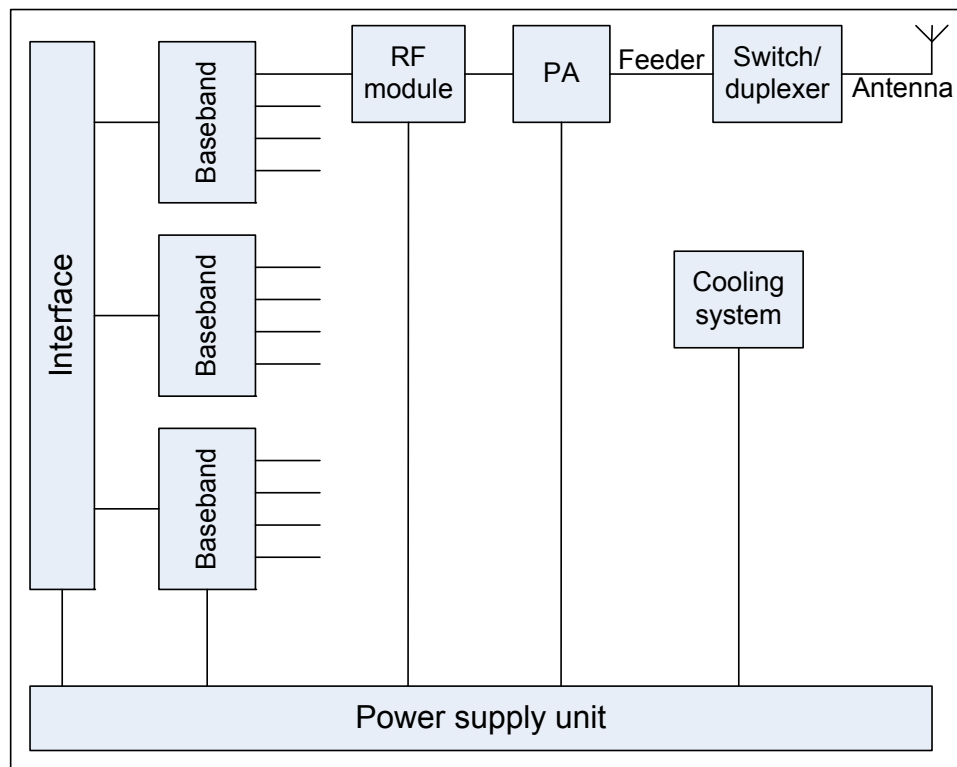
Figure 2.8: An architecture of a 3-sector macrocell BS having four transmit antennas [13].
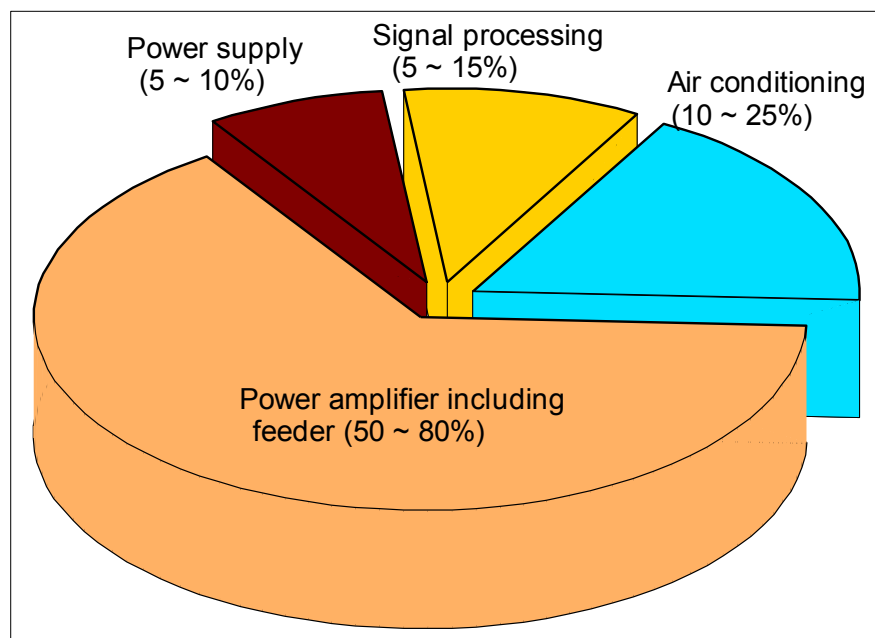
Figure 2.9: Power consumption in different components of a typical macrocell BS [17].
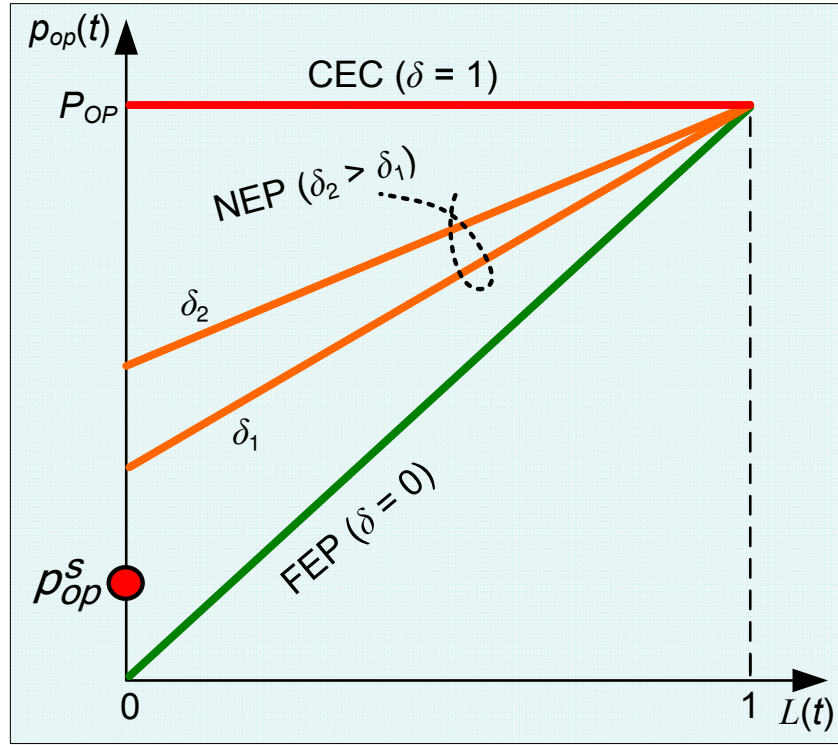
Figure 2.10: Power consumption characteristics of different BS models.

mance metrics are apparently incomplete and potentially misleading as they fail to capture the overall power consumption characteristics of a BS. Therefore, for evaluating the energy efficiency of a cellular network, it is essential to account the total power required for operating a complete set of a BS.

Despite the improved load-dependent energy consumption in the new generation BSs, most of the contemporary BS consumes nearly equal power irrespective of traffic load. Therefore, in the literature, both the constant energy consumption (CEC) model [9], [16], [17], [32], [36], [37], [38], [43], [52], [53], [54], [55], [56] and the non-energy proportional (NEP) linear power consumption model [11], [12], [18], [19], [33], [39], [41] for BSs are widely used. CEC type BSs consume constant power irrespective of traffic load. Whereas, for NEP type BSs, a load-dependent dynamic power consumption part and a load-independent constant power consumption part together constitute the total operating power. In this thesis, a generalized power consumption model capable of capturing a wide range of BSs is adopted for the evaluation of the proposed systems. Under the adopted model, the instantaneous operating power of a single TRX chain can be given as

below [11], [39]

$$p_{op}(t) = \begin{cases} (1-\delta)L(t)P_{Op} + \delta P_{Op} & \text{(active mode)} \\ p_{op}^s & \text{(sleep mode)} \end{cases} \qquad (2.1)$$

where $0 \leq L(t) \leq 1$ is the LF at time t, P_{Op} is the maximum operating power required at full-load (i.e., $L(t) = 1$) and $0 \leq \delta \leq 1$ is a constant determining the level of dependency of $p_{op}(t)$ on $L(t)$ and therefore, it is named as energy-load proportionality constant (ELPC). Now, based on the value of δ, various types of BSs can be modeled, which mainly fall into three different categories: (i) CEC model ($\delta = 1$), (ii) fully energy proportional (FEP) model ($\delta = 0$), and (iii) NEP model ($0 < \delta < 1$). Fig. 2.10 shows the power consumption characteristics of different BS models. FEP type does not consume any power at no-load and consumption linearly increases with the load, which is an ideal case and the ultimate target of BS manufacturers. On the other hand, depending on the design of the BS hardware, sleep mode power p_{op}^s may vary. Total operating power of a BS set can be evaluated by summing the operating power of all its TRX chains.

2.7 Fundamental Approaches for Enhancing Energy Efficiency in Cellular Networks

For transforming the current energy inefficient cellular networks into really "green" ones, it is essential to bring fundamental improvements in every possible aspect. This upgrading can be seen across three different levels of cellular networks, namely, component level, link level and network level features, which are discussed below [17].

2.7.1 Component Level Prospects

Since BSs are the major power hungry elements of cellular networks, reduction in power usage in different components of BSs can provide a significant boost in energy efficiency. For proper operation of PAs under the modulation schemes utilized in UMTS/high speed packet access (HSPA)/LTE systems, they are required to be operated in the linear range much below the saturation region resulting in significantly lower energy efficiency [5], [17]. Thus, improving the efficiency of PAs is of utmost importance, which can be achieved by employing the Doherty design approach; integrating advanced digital predistortion (DPD), linearization and envelope tracking techniques; and so on [17], [57], [58].

Besides, deactivation of PAs at LTE signal-free symbols [57], [58] and other components of BSs (e.g., digital and analog circuits [17]) in LTE discontinuous transmission (DTX) mode, use of low power front-end supporting different transmit power levels [17], and adaptive voltage and frequency scaling [59] can make a BS more energy efficient. In addition, modifications to BS architectures requiring less or no cooling at all (e.g., Ericsson's Tower Tube BS), utilization of software-based remotely configurable BSs (e.g., Flexi BS of Nokia Siemens Networks) and integration of multiple technologies in a single BS set (e.g., Flexi BS and ZTE's *Unified Hardware Platform*) can also reduce the energy cost [57].

2.7.2   Link Level Prospects

Traditionally, radio link protocol and transmission techniques are designed focusing mainly on achieving higher throughput, optimal SE, satisfactory network coverage, low latencies, low power consumption in the user terminals and so on [17]. However, it is high time to focus on the energy efficiency of radio links from BS perspectives. Energy efficient resource allocation, efficient interference management schemes [13] and coordinated multi-point transmission (CoMP) [36], [60], [61] has the potential to lower the RF power requirement. In addition, imposition of a higher priority in scheduling lower frequency bands in a cognitive multi-frequency operation [36], coordinated scheduling of component carriers (CCs) [62] and turning off the corresponding PAs with no scheduled CCs under carrier aggregation [58] can also be considered for energy efficiency of cellular networks. In particular, it is highly important to focus on the joint optimization of SE and energy efficiency for the radio link operations, which can bring significant reduction in energy consumption as well as maintain the service quality [17].

2.7.3   Network Level Prospects

There is substantial prospect of saving energy by designing scenario specific (e.g., dense urban, suburban and sparse rural areas) optimum network deployment and provisioning techniques. From a network deployment perspective, cell size (e.g., macro, micro, femto and pico cells) [63], [64], [65], homogeneous and heterogeneous cell deployment [51], [54], [66], [67], [68], cell densities [52], [69], various sector and antenna configurations in each BS, beam forming, antenna tilting, distributed antenna systems, relays and multi-hop

techniques [13], [17], [58] can be exploited for achieving energy savings. On the other hand, self-organizing network provisioning mechanisms, such as traffic-aware adaptive adjustment of the number, location and coverage of BSs [5], [13], [17], [36], [58], [70], reconfiguration of BSs using various number of sectors and antennas per sector [17], [58], redistribution of traffic among macro, micro, pico and femto cells [17], [36], utilization of hybrid energy sources (i.e., on-grid and renewable energy) and switching between them [57], [71], [72], [73], inter-network cooperation for switching off BSs [36], [74], [75], [76], software controlled network capacity tuning [57], dimming services and carriers [77], and cell breathing [43], [41], [78] are some of the highly prospective options for improving energy efficiency in cellular networks.

2.8 Energy Efficient Dynamic Network Provisioning: Related Research

From the previous discussion of traffic diversity, power consumption breakdown of a network, power profiles of BSs and the conventional network provisioning strategy, it is clearly evident that BSs are the major energy consuming as well as the most energy inefficient equipment in a cellular system. Therefore, enhancing the energy efficiency of cellular networks by inactivating RAN equipment at low-traffic times, namely, BSs and the sectors in each BS, is being considered as one of the most promising techniques. This can be confirmed from the emergence of a large number of BS and sector switching schemes in recent years [5], [10], [30].

The basic concept of all the proposals is fairly simple: *Based on the instantaneous traffic demand, the number of active elements (i.e., BSs and sectors) in a cellular RAN is dynamically minimized, while the remaining active elements provide the coverage for the users located in the inactive elements.* Then the research problem narrows down to the following question: *When, which and how are the RAN elements selected for activation and deactivation as well, while maintaining QoS?* This is also the principal research focus of this thesis. More precisely, this thesis proposes and investigates RAN equipment switching mechanisms for single-tier (i.e., homogeneous) networks deployed with macro-cells only. Therefore, the discussion in this section is kept restricted to the existing related schemes proposed for single-tier networks only.

2.8.1   Base Station Switching: Single Network Scenario

In this section, BS switching based schemes developed for single network scenarios are studied. Aiming to leverage the natural temporal-spatial traffic diversity in cellular networks, 3GPP LTE has included turning off under-loaded BSs at lower traffic times as an use case for saving energy [31]. However, the standard has not specified any implementation scheme and has left the issue of designing appropriate mechanisms open for further research. In light of this, a high level energy efficiency evaluation framework (E^{3}F) for approaching and assessing new designs was developed under the European Union (EU) funded research project "Energy Aware Radio and Network Technologies (EARTH)" [18]. This framework identified that both small-scale short-term system-level metric and large-scale long-term global metric are vital for evaluating any new scheme. Under the large-scale long-term evaluation, global performance metric was proposed to be evaluated by taking the weighted sum of the evaluations carried out over various deployment scenarios (e.g., urban, suburbs and rural areas) involving corresponding daily/weekly traffic profiles. Here below, a critical study of the existing BS switching schemes is presented by grouping them into several categories.

2.8.1.1   Under Delay Intolerant Traffic

By employing predefined deterministic switching patterns of BSs, authors in [32], [33], [34] and [35] proposed manually turning off BSs during low-traffic times and thus, these schemes are applicable only for regular cell layouts. In contrast, proposals for dynamically shutting down some BSs following the daily traffic profile were presented in [36], [37] and [38]. The proposals in [32], [33], [35] and [38] provided no strategy for turning on the BSs during high-traffic times leading to their incompatibility for future SONs. Thus, in case of an emergency situation of a sudden rise in traffic generation during the switched off times, many users may experience service interruption. On the other hand, the schemes in [32], [33], [35] and [37] are developed based on a fairly unrealistic assumption of homogeneous traffic throughout the network and thus, the impact of UE distribution and data rates is completely overlooked. A more complete distributed dynamic scheme with detailed procedures for both switching on and off BSs using the average system load as the algorithm initiator was proposed in [9]. Communications among neighboring BSs are utilized for exchanging load information and disseminating the switching

on/off decisions. However, guaranteed data rate demands from users may significantly affect the load distribution, which is not addressed in this work. Moreover, a more efficient algorithm is expected as the presented one does not implement any intelligence in finding the best subset of neighbors for distributing traffic leading to reduced energy savings.

Proposals in [43] and [79] combined the cell zooming feature with cell sleeping techniques. Under these methods, based on the traffic, each BS expands (contracts) for accepting (offloading) traffic. Under feasible conditions, some BSs are switched to sleep mode as well. In addition, for maintaining coverage, [79] introduced the concept of inner-cell and outer-cell regions operating on different frequency bands, which can be implemented by using vertical sectorization and adaptive tilting under regular cell layout. On the other hand, a theoretical optimization approach for evaluating the potential energy savings from turning off BSs was outlined in [53]. Another theoretical analysis of energy savings from BS sleeping under coverage constraint by utilizing a stochastic geometry based network model was presented in [80]. However, the schemes in [9], [32], [36], [37], [38], [43] and [53] failed to capture the load-dependent power utilization in BSs resulting in overestimations. Moreover, many of them presented either very basic algorithms ignoring the actual data rates and locations of users [37], [33], [38] or no algorithm at all [32], [36], [53], [80].

2.8.1.2   With Delay Tolerant Traffic: Energy-Delay Tradeoff

Many applications (e.g., web browsing, file transfer and e-mail) can tolerate certain service delays, which can be exploited for regulating the energy saving switching operation of BSs. Considering this as an opportunity, [11] and [81] studied the tradeoff between energy savings and delay by formulating several cost minimization problems. However, the systems in [11] and [81] do not guarantee user data rates leading to the potential degradation of service quality for users in the sleep mode BSs. On the other hand, by developing various closed form expressions, [82] and [83] presented comprehensive analyses on the delay-savings tradeoff under several sleep control and power matching mechanisms. A major limitation of these two analyses is the consideration of a single BS scenario and thus, for understanding the more realistic behavior of the system performance, they have to be extended for multi-cell scenarios. Despite the differences in the system models, in general, an inverse relationship between energy savings and delay is demonstrated in all of these four works.

2.8.1.3   Network Segmentation Strategies

For developing energy efficient BS switching schemes, all the works discussed above considered the entire network as a whole. The works in [12], [84] and [85] handled the BS switching problem by dividing the networks into smaller sub-networks. For instance, [12] divided the networks into rectangular grids containing several BSs. Then, a traffic profiling scheme was used to estimate the traffic of each grid. Finally, BS switching algorithm was executed inside each grid independently from the other grids. This system was designed under the framework of wideband code division multiple access (WCDMA)-based 3G systems and no algorithm was presented as well. Thus, changes in the system modeling approach are required to make it compatible for next generation orthogonal frequency division multiple access (OFDMA)-based systems. On the other hand, [84] divided a network into many clusters consisting of three BSs. Then, similar to [12], BS switching is done in each cluster independently. In [85], the total network area is segmented into many sub-areas by dividing the network into columns and rows, which are of equal widths and heights respectively. The division is done in a way such that each column can have a maximum of one BS and thus, the network is represented by an one-dimensional linear model. In the next step, a graph theory based shortest path algorithm is used for finding out the optimal set of active BSs such that there exists no coverage gap between two consecutive BSs. Other BSs are then switched into sleep mode. A common drawback of these sub-network based schemes is that they restrict the scope of cooperation by limiting it within the smaller domains leading to the possibility of sacrificing energy saving performance.

2.8.1.4   Integration of CoMP Transmission

It has been widely recognized that SE of a cellular network can be effectively improved by CoMP transmission, where multiple BSs cooperatively serve the users in multiple cells. This technique particularly can be very useful in urban environments, where the dense deployment of BSs ensures that the users are always within communication distance with multiple BSs. Some of the CoMP transmission techniques are demonstrated in Figs. 2.11 and 2.12 [86]. By implementing such coordinated uplink and downlink transmission/reception, CoMP transmission techniques can achieve a network wide interference reduction resulting in reduced power requirement at both the uplink and the downlink [36]. Consequently, a new network having integrated CoMP transmission facilities can be deployed with fewer BSs leading to enhanced energy efficient operation.

(a) Joint transmission (JT).

(b) Coordinated beamforming (CB).
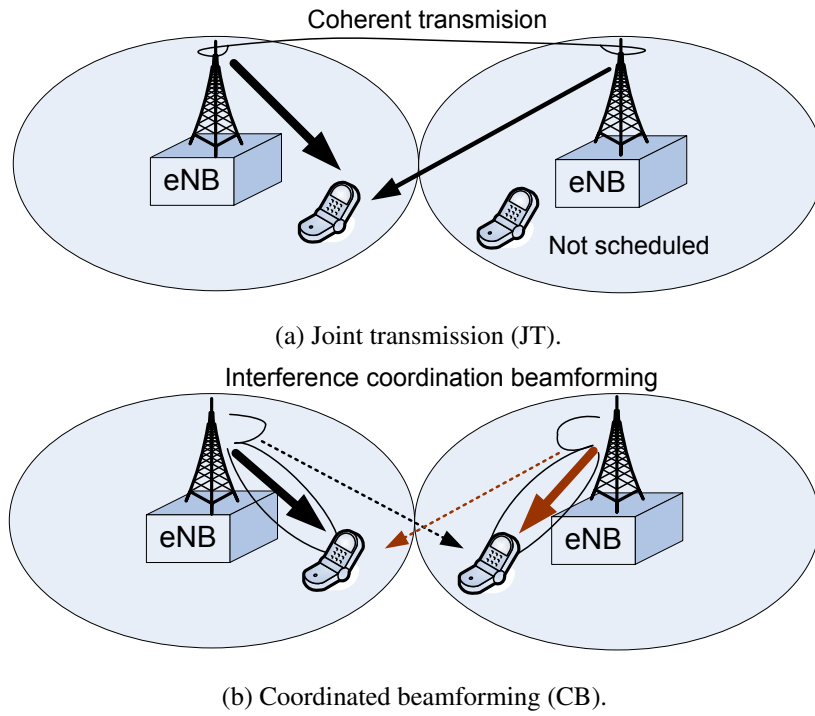
Figure 2.11: Downlink CoMP transmission techniques [86].

(a) Multipoint reception with interference rejection combining (IRC).

(b) Multipoint reception with coordinated scheduling (CS).
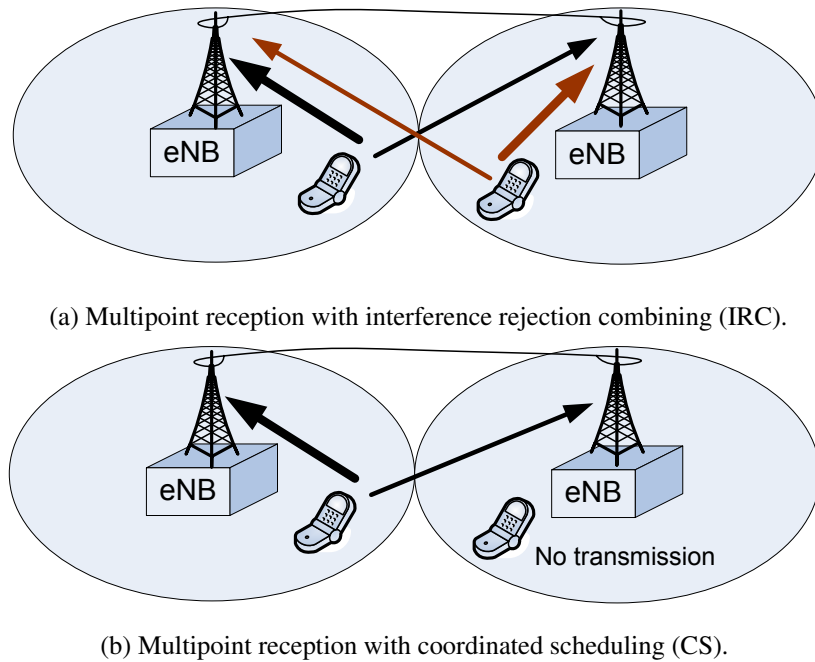
Figure 2.12: Uplink CoMP transmission techniques [86].

Energy efficiency improvement of cellular networks by utilizing CoMP transmission techniques was demonstrated in several previous works [60], [61]. Looking beyond this, [87] and [88] exploited CoMP transmission for facilitating BS switching leading to a higher number of sleep mode BSs. Irrespective of the simplification made for developing the schemes in these two works, it is clearly evident that depending on the data rates, BS power consumption models and other system parameters, BS switching with CoMP transmission has the potential to outperform the BS switching without CoMP in terms of energy efficiency. However, a lot more in-depth analyses under various network scenarios are required before reaching any reasonable conclusion.

2.8.2   Base Station Switching: Multi-Operator Cooperation

Cooperative trading of BSs among the geographically co-located multiple cellular networks can be considered as an additional opportunity for reducing energy utilization. Particularly, in urban environments, BSs from different operators are closely situated, or even on the same tower, and thus, multi-network cooperation can be an attractive approach. Two case studies presented in [36] and [76] also supported this potential for energy savings. On the other hand, authors in [48] considered a case of two operators with the assumption that BSs of the two operators are co-located. The two operators cooperatively share each other's traffic and thus, during low-traffic times, either of the co-located BSs belonging to the two networks switches to sleep mode. Evaluation under various system settings demonstrated a prospect of substantial energy savings. On the other hand, another multi-network cooperative scheme incorporating four operators was presented in [89]. Various priority orders of the operators for switching into sleep mode keeping one of them always active were explored. However, none of these schemes provided any algorithm or implementation framework. Moreover, more general scenarios of BSs belonging to different RANs located at different towers have to be taken into consideration. Developing cooperation policies among the operators, managing cross-operator mobility, user authentication and billing, and so on are some of the other complex challenges, which demand thorough investigation.

2.8.3 Sector Switching

The emergence of energy efficient dynamic BS switching schemes has also exposed numerous incredible difficulties regarding their implementations [36], [43]. For instance, the schemes involving dynamic cooperation among BSs are extremely complex requiring tight coordination and accurate synchronization for rapid coverage adjustments to avoid coverage holes and excessive interference. Under these schemes, the interference is much more dynamic and harder to keep track of than that in the conventional networks and thus, it is extremely difficult to develop efficient techniques for managing it. Moreover, incredible upgrading in BSs in terms of processing power as well as artificial intelligence is essential. For instance, the switching transients (i.e., from active to sleep mode and vice versa) have to be very short, which can otherwise significantly offset the energy savings gain [90].

One attempt to develop alternative solutions with less complexity and ease implementations, yet effective, is the dynamic sectorization technique [17]. Under the dynamic sectorization techniques, each BS is dynamically reconfigured using the minimum number of sectors sufficient for meeting the instantaneous traffic demand, while the TRX chains corresponding to the other sectors are switched off for saving energy. Currently, only a handful of preliminary studies on dynamic sectorization are available in the existing literature, which are discussed here.

Authors in [40], [41], [42] and [91] simply estimated the degree of potential energy savings from dynamic sectorization, while no attempt was made to propose algorithms and develop implementation guidelines. Moreover, major simplifications in system modeling were made by ignoring several crucial factors. Firstly, consideration of the antenna radiation pattern in any realistic evaluation of sectorization techniques is extremely important. This is because, after a BS is switched from one sector configuration to another, the relative position of a UE in a sector and hence, its received signal power may change. This may significantly affect the system performance, which was overlooked in [40], [41] and [91]. Secondly, with the change in transmission beamwidth of an antenna, its gain changes [92]. This comes from the fact of radiating the same amount of power for covering an increased (or decreased) sector area. System performance can again be affected by this antenna feature, which was not considered by any of these studies in [40], [41], [42] and [91]. Furthermore, these works evaluated energy savings by switching BSs mainly

from three-sector to single-sector configuration and thus overlooked other possible antenna settings.

Although the above discussed works demonstrated a substantial energy savings from sectorization, they lack concrete system modeling and comprehensive investigations. Thus, this branch of energy saving mechanisms requires much more attention and vigilant investigation for further exploration.

2.9 Key Technologies for Enabling Network Equipment Switching

2.9.1 Wake-up Technology

As discussed above, switching on/off BSs in accordance with the temporal-spatial traffic diversity for saving energy in cellular networks has become the center of focus of many researchers. The majority of the proposals involve multiple switching operations of BSs (between on and off) per day. Under such scenarios, operator assisted manual switching of BSs is not an efficient solution. Particularly, many subscribers may face difficulty in accessing services in case of a sudden surge in traffic generation during the switch off times. A wake-up mechanism with essential intelligence can be a realistic approach for this purpose, which can enable BSs switching their operating modes without any human intervention. This technology has the potential of making access networks more energy efficient as well as guaranteeing the service availability.

Wake-up technology enables electrical and electronic equipment switching among several power states depending on the instantaneous tasks to be performed. For example, a device can switch to a low power state when it is unnecessary to keep all the sections in power mode and then, wake-up with the reception of a special message to switch into active mode for transmission and/or reception. Power requirements can vary substantially among the operating modes. A desktop personal computer (PC), for example, can generally be operated in four different modes - active, idle, sleep and hibernate. Typical power consumption in these modes are 140 W, 100 W, 1.2 W and 1.0 W respectively [93]. Similarly, a Wi-Fi UE typically consumes 400 mW, 1000 mW and 1100 mW in connected/idle mode, searching mode and active transmission/reception mode respectively [93].

On the other hand, a wake-up module is required to be keept in active mode during the power saving modes of an equipment. This module can intercept any wake-up request and immediately switch the equipment to the desired mode. Power consumption in this module has to be very low, otherwise it could offset the overall energy savings. Low-power milliwatt range wake-up modules are currently being used in wireless local area networks (WLANs). Research on further improvements in terms of energy consumption (e.g., microwatt range) and size of these modules for different applications is currently under way [94], [95], [96].

Applicability and possible incentives of introducing the wake-up technology for various communication networks have been investigated for the last few years [94], [97], [98], [99], [100], [101]. Different wake-up scheduling algorithms for increasing the life time of sensor networks as well as for maintaining the required QoS were proposed in [97], [98]. For Ethernet, power saving mechanisms by deactivating some links and routers during the lower traffic time were studied in [99]. A few analyses of sleep mode and wake-up technology for Wi-Fi access points (APs) and battery powered end user devices are also available from [94], [100]. Further energy saving through switching between wireless and wired networks in office environments based on the data rate requirement by allowing the unused network to go into sleep mode is investigated in [101]. All of these published results have established the great promise of this technology by significantly increasing the life time of battery operated isolated devices and substantially reducing the energy consumption in these networks.

Nevertheless, integration of a wake-up mechanism in cellular systems can be much more complex than in other applications. The highly dynamic nature of cellular networks due to a large number of users with unpredictable mobility patterns and session generation behavior, heterogeneity in various dimensions (e.g., QoS requirements, applications, cell sizes, BS capacities and network technologies), time-variant wireless channel characteristics, frequent operating mode switching of BSs requiring fast coverage adjustments, and switching times of various accessories in BSs (e.g., cooling system, PA and base band module) are some of the key factors to be considered in such a scenario. Therefore, careful design and analysis is required in deploying wake-up technology in cellular networks.

2.9.2 Advanced Antenna Technology: Beam Forming, Fanning and Panning Features

Along with BS switching, future networks are expected to involve dynamic switching of sectors. For maintaining network coverage with a time-varying number of active sectors and BSs, it is essential to have the facilities of dynamic adjustment of the transmission beamwidth, beam direction and the transmission range of each sector. With the advent of smart antenna technology in recent years, this has become a real possibility.

Omnidirectional antennas were primarily used for the deployment of the early days commercial cellular systems, which are typically linear cylinders, resembling a pipe. Next, for overcoming the low capacity issue of Omnidirectional antennas, multi-sector antennas were introduced. Although 3-sector antennas are almost universal in contemporary networks, a recent trend of developing antennas for using in 6-sector cell sites is noticed. Switching from 3-sector to 6-sector antennas can achieve a 70% higher capacity [102], while the number of inter-sector handoffs will increase as well.

Throughout the development process, various facilities, such as beam tilting (remote electrical and mechanical tilting), multi-band support (i.e., combined antennas of multiple frequency bands in a single housing), multi-beam antenna (i.e., multiple beams from a single array of antennas), vertical sectorization capabilities, integration of active electronic devices in the antenna radomes and beam forming capabilities are added [102]. Antennas with such kinds of advanced technologies are popularly known as "smart antennas". Smart antenna is a very general term, which refers to adaptive antennas having all, or a subset of, the aforementioned facilities. Thus, smart antennas enable following relatively slow-varying traffic patterns, forming beams aimed at particular users or steering nulls to reduce interference. In addition, they can have adaptive antenna arrays with the ability to apply separate signals (with controllable amplitude and phase of the input currents) to antenna elements in both the vertical and horizontal axes for forming beams or sectors in the desired planes as well as for implementing multiple-input multiple-output (MIMO) and receive diversity [103], [104].

Furthermore, a new generation of smart antennas known as reconfigurable beam antennas also includes the remotely controlled beam fanning and beam panning capabilities [102]. Beam fanning refers to the technology of reconfiguring transmission beamwidths, while
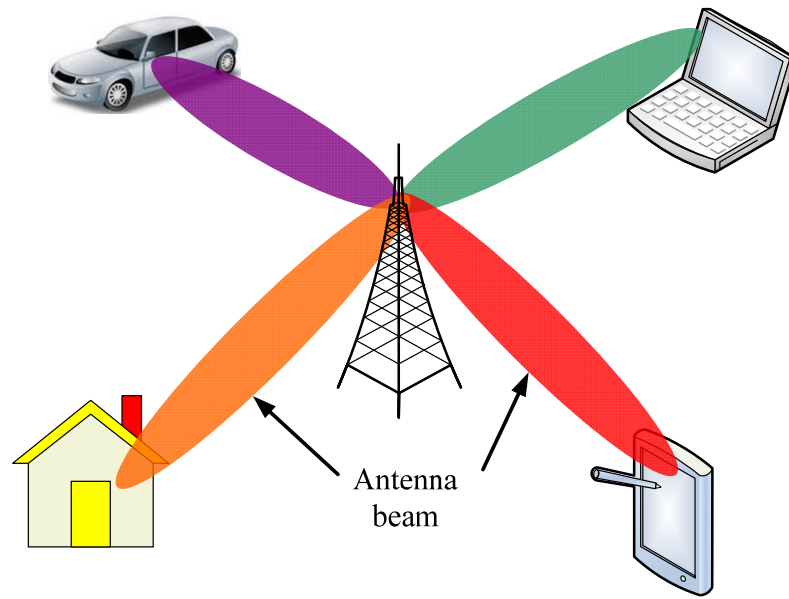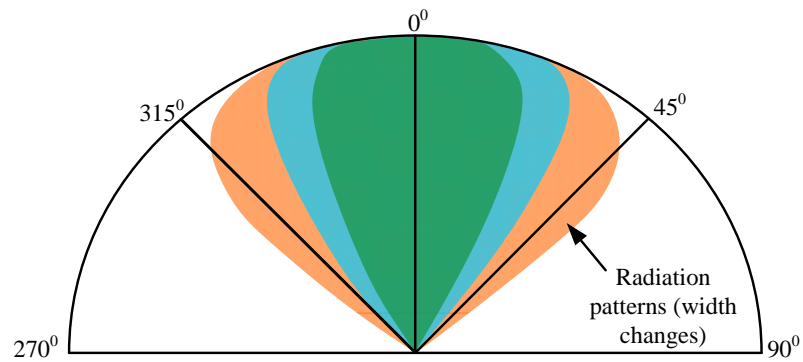
(a) Beam forming.

(b) Beam fanning [102].
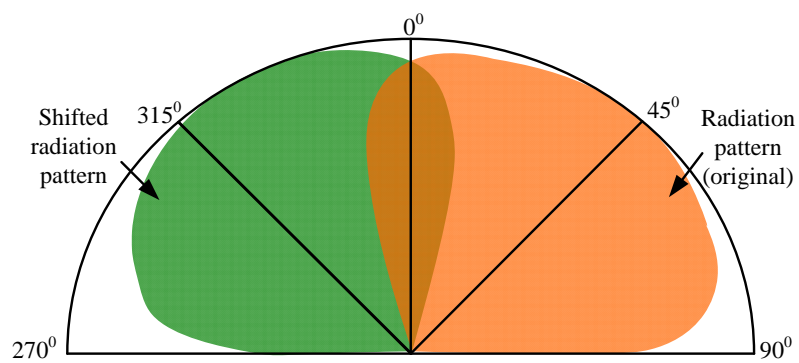
(c) Beam panning [102].

Figure 2.13: Smart antenna features.

beam panning implies the shifting of a beam to a targeted direction. Beam forming, fanning and panning capabilities of smart antennas are demonstrated in Fig. 2.13. Under dynamic switching of sectors, remaining active sectors can implement this beam fanning capability of antennas for widening their beamwidths to cover the entire cell area. In addition, BSs are required to be equipped with the apparatus, control circuitry and artificial intelligence for carrying out sector switching and driving the antennas for coverage maintenance.

2.9.3   Inter-BS Communications

The dramatic rise in the demand for mobile communications and the increasing complexity of the networks necessitate more intelligent network management mechanisms. Provision of multi-cell cooperation through inter-BS coordination and collaboration in cellular access networks is a promising tool for such an environment. The ultimate goal of multi-cell cooperation is to maximize network capacity as well as service quality by utilizing network resources in an optimal fashion and minimizing inter-cell interference [74], [105]. For example, stringent multi-cell coordination is essential for energy saving dynamic network reconfigurations, under which some BSs can be put into sleep mode, while the active BSs cooperatively adjust their transmission ranges to maintain coverage for the sleep mode ones. This type of coordination becomes even more crucial for the implementations of distributed type solutions.

By recognizing the huge potential of multi-cell coordination, inter-BS communication is enabled by integrating links among BSs both in LTE-A [106] and WiMAX [107] architectures. For instance, LTE evolved universal terrestrial radio access network (E-UTRAN), as demonstrated in Fig. 2.14, consists of a network of eNBs with no central coordinator. eNBs are connected to the evolved packet core (EPC) via serving gateways (SGWs) and mobility management entities (MMEs). As shown in the figure, eNBs are interconnected with each other using an "X2" interface, which is introduced for inter-BS message exchange in various coordination and cooperation phases. Similarly, the "R8" interface in the WiMAX access network plays a similar role to the "X2" interface [107], [108]. It is worthwhile to mention that 2G/3G based cellular systems do not have any inter-BS communication link.
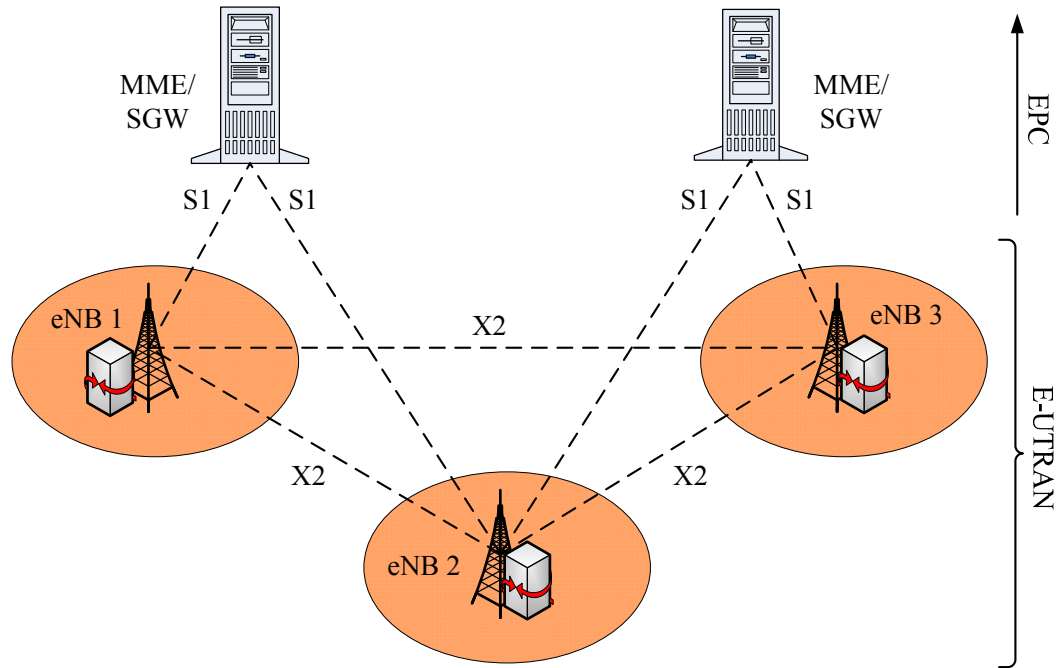
Figure 2.14: LTE architecture.

2.9.4 Inspiration from Ecological Self-Sustainability

The best example of a self-sustainable system is the Earth's ecosystem. Despite natural changes and instability in the ecosystem, the entire system regains its stability through millions of years of evolution. Thus, it is arguably in a highly balanced and stable state with intrinsic adaptivity to varying environmental conditions, inherent resiliency to failures and damages, successful and collaborative operation on the basis of a limited set of rules, and global intelligence [109]. Self-organizing, self-managing, self-adapting and self-optimizing capabilities are the fundamental properties behind the self-sustainability of the Earth's ecosystem.

A self-organizing system in ecology consists of numerous small components, which work based on some basic local rules. These rules specifying interactions among the system components are executed using only local information, without reference to the global pattern. Systems of this class, starting from an initial random state, with no guidance or help from any external body, emerge spontaneously in a well-organized structured system [110]. On the other hand, a self-adaptive system works in a top-down manner and is capable to adjust to changes in the environment without endangering its essential

organization. Such a system can evaluate its own global behavior and change it when the evaluation indicates that it is not accomplishing what it was intended to do, or when better functionality or performance is possible.

Whereas, a self-managing system is capable in managing its resources and organization by itself. This management can be either optimal or non-optimal. A self-optimizing system is also capable to manage its resources. However, it always attempts to optimize the utilization of its available resources. Such a self-optimizing system learns from interactions with the changing environment and optimizes its performance during the entire life cycle [26].

Besides, different types of interactions among a large number of homogeneous and heterogeneous components in an ecosystem play a key role in maintaining its sustainability. Mutualism/cooperation, competition, altruism, predation, parasitism, coopetition, protocooperation, commensalism and detritivory are the main interactions observed in the ecosystem [111], [112]. An interacting species either gets benefits or loses something, or neither gets benefits nor loses anything from the interaction.

On the other hand, future networks are expected to be interconnected networks of heterogeneous technologies, relatively large and highly dynamic in nature [24], [25], [113]. Managing such networks using traditional operator assisted manual techniques is inefficient and impractical. Under such complex scenarios, the self-organizing operation of networks requiring minimum human intervention is being considered as a prospective solution expecting various potential gains including reduced cost and complexity [23], [26]. This potential has been recognized by all the major telecommunication standard developers, such as 3GPP LTE, WiMAX and NGMN alliance [27], [28], [29]. Definitions of SONs by these standards encompass self-configuration, self-optimization and self-healing features.

If a HWN is considered as an ecosystem, then different networks comprising it can be thought to be analogous to different components of the Earth's heterogeneous ecosystem. Therefore, network operation mechanisms developed based on ecological principles have a huge potential to be real solutions for the envisaged self-organizing HWNs. The prospect of incorporating ecological principles in communication networks design has been demonstrated in several previous works [109]. For instance, being inspired by

the "adaptation by evolution" feature of organisms, a distributed framework for service evolution with varying network characteristics was proposed in [113]. Whereas, [114] presented an ecological population dynamics based approach for modeling the life time and the energy distribution of battery constrained sensor networks. Moreover, swarm intelligence [115], coordination among social insects [116], animal foraging behaviour [117], synchronization of fireflies [118], adaptive nature of the mammalian immune system [119] and so on were all exploited in developing various features of communication systems.

2.10   Chapter Summary

The first part of this chapter has presented the basic architecture of a typical cellular system including the conventional single-tier and emerging multi-tier networks. An in-depth analysis of the natural high-degree temporal-spatial traffic diversity, the explosive growth in global mobile data traffic and the incredible rise in power consumption in cellular networks are also presented. Moreover, a detailed breakdown of power utilization in different components of the state-of-the-art BSs as well as a study of the power consumption profiles of BSs has been presented. This has identified that the reduction of energy utilization in BSs can make the existing networks much more energy efficient. In the second part of this chapter, a comprehensive discussion on the component level, link level and network level fundamental approaches for achieving energy efficient cellular networks has been provided. Existing energy saving proposals integrating dynamic switching of BSs as well as sectors have then been grouped into various categories and studied critically. Finally, wake-up technology, smart antennas with advance features, tight inter-BS coordination and integration of ecological principles in network operations are identified as the critical factors for enabling self-organizing type dynamic switching of network equipment. Thus, this chapter has established the background for introducing various novel energy saving frameworks in the following chapters.

Chapter 3

Eco-Inspired Cellular Network Operations

Chapter 2 has identified that the inclusion of ecological principles in operational mechanisms has the great prospects in achieving self-organizing network management. Therefore, by establishing an analogy between the ecosystem and the HWNs, this chapter introduces a new design paradigm for cellular networks incorporating the principles of ecosystem on Earth. Applicability of the ecological principles to cellular networks is demonstrated by proposing an eco-inspired RRM mechanism. Based on the theory of ecological multi-species multi-resource competition, an analytical model for characterizing the unfairness and instability in HWNs resulting from the intense competition among users from multiple networks with diverse resource requirements is developed first. The proposed RRM scheme is then imposed for ensuring the coexistence of users from all classes, even under extreme situations and sudden network environment disruptions. Effectiveness of the proposed RRM scheme is demonstrated through extensive simulations. The contribution in this chapter has been published in [120].

3.1   An Eco-Inspired Resource Management Scheme

This section proposes a RRM framework for HWNs aiming to demonstrate the applicability of ecological principles to cellular networks. The proposed framework is developed

based on the ecological competition among multiple species for multiple resources, which can model both the user dynamics and the resource dynamics for complex HWNs having variable number of networks, user classes and resource types.

3.1.1 Motivations and Related Works

Proposals for future wireless network architectures encompassing interworked HWNs offer different applications having diverse resource requirements. Users of different classes (e.g., voice, video and data) from different networks having widely varying QoS in terms of resources (e.g., bandwidth and power) come together and compete for resources. These inevitable intense competitions may result in unfair resource distribution among different classes of users and consequently, the probability of being left out for some of these user classes is high. This phenomenon is known as competitive exclusion in ecology. In HWNs, especially during peak-traffic times or in regions of high user density, the phenomenon of competitive exclusion is a very likely possibility. Thus, the sustainability of future HWNs is at high risk. Sustainable networks have to be capable of fair allocation of all the network resources for seamless connectivity and mobility to all kinds of subscribers as well as of fulfilling the requirements of the service providers. Therefore, design of RRM mechanisms through proper resource control, congestion control and admission control is of extreme importance for HWNs [121], [122].

Existing RRM approaches can be aligned with three distinctive categories: network-centric, user-centric and collaborative [122]. In network-centric and user-centric RRM schemes, the networks and the users respectively focus on maximizing their own utility [121], [123], [124], [125], [126]. Contrarily, in the collaborative approach, both the networks and the users jointly make the decisions for optimizing their combined utility [127]. For instance, a simulation based network-centric admission control policy for RRM of HWNs was presented in [123]. In [124], a Markov chain model was used for analyzing the RRM of a HWN, where the authors considered only two classes of users with no indication of the achieved throughput by each class. On the other hand, a user oriented vertical handoff based scheme aiming to maximize user profit and improve load balancing among multiple networks was investigated in [125]. While, a RRM scheme for parallel transmission was proposed in [126], where each UE is allowed to transmit over multiple RANs simultaneously. However, both [125] and [126] are user-centric approach leading to a potential selfish behaviour of users. Furthermore, being inspired by the anal-

ogy between the HWNs and the heterogeneous systems of other fields, many researchers imported theories from those fields for devising RRM schemes [121], [127], [128], [129]. As an example, authors in [128] used an economic model for formulating a RRM scheme and evaluated the network social welfare for quantizing its performance. But, the user data rate considered for the evaluation was 8-12 kbps, which does not represent a real network having widely differing data rates.

Furthermore, in developing any standard and scheme for attaining sustainable HWNs, all types of network resources have to be taken into account. For example, for developing energy efficient HWNs, any RRM scheme should jointly consider both BW and power as independent resources [17]. However, in the recent literature, the majority of authors have considered either BW or power as the resource. Moreover, none has modeled the phenomenon in which each class of users in the network individually has enough subscribers for acquiring the entire resources, i.e., an extreme scenario where the network stability may collapse. Additional motivation for developing the proposed RRM scheme based on the ecological principle has come from the previously mentioned great analogy between HWNs and the ecosystem [129], [130], which is presented in detail in the following section.

3.1.2 Proposed RRM Framework

3.1.2.1 Ecological Resource Competition Dynamics

In ecology, a resource is defined as a factor contributing to a higher growth rate resulting in higher population densities with the increase of its availability and consumption by the species. Such resources include food, water, sunlight, habitat, minerals, CO_2, O_2 and so on. Competition within the same species (intraspecific) as well as among the species (interspecific) is the most commonly observed interaction, where a group of species tries to optimize their own share of resources for their sustainable existence. In ecology, there is no visible regulator in controlling these competitions. The outcomes of these competitions dictate the growth of species resulting in the coexistence or extinction of incompetent species from certain areas and thus influence the biodiversity on Earth.

Resources in ecology are broadly classified as perfectly complementary, imperfectly complementary and perfectly substitutable [131]. Perfectly complementary resources are all

essential for species survival and one can't be compensated by another. In this case, the population growth of a species is governed by the least available resource. In such a scenario of G genus[1] having p different species competing for r different perfectly complementary resources, the joint population dynamics and resource dynamics can be expressed as below [131]

$$\frac{dN_i(t)}{dt} = N_i(t) \left[min_j \left\{ \frac{g_{i,j}(R_j(t))}{q_{i,j}} \right\} - D_i(t) \right] \tag{3.1}$$

$$\frac{dR_j(t)}{dt} = S_j(t) - \sum_{m=1}^{p} q_{m,j} \left[min_n \left\{ \frac{g_{m,n}(R_n(t))}{q_{m,n}} \right\} \right] N_m(t) \tag{3.2}$$

$$i = 1, 2, ..., p; j = 1, 2, ..., r; n = 1, 2, ..., r$$

$$\text{Initial conditions: } N_i(0) = N_0, R_i(0) = R_0 \tag{3.3}$$

where $N_i(t)$ denotes the population density of ith species, $R_j(t)$ is the biomass density of jth resource, D_i is the per capita death rate of ith species, $S_j(t)$ is the net supply rate of jth resource, $g_{i,j}(R_j)$ is the removal rate of jth resource by an individual of ith species, $q_{i,j}$ is the amount of jth resource required to produce each individual of ith species and $B_i(t) = min_j \left\{ \frac{g_{i,j}(R_j(t))}{q_{i,j}} \right\}$ is the per capita birth rate of ith species. In ecology, Michaelis-Menten form is usually used for $g_{i,j}(R_j)$ [131]. The competition among species for resources has been accounted for in the second part of (3.2). The equation implies that when one species group consumes more resources resulting in an increase of its population, it reduces the resource availability to other species groups and thus limits their growth.

In an ecologically balanced (equilibrium) system, the rate of changes of population of all species and resource densities is zero. Setting $\frac{dN_i(t)}{dt} = 0$ and $\frac{dR_j(t)}{dt} = 0$ in (3.1)-(3.2), we can derive the conditions of equilibrium for this competition as below

$$B_i(t) - D_i(t) = 0 \tag{3.4}$$

$$S_j(t) - \sum_{m=1}^{p} q_{m,j} B_m(t) N_m(t) = 0 \tag{3.5}$$

Imposing additional conditions on top of (3.4)-(3.5), one can define a desired balanced state. All of these conditions in combination determine the population densities and resource availabilities at the equilibrium state of the system.

---

[1]Several species combinely form a genus.

3.1.2.2 Heterogeneous Wireless Networks as an Ecosystem

Future HWNs can be considered as analogous to the ecosystem of Earth having different homogeneous and heterogeneous systems [129], [130]. Therefore, here it is named the heterogeneous wireless network ecosystem (HWNE). In HWNs, the service requirements of users vary widely and hence, users are grouped into different classes. Such requirements mainly include bandwidth (BW), power and QoS. Usually, a set of different classes of users is served by a RAN, which can be assumed equivalent to a genus. Thus, each class of users is analogous to a species. Then, the number of active users of a particular class is analogous to species population density. Similarly, call generation and call ending in the networks are equivalent to birth and death of a species population respectively. A complete relationship between the ecosystem and the HWNE is presented in Table 3.1.

3.1.2.3 Competition Model in Heterogeneous Wireless Networks

A scenario of HWN consisting of UMTS and WiMAX cellular systems is considered here for investigation, where BSs from the two networks overlap each other over a fraction of their coverage as shown in Fig. 3.1. Four classes of users $N_i(i = 1, 2, ..., 4)$ with different resource requirements are assumed - N_1 and N_2 originally belong to UMTS, while N_3 and N_4 to WiMAX. On the other hand, BW and transmit power (TP) of BSs are considered as the two different resources (i.e., $r = 2$) subject to competition. For serving a user, both BW and TP must be allocated for it. These two resources can't compensate each other. Therefore, BW and TP can be grouped as completely complementary resources. It is also assumed that UEs have dual-band interface to support both RANs and are capable to adaptively select, connect and switch to either of them based on coverage and resource availability.

For analytical purpose, two hypothetical resource pools, R_1 and R_2 for BW and TP respectively are formed, which is accessible to the users from both the networks located in the common coverage. Each pair of two BSs, one from UMTS and the other from WiMAX, allocates a certain portion of their BW and TP to these R_1 and R_2 pools and thus, form a resource group for shared access. The portion of resources allocated in the pools for sharing can be set through negotiation between the operators. When a user located in the common coverage area wants to access service, it needs to be allocated resources from both the pools simultaneously. This common coverage area is also the

Table 3.1: Analogy between the ecosystem on Earth and the HWNE

Symbol	Ecosystem	HWNE
G	Genus	RAN
N_i	Population of ith species	Active users of ith class
R_j	Biomass density of jth resource	Unused amount of jth resource
D_i	Death rate of ith species	Call ending rate of ith class
S_j	Net supply rate of jth resource from the death of species and reproduction of resources	Total release rate of jth resource due to the call ending of all classes
$g_{i,j}(R_j)$	Removal rate of jth resource by each individual of ith species	Removal rate of jth resource by each user of ith class
$q_{i,j}$	j^{th} resource essential to produce each individual of ith species	j^{th} resource essential to serve each user of ith class
$B_i(t)$	Per capita birth rate of ith species	Call generation rate per user of ith class
p	Number of species	Number of class of users
r	Number of ecological resources	Number of radio resources
$R_{i,max}$	Maximum amount of ith ecological resource	Maximum amount of ith radio resource
t	Time	Time

network area where the competition among the users takes place for gaining the resources from the R_1 and R_2 pools.

Under unregulated competition, resource allocation among the classes is likely to be iniquitous and potential competitive exclusion of particular classes is expected. To abolish the jeopardy of such unfairness for realizing a stable coexistence of all classes, ecological MSMRC-based RRM (explained in Section 3.1.2.5) scheme is proposed. For every resource group, i.e., for every pair of BSs sharing resources, a functional block with the scheme is setup as shown in Fig. 3.1. This block can be located at a place so that it
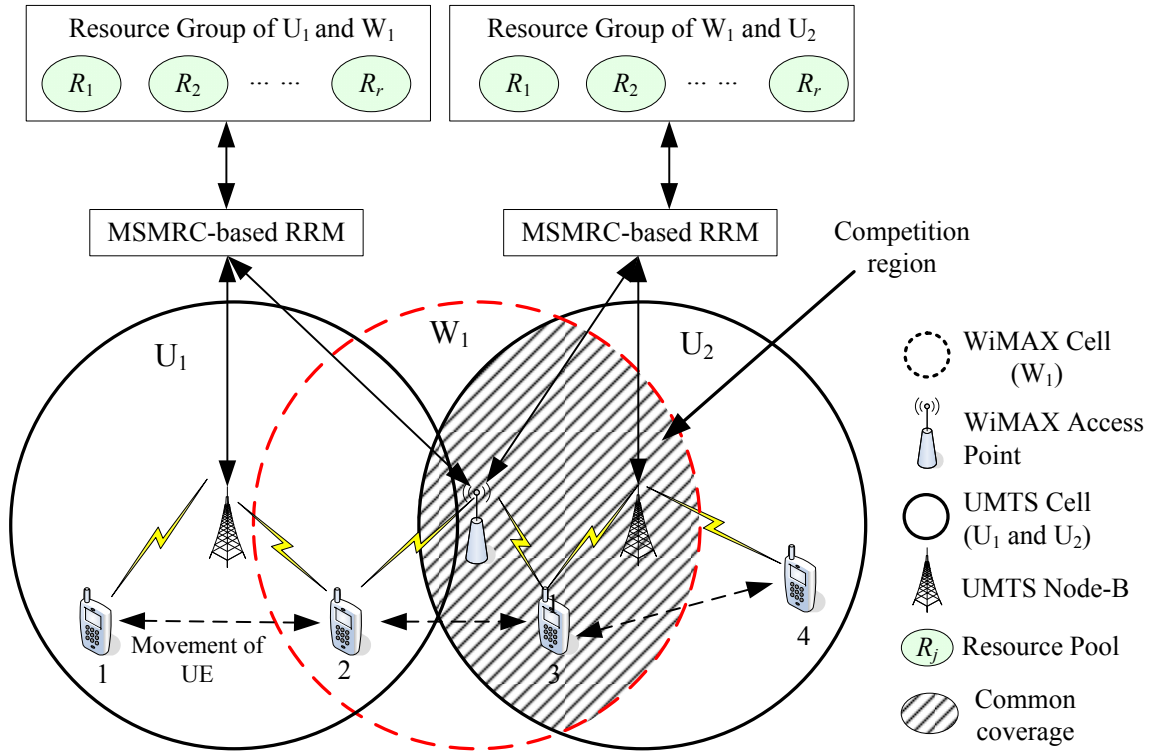
Figure 3.1: System model.

can access information from both BSs making the proposed scheme of distributed type. Therefore, users from both the networks in the common coverage area can compete for gaining resources under the control of the proposed RRM scheme.

3.1.2.4 Coexistence of Multiple User Classes

For the assumed system scenario with four user classes and two resources, (3.4)-(3.5) can be manipulated for evaluating the conditions of network equilibrium and coexistence of different classes. Replacing (3.4) into (3.5), we have

$$S_1(t) = q_{1,1}D_1(t)N_1(t) + q_{2,1}D_2(t)N_2(t) + q_{3,1}D_3(t)N_3(t) + q_{4,1}D_4(t)N_4(t) \quad (3.6)$$

$$S_2(t) = q_{1,2}D_1(t)N_1(t) + q_{2,2}D_2(t)N_2(t) + q_{3,2}D_3(t)N_3(t) + q_{4,2}D_4(t)N_4(t) \quad (3.7)$$

An additional condition that users from all classes combinedly consume the entire available BW at equilibrium condition is imposed, which can be written as

$$q_{1,1}N_1(t) + q_{2,1}N_2(t) + q_{3,1}N_3(t) + q_{4,1}N_4(t) = R_{1,max} \quad (3.8)$$

Furthermore, for the convenience to evaluate the conditions using matrix algebra, one more condition is evaluated from (3.4) as below

$$D_i(t) = min_j \left\{ \frac{g_{i,j}(R_j(t))}{q_{i,j}} \right\} = min_j \left\{ \frac{g_{i,j}^*(R_j(t))}{q_{i,j}N_i(t)} \right\} \tag{3.9}$$

Here, $g_{i,j}^*(.)$ is the rate of removal of resource j by all users of ith class together. In wireless network scenario, $g_{i,j}^*(.)$ can be modeled as $R_j/T_{h,i}$, where $T_{h,i}$ is the call holding time of ith class. Setting $i = 1$ in (3.9), we get

$$N_1(t) = min_j \left\{ \frac{g_{1,j}^*(R_j(t))}{q_{1,j}D_1(t)} \right\} = y_1^{min}(t) \tag{3.10}$$

Writing (3.6)-(3.8) and (3.10) in matrix form

$$\begin{bmatrix} q_{1,1}D_1 & q_{2,1}D_2 & q_{3,1}D_3 & q_{4,1}D_4 \\ q_{1,2}D_1 & q_{2,2}D_2 & q_{3,2}D_3 & q_{4,2}D_4 \\ q_{1,1} & q_{2,1} & q_{3,1} & q_{4,1} \\ 1 & 0 & 0 & 0 \end{bmatrix} \begin{bmatrix} N_1 \\ N_2 \\ N_3 \\ N_4 \end{bmatrix} = \begin{bmatrix} S_1 \\ S_2 \\ R_{1,max} \\ y_1^{min} \end{bmatrix} \tag{3.11}$$

In matrix notation, at equilibrium of the system, it can be written as

$$\mathbf{QN} = \mathbf{R}, i.e., \mathbf{N} = \mathbf{Q}^{-1}\mathbf{R} = \mathbf{PR} \tag{3.12}$$

where

$$\mathbf{N} = \begin{bmatrix} N_1 \\ N_2 \\ N_3 \\ N_4 \end{bmatrix}, \mathbf{P} = \mathbf{Q}^{-1} = \begin{bmatrix} p_{1,1} & p_{1,2} & p_{1,3} & p_{1,4} \\ p_{2,1} & p_{2,2} & p_{2,3} & p_{2,4} \\ p_{3,1} & p_{3,2} & p_{3,3} & p_{3,4} \\ p_{4,1} & p_{4,2} & p_{4,3} & p_{4,4} \end{bmatrix}, \mathbf{R} = \begin{bmatrix} S_1 \\ S_2 \\ R_{1,max} \\ y_1^{min} \end{bmatrix} \tag{3.13}$$

As N_1, N_2, N_3 and N_4 have to be positive for any meaningful coexisting equilibrium, the conditions of both equilibrium and coexistence of all the user classes in the considered HWN can then be given by

$$C_d = p_{d,1}S_1 + p_{d,2}S_2 + p_{d,3}R_{1,max} + p_{d,4}y_1^{min} > 0, \forall d = 1, 2, ..., 4 \tag{3.14}$$
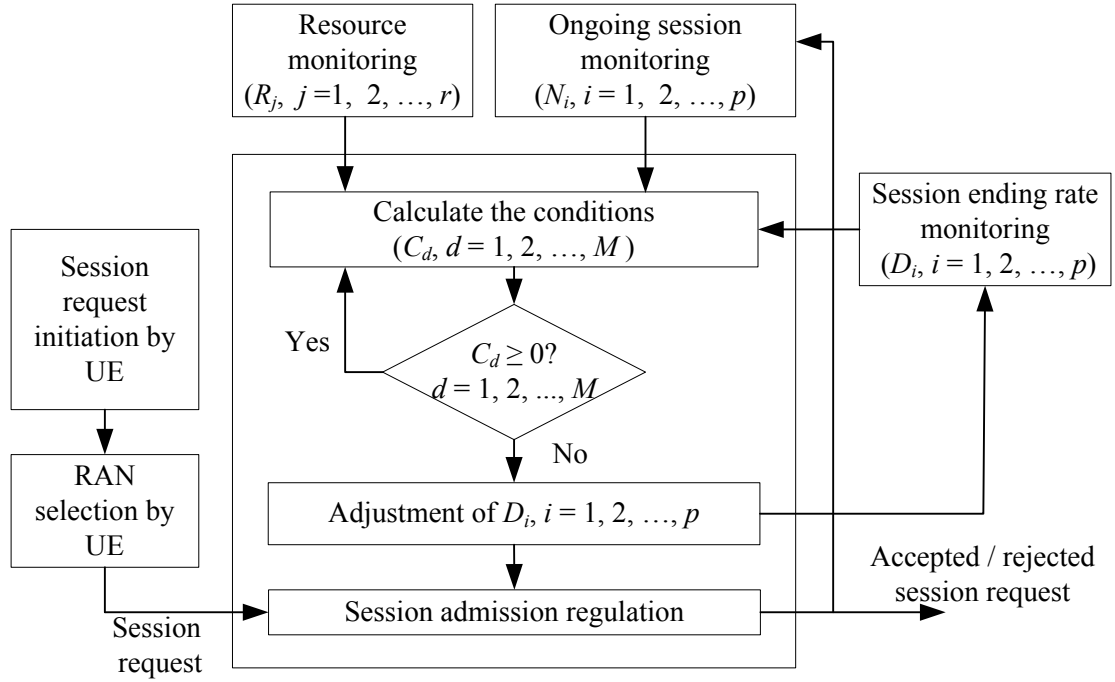
Figure 3.2: Ecological resource competition based MSMRC RRM scheme.

3.1.2.5 MSMRC-based Scheme for RRM

The complete framework of the proposed MSMRC-based resource management scheme is shown in Fig. 3.2. In the proposed scheme, number of ongoing sessions from different classes (N_i), available resources in the shared pools (R_j) and the call ending rates (D_i) are monitored periodically. In the decision making phase, parameters obtained from the monitoring phase are used for making the decisions on session admission requests made by UEs.

For requesting a new session, a RAN selection policy for UEs is proposed here, whose flow diagram is shown in Fig. 3.3. When a UE is in the common coverage area, it uses the resources from the shared pools. If sufficient resources in the pools donated by the same network (say UMTS) to which the UE is originally attached (i.e., UMTS) are available, the UE then selects that RAN (i.e., UMTS) and attempts to connect to it. Otherwise, it selects and attempts to connect the other RAN (i.e., WiMAX) accessing the unused resources in the pools allocated by that RAN (WiMAX). In contrast, if a UE is in the coverage of single RAN and this RAN is its original RAN, the UE select this RAN. Otherwise, the session request of the UE is blocked. Resources to be allocated to this UE

come from the resources of its original RAN left after donating to the shared pools.
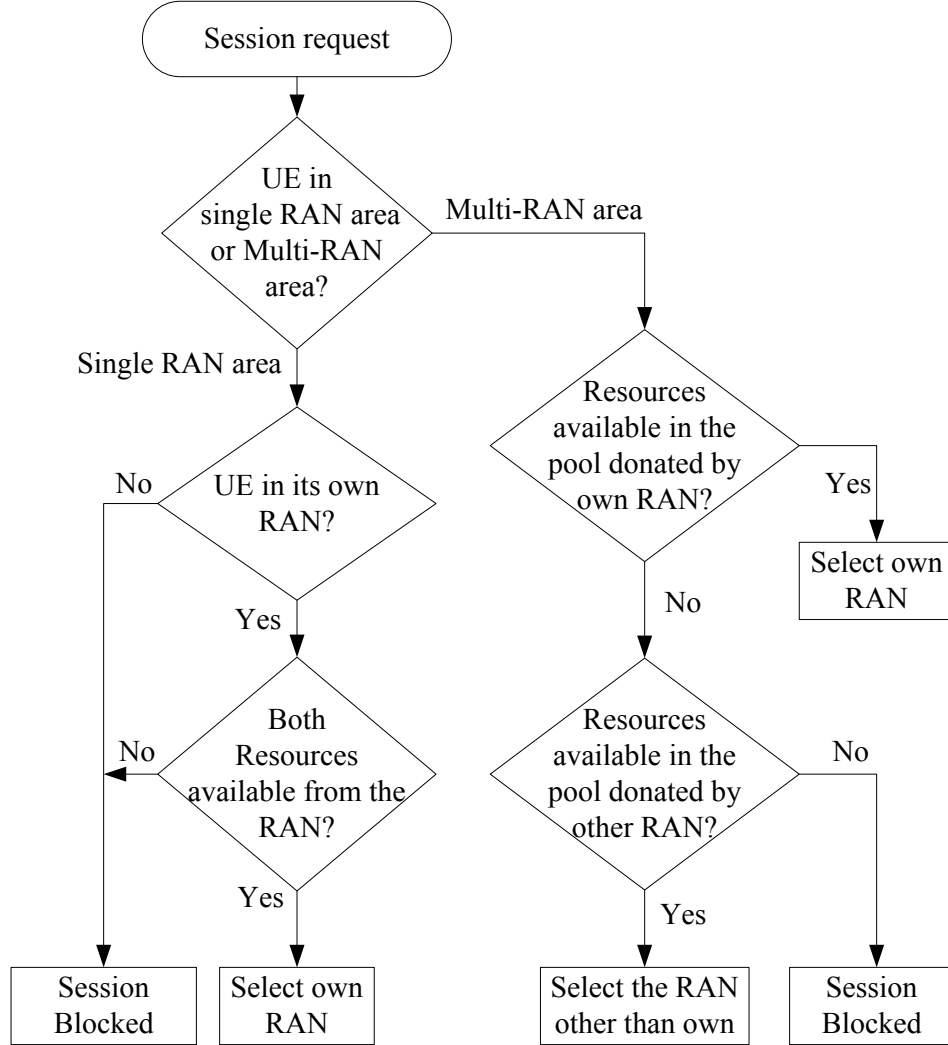
Figure 3.3: RAN selection policy of UEs.

After the selection of a RAN by a UE, the decision of session request acceptance or rejection has to be made by the proposed RRM scheme. Using the monitored parameters, conditions $C_d, \forall d \in (1, 2, .., M)$ for a coexisting stable equilibrium are evaluated using (3.14), where M is the number of conditions. If all the conditions are positive, the system parameters are kept unchanged. When any of the conditions in (3.14) is negative, adjustments in the call ending rates $D_i, \forall i \in (1, 2, ..., p)$ are made. The adjustments are done based on the values of $\frac{dN_i(t)}{dt}, \forall i \in (1, 2, ..., p)$. If $\frac{dN_i(t)}{dt} > 0$ which implies an increasing trend in N_i, D_i is increased by a very small value, say Δ. The opposite is done for those classes whose $\frac{dN_i(t)}{dt} < 0$, i.e., D_i is decreased by Δ. On the other hand, no adjustment in

D_i is made for those classes having $\frac{dN_i(t)}{dt} = 0$.

$D_i, \forall i \in (1, 2, ..., p)$ is adjusted within the range $[D_{i,min}, D_{i,max}]$, while $D_{i,min}$ and $D_{i,max}$ can be different for different classes. However, $D_{i,min}$ is the initial value, which only includes session ending due to termination by the user itself and handoff. Any adjusted new value of D_i greater than $D_{i,min}$ is implemented by intentionally blocking new session requests and dropping ongoing sessions. Dropping an ongoing session is not practised as long as blocking new session request is sufficient to meet the new D_i. On the other hand, decrease in D_i is realized by allowing more sessions from class i. Thus, based on the latest adjusted $D_i, \forall i \in (1, 2, ..., p)$, a new session request is accepted or rejected.

3.1.2.6 Simulation Setup

MATLAB has been used for evaluating the performance of the proposed RRM scheme. Differential equation set (3.1) - (3.2) is numerically evaluated using the fourth-order Runge-Kutta method [132]. The time scale is in second.

For the simulations, cell radius for both the networks is assumed 1 km. In WCDMA based UMTS system, transmission BW is 5 MHz. For achieving a cell capacity equal to 2 Mbps with a minimum required received signal-to-noise-ratio (SNR) at UE 5.5 dB, total TP requirement for serving an UMTS cell of 1 km radius is approximately 60 W [133] and thus, the average TP per kbps is 30/1024 W. On the other hand, with a higher BW, a WiMAX BS can support much higher bit rate. Assuming required SNR at UE equal to 15 dB for 3/4 16-QAM scheme and a path-loss exponent equal to 3, a WiMAX BS requires a TP of approximately 24 W for supporting 2 Mbps over a coverage area of 1 km radius [133]. Therefore, average TP per kbps in WiMAX is 12/1024 W. For the simulations, it is assumed that in the shared resource pools, UMTS allocates 1 Mbps and 30 W, while the contributions of WiMAX are 10 Mbps and 120 W. Thus, the total BW and TP in the pools are 11 Mbps and 150 W respectively.

Four classes of users are considered requiring 12.2 kbps (class 1), 128 kbps (class 2), 64 kbps (class 3) and 384 kbps (class 4) BW. Corresponding active number of sessions are denoted by N_1, N_2, N_3 and N_4 respectively. Therefore, $q_{1,1} = 12.2$ kbps, $q_{2,1} = 128$ kbps, $q_{3,1} = 64$ kbps and $q_{4,1} = 384$ kbps. Correspondingly, $q_{1,2} = 0.357$ W, $q_{2,2} = 3.75$ W, $q_{3,2} = 0.75$ W and $q_{4,2} = 4.5$ W respectively. For simulating the network in extreme situation, it is assumed that each class individually has sufficient users to acquire all the
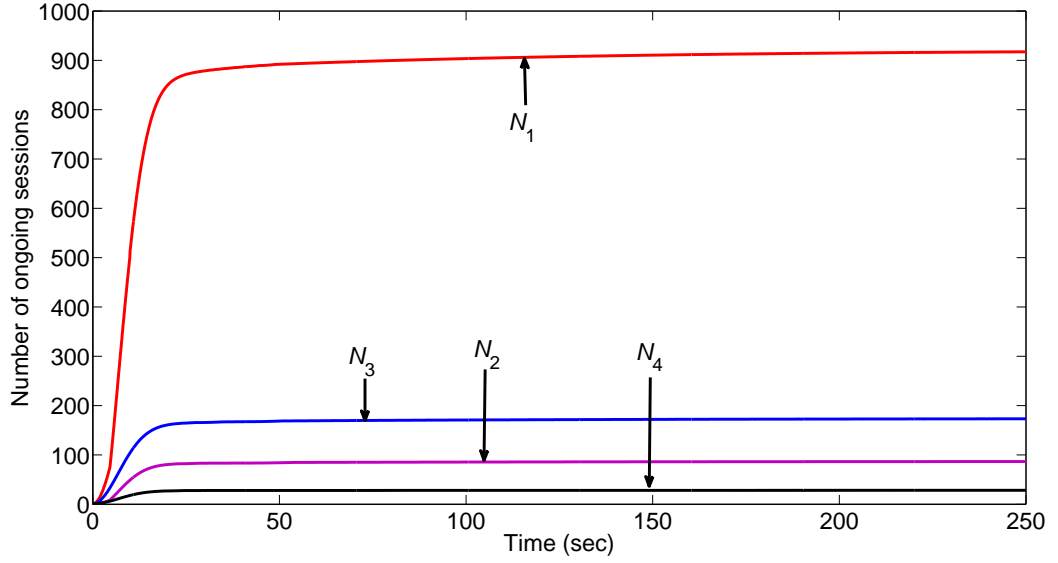
Figure 3.4: Sessions of each class with entire resources being allocated.

resources in the shared pools. Assuming that movement of users is the only cause of change in the received power at UEs, downlink TP adjustments are made so that the bit rate remains constant. Average velocity of users is considered as 36 km/h, i.e., 10 m/sec. The speed and the direction of movement of users are considered as two random variables (RV) with triangular and uniform distribution respectively. Cell residence time depends on the mobility of the users. For a cell of radius equal to R and a triangular probability density function (pdf) of speed in the range $[0, 2V]$, where V is the average speed, cell residence time is equal to $\frac{4Rln(2)}{V}$ [35]. Assuming an overlap of the two BSs by 50%, the patterned area in Fig. 3.1 can be approximated by a circle of radius $R^* \approx 0.625R = 625$ m. Thus, for V = 36 km/h, cell residence time is approximately 173 sec. Therefore, assuming average session duration of 240 sec, average session ending rate becomes equal to 0.01 calls/sec. This is the initial and minimum value of $D_i, \forall i \in (1, 2, ..., 4)$ used for the evaluations. Also, $D_{i,max} = 1.0, \forall i$ and $\Delta = 0.001$ are taken for all the simulations.

3.1.2.7 Results and Discussions

The analytical model in (3.1)-(3.2) is first used for evaluating the maximum number of concurrent users from each class, which can be served if all the resources in the shared pools are allocated for each class separately. Corresponding result is presented in Fig. 3.4 illustrating that at best 921, 87, 174, and 28 users can be served from class 1, 2, 3 and 4
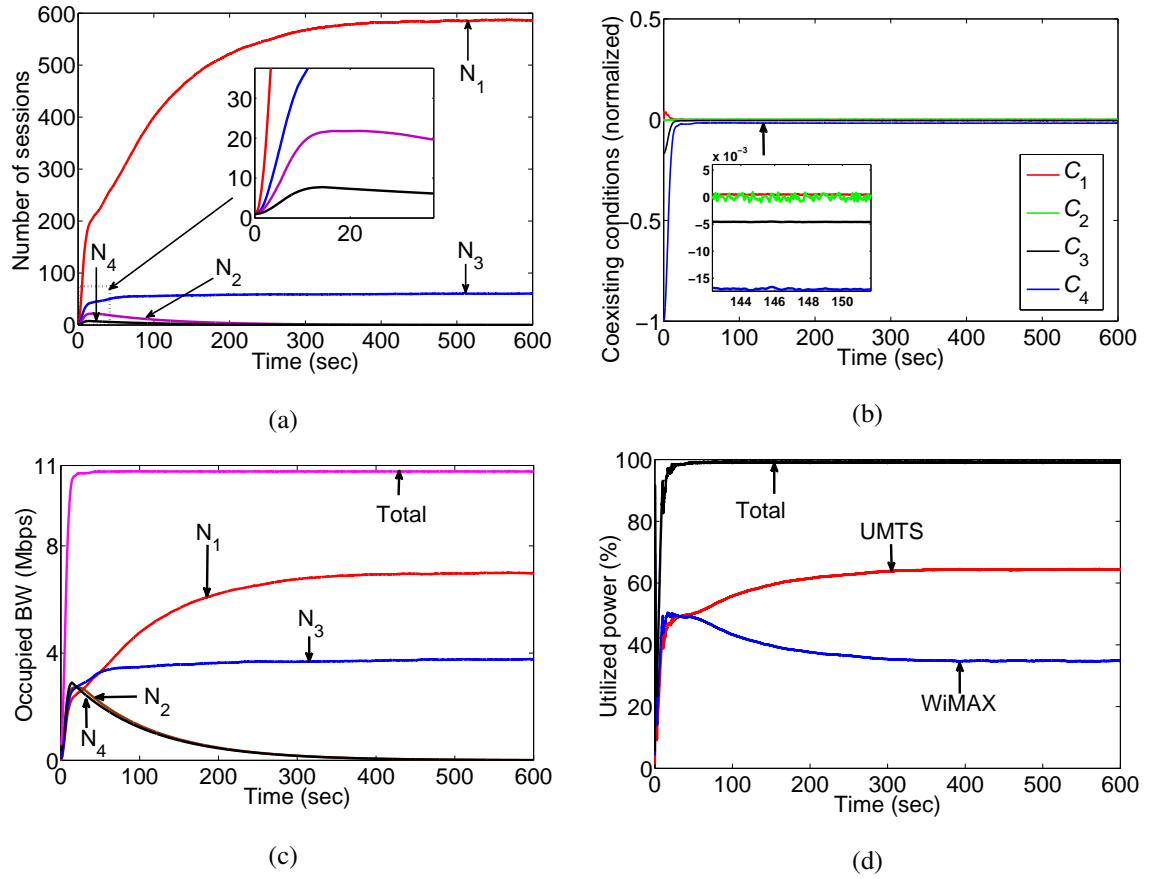
Figure 3.5: System performance under natural competition as in ecosystem.

respectively with the entire resources.

Then the model is simulated by allowing the users to compete freely such that new session requests are allocated resources in their arrival sequence. This scenario is equivalent to the natural competition observed in ecosystem with no resource controller. Corresponding outcomes are presented in Fig. 3.5. As shown in Fig. 3.5(a), initially, the number of user increases for all the classes. This trend continues for N_1 and N_3, and eventually becomes constant. In contrast, after certain time, the number starts to decline for N_2 and N_4 dropping to zero after 330 sec and 220 sec respectively. This can be explained as below: Both class 2 and 4 require much higher resources compared to class 1 and 3, and consequently, they are competitively excluded from the network leading to the collapse of the network stability. Within the first few seconds, as seen from Fig. 3.5(c) and Fig. 3.5(d), due to very high new session generation rate, almost entire amounts of both the resources are allocated among the classes. After that, whenever one session ends, say
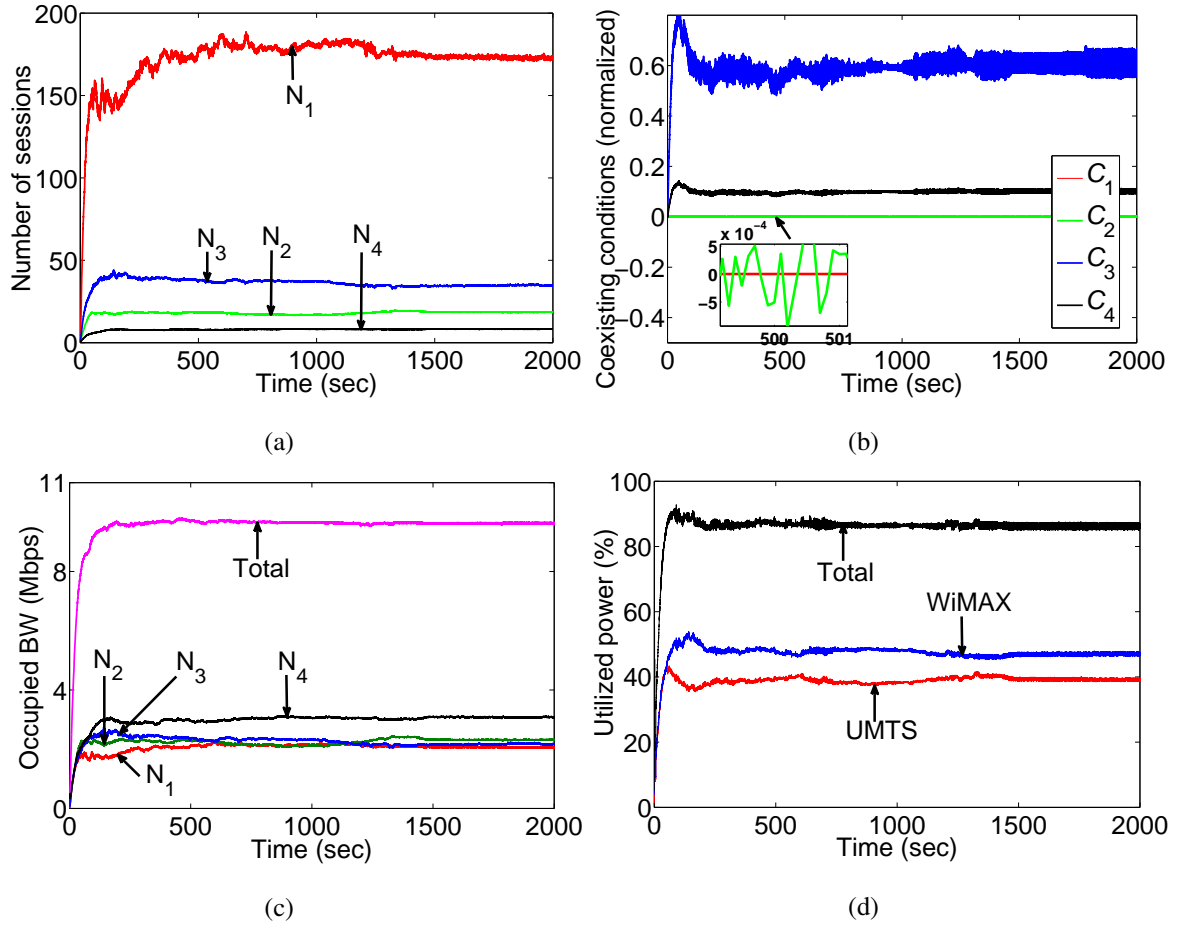
Figure 3.6: System performance under the proposed MSMRC-based RRM.

from class 1 or 3, the released resources are not enough for a session of class 2 and 4. Thus, the released resources are taken away by the other users from class 1 or 3. On the other hand, when one session ends from class 2 or 4, it can be occupied by users from class 1 and 3 also. However, if once the released resources from class 2 and 4 are taken away by class 1 or 3, no new users from class 2 and 4 are able to get connection leading to the eventual extinction of these classes. Furthermore, the normalized conditions for stable coexistence have shown in Fig. 3.5(b). Zooming close, it can be seen that two of them are negative, one is positive and the other alternates between positive and negative. This confirms the non-coexistence of all classes and break down of system stability as observed. On the other hand, Fig. 3.5(d) shows that although UMTS system provides only 20% (30 W) of the total power (150 W), it has occupied the most amounting 64%.

The system is then simulated with the proposed RRM scheme, where the users compete
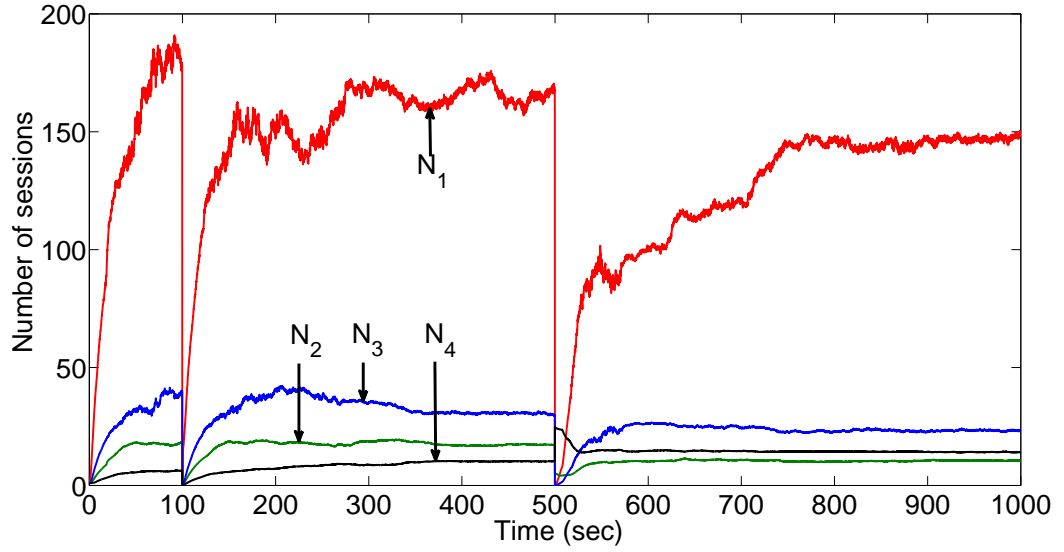
Figure 3.7: Sustainability of the system under the proposed RRM scheme.

under a regulated environment. From the results presented in Fig. 3.6(a), it is seen that the proposed RRM scheme has removed any chance of competitive exclusion of any class of users, rather ensures the coexistence of all of them. For example, at 2000 seconds, 173, 18, 35 and 8 users of class 1, 2, 3 and 4 respectively are receiving services from the network. Furthermore, Fig. 3.6(c) and Fig 3.6(d) identify that at any time, maximum 86% of resources (both TP and BW) is being used for serving the users. Remaining 14% resources can be explained as left as reserve always, which is eventually maintaining the coexistence. Notably, although the scheme has shown its capability in preserving the coexistence, the network is not in an equilibrium state as evident from the continuous changes in the number of users in Fig. 3.6(a). This is also supported by Fig. 3.6(b) as three conditions are always positive, while the other alternates between positive and negative values.

The self-sustainability feature of the proposed RRM scheme in terms of the coexistence of all the user classes is further demonstrated in Fig. 3.7. Here, during the simulation, the network is intentionally disrupted by abruptly changing the number of users at two different instances. At $t = 100$ sec, $\{N_1 = 0, N_2 = 0, N_3 = 0, N_4 = 0\}$, while at $t = 500$ sec, $\{N_1 = 0, N_2 = 5, N_3 = 0, N_4 = 25\}$ are set. As evident from the figure, at both the occasions, the RRM scheme restores the network to a state of coexistence of users from all the four classes.

3.2   Chapter Summary

This chapter have introduced an eco-inspired network designing approach by integrating ecological principles in cellular network operations. Effectiveness of this new notion is demonstrated by proposing a multi-species multi-resource competition based MSMRC RRM mechanism. The proposed RRM scheme has shown its capability in sustainable resource allocation for guaranteeing the coexistence of users with diverse resource requirements under the extreme competitive situations as well as sudden disruptions in network environment. Therefore, by being motivated from this proven rationale of eco-inspired design, the next chapter presents an ecological self-organization based inter-BS cooperation oriented dynamic BS switching scheme for energy efficiency in cellular networks.

Chapter 4

Distributed Dynamic Switching of Base Station: Single Network Scenario

This chapter proposes a distributed inter-BS cooperation assisted load balancing framework, named dynamic switching of BS (DSBS), for improving the energy efficiency of cellular access networks. The proposed cooperation is formulated following the principle of ecological self-organization and thus, ruling out the necessity of any human assistance. The proposed DSBS mechanism exploits the inherent traffic diversity to engage BSs into mutual cooperation for distributing traffic among themselves and thus, the number of active BSs is dynamically adjusted for achieving energy savings. For reducing the number of communications among BSs, a three-step measure is taken by using predicted LF, initializing the algorithm with only the active BSs and differentiating neighboring BSs according to their operating modes for distributing traffic. An EWMA-based technique is proposed for predicting the LF in advance based on the historical data. Various selection schemes for finding the best BSs to distribute traffic are also explored. Furthermore, an analytical formulation for modeling the BS switching dynamics under the proposed DSBS mechanism is also presented. A thorough investigation of the system performance under a wide range of network settings is carried out. The content in this chapter has contributed to [134], [135], [136] and [137].

4.1 System Model

This section presents the core concept of the network operation under the proposed framework. In addition, various schemes for selecting the best neighboring BSs for distributing the traffic of an imminent sleep mode BSs is outlined.

4.1.1 Ecological Self-Organization

Proposed cellular access network model is developed based on the principle of ecological self-organization. A self-organizing system in ecology has many small components, which follows a set of basic local rules. The interactions among the components are executed using only local information, without being aware of the global pattern. This global pattern is an emergent property, which emerges spontaneously in a well-organized structured system starting from an initial random state and without any guidance or control from any external body [24], [110].

The concept of an ecological self-organizing system is presented in Fig. 4.1. Local interaction domain of node N_1 and N_2 are illustrated by the dashed lines. The solid lines between any two nodes represent the interaction between them. For instance, as shown in the figure, node N_1 and its neighboring nodes $N_3 - N_9$ are interacting using their own local rules. Here, N_1 has no knowledge on the behavior of the other nodes beyond its own domain (i.e., N_2 and $N_{10} - N_{14}$). However, neighboring nodes of N_1 are also interacting with their respective neighboring nodes, and thus, N_1 is indirectly influencing the behavior of all the nodes in the system. In turn, local behaviors of all the nodes generate the global behavioral pattern of the system. This kind of interaction is commonly observed among different species, for example, a flock of birds, a group of termites, a school of fishes and a group of bees.

4.1.2 Proposed Energy Efficient Cellular Access Network

Load balancing schemes are traditionally proposed for mitigating the load imbalance problem by redistributing traffic among BSs leading to efficient utilization of radio resources, enhanced coverage for cell edge users and improvement in the overall network throughput [138], [139]. In contrast, a network wide distributed inter-BS cooperation assisted load balancing scheme is employed here for improving the energy efficiency of
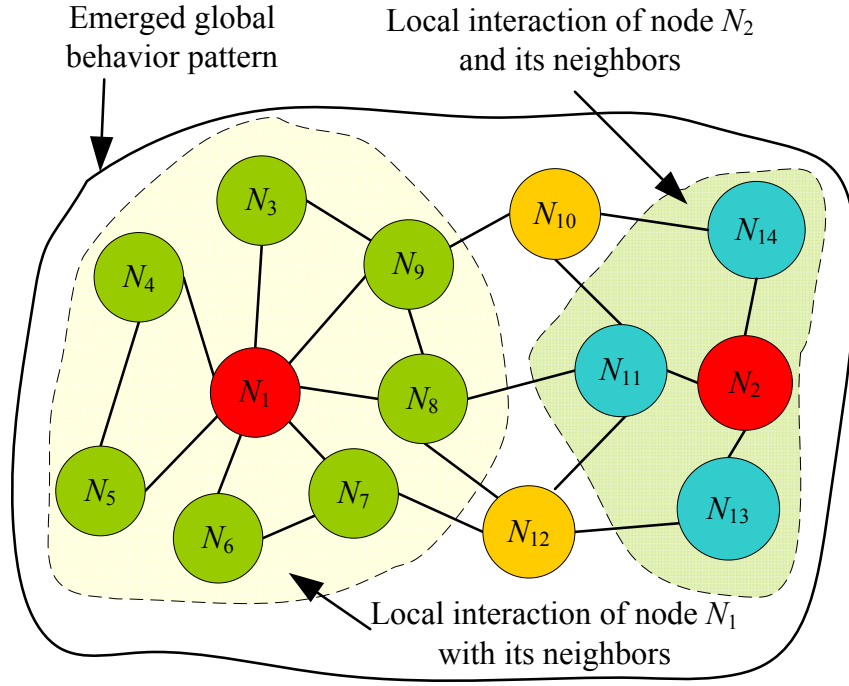
Figure 4.1: Ecological self-organization.

cellular access networks. Concept of the proposed network operation under DSBS is demonstrated in Fig. 4.2. Similar to the ecological system explained in Fig. 4.1, proposed cooperation between a BS and its neighbors is governed by the traffic of itself and its neighbors, QoS requirements and other design parameters. Here, adjacent BSs capable to reach each other (e.g., over X2 interface in LTE) are considered as neighbors. For instance, BS $\mathcal{B}_2$, $\mathcal{B}_4$ and $\mathcal{B}_5$ are serving as acceptors for $\mathcal{B}_1$ by cooperatively sharing its traffic (as shown by the arrows) and thus, allow $\mathcal{B}_1$ to switch into sleep mode for saving energy. At the same time, for supporting the extended coverage zones, transmit power of these acceptors $\mathcal{B}_2$, $\mathcal{B}_4$ and $\mathcal{B}_5$ may need to be adjusted. Here, BS $\mathcal{B}_1$ is totally unaware about the traffic environment of the other BSs except $\mathcal{B}_2, \mathcal{B}_3, \mathcal{B}_4$ and $\mathcal{B}_5$.

It is considered that after the decision of switching to sleep mode by a BS, no new session is accepted by that BS and the active users are forced to handoff to the acceptors. However, before switching to sleep mode, a BS decreases its transmit power over a short interval, which allows smooth handover for its users. On the other hand, during the high-traffic time, upon receiving any wake-up request from other active BSs, sleep mode BSs switch to active mode for reducing the traffic load on others. Through this dynamic switching of BSs, number of active BSs is adaptively adjusted and thus, energy savings is
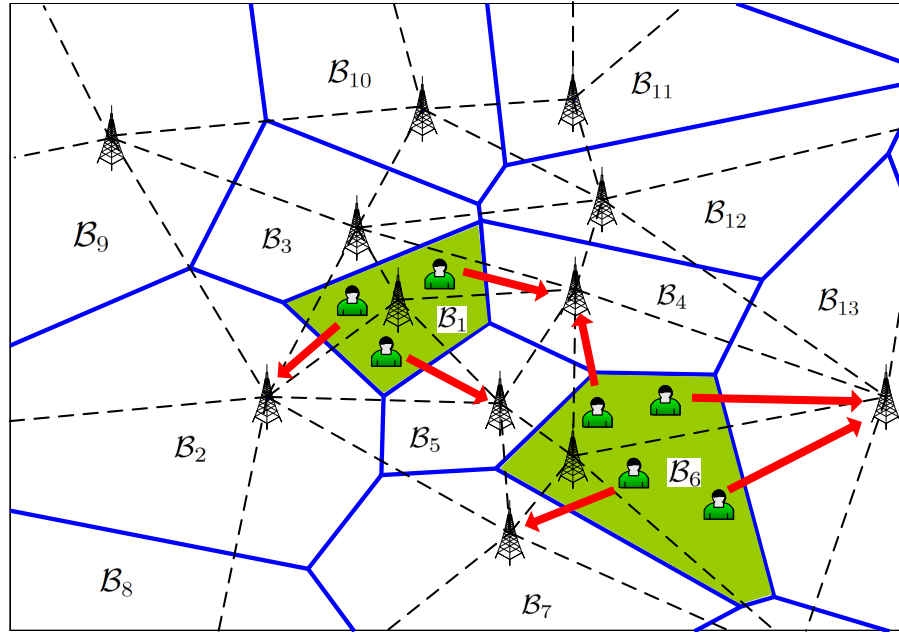
Figure 4.2: Concept of the proposed DSBS mechanism (Shaded BSs $\mathcal{B}_1$ and $\mathcal{B}_6$ are in sleep mode).

achieved. For the entire procedure, no human intervention is essential making the scheme self-organizing in nature.

Each BS is assumed to have a sleep-wake module (SWM) enabling it to switch between active and sleep modes. An active mode BS has the full functionality as of conventional BSs. In contrast, a sleep mode BS neither carries any user traffic nor performs any control signaling. However, the SWM of a sleep mode BS can intercept any wake-up request upon receiving which it can switch to active mode. Energy requirement for a SWM compared to that of an entire BS set is also considered insignificant. Furthermore, adaptive transmit power allocation in downlink for maintaining the required signal strength at UEs is assumed. Hence, user data rates are not affected due to handover from an imminent sleeping BS to a neighbor.

4.1.3 Schemes for Selecting the Best BSs for Traffic Distribution

Candidate space of a BS is the collection of all the possible combinations of its neighbors. For distributing its traffic, a BS has to select the best combination from the candidate space, which can support its traffic as well as maintain QoS within target limits.

Therefore, various selection schemes for deciding on the best combination of neighboring BSs are proposed. Let S_n be a selection scheme. This implies that the candidate space for a BS contains all the candidate combinations of up to n BSs taken from its neighbors. If K_i is the number of neighbors of BS $\mathcal{B}_i$ and the selection scheme is $S_n(n \leq K_i)$, then the total number of candidate combinations for $\mathcal{B}_i$ is equal to $\sum_{c=1}^{n} \binom{K_i}{c}$. For example, in Fig. 4.2, $\mathcal{B}_1$ has four neighbors $\mathcal{B}_2$, $\mathcal{B}_3$, $\mathcal{B}_4$ and $\mathcal{B}_5$. If the selection scheme is S_2, then the candidate space for $\mathcal{B}_1$ contains the following ten combinations of BSs: $\{\mathcal{B}_2\}, \{\mathcal{B}_3\}, \{\mathcal{B}_4\}, \{\mathcal{B}_5\}, \{\mathcal{B}_2, \mathcal{B}_3\}, \{\mathcal{B}_2, \mathcal{B}_4\}, \{\mathcal{B}_2, \mathcal{B}_5\}, \{\mathcal{B}_3, \mathcal{B}_4\}, \{\mathcal{B}_3, \mathcal{B}_5\}$ and $\{\mathcal{B}_4, \mathcal{B}_5\}$.

4.2 Network Description

Different aspects of the system model, namely, the network layout, admission control policy, traffic model, power consumption profile of BSs and the interference model are presented in this section. Network model is presented in the context of OFDMA-based LTE systems, which may also be adopted to WiMAX systems.

4.2.1 Network Layout

The downlink of a multi-cell OFDMA-based cellular network having a set of N BSs $\mathcal{B} = \{\mathcal{B}_1, \mathcal{B}_2, ..., \mathcal{B}_N\}$ is considered here. It is assumed that the sectors in a BS are assigned orthogonal frequency bands, while the same frequency bands are reused among BSs. Furthermore, under the proposed network, it is considered that the available RBs and the transmit power can be shared among the sectors of a BS.

4.2.2 Power Consumption Model of BSs

Let BS $\mathcal{B}_i$ has total N_{TRX} TRX chains. Now, assuming equal maximum operating power $P_{i,Op}$, equal sleep mode power $p_{i,op}^s$ and equal ELPC δ_i for all of these N_{TRX} chains of $\mathcal{B}_i$, total instantaneous operating power of $\mathcal{B}_i$ can be written as below [11], [39]

$$p_{i,op}(t) = \begin{cases} \sum_{j=1}^{N_{TRX}} \left[(1-\delta_i)L_i^{(j)}(t)P_{i,Op} + \delta_i P_{i,Op} \right] & \text{(active mode)} \\ \sum_{j=1}^{N_{TRX}} p_{i,op}^s & \text{(sleep mode)} \end{cases} \qquad (4.1)$$
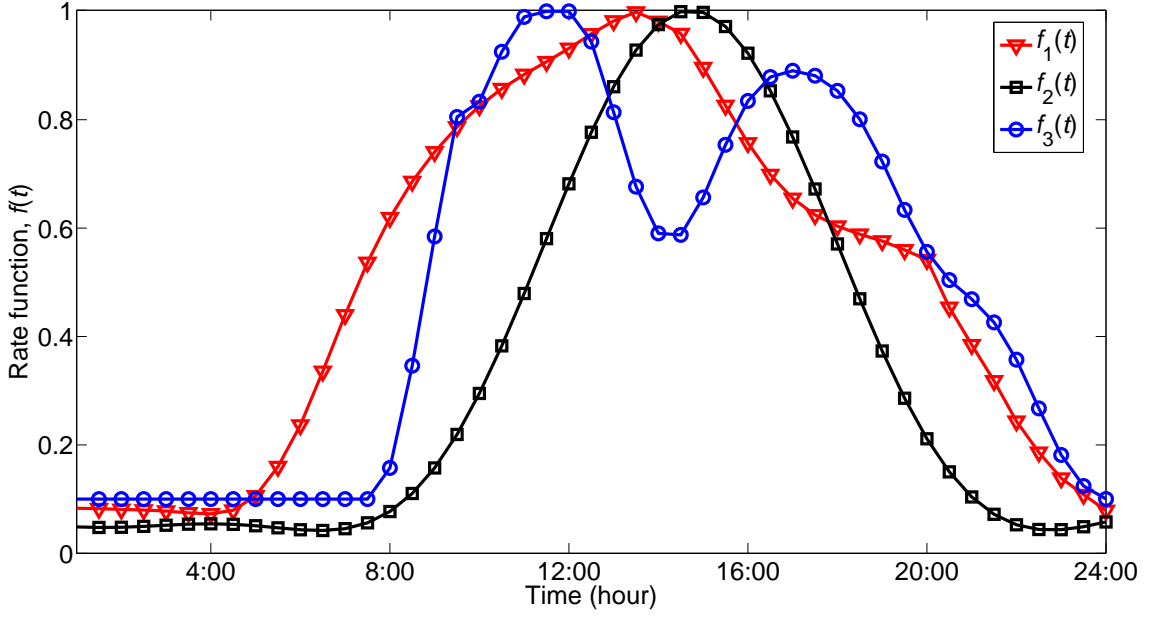
Figure 4.3: Rate functions for generating inhomogeneous traffic.

where $0 \leq L_i^{(j)}(t) \leq 1$ is the LF of the jth TRX chain at time t, while the LF of BS $\mathcal{B}_i$ can be written as $L_i(t) = \frac{1}{N_{TRX}} \sum_{j=1}^{N_{TRX}} L_i^{(j)}$. LF in an LTE system can be defined as the ratio of the number of resource blocks (RBs) in use to the total number of available RBs [140], [141]. On the other hand, $P_{i,Op} = g_i P_{i,Tx} + h_i$. Here, $P_{i,Tx}$ is the maximum transmit power of a chain, and g_i and h_i are constants [11], [52]. In addition, for covering different levels of sleep mode power, it is modeled as $p_{i,op}^s = \delta_i h_i$.

4.2.3 Traffic Model

In cellular networks, traffic generation is naturally inhomogeneous, where the arrival rate varies both in time and space. In this thesis, an inhomogeneous process is modeled by multiplying a homogeneous process with a time-varying rate function $0 \leq f(t) \leq 1$ and a space varying constant $\alpha(l_i) \in [0, 1]$, where $l_i \in \mathbb{R}^2$ is the location of $\mathcal{B}_i$. Therefore, considering a homogeneous traffic generation process with an average rate λ_h, the rate parameter of the inhomogeneous process $\lambda(l_i, t)$ for $\mathcal{B}_i$ can be written as

$$\lambda(l_i, t) = \alpha(l_i) f(t - \theta(l_i)) \lambda_h, \forall i \tag{4.2}$$

For all BSs, same rate function is assumed here. Three typical rate functions are shown in Fig. 4.3, which closely match with many real daily traffic profiles [9], [12], [32], [36],

[48]. Here, $\alpha(l_i)$ can capture the inter-BS traffic level variation. Also, $\theta(l_i) \in [0, 24)$ hours models the peak-time and the off-peak time variation among BSs.

4.2.4 Resource Block Allocation

Received SINR at u^{th} UE located in BS $\mathcal{B}_i$ can be given by

$$\gamma_{i,u} = \frac{P_{i,u}^{Rx}}{\mathcal{I}_{i,u}^{intra} + \mathcal{I}_{i,u}^{inter} + \mathcal{P}_N} \tag{4.3}$$

where $P_{i,u}^{Rx}, \mathcal{I}_{i,u}^{intra}, \mathcal{I}_{i,u}^{inter}$ and $\mathcal{P}_N$ are the received power, intra-cell interference, inter-cell interference and the additive white Gaussian noise (AWGN) power respectively. Now, considering adaptive modulation and coding (AMC), received SINR $\gamma_{i,u}$ can then be mapped to the SE given in bps/Hz [142]

$$\psi_{i,u} = \begin{cases} 0 & \textit{if } \gamma_{i,u} < \gamma_{min} \\ \xi \log_2(1 + \gamma_{i,u}) & \textit{if } \gamma_{min} \leq \gamma_{i,u} < \gamma_{max} \\ \psi_{max} & \textit{if } \gamma_{i,u} \geq \gamma_{max} \end{cases} \tag{4.4}$$

where $0 \leq \xi \leq 1$, γ_{min}, ψ_{max} and γ_{max} are the attenuation factor accounting implementation loss [142], [143], minimum SINR, maximum SE and the SINR at which ψ_{max} is achieved. Then the number of required RBs can be estimated by

$$\beta_{i,u} = \left\lceil \frac{R_{i,u}}{W_{RB}\psi_{i,u}} \right\rceil \tag{4.5}$$

where $R_{i,u}$ is the required data rate in bps, W_{RB} is the bandwidth per RB in Hz (e.g., 180 kHz in LTE), and $\lceil x \rceil$ is the nearest integer equal to or larger than x. On the other hand, if the number of RBs per UE is set fixed, (4.4) - (4.5) can be used for estimating the required SINR for any data rate.

4.2.5 Interference Estimation

Use of orthogonal frequency bands in the sectors results in no intra-cell interference. On the other hand, because of dynamic switching of BSs, inter-cell interference can alter throughout the network, which is extremely challenging to keep track. Therefore, for the sake of computational tractability, with the following reasoning, dynamic inter-cell interference is ignored and considered it as Gaussian-like noise. Firstly, the time scale of dynamic inter-cell interference is much smaller than the session durations [11], [39].

Secondly, interpreting inter-cell interference as Gaussian noise can be considered as the worst possible interference scenario [144], [145], [146]. This assumption is more realistic under the condition when the RBs are randomly assigned to UEs or the information of the assigned RBs to UEs in other BSs is unknown [146]. As explained later in Section 4.2.6, no coordination among BSs for assigning RBs to their respective UEs is considered. Moreover, availability of intelligent frequency planning (e.g., fractional frequency reuse (FFR) and soft frequency reuse (SFR) [138], [147], [148]) and interference randomization [149] schemes, which can be accommodated in the system, leads the assumption to a feasible one [11]. Considering these factors, other energy efficient works also adopted this type of model for inter-cell interference [11], [39], [54], [56], [61]. Nevertheless, the variance (i.e., power) of the Gaussian-like interference depends on the active set of BSs, and their traffic load, transmitted power and antenna gains, as well as the channel model [150].

4.2.6   Session Admission Control

As session admission control (SAC) is not the main focus of this research, for the convenience of analysis, a simple first-come/first-served based SAC is adopted throughput the thesis. Only real-time services with constant bit rate (CBR) requirement are considered. Therefore, it is assumed that the blocked calls are lost immediately and the allocated RBs are left dedicated for the entire session durations. No coordination among BSs for scheduling their UEs to RBs is considered as well.

It is also assumed that all UEs from service class q can be allocated equal number of RBs, i.e, $\beta_{i,u} = \beta_q, \forall i, \forall u$. Thus, when a session request arrives, based on the requested data rate $R_{i,u}$, required RB(s) $\beta_{i,u}$ and the location of UE, (4.4) - (4.5) along with a path loss model are used for estimating the required SINR $\gamma_{i,u}$, transmit power $P_{i,u}^{Tx}$, and the modulation and coding scheme (MCS). If $\beta_{i,u}$ RBs and transmit power equal to $P_{i,u}^{Tx}$ are available in $\mathcal{B}_i$, the session is admitted. Otherwise, the session request is blocked.

It is to be noted that although LTE is envisaged to be an all-Internet protocol (IP) network, circuit switch type SAC is suitable for analyzing the aforementioned assumed service type. Also, this type of SCA is widely practised in literatures for evaluating LTE systems [151]. System performance under guaranteed bit rate (GBR) and best effort services is left for the future works. It can be inferred that energy savings for non-CBR services would

be higher as UE data rates do not need to be strictly maintained like CBR services. In this sense, use of CBR services in evaluating the system performance can be considered as a conservative approach.

4.3 Proposed Distributed DSBS Algorithm

An energy saving load balancing algorithm for swapping traffic and switching BSs by employing distributed inter-BS cooperation is presented here. It is assumed that the algorithm is implemented in each BS and carried out periodically in every T_d time units, where T_d is an adjustable parameter. For avoiding potential simultaneous load distribution by two neighbors, BSs are allowed to distribute traffic one after another. The sequence of BSs in which this distribution is carried out is assumed to be preset by the network controller. Without losing the generality, this sequence is taken as $\mathcal{B}_1, \mathcal{B}_2, ..., \mathcal{B}_N$[1].

For realizing the distributed cooperation, three LF thresholds normalized to unity are defined - lower threshold L_f, upper threshold H_f and acceptance threshold A_f. They are related as $A_f > H_f \geq L_f > 0$. Here, L_f and H_f are equally applicable for each BS and the total network as well, while A_f is only defined for BSs.

Now, let $\widehat{L}(t)$ be the LF for the aggregated traffic of the network at time t. Then, if $\widehat{L}(t) < L_f$ or $\widehat{L}(t) \geq H_f$, load distribution process is triggered by the network controller. Once the process is initiated, each BS in its turn uses the thresholds for distributing its traffic. Thus, at the beginning of $\mathcal{B}_i$'s turn, if it is in active mode, it checks its LF with the thresholds whether $L_i(t) < L_f$ or $L_i(t) \geq L_f$ for starting its load distribution, where $L_i(t)$ is the actual LF of $\mathcal{B}_i$. On the other hand, BS $\mathcal{B}_i$ can accept traffic from other BS(s) as long as its new LF (i.e., own traffic plus shared traffic) $L_i^{(+)}(t) < A_f$ and session blocking is within target limit.

If either of the aforementioned criterion is true for $\mathcal{B}_i$, it sends request to the active mode neighbors for the information of available RBs and the remaining transmit power. It is to be noted that exchange of information among BSs is supported in both 3GPP LTE [31] and WiMAX [107]. On the other hand, information on itself, namely, RBs and

---

[1]This sequence of BSs can also be dynamically evaluated based on different strategies, such as the instantaneous traffic levels, power profiles of BSs or even randomly. It is worth noting that the proposed algorithm is independent of the underlying sequencing strategies and can work well with any of them.

transmit power usage data, locations of own UEs, operating modes of the neighbors, list of neighbors whose traffic is sharing $\mathbf{S}_i = \{S_1, S_2, ..., S_{z_i}\}$, and the candidate space $\mathbf{C}_i = \{\mathbf{C}_{i,1}, \mathbf{C}_{i,2}, ..., \mathbf{C}_{i,M_i}\}$ are required. Here, $\mathbf{C}_{i,n}, (n = 1, 2, ..., M_i)$ is the nth candidate combination of $\mathcal{B}_i$. Using the gathered information, $\mathcal{B}_i$ decides its best neighbors for distributing its traffic as well as the necessary transmission range adjustments for itself and the neighbors for maintaining coverage. The formulated decision message is then propagated among its neighbors. The neighbors send back acknowledgements to $\mathcal{B}_i$ after their execution of the decisions followed by $\mathcal{B}_i$'s own execution. Thereafter, $\mathcal{B}_i$ confirms the network controller of its completion of load distribution procedure. Upon receiving the acknowledgement from $\mathcal{B}_i$, network controller then instructs the next BS $\mathcal{B}_{i+1}$ for starting its load distribution procedure. Thus the algorithm proceeds from one BS to the other. On the other hand, in sleep mode, BS $\mathcal{B}_i$ monitors for any wake-up request from its neighbors and if there is any, it switches to active mode. Fig. 4.4 presents a summary of the coordination between $\mathcal{B}_i$ and its neighbors during its both the operating modes. It is worth mentioning that the accounting of the operating status of BSs as explained above reduces the computations compared to the other schemes in [11], [37], [38], [39], [54], which start their algorithms assuming all BSs are in active mode.

At one instance, BS $\mathcal{B}_i$ can switch to sleep mode, while it can immediately be switched back to active mode by the next BS $\mathcal{B}_{i+1}$ or so on resulting in Ping-Pong effect. For reducing this switching, by utilizing the knowledge of operating modes of the neighbors, $\mathcal{B}_i$ divides its candidate space $\mathbf{C}_i$ into two mutually exclusive subsets: i) $\mathbf{C}_{i,a} = \{\mathbf{X}_{i,1}, \mathbf{X}_{i,2}, ..., \mathbf{X}_{i,q}\} \subseteq \mathbf{C}_i$, where each BS in $\mathbf{X}_{i,k} = \{x_1, x_2, ..., x_{P_k}\}, \forall k \in (1, 2, ..., q)$ is in active mode, and ii) $\mathbf{C}_{i,s} = \{\mathbf{Y}_{i,1}, \mathbf{Y}_{i,2}, ..., \mathbf{Y}_{i,r}\} \subseteq \mathbf{C}_i$, where at least one BS in $\mathbf{Y}_{i,k} = \{y_1, y_2, ..., y_{P_k}\}, \forall k \in (1, 2, ..., r)$ is in sleep mode. BS $\mathcal{B}_i$ has to choose the best combination of neighboring BSs denoted by $\mathbf{B}_i^*$ from either of these two subsets for distributing its traffic. The algorithm then imposes a higher priority on $\mathbf{C}_{i,a}$ over $\mathbf{C}_{i,s}$ for choosing the neighbors to distribute the traffic of $\mathcal{B}_i$, which ensures that the sleep mode BSs are not switched to active mode unless it is absolutely necessary for maintaining QoS. This in turn limits the Ping-Pong effect as well as the computational load. The algorithm treats the low-traffic period and the high-traffic period in different ways, which are presented in detail below.
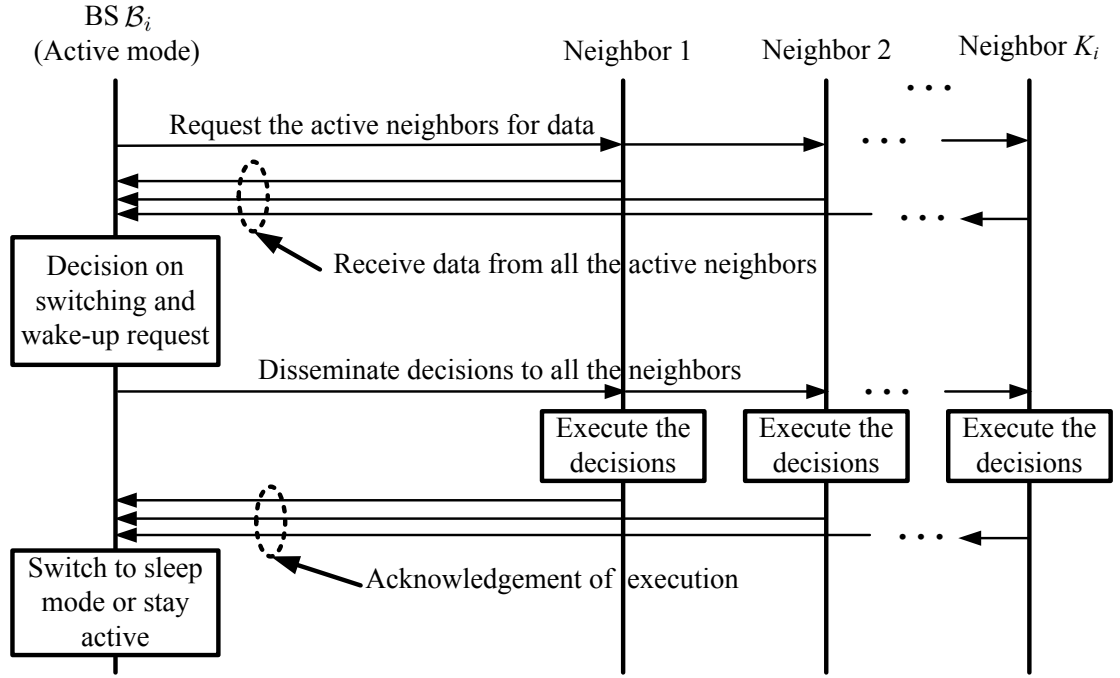
(a) $\mathcal{B}_i$ is in active mode.
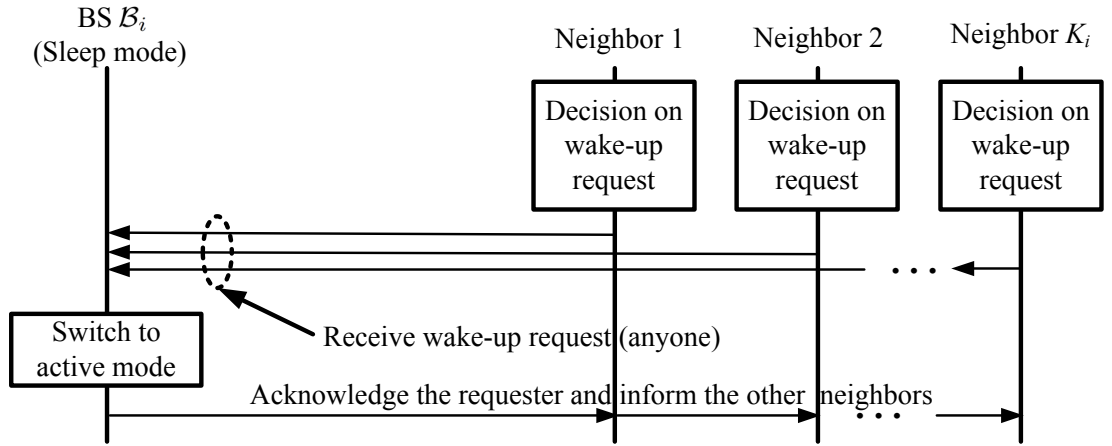
(b) $\mathcal{B}_i$ is in sleep mode.

Figure 4.4: Summary of coordination between BS $\mathcal{B}_i$ and its K_i neighbors.

4.3.1 Low-Traffic Period of $\mathcal{B}_i$

This part of the algorithm is activated when $L_i(t) < L_f$. In this case, $\mathcal{B}_i$ searches for the best combination $\mathbf{B}_i^*$ only in $\mathbf{C}_{i,a}$. This policy of not choosing $\mathbf{B}_i^*$ from $\mathbf{C}_{i,s}$ avoids the unnecessary switching of sleep mode BSs.

i) If $\mathcal{B}_i$ is in active mode and $\mathbf{S}_i = \emptyset$, $\mathcal{B}_i$ looks for the best combination $\mathbf{B}_i^* \in \mathbf{C}_{i,a}$ (as explained in Section 4.3.3) for distributing its full traffic such that it can switch to sleep mode. If $\mathbf{C}_{i,a} = \emptyset$, then $\mathcal{B}_i$ stops searching.

ii) Else, if $\mathcal{B}_i$ is in active mode and $z_i > 0$ (i.e, $\mathbf{S}_i \neq \emptyset$), $\mathcal{B}_i$ switches to sleep mode only when it can redistribute its traffic to all the z_i BSs in $\mathbf{S}_i$. Hence, $\mathcal{B}_i$ searches for the best combination $\mathbf{B}_i^*$ among those $\mathbf{X}_{i,k} \in \mathbf{C}_{i,a}, (1 \leq k \leq q)$ such that $\mathbf{S}_i \subseteq \mathbf{X}_{i,k}$.

If the best combination is found, $\mathcal{B}_i$ distributes its full traffic to BSs in $\mathbf{B}_i^*$ and then, switches to sleep mode. Otherwise, $\mathcal{B}_i$ stays in active mode. Pseudo code for this part of the algorithm is presented in Table 4.1.

Table 4.1: Traffic distribution of $\mathcal{B}_i$ during low-traffic period

---

1:    Initialize $\mathbf{B}_i^* = \emptyset$

2:    **If** $s_i = 1^a$, $L_i(t) < L_f$, $z_i = 0$ and $\mathbf{C}_{i,a} \neq \emptyset$

3:      Find $\mathbf{B}_i^* \subseteq \mathbf{C}_{i,a}$

4:      **Elseif** $s_i = 1$, $L_i < L_f$, $z_i \neq 0$ and $\mathbf{C}_{i,a} \neq \emptyset$

5:        Find $\mathbf{B}_i^* \subseteq \mathbf{C}_{i,a}$ such that $\mathbf{S}_i \subseteq \mathbf{B}_i^*$

6:    **End If**

7:    **If** $\mathbf{B}_i^* \neq \emptyset$

8:      Set $s_i = 0, p_i = 0, L_i(t) = 0$ and $\mathbf{S}_i = \emptyset$

9:      Update $s_m, L_m(t), \mathbf{S}_m$ and the coverage $\forall \mathcal{B}_m \in \mathbf{B}_i^*$

10:   **End If**

---

[a]Here, $s_i(t) \in \{0, 1\}$ is the operating mode indicator of $\mathcal{B}_i$ at time t. Active mode of $\mathcal{B}_i$ is indicated by $s_i(t) = 1$, while $s_i(t) = 0$ if $\mathcal{B}_i$ is in sleep mode.

4.3.2   High-Traffic Period of $\mathcal{B}_i$

High traffic period refers to the scenario when $L_i(t) \geq H_f$. In this case, four alternatives are attempted one-after-another by BS $\mathcal{B}_i$ for distributing its traffic. This priority order allows the sleep mode BSs to stay in sleep mode for longer duration. If none of these four alternatives are met, $\mathcal{B}_i$ continues to operate in the active mode. The alternatives are presented as below:

i) Total traffic distribution among BSs in $\mathbf{B}_i^* \in \mathbf{C}_{i,a}$: The procedure of traffic distribution in this option is same as Section 4.3.1 except the condition that this procedure starts when $L_i(t) \geq H_f$. If this alternative is met, $\mathcal{B}_i$ switches to sleep mode after distributing its traffic to the BSs in $\mathbf{B}_i^*$.

ii) Partial traffic distribution among BSs in $\mathbf{B}_i^* \in \mathbf{C}_{i,a}$: The procedure is similar to Section 4.3.1 with two exceptions. Along with the condition of $L_i(t) \geq H_f$, the other exception is that the best combination has to be capable to share the excess traffic equal to $(L_i(t) - H_f)$. If $\mathbf{B}_i^*$ is found, the excess traffic is distributed to BSs in $\mathbf{B}_i^*$, while $\mathcal{B}_i$ stays in active mode with its new lower traffic. This partial load distribution results in better load balancing.

iii) Total traffic distribution among BSs in $\mathbf{B}_i^* \in \mathbf{C}_{i,s}$: In this option, $\mathcal{B}_i$ looks for the best combination $\mathbf{B}_i^*$ in $\mathbf{C}_{i,s}$. Except this change and the condition of $L_i(t) \geq H_f$, the procedure is same as Section 4.3.1. However, the result is quite different. If $\mathbf{B}_i^*$ is found, $\mathcal{B}_i$ switches to sleep mode and at the same time, sleeping BSs in $\mathbf{B}_i^*$ switch to active mode for supporting its traffic.

iv) Partial traffic distribution among BSs in $\mathbf{B}_i^* \in \mathbf{C}_{i,s}$: This step is same as Section 4.3.2(ii) except that the best combination $\mathbf{B}_i^*$ is determined from $\mathbf{C}_{i,s}$. Thus, $\mathcal{B}_i$ continues to operate with the new lower traffic and at the same time, other sleep mode BSs in $\mathbf{B}_i^*$ wake-up to share its excess traffic.

Pseudo code of this second part of the algorithm is presented in Table 4.2. The complete flow diagram of the algorithm is also presented in Fig. 4.5.

Table 4.2: Traffic distribution of $\mathcal{B}_i$ during high-traffic period

---

1:     Initialize $\mathbf{B}_i^* = \emptyset$

2:    **If** $s_i = 1$, $L_i(t) \geq H_f$, $z_i = 0$ and $\mathbf{C}_{i,a} \neq \emptyset$

3:       Find $\mathbf{B}_i^* \subseteq \mathbf{C}_{i,a}$

4:      **Elseif** $s_i = 1$, $L_i(t) \geq H_f$, $z_i \neq 0$ and $\mathbf{C}_{i,a} \neq \emptyset$

5:        Find $\mathbf{B}_i^* \subseteq \mathbf{C}_{i,a}$ such that $\mathbf{S}_i \subseteq \mathbf{B}_i^*$

6:    **End If**

7:    **If** $\mathbf{B}_i^* \neq \emptyset$

8:       Set $s_i = 0$, $p_i = 0$, $L_i(t) = 0$ and $\mathbf{S}_i = \emptyset$

9:       Update s_m, $L_m(t)$, $\mathbf{S}_m$ and the coverage $\forall \mathcal{B}_m \in \mathbf{B}_i^*$

10:      Stop the algorithm

11:     **Else** Find $\mathbf{B}_i^* \subseteq \mathbf{C}_{i,a}$ for distributing $(L_i(t) - H_f)$

12:        **If** $\mathbf{B}_i^* \neq \emptyset$

13:          Set $L_i(t) = H_f$ and update the coverage of $\mathcal{B}_i$

14:          Update $L_m(t)$ and the coverage $\forall \mathcal{B}_m \in \mathbf{B}_i^*$

15:          Stop the algorithm

16:        **End If**

17:    **End If**

18:    **If** $s_i = 1$, $L_i(t) \geq H_f$, $z_i = 0$ and $\mathbf{C}_{i,s} \neq \emptyset$

19:       Find $\mathbf{B}_i^* \subseteq \mathbf{C}_{i,s}$

20:      **Elseif** $s_i = 1$, $L_i(t) \geq H_f$, $z_i \neq 0$ and $\mathbf{C}_{i,s} \neq \emptyset$

21:        Find $\mathbf{B}_i^* \subseteq \mathbf{C}_{i,s}$ such that $\mathbf{S}_i \subseteq \mathbf{B}_i^*$

22:    **End If**

23:    **If** $\mathbf{B}_i^* \neq \emptyset$

24:       Set $s_i = 0$, $p_i = 0$, $L_i(t) = 0$ and $\mathbf{S}_i = \emptyset$

25:       Update s_m, $L_m(t)$, $\mathbf{S}_m$ and the coverage $\forall \mathcal{B}_m \in \mathbf{B}_i^*$

26:      **Else** Find $\mathbf{B}_i^* \subseteq \mathbf{C}_{i,s}$ for distributing $(L_i(t) - H_f)$

27:        **If** $\mathbf{B}_i^* \neq \emptyset$

28:          Set $L_i(t) = H_f$ and update p_i

29:          Update s_m, $L_m(t)$ and the coverage $\forall \mathcal{B}_m \in \mathbf{B}_i^*$

30:        **End If**

31:    **End If**

Figure 4.5: Flow diagram of the algorithm.

4.3.3 Selecting the Best Combination for Traffic Distribution

As stated above, a BS has to select the best combination of neighbors $\mathbf{B}_i^*$ for distributing its traffic. For the sake of brevity, the procedure of selecting $\mathbf{B}_i^*$ by $\mathcal{B}_i$ for low-traffic period is explained here. Similar concept is used for finding the best combinations for high-traffic period.

For evaluating $\mathbf{B}_i^*$, expected LF (ELF) and the required additional transmit power for all BSs in all the candidate combinations $\mathbf{X}_{i,k} \in \mathbf{C}_{i,a}, \forall k \in (1, 2, ..., q)$ are first calculated. In calculating the ELFs of P_k BSs in $\mathbf{X}_{i,k}$, $\mathcal{B}_i$ first gathers the data of the number of available RBs in these P_k BSs. Then, based on the resource allocation policy, number of

Figure 4.6: Coverage extension of $\mathcal{B}_2$ and $\mathcal{B}_5$ for serving the sleep mode BS $\mathcal{B}_1$.

RBs required in each of the P_k BSs for supporting all the users of $\mathcal{B}_i$ and their own users is calculated, which gives the ELFs. In this calculation, it is assumed that if $\mathcal{B}_i$ could switch to sleep mode, a UE in $\mathcal{B}_i$ would handoff to the nearest BS in $\mathbf{X}_{i,k}$. Feedback from UEs to the serving BSs is considered for receiving their location data. Similarly, required additional transmit power for supporting the UEs of $\mathcal{B}_i$ is calculated.

Then, the *minimax* value among these ELFs is determined, which is equal to the minimum of the maximum values taken from each combination in $\mathbf{C}_{i,a}$. The combination corresponding to this *minimax* value is the probable $\mathbf{B}_i^*$ and let us denote it as $\widetilde{\mathbf{B}}_i^*$. Next, the expected session blocking probability in all BSs in $\widetilde{\mathbf{B}}_i^*$ is evaluated. Now, if *minimax* $< A_f$, session blocking is within the target and all BSs of $\widetilde{\mathbf{B}}_i^*$ can provide the respective required additional transmit power, then $\mathbf{B}_i^* = \widetilde{\mathbf{B}}_i^*$ for $\mathcal{B}_i$. Use of *minimax* value implements traffic distribution to the least loaded BS combination and helps to reduce session blocking.

4.3.4 Coverage for the Sleep Mode BSs

As stated in the algorithm section, for providing the full coverage for a sleep mode BS $\mathcal{B}_i$, necessary adjustments in the transmission range of all BSs in $\mathbf{B}_i^*$ are made. One simple example of coverage extension by the neighboring BSs under hexagonal cell layout is demonstrated in Fig. 4.6. Here, $\mathcal{B}_2$ and $\mathcal{B}_5$ are instructed by $\mathcal{B}_1$ for increasing their

transmit ranges in the specified directions by the specified amounts. In cellular networks, this coverage extension can be done by adjusting the pilot channel (e.g., physical down-link control channel (PDCCH) in LTE [152]) signal power. Advanced beam-forming techniques [33], [75], or any other suitable technique can also be used for this purpose. In addition, an increase in the maximum transmit power rating of BSs might also be required. After the completion of this adjustment, $\mathcal{B}_1$ can then be switched to sleep mode.

4.3.5 On the Selection of Thresholds

Proposed cooperation is governed by the preset aforementioned LF thresholds, which are network specific. These thresholds can be set equal for all BSs or varied among them. On the other hand, depending on the network traffic growth trends, they may need to be updated on a periodic basis. For instance, in a network where traffic load difference be-tween consecutive days is relatively small, less frequent updating would be required, and vice versa. In this chapter, the methodology for selecting and updating these thresholds is not specified and left for future works. Instead, the system performance under various settings of these thresholds has been thoroughly analyzed. Nevertheless, for a given his-torical traffic load database, an offline optimization technique can be used by the network controller for estimating their values corresponding to the maximum energy savings un-der the proposed algorithm. Once the optimal values of L_f, H_f and A_f are found, each BS has to be instructed accordingly by the network controller.

4.4 EWMA-based LF Prediction

As explained in the algorithm, aggregated network LF is used in triggering the traffic dis-tribution operation for network reconfiguration. Either the instantaneous or a predicted LF can be used for this purpose. Let N_d be the number of instances per day at which traffic distribution is planned to be attempted. Use of instantaneous LF implies the ne-cessity of gathering network parameters and attempting to distribute traffic at all these N_d instances, which imposes a lot of signaling and computational burden. In contrast, from the predicted envelope, it is possible to eliminate a subset of N_d instances *a priori* at which reconfiguring procedure is not feasible. Thus, unnecessary attempts of network reconfiguring procedure can be avoided resulting in reduced number of computations. It is to be noted that the estimated LF is used for deciding whether to initiate the traffic

distribution event. Whereas, the actual traffic environment, for example, the data rate and the locations of the active UEs, is used for the traffic distribution. In light of this, an EWMA-based technique for predicting the LF envelope of an entire day in advance from the historical LF data is proposed here. Since the traffic level differs much from weekdays to weekends, weekday (weekend) LF is estimated from the weekday (weekend) data.

Let the target is to estimate the LF for $(D+1)^{th}$ day from the given $D \times N_d$ LF matrix $\mathbf{L} = [\mathbf{L}_1; \mathbf{L}_2; ...; \mathbf{L}_D]$, where $\mathbf{L}_n, n = 1, 2, ..., D$ is a row vector containing N_d samples of LFs taken over n^{th} day. A robust version of local regression technique using weighted linear least squares is then applied on each day LF data, which produces a smooth version of the LF data by reducing abruptness [153]. Modified LF matrix can be written as $\widetilde{\mathbf{L}} = [max(\mathbf{L}_1, Sm(\mathbf{L}_1)); max(\mathbf{L}_2, Sm(\mathbf{L}_2)); ...; max(\mathbf{L}_D, Sm(\mathbf{L}_D))] = [\widetilde{\mathbf{L}}_1; \widetilde{\mathbf{L}}_2; ...; \widetilde{\mathbf{L}}_D]$. Here, $Sm(.)$ does the smoothing operation and $max(\mathbf{L}_n, Sm(\mathbf{L}_n))$ takes the sample-wise maximum between $\mathbf{L}_n$ and $Sm(\mathbf{L}_n)$, which increases the reliability of not underestimating the envelope. Overestimation can decrease the potential energy savings. However, it is a conservative approach for suppressing the potential false triggering of load distribution procedure at infeasible instances. Then, the moving average $\overline{\mathbf{L}}_{D+1}$, the standard deviation $\overline{\sigma}_{D+1}$ and the predicted LF $\widehat{\mathbf{L}}_{D+1}$ for $(D+1)^{th}$ day are given by [12], [154]

$$\overline{\mathbf{L}}_{D+1} = (1 - \beta)\overline{\mathbf{L}}_D + \beta\widetilde{\mathbf{L}}_D \tag{4.6}$$

$$\overline{\sigma}_{D+1} = (1 - \varrho)\overline{\sigma}_D + \varrho|\overline{\mathbf{L}}_D - \widetilde{\mathbf{L}}_D| \tag{4.7}$$

$$\widehat{\mathbf{L}}_{D+1} = \overline{\mathbf{L}}_{D+1} + \zeta\overline{\sigma}_{D+1} \tag{4.8}$$

where $0 < \beta, \varrho < 1$ are smoothing constants, which determines the level of smoothing. If the smoothing constant is small (i.e., close to 0), more weight is given to the observations from the more distant past and thus, a high level of smoothing is achieved. On the other hand, for a higher value (i.e., close to 1), more weight is given to the more recent observations, which reduces the level of smoothing. It has been found that the best values of smoothing constant lies between 0.2 and 0.3 [154]. For the proposed systems in this thesis, $\beta = \varrho = 0.2$ are used, which is determined from a number of simulations. Here, ζ is another constant usually taken equal to 3, which is also known as the three-sigma rule [154]. At the end of each day, LF database used for estimation is updated by appending the actual LF data of the day and deleting that of the oldest day.

4.5   Performance Parameters

This section summarizes the performance metrics of the proposed system, namely, the percentage of sleep mode BSs, net energy savings, number of switching in each BS and the network capacity utilization.

4.5.1   Percentage of Sleep Mode BSs

Percentage of sleep mode BSs at time t and the average percentage of sleep mode BSs over time T denoted by $P_{s,N}(t)$ and P_s respectively can be given by

$$P_{s,N}(t) = \left[\frac{1}{N} \sum_{i=1}^{N} \{1 - s_i(t)\} \right] \times 100\% \tag{4.9}$$

$$P_s = \left[\frac{1}{T} \int_0^T P_{s,N}(t)dt \right] \times 100\% \tag{4.10}$$

These expressions also represent the probabilities of a BS to switch into sleep mode.

4.5.2   Net Energy Savings

Let E_i^{Org} and E_i^{Pro} be the total energy consumption over time T in $\mathcal{B}_i$ in the original network (i.e., always active) and the proposed energy saving network respectively, which can be written as below

$$E_i^{Org} = \int_0^T \sum_{j=1}^{N_{TRX}} \left[(1 - \delta_i) L_i^{(j)}(t) P_{i,Op} + \delta_i P_{i,Op} \right] dt, \forall i \tag{4.11}$$

$$E_i^{Pro} = \int_0^T \sum_{j=1}^{N_{TRX}} \left\{ s_i(t) \left[(1 - \delta_i) L_i^{j+}(t) P_{i,Op}^{(+)} + \delta_i P_{i,Op}^{(+)} \right] + \left[(1 - s_i(t)) p_{i,op}^s \right] \right\} dt, \forall i \tag{4.12}$$

In (4.12), $L_i^{j+}(t)$ is the new LF of the jth TRX chain of $\mathcal{B}_i$ and $P_{i,Op}^{(+)}(t)$ is the new maximum operating power after the coverage extension of $\mathcal{B}_i$. Thus the average net energy savings per BS over time T can be written as

$$E_s = \left[\frac{\sum_{i=1}^{N} E_i^{Org} - \sum_{i=1}^{N} E_i^{Pro}}{\sum_{i=1}^{N} E_i^{Org}} \right] \times 100\% \tag{4.13}$$

4.5.3 Number of Switching

Let N_T be the total number of instances over time T per BS at which the traffic distribution algorithm is executed by $\mathcal{B}_i$. Average percentage of instances at which switching occurs can then be written as

$$\mathcal{N}_{Sw} = \frac{1}{NN_T} \sum_{i=1}^{N} \left[\sum_{k=1}^{N_T} XOR\left(s_i(k), s_i(k-1)\right) \right] \times 100\%, s_i(k) = 1 \text{ for } k \leq 0, \forall i \tag{4.14}$$

4.5.4 Capacity Utilization Gain

The parameter capacity utilization gain (CUG) is defined for quantifying the gain in network capacity (e.g., number of RBs in LTE) utilization by the proposed system. First, capacity utilization efficiency (CUE) for a network over time T is defined as below

$$CUE = \frac{1}{N} \sum_{i=1}^{N} \frac{\int_{T_{i,a}} L_i(t)dt}{T_{i,a}} \tag{4.15}$$

where $T_{i,a}$ is the total active time of $\mathcal{B}_i$. Thus, $T_{i,a} = T$ and $T_{i,a} \leq T$ under the original and proposed networks respectively. CUG can then be defined as

$$CUG = \frac{CUE_{Pro}}{CUE_{Org}} \times 100\% \tag{4.16}$$

where CUE_{Org} and CUE_{Pro} are the CUEs under the original and the proposed networks respectively. For LTE, this parameter CUG is equivalent to the ratio of the number of utilized RBs per BS under the proposed network to that of the original network.

4.6 Analytical Modeling

In this section, an analytical model for evaluating the probabilities of BSs to switch into sleep mode under the proposed network operation is formulated. In the proposed algorithm, decision on the operating modes of BSs in the next instance depends only on the current operating modes of all BSs and their current traffic. Therefore, the proposed BS switching process can be modeled as a Markov process. Markov modeling also greatly simplifies the modeling of system behavior as well requires less computational power.

Now, a state of the network at any time t is one of the possible combinations of the operating modes of all BSs denoted by $\mathbb{S}(t) = (s_1(t), s_2(t), ..., s_N(t))$. Thus, the total number

of states is 2^N growing exponentially with N, which makes it challenging for solving using Markov chains. For reducing the complexity, following the proposed algorithm, a heuristically guided formulation is presented here. For the convenience of presentation, the time index from some of the following equations is omitted and brought back later.

Let S_{P_i}, $N_i = \{\mathcal{B}_{i,1}, \mathcal{B}_{i,2}, ..., \mathcal{B}_{i,K_i}\} \subset \mathcal{B}$ and $\mathbf{C}_{i,n} = \{C_{i,n}^{(1)}, C_{i,n}^{(2)}, ..., C_{i,n}^{(P_n)}\} \in \mathbf{C}_i$ be the selection scheme, set of neighbors and the nth candidate combination of $\mathcal{B}_i$ respectively. Here, $C_{i,n}^{(k)} \in N_i$ and $P_n \leq P_i, \forall i, \forall n, \forall k$.

Let us define the following two events:
$E_{i,n} = \{\mathcal{B}_i$ distributes traffic to $\mathbf{C}_{i,n}$ and switches into sleep mode$\}, \forall i, \forall n$, and
$A_{i,n}^{(k)} = \{C_{i,n}^{(k)}$ is in active mode$\}, \forall i, \forall n, \forall k$

Assuming that $\mathcal{B}_i$ is not sharing the traffic of any of its neighbors, probability of occurring event $E_{i,n}(n = 1, 2, ..., M_i)$ at time t can be written as below

$$P\{E_{i,n}\} = \left[P\{L_i < L_f\} \prod_{k=1}^{P_n} P^\Delta \left\{A_{i,n}^{(k)}\right\} + P\{L_i \geq H_f\} \right]$$
$$\times \prod_{k=1}^{P_n} \left[P\left\{A_f - L_{i,n}^{(k)} > \psi_{i,k} L_i\right\} P\left\{P_{i,n}^{(k)} \leq P_b^{th}\right\} \right] \quad (4.17)$$

where $L_{i,n}^{(k)}$ and $P_{i,n}^{(k)}$ are the actual LF and the session blocking in $C_{i,n}^{(k)}$ respectively; $\psi_{i,k}$ is the fraction of L_i to be distributed to $C_{i,n}^{(k)}$ and thus, $\sum_{k=1}^{P_n} \psi_{i,k} = 1$; $P^\Delta \left\{A_{i,n}^{(k)}\right\}$ is the probability that $C_{i,n}^{(k)}$ was active at the last instance, while $P^\Delta \left\{A_{i,n}^{(k)}\right\} = 1, \forall t \leq 0, \forall i, \forall n, \forall k$. If there is no candidate combination for $\mathcal{B}_i$, $P\{E_{i,n}\} = 0$. Also, P_b^{th} is the target session blocking. Simple manipulation of the indices of the equations derived in Appendix A will result in the probabilities in (4.17).

However, if $\mathcal{B}_i$ has been supporting the traffic of any of its neighboring BSs other than those in $\mathbf{C}_{i,n}$, as discussed in Section 4.3, the algorithm does not allow $\mathcal{B}_i$ to switch into sleep mode by distributing its current traffic to this n^{th} combination. For accounting this, the probability that $\mathcal{B}_i$ is not the acceptor for any of the remaining $(K_i - P_n)$ BSs is calculated as below

$$P\{X_n\} = \prod_{\substack{k=1 \\ \mathcal{B}_{i,k} \notin \mathbf{C}_{i,n}}}^{K_i} \left(1 - F_{i,k} P^\Delta \{s_{i,k}\}\right) \quad (4.18)$$

where $P^\Delta \{s_{i,k}\}$ is the probability that $\mathcal{B}_{i,k}$ was in the sleep mode at the last instance, and

$$F_{i,k} = \begin{cases} \frac{G_{i,k}}{M_{i,k}} & \text{if } M_{i,k} \neq 0 \\ 0 & \text{if } M_{i,k} = 0 \end{cases} \tag{4.19}$$

where $M_{i,k}$ is the number of candidate combinations for $\mathcal{B}_{i,k}$ and $G_{i,k} \leq M_{i,k}$ is the number of these $M_{i,k}$ combinations containing $\mathcal{B}_{i,k}$. Therefore, the modified $P_i \{E_{i,n}\}$ can be given as

$$\widetilde{P} \{E_{i,n}\} = P \{E_{i,n}\} \times P \{X_n\} \tag{4.20}$$

Since the events of distributing traffic of $\mathcal{B}_i$ to one of the M_i candidate combinations are independent, probability of switching of $\mathcal{B}_i$ into sleep mode at time t can be written as

$$P_i(t) = \widetilde{P} \left\{ \bigcup_{n=1}^{M_i} E_{i,n} \right\} = \sum_{d=1}^{M_i} (-1)^{d+1} \sum_{\substack{n_1,n_2,...,n_d: \\ 1 \leq n_1 \leq n_2 .... \leq n_d \leq M_i}} \widetilde{P} \{E_{i,n_1}\} \widetilde{P} \{E_{i,n_2}\} ... \widetilde{P} \{E_{i,n_d}\} \tag{4.21}$$

Averaging over all N BSs, we can write the probability that a BS switches to sleep mode at time t as below

$$P_{s,N}^{ana}(t) = \left[\frac{1}{N} \sum_{i=1}^{N} P_i(t) \right] \times 100\% \tag{4.22}$$

Average sleeping probability P_s^{ana} per BS over any duration T can then be written as

$$P_s^{ana} = \left[\frac{1}{T} \int_0^T P_{s,N}^{ana}(t)dt \right] \times 100\% \tag{4.23}$$

4.7 Results and Discussions

4.7.1 Simulation Setup

Although the proposed scheme is equally applicable for any cell layout, with the aim to create a benchmark, a hexagonal cell layout is chosen for the evaluation of the proposed network model. Simulated network serves a geographical area covered by three-sector 50 macro cells having an inter-site distance equal to $\sqrt{3} \times 500$ m and uniformly distributed UEs. Carrier frequency = 2 GHz, channel bandwidth = 5 MHz per sector (i.e., 25 RBs) and BS transmit power = 43 dBm per sector are assumed. WINNER+ non-line-of-sight

(NLOS) urban macro-cell channel model is adopted, which gives a path loss $P_L = 138.4 + 35.74 log_{10}(d)$ dB with antenna height $h_{BS} = 25$ m and $h_{UE} = 1.5$ m for BS and UE respectively [155]. Shadow fading standard deviation = 8 dB, penetration loss = 10 dB [156] and the AWGN power density = -174 dBm/Hz are used. AMC code set parameters $\{\xi = 0.75, \gamma_{min} = -6.5$ dB, $\gamma_{max} = 19$ dB, $\phi_{max} = 4.8$ bps/Hz$\}$, noise figure (NF) = 9 dB (5 dB) for UE (BS) and BS antenna gain including feeder loss = 15 dBi are chosen in reference to the 3GPP LTE suggestions [142].

Three classes of real-time CBR services having data rates equal to 64 kbps, 384 kbps and 512 kbps including packet headers and payloads are considered. New sessions arrive following Poisson process. It is assumed that only one RB can be allocated to a UE from any class. Thus, the required SINR for the three classes, calculated using (4.4) - (4.5), are found equal to -4.1 dB, 7.9 dB and 11.1 dB respectively. LTE Frequency division duplexing (FDD) frame structure is considered with the assumption that one transmission time interval (TTI) of 1 ms carries exactly one packet. Furthermore, for a fair comparison and without losing the generality, constant session duration equal to 3 minutes are assumed for all the classes. Target session blocking is set equal to 1%. For generating the time-inhomogeneous traffic, normalized rate functions $f_1(t)$ and $f_2(t)$ as shown in Fig. 4.3 are used. Only temporal variation (i.e., $\theta(l_i) = 0, \forall i$) with equal peak traffic for all BSs (i.e., $\alpha(l_i) = \alpha, \forall i$) is considered. Session arrival rate parameter λ_h = 5.375 sessions/min for each sector is chosen such that the peak-time session blocking in the original network becomes equal to 1%. On the other hand, without losing the generality, BS power profile parameters $\delta_i = \delta$, $g_i = g$, $h_i = h$ and $p_{i,op}^s = p_{op}^s$, $\forall i$ are assumed. Two settings for BS power profile are considered. They are: Set1: $g = 21.45$, h = 354.44 [52], and Set2: $g = 7.8$, $h = 605$ [55]. These parameters provide the maximum operating power of a sector. Moreover, due to the utilization of the inbuilt signalling facilities in the networks and the provision of inter-BS optical backhaul link having a very low energy requirement ($\sim$1pJ/bit/m [157]), signaling energy cost compared to that of the total network is assumed negligible.

4.7.2 Sleep Mode BSs and RB Utilization

Figs. 4.7 and 4.8 present the average percentage of sleep mode BSs per day P_s (i.e., probability of sleeping of BSs) with the thresholds L_f and A_f respectively. Simulation parameters are also shown in the figures. As seen, P_s has an increasing trend with the
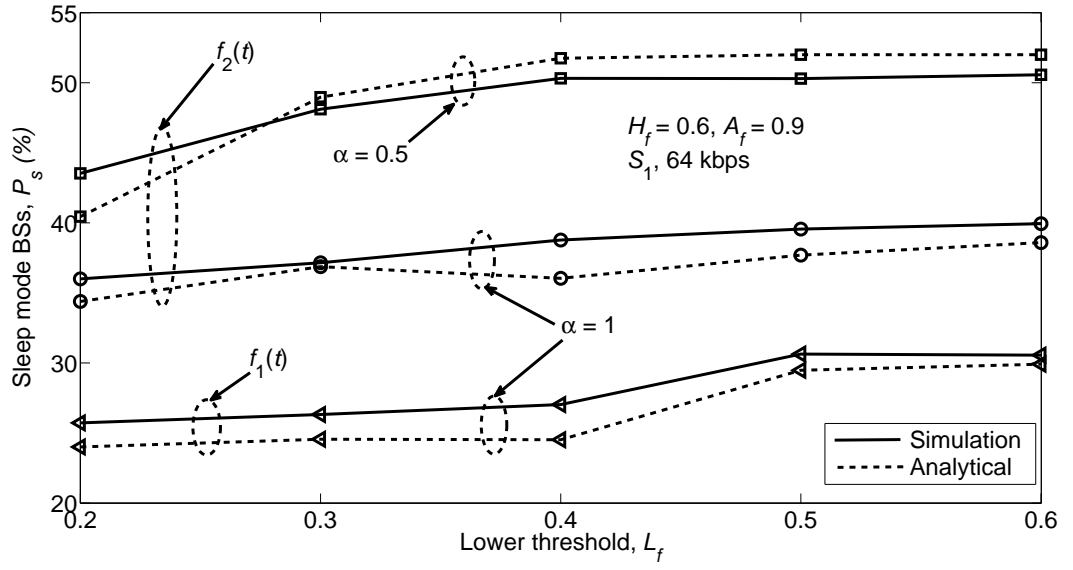
Figure 4.7: Percentage of sleep mode BSs per day with L_f.
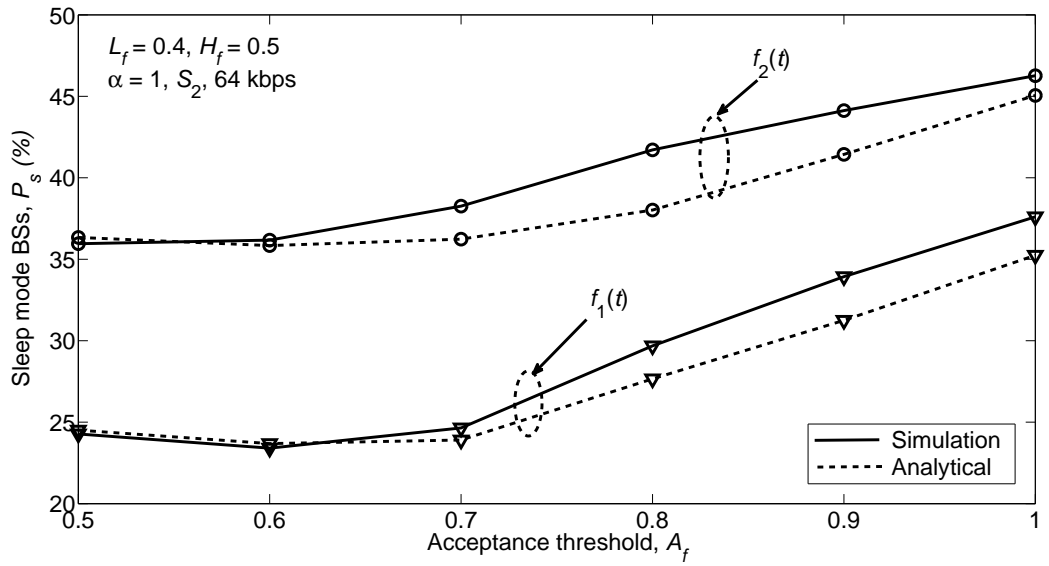
Figure 4.8: Percentage of sleep mode BSs per day with A_f.
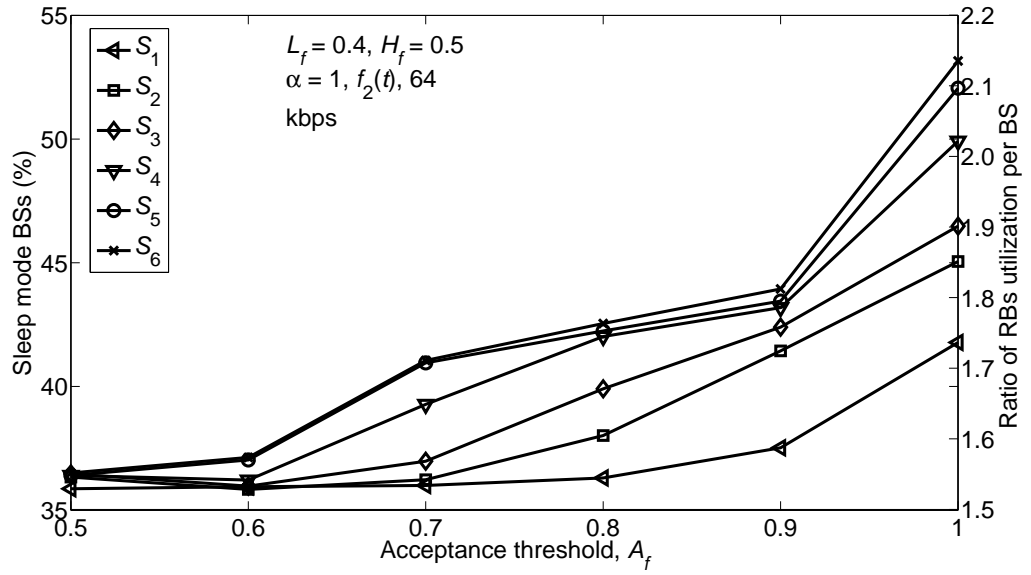
Figure 4.9: Percentage of sleep mode BSs and the ratio of RBs utilization per day with the selection schemes.

increase of both L_f and A_f. For a higher value of L_f, higher number of BSs has the probability to have LF less than L_f. Consequently, higher number of BSs has the chance of distributing their traffic to other BSs and switching to sleep mode. On the other hand, higher value of A_f implies that BSs are capable to accept more traffic from the others. Therefore, higher number of BSs can switch to sleep mode.

Impact of the rate functions is also evident from both the figures. Rate function $f_2(t)$ corresponds to lower traffic generation than that with $f_1(t)$. Therefore, in a network with $f_2(t)$, higher percentage of BSs can switch to sleep mode than that in a network with $f_1(t)$. In addition, impact of traffic parameter α is also included in Fig. 4.7. A value of $\alpha < 1$ refers to a lower level of loading of BSs than their available capacities. Therefore, a higher number of BS can switch to sleep mode by offloading their traffic to the neighboring BSs. Moreover, for all the cases, analytical results are quite close to the simulation results, which validate the simulation model.

Impact of the candidate selection schemes for distributing traffic is illustrated in Fig. 4.9. From the figure, it is observed that as we move from S_1 to S_6, higher percentage of BSs can switch into sleep mode. For example, at $A_f = 1$, on an average 42% BSs switch into sleep mode under S_1 scheme, while the figure is much higher in S_6 scheme amounting

to 53%. For S_1, only 1-BS combinations from the neighbors are selected for distributing traffic. On the other hand, all the possible combinations of neighbors are considered in S_6 scheme causing a higher P_s. Fig. 4.9 can also be explained as a tradeoff between the number of computations and P_s. For example, due to the inclusion of all the possible combinations, S_6 scheme involves the highest number of computations. At the same time, under S_6, number of sleep mode BSs is the highest under S_6.

Notably, in both the Figs. 4.8 and 4.9, the lines are almost flat in the lower range of A_f (up to $A_f = 0.6 \sim 0.7$) and thereafter, they become steeper. This is due to the settings of the simulation parameters, mainly because of $H_f = 0.5$. Due to this setting, in the lower range of A_f, probability of traffic distribution during high traffic period (i.e., LF $\geq H_f$) is less likely. Consequently, the sleep mode BSs in the lower range of A_f is mainly contributed by the traffic distribution events happening when LF $< L_f$. On the other hand, as A_f increases to higher values, probability of occurring traffic distribution during LF $\geq H_f$ also increases. Thus, the sleep mode BSs presented in the figures over the higher range of A_f is due to the traffic distribution during LF $< L_f$ as well as LF $\geq H_f$ resulting in steeper lines.

Ratio of the utilized RBs per BS in the proposed network to that of the original network also follows the same trends of P_s and its scale is shown on the right hand side of Fig. 4.9. Under the proposed network, fewer BSs serve the same number of UEs in the original network, and hence, RB utilization per BS has increased by a factor up to over two as evident from the figure.

4.7.3 Energy Saving Performance

Average daily energy savings of a network corresponding to $f_2(t)$ and S_6 scheme with various data rates is presented in Fig. 4.10. Similar to P_s, energy savings per day is also found to have an increasing trend with A_f. Furthermore, increase of energy savings with the decrease of data rates is evident from the figure. Since a higher data rate requires higher SINR, i.e., higher transmit power, additional power requirement increases with the increase of UE data rates resulting in reduced energy savings. A case where 60% UEs from 384 kbps and the other 40% requiring 512 kbps denoted as 'Mixed' is also considered. Energy savings line for the 'Mixed' case lies between those of 384 kbps and 512 kbps.
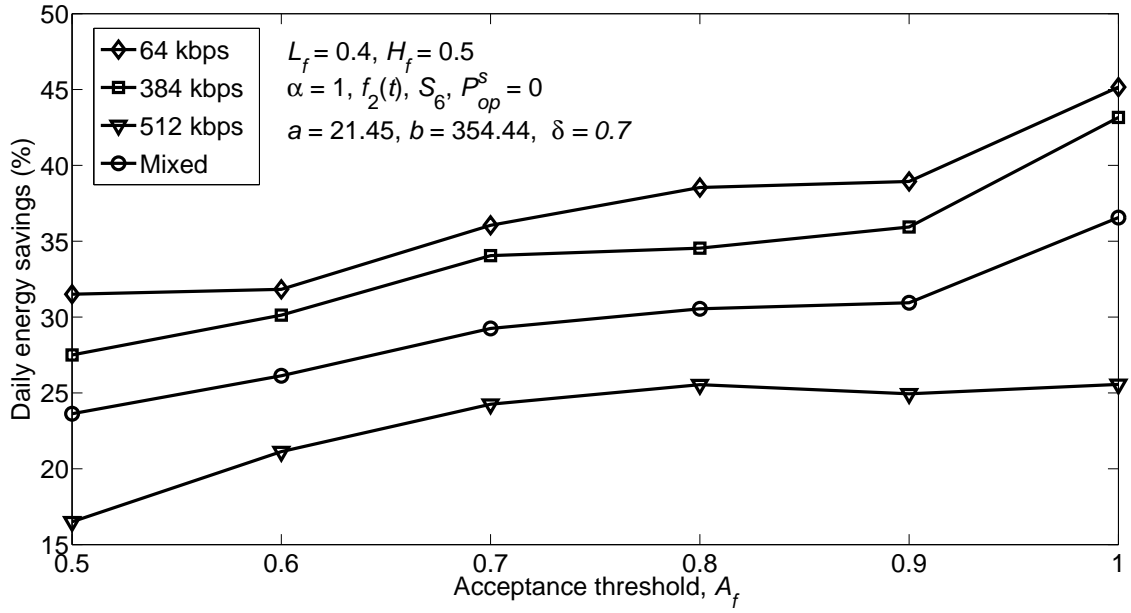
Figure 4.10: Daily energy savings for various data rates.
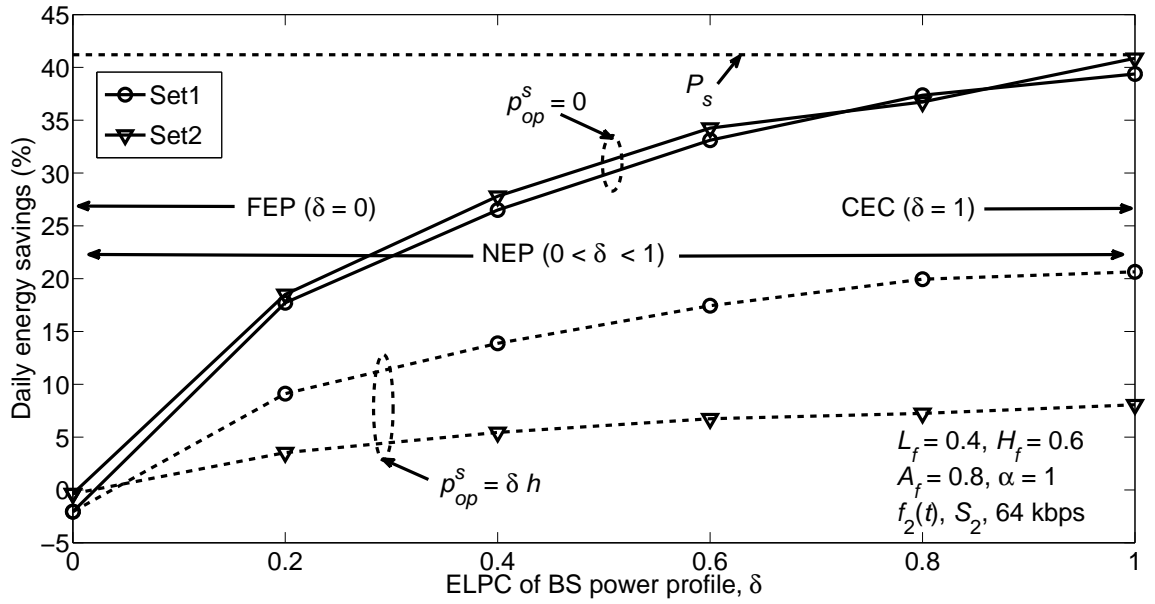
Figure 4.11: Impact of BS power profile parameter δ and sleep mode power on daily energy savings.
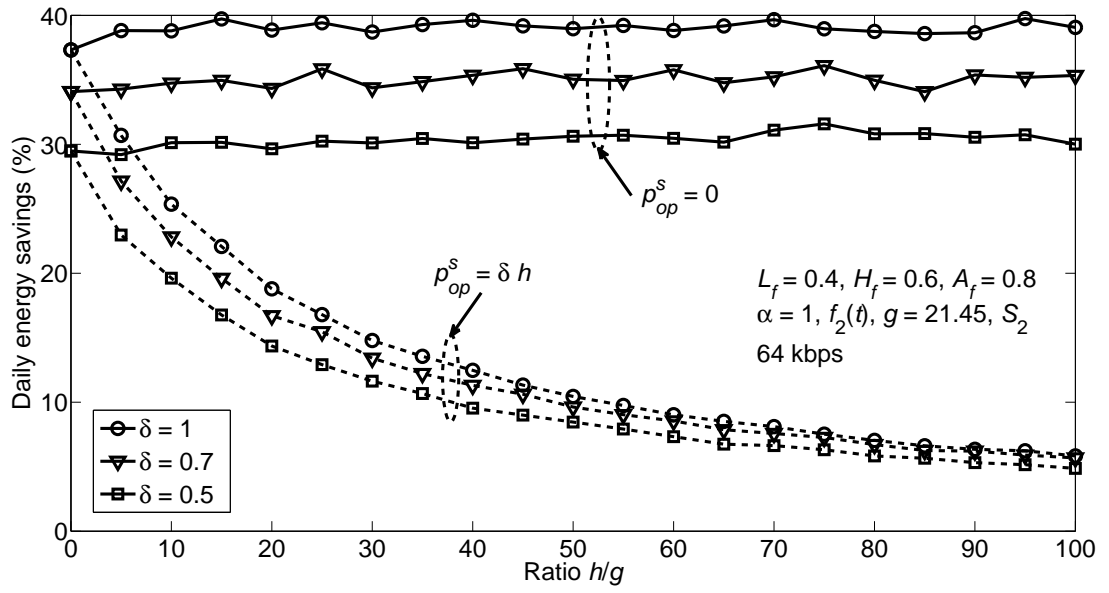
Figure 4.12: Impact of BS power profile parameters g and h on the daily energy savings.

Figs. 4.11 and 4.12 demonstrate the dependency of energy savings on the BS power profile parameters. Since ELPC $\delta = 1$ corresponds to the CEC BSs, which require constant power irrespective of traffic level leading to the highest wastage of energy, proposed system can extract the highest energy savings as illustrated in Fig. 4.11. Then, as δ moves toward zero, BS hardware tends to be more and more energy proportional resulting in diminishing amount of energy wastage and energy savings as well. When $\delta = 0$, BSs are of FEP type consuming power proportional to LF with no wastage and correspondingly, no additional energy savings is possible from switching BSs. Instead, the system may consume extra power because of additional transmit power. In addition, non-zero sleep mode power (i.e., $p_{op}^s > 0$) can drastically reduce the energy savings as evident from the figure. It is also identified that Set1 and Set2 achieve approximately equal savings for $p_{op}^s = 0$, while the savings significantly differs for $p_{op}^s = \delta h$. Since $h = 605$ for Set2, which is much higher than that of Set1 ($h = 354.44$), BSs of Set1 consumes much less power in sleep mode leading to higher savings than that of Set2.

On the other hand, impact of the ratio h/g is demonstrated in Fig. 4.12. The ratio h/g is varied by varying h and keeping g equal to 21.45. As shown, for $p_{op}^s = 0$, the ratio h/g has almost no impact on the energy savings of the network. However, for the case of $p_{op}^s > 0$, h/g has significant impact on the savings. As h/g, i.e., h continues to increase, an increasing amount of power consumption occurs in the sleep mode of BSs, which

significantly offsets the network energy savings.

4.7.4   Switching in BSs
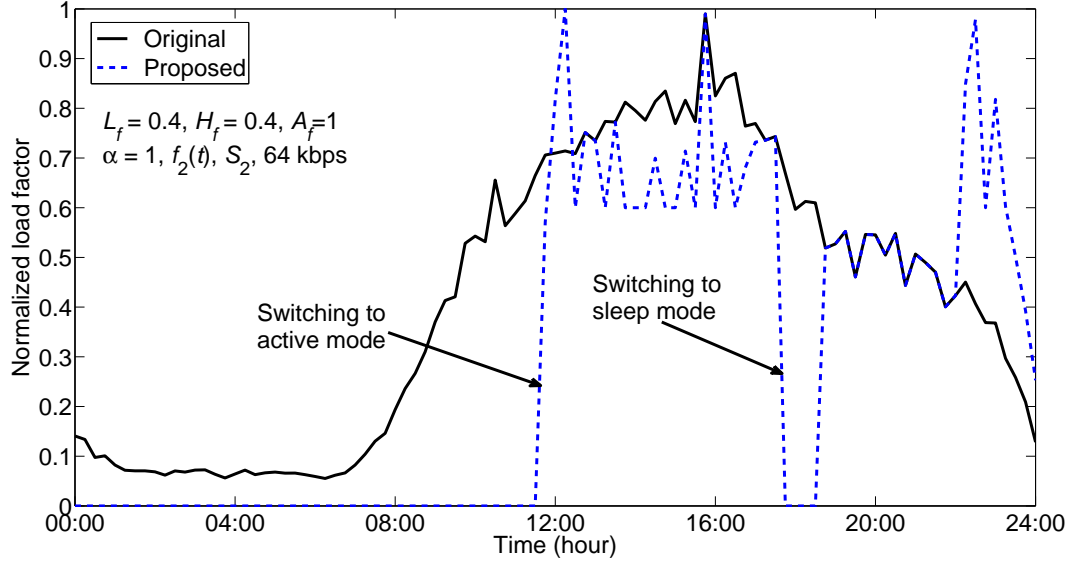
(a) Randomly taken BS 1.
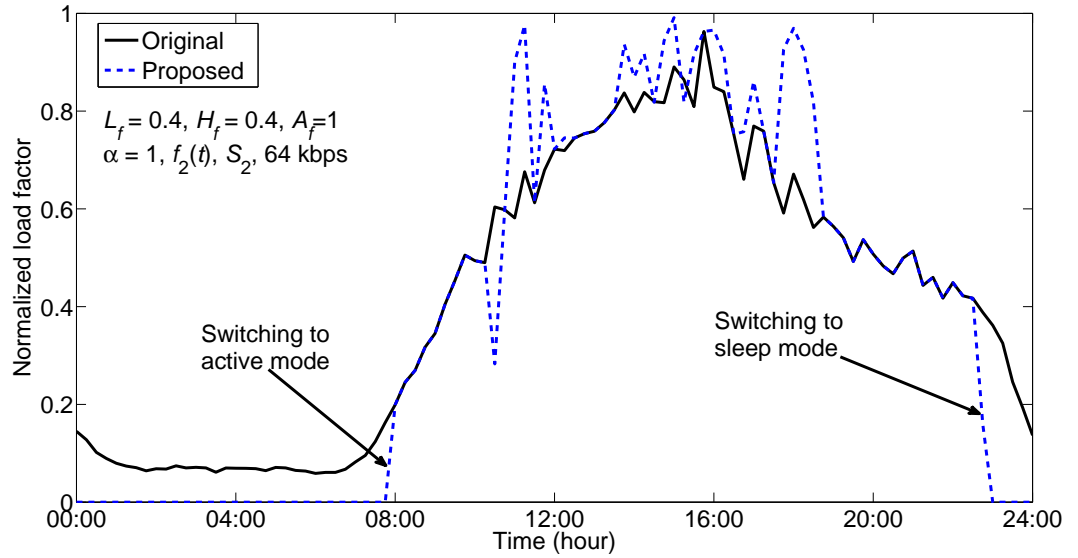
(b) Randomly taken BS 2.

Figure 4.13: Illustration of switching in two different BSs over a day.

During the dynamic network reconfiguration, each BS can experience multiple switching over a day. For demonstrating this, instantaneous traffic of two randomly chosen BSs are
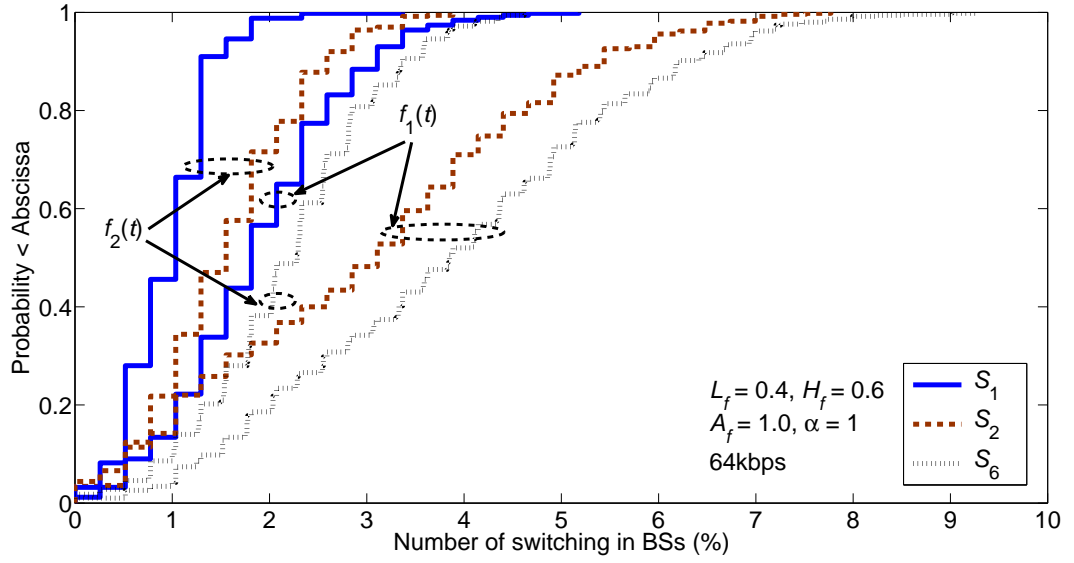
Figure 4.14: The cumulative distribution function of number of switching in BSs per day.

presented in Fig. 4.13. As seen, both the BSs are switched from active to sleep mode and vice versa for multiple times over 24 hours. For instance, BS 1 goes to sleep mode at 00:00 hours and remains in sleep mode until 11:30 hours. After switching to active mode at 11:30 hours, it continues to operate over the rest of the day except another short sleeping phase between 17:30-18:30 hours. Thus, BS 1 switches twice from active to sleep mode and twice from sleep to active mode as well. It is also observed that for certain periods, both the BSs carry higher traffic than their own, which corresponds to the shared traffic from the neighboring BSs.

Fig. 4.14 presents the cumulative distribution function (*cdf*) of the percentage of the instances of the algorithm execution at which switching from active to sleep mode occurs in each BS. From the figure, it is clear that the number of switching in BSs can vary significantly with the selection schemes and the rate function of a network. For instance, in all the schemes, the occurrence of switching in BSs is more probable in a network with $f_1(t)$ compared to that with $f_2(t)$. Also, the non-zero probability at 0% switching indicates that some BSs never switch to sleep mode and conserve no energy for themselves. However, they contribute to the savings by sharing the traffic of other BSs and allowing them to stay in sleep mode.
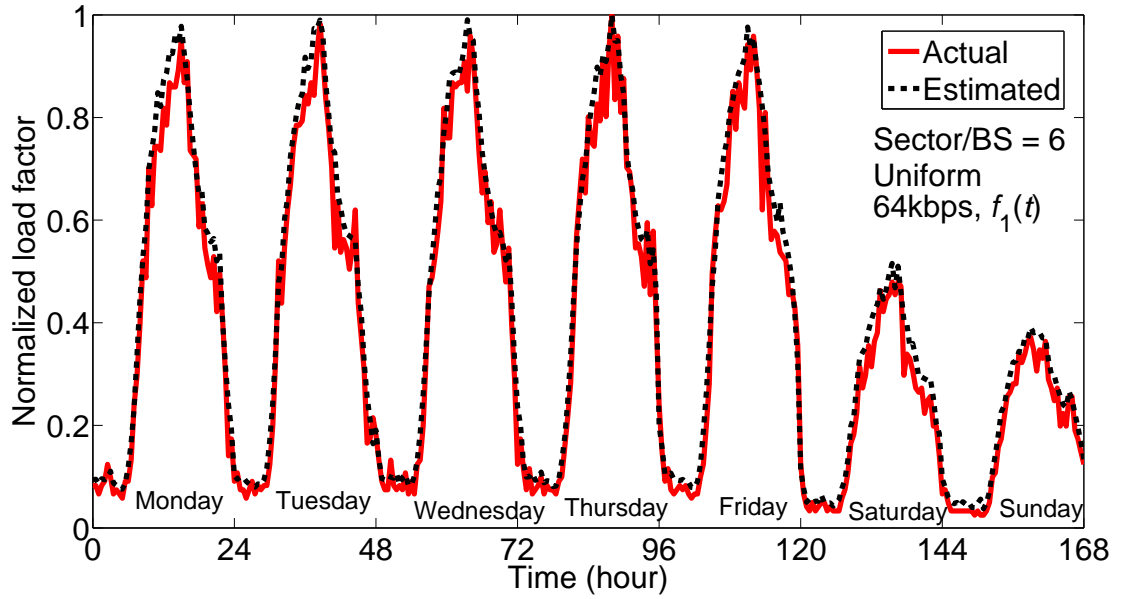
Figure 4.15: LF envelope prediction using the proposed EWMA-based estimator.

4.7.5 Performance under the EWMA-based LF Predictor

Performance of the proposed EWMA-based LF prediction technique is demonstrated in Fig. 4.15. First, LF data for four weeks is generated, which is then used for estimating the LF of the next one week. For generating the LF data, the rate function $f_1(t)$ (Fig. 4.3), $\alpha = 1$, sampling interval = 30 minutes and 64 kbps user data rate is considered. Weekday and weekend data are separated for estimating the envelope for the corresponding days. From the figure, it is clear that the estimated values are very close and almost always higher than the actual data.

Percentage of reduction in the number of instances at which a BS communicates with its neighbors under this EWMA predictor is presented in Fig. 4.16. This reduction of communications results from the combined effect of the use of predicted LF envelope, allowing only the active mode BSs for deciding on the traffic distributions and accounting the operating modes of the neighbors for prioritizing them in choosing the best combinations. As seen, depending on the network parameters, as high as 80% reduction is achieved. Also, the higher the gap between L_f and H_f, the higher is the reduction. Reduction corresponding to $L_f = H_f$ solely results from checking the operating status of each BS amounting around 30% and 40% for $f_1(t)$ and $f_2(t)$ respectively.
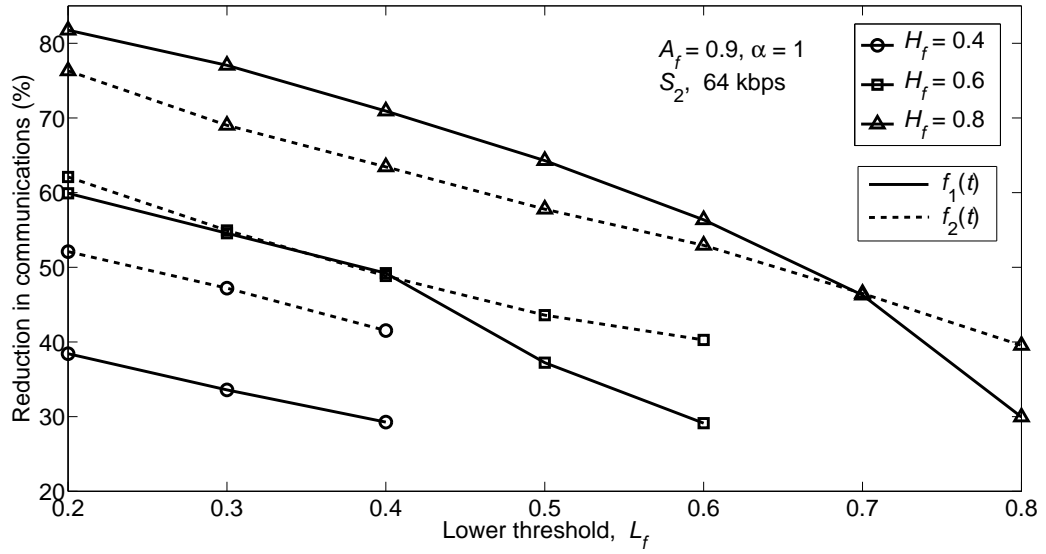
Figure 4.16: Reduction in the number of communications among BSs.

4.8   Chapter Summary

An ecological self-organization inspired distributed inter-BS cooperation assisted energy efficient load balancing DSBS framework for OFDMA-based cellular access networks has been presented in this paper. BSs in the proposed system mutually cooperate for dynamically switching the selected BSs into sleep mode for saving energy. Various schemes for selecting the best BSs for distributing traffic are also exploited. Utilization of the predicted LF by the proposed EWMA-based predictor, consideration of the operating modes of BSs for initializing the algorithm and the prioritization of the active neighbors over sleeping BSs are also explored for reducing the number of computations. Moreover, an analytical model for evaluating the probabilities of BSs switching into sleep mode is also presented. System performance over a wide range of traffic level, BS selection schemes, BS power models, switching thresholds and data rates has been investigated. Higher savings is identified for the networks with lower data rate users. Furthermore, energy savings increases with the increase of non-proportionality in power consumption of BSs. In addition, depending on the network settings, an increment in RB utilization is observed by a factor over two and the communications among BSs is reduced by more than 80%. Now, in many cases, a geographical area can be covered by several network operators. Therefore, the next chapter focuses on developing energy efficient dynamic BS switching mechanisms through mutual cooperation among these colocated networks.

Chapter 5

Distributed Dynamic Switching of Base Station: Multi-Network Scenario

An energy saving distributed DSBS mechanism by utilizing mutual cooperation among BSs belong to a single network has been presented in Chapter 4. Since the interacting BSs are from the same network, the cooperation technique can be named as intra-network co-operation. This chapter extends the focus on exploiting the existence of multiple cellular networks for extracting any potential savings by employing mutual cooperation among themselves. Two alternative schemes of DSBS involving traffic-sensitive distributed and self-organizing type intelligent cooperation mechanisms among BSs belong to different networks are presented in this chapter. They are named inter-network cooperation and joint cooperation respectively. Analytical models for evaluating the switching dynamics of BSs under these mechanisms are also formulated. System performance is thoroughly investigated under different number of cooperating networks, traffic scenarios, BS power profiles and their switching thresholds. Optimal energy savings, while maintaining QoS, is also evaluated. System performance in terms of network capacity utilization, additional transmit power and BS sleeping patterns is also investigated. The content of this chapter has appeared in [158], [159] and [160].

5.1   Inter-network Cooperation for DSBS

Nowadays, almost any city around the world is under the coverage of multiple cellular mobile operators [36], [89]. This multi-RAN scenario can be considered as an opportunity for developing energy saving DSBS mechanisms by implementing cooperative sharing of each other's traffic. Fig. 5.1 illustrates the various options of energy saving cooperation among BSs of N co-located RANs. For reducing the complexity in evaluation and developing analytical models, hexagonal layout is chosen and the co-located BSs belong to different RANs are assumed of equal size. Although the second assumption simplifies the system modeling and analysis, it is a quite reasonable consideration, particularly for urban areas, where the cell sites are located very close or even in the same tower [36]. Without losing the generality, equal number of BSs is considered for all the networks. Thus, at a particular location, there are N BSs from the N RANs engaged in mutual cooperation.

Under the proposed inter-network cooperation, based on the instantaneous total traffic load of the N co-located BSs, traffic is dynamically redistributed among these N BSs. Thus, some of these N BSs can switch to sleep mode and reduce the overall energy consumption. Sufficient number of BSs are left active for supporting the total load of this location. These N BSs communicate and coordinate over inter-RAN interface requiring no operator assistance. For instance, the S4 and S12 interfaces in LTE RANs can be utilized for exchanging information with 2G and 3G access networks via SGWs [161]. IP network can also be considered as an alternate option for the inter-RAN correspondence. For distributed type implementation as like the one proposed here, a new direct link among BSs of multiple RANs would be a better option for reduced latency and signaling overhead.

On the other hand, an agreement has to be established among the cooperating network operators. This agreement may include the priority sequence of operators for distributing traffic load, a business model of distributing the profit gained from energy saving cooperation and so on. For traffic distribution, a pre-defined fixed ranking of the networks or a dynamic ranking derived from the instantaneous load can be used. In this chapter, a pre-defined ranking policy is adopted. Without losing the generality, the indices used for the RANs are taken as their ranks, i.e., RAN 1 has the highest priority in distributing its traffic, while the lowest priority is assigned to N^{th} RAN. The notations used in this chapter are summarized in Table 5.1.
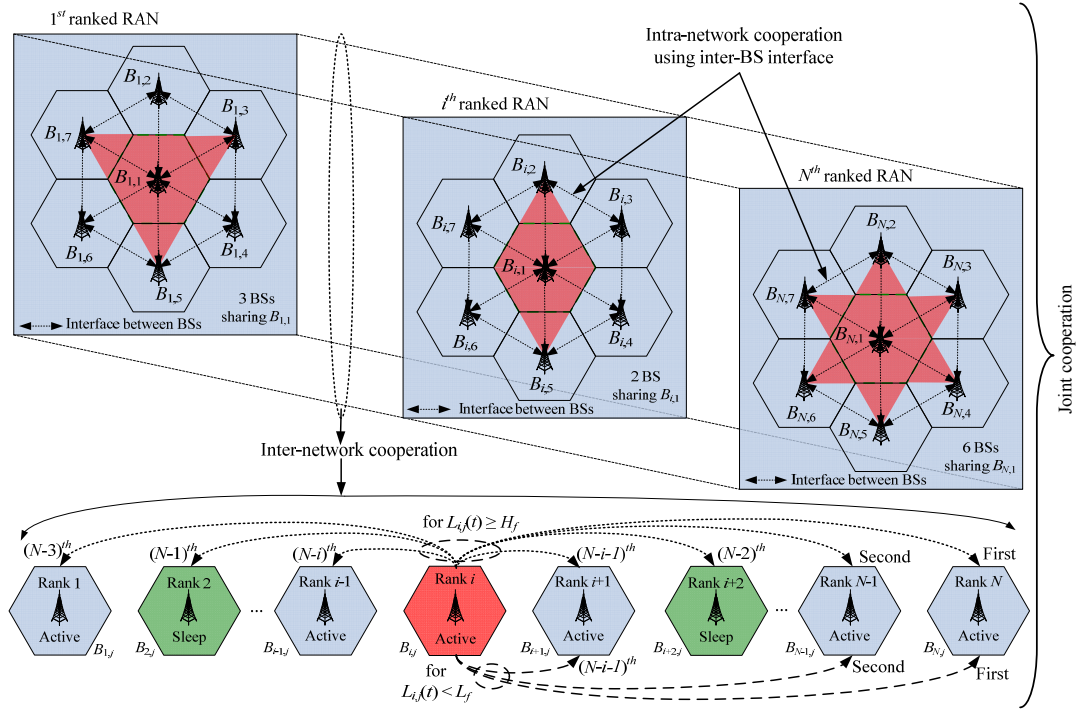
Figure 5.1: Energy saving cellular access network under multi-RAN scenarios.

Table 5.1: Summary of the notations used in this chapter

N	Number of cooperating networks	$\mathbf{C}_{i,j}^{(m)}, \mathbb{D}_{i,j}$	Candidate combination of $\mathcal{B}_{i,j}$
N_T	Number of BSs in a network	$C_{i,j}^{m,k}$	k^{th} BS in $\mathbf{C}_{i,j}^{(m)}$
$\mathcal{B}_{i,j}$	j^{th} BS of ith network	$\mathcal{B}_{i,j}^{(k)}$	k^{th} candidate BS of $\mathcal{B}_{i,j}$
$L_{i,j}$	Load factor of $\mathcal{B}_{i,j}$	$L_{i,j}^{(k)}$	Load factor of $\mathcal{B}_{i,j}^{(k)}$
$s_{i,j}$	Operating mode of $\mathcal{B}_{i,j}$ 0: Sleep, 1: Active	$s_{i,j}^{(k)}$	Operating mode of $\mathcal{B}_{i,j}^{(k)}$ 0: Sleep, 1: Active
$p_{i,j}$	Transmit power of $\mathcal{B}_{i,j}$	$p_{i,j}^{(k)}$	Transmit power of $\mathcal{B}_{i,j}^{(k)}$
$f_{i,j}$	Rate function of $\mathcal{B}_{i,j}$	$\lambda_{i,j}^{(q)}$	q^{th} class Poisson parameter
$\beta_{i,j}$	Total number of RBs in $\mathcal{B}_{i,j}$	$h_{i,q}$	q^{th} class session duration
Q	Number of service classes	$\eta_{i,q}$	q^{th} class RB requirement
L_f	Lower threshold	$(.)^T$	Transpose of a matrix
H_f	Upper threshold	$|\mathbb{D}|$	Cardinality of vector $\mathbb{D}$
A_f	Acceptance threshold	$Q(.)$	Q-function

5.1.1 Algorithm

Proposed algorithm is executed periodically at all the N_T locations. For j^{th} location, $\mathcal{B}_{1,j}$ has the first priority in distributing its traffic and hence, the other $(N-1)$ BSs of this location comply with the decisions made by $\mathcal{B}_{1,j}$. After $\mathcal{B}_{1,j}$ finishes its turn, the authority of making decision moves to $\mathcal{B}_{2,j}$ and so on. Thus, the strategy is analogous to dynamic clustering techniques, where every BS works as the cluster head in its turn.

Let $\mathbb{D}_{i,j} = \left\{ \mathcal{B}_{i,j}^{(k)} : k = 1, 2, ..., N, k \neq i \right\}$, $\mathcal{L}_{i,j} = \left\{ L_{i,j}^{(k)} : k = 1, 2, ..., N, k \neq i \right\}$, $\mathcal{S}_{i,j} = \left\{ s_{i,j}^{(k)} : k = 1, 2, ..., N, k \neq i \right\}$ and $\mathcal{P}_{i,j} = \left\{ p_{i,j}^{(k)} : k = 1, 2, ..., N, k \neq i \right\}$ be the ID, LF, operating mode and the transmit power sets of the candidate BSs for $\mathcal{B}_{i,j}$ respectively. Now, similar to the intra-network cooperation presented in Chapter 4, the two cases - a) low-traffic period (i.e., $L_{i,j} < L_f$), and b) high-traffic period (i.e., $L_{i,j} \geq H_f$) are dealt in different ways. Therefore, based on the network ranking and the operating mode of the candidate BSs, $\mathbb{D}_{i,j}$ is divided into four mutually exclusive sets: $\mathbb{D}_{i,j}^{L,a} = \left\{ \mathcal{B}_{i,j}^{(k)} : k > i, s_{i,j}^{(k)} = 1 \right\}$, $\mathbb{D}_{i,j}^{L,s} = \left\{ \mathcal{B}_{i,j}^{(k)} : k > i, s_{i,j}^{(k)} = 0 \right\}$, $\mathbb{D}_{i,j}^{H,a} = \left\{ \mathcal{B}_{i,j}^{(k)} : k < i, s_{i,j}^{(k)} = 1 \right\}$, and $\mathbb{D}_{i,j}^{H,s} = \left\{ \mathcal{B}_{i,j}^{(k)} : k < i, s_{i,j}^{(k)} = 0 \right\}$. Here, the superscripts "L", "H", "a" and "s" stand for "lower ranked", "higher ranked", "active mode" and "sleep mode" respectively. As an example, $\mathbb{D}_{i,j}^{L,a}$ is the set of all the active mode BSs ranked lower than $\mathcal{B}_{i,j}$.

For case (a), $\mathcal{B}_{i,j}$ is allowed to distribute traffic only to the lower ranked active BSs, i.e., to BSs in $\mathbb{D}_{i,j}^{L,a}$ only. However, for (b), following the order defined in $\mathbb{S} = \left(\mathbb{D}_{i,j}^{L,a} \Rightarrow \mathbb{D}_{i,j}^{H,a} \Rightarrow \mathbb{D}_{i,j}^{L,s} \Rightarrow \mathbb{D}_{i,j}^{H,s} \right)$, $\mathcal{B}_{i,j}$ is permitted to attempt all the four sets for distributing its traffic. During the traffic distribution to a particular set, $\mathcal{B}_{i,j}$ distributes sequentially to BSs of that set starting from the lowest ranked one. Thus, this proposed sequence preserves the network ranking as well as the higher preference of selecting active BSs over the sleep mode BSs for distributing traffic. As an instance, load distributions by $\mathcal{B}_{i,j}$ under inter-network cooperation for both a low-traffic and a high-traffic periods are shown at the bottom part of the Fig. 5.1. BSs $\mathcal{B}_{i,j}$ and $\mathcal{B}_{i+2,j}$ are in sleep mode. The indices used with the broken lines indicate the sequence of attempted BSs by $\mathcal{B}_{i,j}$ for distributing its traffic. For example, as shown in the diagram, during $L_{i,j} < L_f$, $\mathcal{B}_{i,j}$ approaches only the lower ranked active BSs starting from the lowest ranked $\mathcal{B}_{N,j}$. Pseudo code of the traffic distribution algorithms are presented in Table 5.2 and 5.3.

Table 5.2: Traffic distribution of $\mathcal{B}_{i,j}$ during low-traffic period

1:	Initialize $s_{i,j}, p_{i,j}, \mathcal{L}_{i,j}, \mathcal{S}_{i,j}, \mathcal{P}_{i,j}, \mathbb{D}_{i,j}$
2:	**If** $s_{i,j} = 1$, $L_{i,j} < L_f$ and $\mathbb{D}_{i,j}^{L,a} \neq \emptyset$
3:	**If** $\sum_{k=1}^{|\mathbb{D}_{i,j}^{L,a}|} \left(A_f - L_{i,j}^{(k)} \right) \geq L_{i,j}$, where $\mathcal{B}_{i,j}^{(k)} \in \mathbb{D}_{i,j}^{L,a}$
4:	Distribute $L_{i,j}$ to $\mathcal{B}_{i,j}^{(k)} \in \mathbb{D}_{i,j}^{L,a}$, $k = 1, 2, ..., |\mathbb{D}_{i,j}^{L,a}|$
5:	Set $L_{i,j} = 0$, $s_{i,j} = 0$ and $p_{i,j} = 0$
6:	Update $L_{i,j}^{(k)}, s_{i,j}^{(k)}$ and $p_{i,j}^{(k)} \forall \mathcal{B}_{i,j}^{(k)} \in \mathbb{D}_{i,j}^{L,a}$
7:	**End If**
8:	**End If**

Table 5.3: Traffic distribution of $\mathcal{B}_{i,j}$ during high-traffic period

1:	Initialize $s_{i,j}, p_{i,j}, \mathcal{L}_{i,j}, \mathcal{S}_{i,j}, \mathcal{P}_{i,j}, \mathbb{D}_{i,j}$
2:	**If** $s_{i,j} = 1$, $L_{i,j} \geq H_f$ and $\mathbb{D}_{i,j} \neq \emptyset$
3:	**If** $\sum_{k=1}^{|\mathbb{D}_{i,j}|} \left(A_f - L_{i,j}^{(k)} \right) \geq L_{i,j}$, where $\mathcal{B}_{i,j}^{(k)} \in \mathbb{D}_{i,j}$
4:	Distribute $L_{i,j}$ to $\mathcal{B}_{i,j}^{(k)} \in \mathbb{D}_{i,j}$ according to $\mathbb{S}$
5:	Set $L_{i,j} = 0$, $s_{i,j} = 0$ and $p_{i,j} = 0$
6:	Update $L_{i,j}^{(k)}, s_{i,j}^{(k)}$ and $p_{i,j}^{(k)} \forall \mathcal{B}_{i,j}^{(k)} \in \mathbb{D}_{i,j}$
7:	**Elseif** $\sum_{k=1}^{|\mathbb{D}_{i,j}|} \left(A_f - L_{i,j}^{(k)} \right) \geq (L_{i,j} - H_f)$, where $\mathcal{B}_{i,j}^{(k)} \in \mathbb{D}_{i,j}$
8:	Distribute $(L_{i,j} - H_f)$ to $\mathcal{B}_{i,j}^{(k)} \in \mathbb{D}_{i,j}$ according to $\mathbb{S}$
9:	Set $L_{i,j} = H_f$ and update $p_{i,j}$
10:	Update $L_{i,j}^{(k)}, s_{i,j}^{(k)}$ and $p_{i,j}^{(k)} \forall \mathcal{B}_{i,j}^{(k)} \in \mathbb{D}_{i,j}$
11:	**End If**
12:	**End If**

5.1.2 Analytical Model

Switching of operating modes of N BSs from N RANs at j^{th} location can be modeled as a Markov process. A state of the process for j^{th} location can be denoted as $\{s_{1,j}, s_{2,j}, ..., s_{N,j}\}$. Thus the number of states for j^{th} location is 2^N, which increases exponentially with N. Therefore, for reducing the complexity in verification, an analyt-
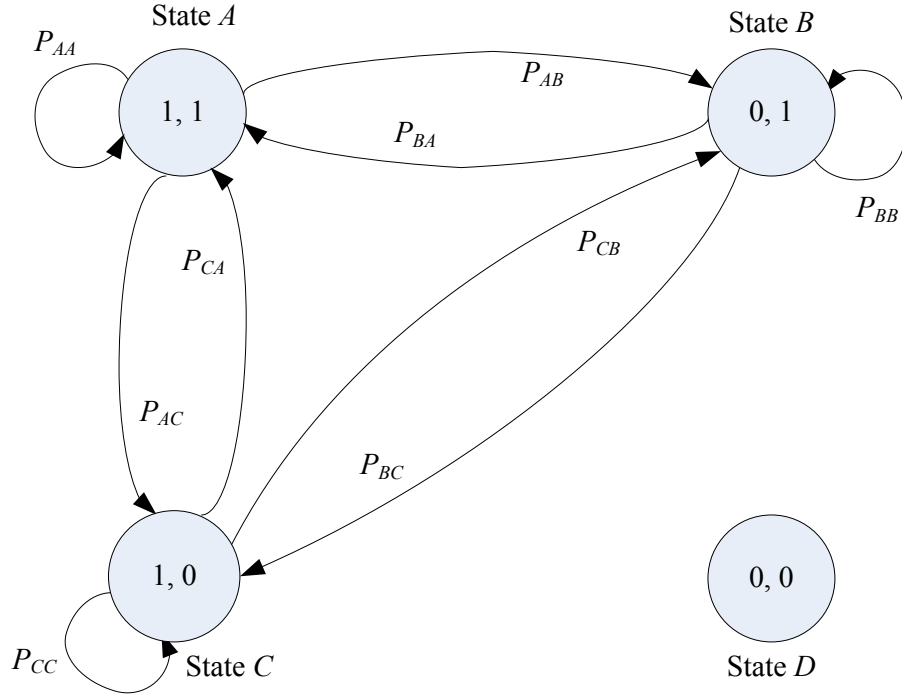
Figure 5.2: Transition diagram for inter-network cooperation between two RANs.

ical model of inter-network cooperation between two RANs is developed here. For the convenience and clarity, the time index is omitted from some of the following equations.

Transition diagram for the system is shown in Fig. 5.2. Number of distinct states in this case is equal to four, which are denoted as $A = (1,1), B = (0,1), C = (1,0)$ and $D = (0,0)$. The two digits in the states denote the operating modes of BSs from RAN 1 and RAN 2 respectively. The state probabilities at j^{th} location are denoted by a vector $\mathbf{P_j^{S,Inter}} = [P_j^A \ P_j^B \ P_j^C \ P_j^D]$, where P_j^A is the probability that the system is in state A. Transition matrix of the system can be written as

$$\prod_j = \begin{bmatrix} \mathbf{T_j^1} & \mathbf{T_j^2} & \mathbf{T_j^3} & \mathbf{T_j^4} \end{bmatrix} = \begin{bmatrix} P_{AA} & P_{AB} & P_{AC} & P_{AD} \\ P_{BA} & P_{BB} & P_{BC} & P_{BD} \\ P_{CA} & P_{CB} & P_{CC} & P_{CD} \\ P_{DA} & P_{DB} & P_{DC} & P_{DD} \end{bmatrix} \tag{5.1}$$

where $\mathbf{T_j^q}(q = 1, 2, ..., 4)$ is the qth column of $\prod_j$. The probabilities in $\prod_j$ can be derived

as below

$$
\left.\begin{aligned}
P_{AB} &= [Pr\{L_{1,j} < L_f\} + Pr\{L_{1,j} \geq H_f\}] \times Pr\{L_{1,j} + L_{2,j} < A_f\} \\
P_{AC} &= Pr\{L_f \leq L_{1,j} < H_f\} \times Pr\{L_{1,j} + L_{2,j} < A_f\} \times Pr\{L_{2,j} \geq H_f\} \\
P_{BA} &= Pr\{L_{1,j} + L_{2,j} \geq A_f\} \\
P_{BC} &= Pr\{L_{1,j} + L_{2,j} < A_f\} \times Pr\{L_{2,j} \geq H_f\} \\
P_{AA} &= 1 - P_{AB} - P_{AC} - P_{AD}, P_{BB} = 1 - P_{BA} - P_{BC} - P_{BD} \\
P_{CC} &= 1 - P_{CA} - P_{CB} - P_{CD}, P_{CA} = P_{BA} \\
P_{CB} &= P_{AB}, P_{AD} = P_{BD} = P_{CD} = P_{DA} = P_{DB} = P_{DC} = P_{DD} = 0
\end{aligned}\right\} \tag{5.2}
$$

State probabilities for j^{th} location at time t is then given by

$$
\mathbf{P_j^{S,Inter}} = \mathbf{P_j^{S,\Delta}} \prod_j, \; \forall j \tag{5.3}
$$

where $\mathbf{P_j^{S,\Delta}} = \begin{bmatrix} P_j^{A,\Delta} & P_j^{B,\Delta} & P_j^{C,\Delta} & P_j^{D,\Delta} \end{bmatrix}$ is the state probability vector $\mathbf{P_j^{S,Inter}}$ at the last instance. Initial state probability vector $\mathbf{P_j^{S,Inter}} = [1\ 0\ 0\ 0], \forall t \leq 0, \forall j$. We can then write

$$
Pr\{\mathcal{B}_{1,j}\ \text{sleeps at time}\ t\} = P_{1,j}^{S,Inter} = \mathbf{P_j^{S,\Delta}} \cdot \left(\mathbf{T_j^2}\right)^T, \; \forall j \tag{5.4}
$$

$$
Pr\{\mathcal{B}_{2,j}\ \text{sleeps at time}\ t\} = P_{2,j}^{S,Inter} = \mathbf{P_j^{S,\Delta}} \cdot \left(\mathbf{T_j^3}\right)^T, \; \forall j \tag{5.5}
$$

Considering the traffic model parameter α (defined in Chapter 4) as an uniform RV over a range $[a, b]$, conditional probabilities $P_{i,j}^{S,Inter}|_\alpha (i = 1, 2)$ conditioned on α can be simplified as below

$$
P_{1,j}^{S,Inter}|_\alpha = \left[P_j^{A,\Delta} + P_j^{C,\Delta}\right](1 - q_1 + q_2)(1 - q_5)
$$
$$
+ P_j^{B,\Delta}\left[1 - q_3(1 - q_4) - q_5\right] \tag{5.6}
$$

$$
P_{2,j}^{S,Inter}|_\alpha = \left[P_j^{A,\Delta}(q_1 - q_2) + P_j^{B,\Delta}\right]q_3(1 - q_4)
$$
$$
+ P_j^{C,\Delta}\left[1 - (1 - q1 + q_2)(1 - q_5) - q_4\right] \tag{5.7}
$$

$$
\left.\begin{aligned}
\text{where } q_1 &= Q\left(\frac{\frac{\beta_{1,j} L_f}{\alpha f_{1,j}(t)} - \mu_{x_{1,j}}}{\sqrt{\sigma_{x_{1,j}}^2}}\right), \quad q_2 = Q\left(\frac{\frac{\beta_{1,j} H_f}{\alpha f_{1,j}(t)} - \mu_{x_{1,j}}}{\sqrt{\sigma_{x_{1,j}}^2}}\right) \\
q_3 &= Q\left(\frac{\frac{\beta_{2,j} H_f}{\alpha f_{2,j}(t)} - \mu_{x_{2,j}}}{\sqrt{\sigma_{x_{2,j}}^2}}\right), \quad q_4 = Q\left(\frac{\frac{A_f}{\alpha} - \mu_{z_{2,j}}}{\sqrt{\sigma_{z_{2,j}}^2}}\right) \\
q_5 &= Q\left(\frac{\frac{A_f}{\alpha} - \mu_{z_{2,j}}}{\sqrt{\sigma_{z_{2,j}}^2}}\right)
\end{aligned}\right\} \tag{5.8}
$$

By utilizing the derivation presented in Appendix A into (5.2) and after some simple algebra, the expressions in (5.6)-(5.8) can be reached. Now, bringing back the time index, for location j at time t, we can write the unconditional probabilities as below

$$P_{i,j}^{S,Inter}(t) = \frac{1}{b-a} \int_a^b P_{i,j}^{S,Inter}|_\alpha \, d\alpha, \ i = 1,2 \tag{5.9}$$

Thus the average sleeping probability of a BS in the combined network can be given by

$$P_{avg}^{S,Inter} = \left[\frac{1}{N N_T T} \sum_{i=1}^{N} \sum_{j=1}^{N_T} \int_0^T P_{i,j}^{S,Inter}(t) dt \right] \times 100\% \tag{5.10}$$

5.2 Joint Cooperation for DSBS

Under the proposed joint cooperation, both the intra-network cooperation and the inter-network cooperation are applied together for achieving a higher level of energy savings by switching higher number of BSs into sleep mode.

5.2.1 Algorithmic Framework

At each instance of the execution of the joint cooperation, the intra-network and the inter-network cooperation techniques are performed one after another. Either of the them can be executed first followed by the other. Under the scheme investigated here, the intra-network cooperation is performed inside each network in the first phase, which reconfigures respective networks with the reduced number of active BSs. Then, in the second phase, the inter-network cooperation among the networks is carried out for further reducing the number of active BSs.

5.2.2 Analytical Modeling

BS $\mathcal{B}_{i,j}$, under the proposed joint cooperation scheme, can switch from active to sleep mode and vice versa due to either the intra-network cooperation or the inter-network cooperation. Therefore, the probability of switching of $\mathcal{B}_{i,j}$ into sleep mode at any time t can be given by

$$P_{i,j}^{S,Joint}(t) = \frac{1}{b-a} \int_a^b \left[P_{i,j}^{S,Intra}(t)|_\alpha + P_{i,j}^{S,Inter}(t)|_\alpha \right.$$

$$-P_{i,j}^{S,Intra}(t)|_{\alpha} \times P_{i,j}^{S,Inter}(t)|_{\alpha}\Big] d\alpha, \ \forall i, \forall j, \forall t \qquad (5.11)$$

where $P_{i,j}^{S,Intra}(t)|_{\alpha}$ is the conditional probability of $\mathcal{B}_{i,j}$ to switch into sleep mode under the intra-network cooperation. Following the similar procedure presented in Chapter 4, expression of $P_{i,j}^{S,Intra}(t)|_{\alpha}$ for a hexagonal layout can be derived as below.

$$P_{i,j}^{S,Intra}(t)|_{\alpha} = 1 - \prod_{n=1}^{M_{i,j}} \left[1 - \left[\left\{ 1 - Q\left(\frac{\frac{L_f \beta_{i,j}}{\alpha f_{i,j}(t)} - \mu_{x_{i,j}}}{\sqrt{\sigma_{x_{i,j}}^2}} \right) \right\} \times \prod_{k=1}^{P} P^{\Delta}\left\{ A_{i,j}^{n,k} \right\} \right. \right.$$

$$\left. \left. + Q\left(\frac{\frac{H_f \beta_{i,j}}{\alpha f_{i,j}(t)} - \mu_{x_{i,j}}}{\sqrt{\sigma_{x_{i,j}}^2}} \right) \right] \times \prod_{k=1}^{P} \left\{ 1 - Q\left(\frac{A_f - \mu_{y_{i,j}}}{\sqrt{\sigma_{y_{i,j}}^2}} \right) \right\} \times Pr\left\{ \overline{X_{i,j}^{(n)}} \right\} \right] \qquad (5.12)$$

where

$$Pr\left\{ \overline{X_{i,j}^{(n)}} \right\} = \left[\prod_{\substack{k=1 \\ m=1, m \neq n}}^{P} \left[1 - F_{i,j}^{m,k} P^{\Delta}\left\{ S_{i,j}^{m,k} \right\} \right] \right] \times \left[\prod_{\substack{k=1 \\ m=2, m \neq n}}^{P} \left[1 - F_{i,j}^{m,k} P^{\Delta}\left\{ S_{i,j}^{m,k} \right\} \right] \right]$$

$$\times \dots \times \left[\prod_{\substack{k=1 \\ m=M_{i,j}, m \neq n}}^{P} \left[1 - F_{i,j}^{m,k} P^{\Delta}\left\{ S_{i,j}^{m,k} \right\} \right] \right] \qquad (5.13)$$

Here, $P^{\Delta}\left\{ A_{i,j}^{m,k} \right\}$ is the probability that $C_{i,j}^{m,k}$ is in active mode at the last instance and $P^{\Delta}\left\{ S_{i,j}^{m,k} \right\} = 1 - P^{\Delta}\left\{ A_{i,j}^{m,k} \right\}$. BS $C_{i,j}^{m,k}$ is the kth element of $\mathcal{B}_{i,j}$'s m^{th} candidate combination $\mathbf{C}_{i,j}^{(m)} = \left[C_{i,j}^{m,1}, C_{i,j}^{m,2}, \dots, C_{i,j}^{m,P} \right]$. The factor $F_{i,j}^{m,k} = 1/M_{i,j}^{m,k}$ for $M_{i,j}^{m,k} \neq 0$, while $F_{i,j}^{m,k} = 0$ for $M_{i,j}^{m,k} = 0$. Also, $M_{i,j}$ and $M_{i,j}^{m,k}$ are the number of candidate combinations for $\mathcal{B}_{i,j}$ and $C_{i,j}^{m,k}$ respectively. For the derivation of (5.12) and (5.13), it is assumed that all the candidate combinations of $\mathcal{B}_{i,j}$ are formed using P BSs from the neighbors. The Q-functions in (5.12) follows from the equations derived in Appendix A.

Now, averaging over time t, all BSs and all the cooperating RANs, overall probability that a BS sleeps under the joint cooperation can then be given by

$$P_{avg}^{S,Joint} = \left[\frac{1}{N N_T T} \sum_{i=1}^{N} \sum_{j=1}^{N_T} \int_0^T P_{i,j}^{S,Joint}(t) dt \right] \times 100\% \qquad (5.14)$$

5.3   Energy Saving Optimization Problems

Three optimization problems for evaluating the maximum energy savings and the corresponding parameters are defined here. Exhaustive search technique is used for the

evaluations. First optimization problem, denoted as P1, defines the optimal savings as the achievable maximum energy savings keeping session blocking probability $P_{i,b}, (i = 1, 2, ..., N)$ within a target limit P_b^{th}, while imposing no restrictions on the average number of switching $\mathcal{N}_{Sw}$. The second optimization problem P2 maximizes energy savings as well as minimizes $\mathcal{N}_{Sw}$, while maintains session blocking within P_b^{th}. The last optimization objective P3 evaluates the maximum energy savings keeping both $P_{i,b}$ and $\mathcal{N}_{Sw}$ within their respective target limits. The optimization problems are presented as below

$$(\text{P1}) \underset{L_f, H_f, A_f}{\arg\max} \ E_s \qquad (\text{P2}) \underset{L_f, H_f, A_f}{\arg\max} \ E_s \qquad (\text{P3}) \underset{L_f, H_f, A_f}{\arg\max} \ E_s$$

$$s.t., \quad P_{i,b} \leq P_b^{th}, \forall i \qquad s.t., \quad P_{i,b} \leq P_b^{th}, \forall i \qquad s.t., \quad P_{i,b} \leq P_b^{th}, \forall i$$

$$\min \mathcal{N}_{Sw} \qquad \qquad \mathcal{N}_{Sw} \leq \mathcal{N}_{Sw}^{th}$$

Additional conditions for P1, P2, P3:

$$H_f \geq L_f, A_f > L_f, A_f > H_f$$
$$A_f, H_f, L_f > 0$$

5.4 Results and Discussions

5.4.1 Simulation Setup

For evaluating the proposed energy saving cooperative network models, a scenario of multiple colocated LTE RANs is used as the simulation platform. Each of the networks covers a geographical area using $N_T = 50$ single-sector macrocells of radius equal to 1 km deployed using hexagonal layout. Carrier frequency = 2 GHz and channel bandwidth = 20 MHz equivalent to 100 RBs are assumed. Other link budget parameters, namely, BS transmit power = 46 dBm, BS antenna gain = 10 dBi [71], feeder loss = 3 dB, UE antenna gain = 0 dB, BS NF = 5 dB, UE NF = 9 dB, minimum downlink SINR = -4.1 dB, MIMO gain = 3.5 dB [55], shadow fading standard deviation = 8 dB, Gaussian noise power density = -174 dBm/Hz and the WINNER+ NLOS urban macro-cell channel model are used for the simulations. For the computational tractability, similar to [56], [61] and [162], it is assumed that the inter-cell interference can be managed by adopting certain

interference averaging schemes resulting in equal interference throughout the network. For the simulations, an inter-cell interference margin equal to 6 dB is taken [152].

On the other hand, it is considered that the cooperating networks originally support $Q = 2$ classes of CBR services requiring $\eta_{i,1} = 1$ and $\eta_{i,2} = 2, \forall i$, dedicated RBs. For the convenience of simulations, constant session durations $h_{i,1} = 3$ minutes and $h_{i,2} = 5$ minutes are taken for the two classes. Whereas, traffic generation rates equal to $\lambda_{i,j}^{(1)} = 13.9$ call/min and $\lambda_{i,j}^{(2)} = 4$ call/min are chosen. For traffic parameter $\alpha = 1$, these settings result in 1% and 2% peak-time session blocking for class 1 and 2 respectively. Equations for calculating session blocking probabilities under multi-class services is presented in Appendix B. Rate functions $f_2(t)$ and $f_3(t)$ shown in Fig. 4.3 are used for generating inhomogeneous traffic. Two different traffic scenarios designated as S1 and S2 are simulated for inhomogeneous case. Scenario S1 simulates the temporal variation only, whereas S2 simulates both temporal and spatial variations of traffic generations. It is also assumed that UEs are uniformly distributed in the networks, while the total number of users may vary among BSs and the networks (e.g., when α is a RV).

The system is evaluated for both the CEC and the NEP BSs having power profile parameter $g = 21.45$ and $h = 354.44$ [52]. Two different settings of sleep mode power P_{op}^s are considered for each of the two models. For the CEC model (i.e., $\delta = 1$), the two settings are 0 W and h W, which are designated as CEC1 and CEC2 respectively. The two variants of the NEP model are named as NEP1 and NEP2 having sleep mode power equal to 0 W and δh W respectively. Table 5.4 summarizes the power models used for the simulations in this chapter. Unless otherwise specified, presented results correspond to a network comprises of two RANs (i.e., $N = 2$) with only temporal variation in traffic (i.e., scenario S1), rate function $f_3(t)$, CEC1 power model, $\alpha = 1$ and $P = 2$.

Table 5.4: Power models used for the system evaluation

BS Power Model	ELPC (δ)	P_{op}^s (W)
CEC1	1	0
CEC2	1	δh
NEP1	0.7	0
NEP2	0.7	δh

5.4.2   Inhomogeneous Traffic Scenario

5.4.2.1   Sleep Mode BSs

Percentage of sleep mode BSs with L_f and A_f under the proposed cooperation mechanisms is presented in Figs. 5.3(a) and 5.3(b) respectively. Other simulation parameters are also shown in the figures. For the comparison purpose, results corresponding to the intra-network cooperation are also included in the figures. Now, because of the same reasons explained in Chapter 4, increasing trends in the number of sleep mode BSs with the increase of L_f as well as A_f are observed under all the three cooperation techniques. It is also evident that out of the three cooperation techniques, BSs under the joint cooperation have the highest chance to switch into sleep mode. In addition, a scenario with $\alpha \sim U[0.5, 1.0]$ representing varying traffic levels among BSs is also simulated and the corresponding result is included in Fig. 5.3(b). Because of the lower traffic in some BSs, this setting leads to a higher percentage of sleep mode BSs than that with $\alpha = 1$. Furthermore, from both the figures, it is evident that the analytical results are in close agreement with the simulation results, which validate the simulation models.

5.4.2.2   Additional Transmit Power

First of all, the average additional transmit power required per BS over a day for providing the coverage for UEs located in the sleep mode BSs denoted by P_{Tx}^{add} is demonstrated in Fig. 5.4. As seen, a network with rate function $f_2(t)$ requires lower P_{Tx}^{add} than that of a network having rate function $f_3(t)$. This is because, a network corresponding to $f_2(t)$ has relatively lower traffic compared to that of $f_3(t)$. In such a network, active BSs have to share lower amount of traffic from the sleep mode BSs leading to lower P_{Tx}^{add} requirement. On the other hand, it is also identified that for both the rate functions, P_{Tx}^{add} is significantly higher in scenario S2 ($> 23\%$) than that in S1 ($< 5\%$). Under scenario S1, there is no sleep mode BS during peak-traffic period requiring no additional power. However, in scenario S2, there are always some sleep mode BSs in a day, while the other active BSs share their traffic with extended coverage. Therefore, the active BSs under S2 require additional power over the day resulting in higher P_{Tx}^{add}.
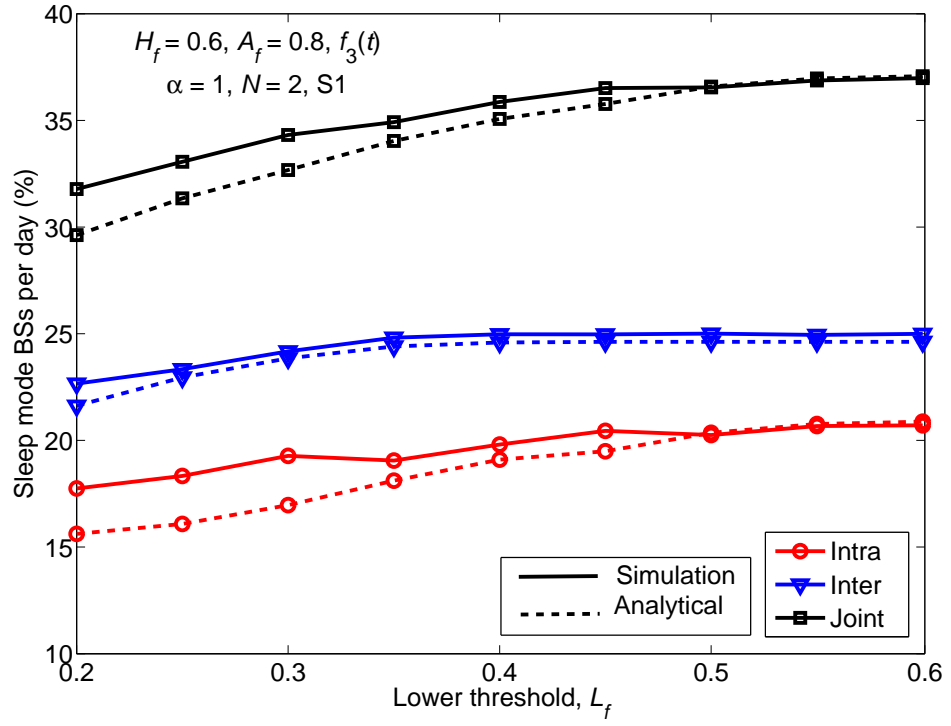
(a) With L_f.
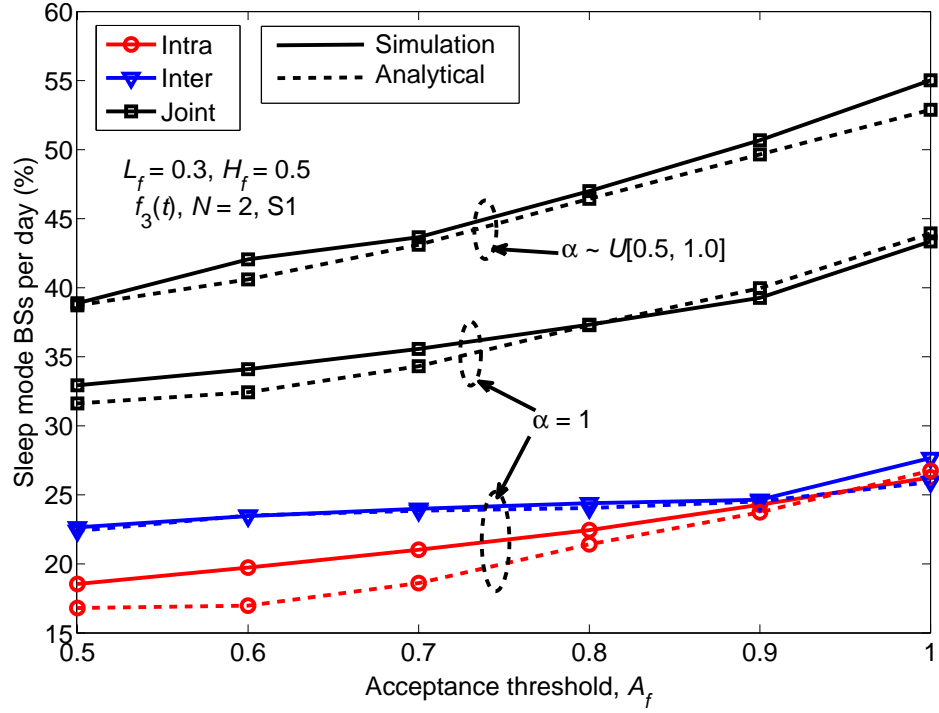
(b) With A_f.

Figure 5.3: Percentage of sleep mode BSs per day under scenario S1.
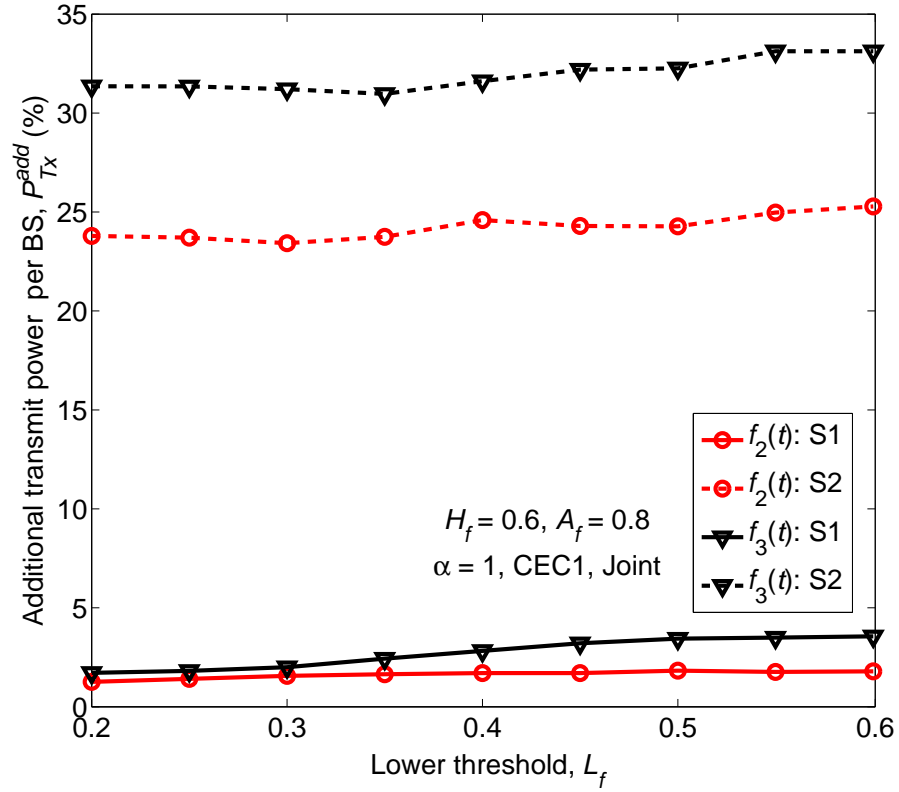
Figure 5.4: Percentage of additional transmit power per BS over a day under the joint cooperation.

5.4.2.3 Daily Energy Savings

Average net energy savings per day under joint cooperation is illustrated in Figs. 5.5 and 5.6. For the convenience of comparison, percentage of sleep mode BSs is also included in the figures. Impacts of the switching thresholds, number of RANs, rate functions, power consumption profiles of BSs and the traffic scenarios on the net energy savings are demonstrated in detail in the two figures.

From the comparison of the two graphs in Fig. 5.5, it is clearly evident that with the increase of the number of cooperating networks, a higher amount of energy savings is realizable. For instance, energy savings at $L_f = 0.7$ for the CEC1 type BSs is increased from 34% to 45% with the increase of RANs from $N = 2$ to $N = 4$. Fig. 5.5 also indicates the substantial dependence of net energy savings on the power models of BSs. For example, the CEC1 and the NEP1 models save much higher than with the CEC2 and the NEP2 models respectively. This is because, BSs of the CEC1 and the NEP1 models
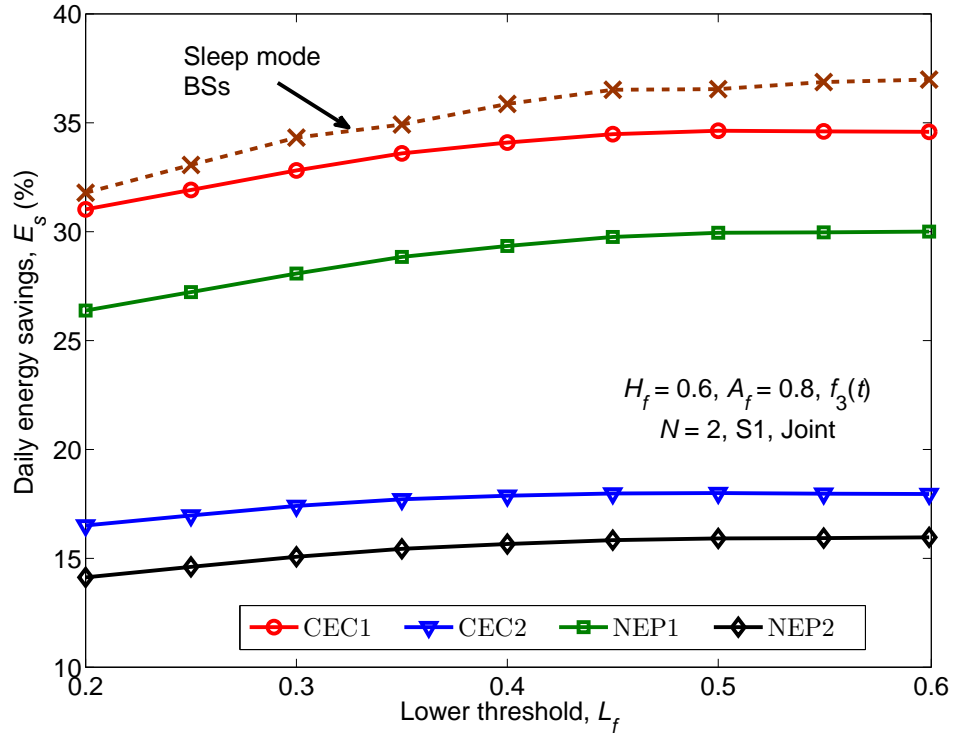
(a) $N = 2$.
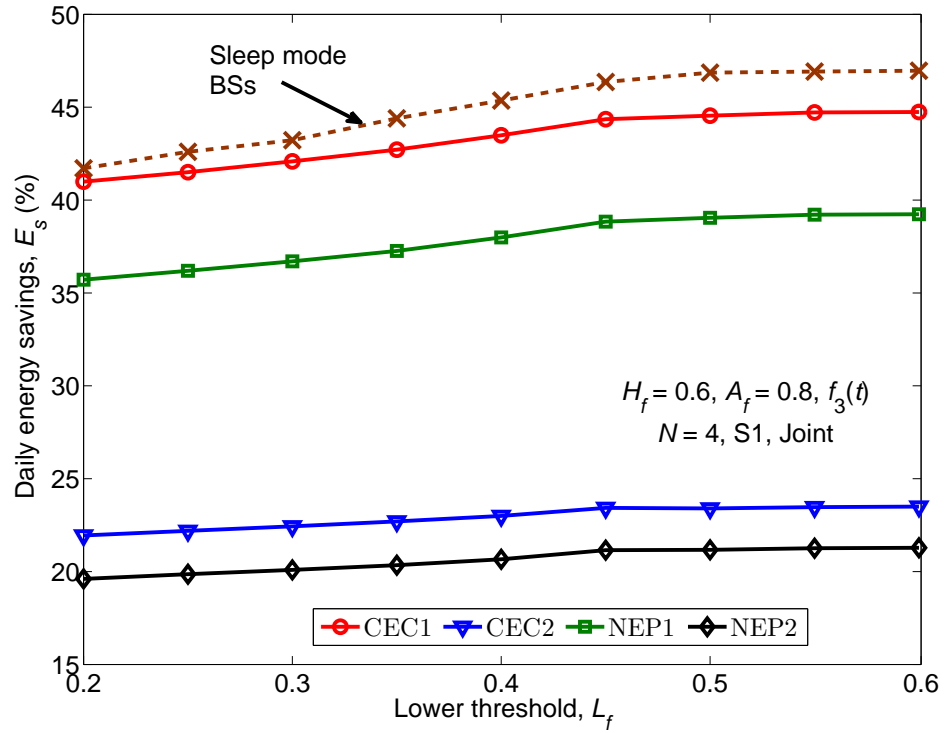
(b) $N = 4$.

Figure 5.5: Daily energy savings under the joint cooperation in scenario S1.
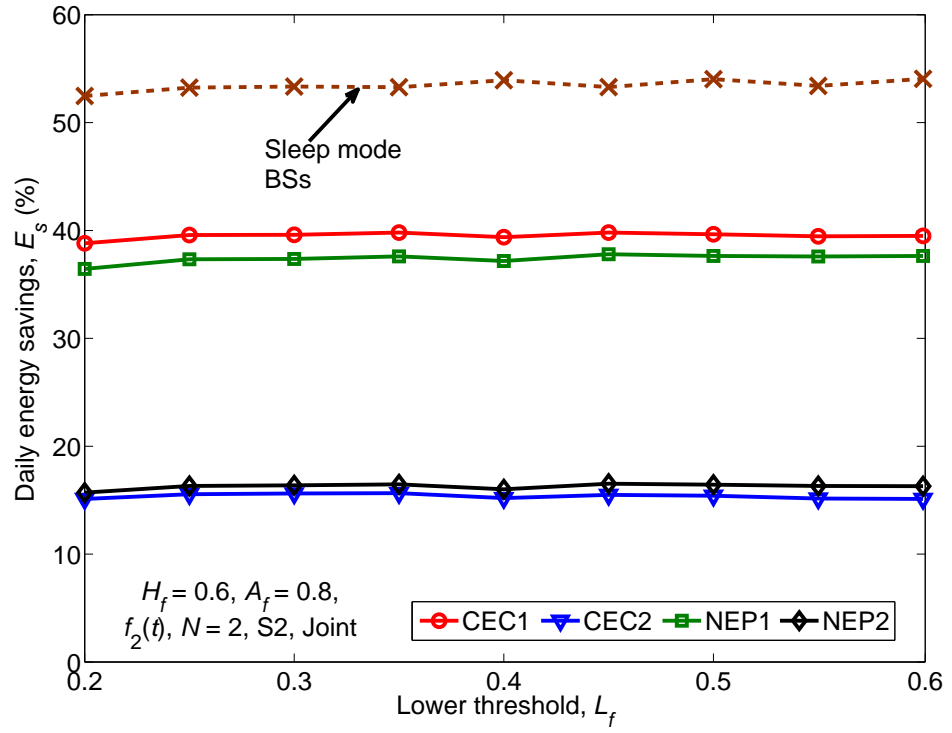
(a) $f_2(t)$.
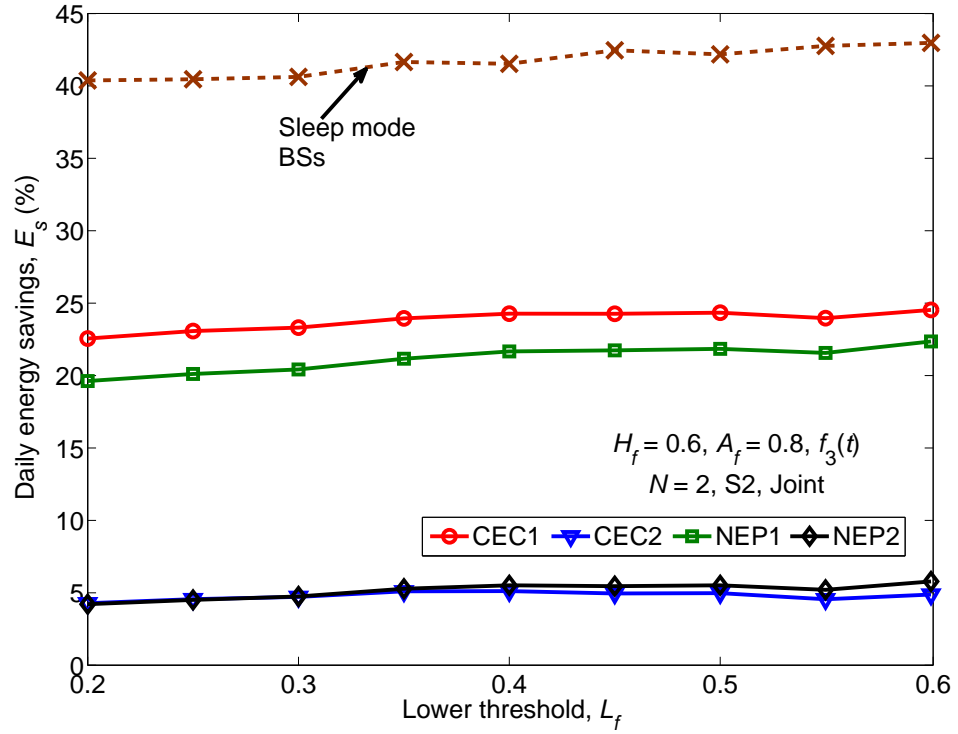
(b) $f_3(t)$.

Figure 5.6: Daily energy savings under the joint cooperation in scenario S2.
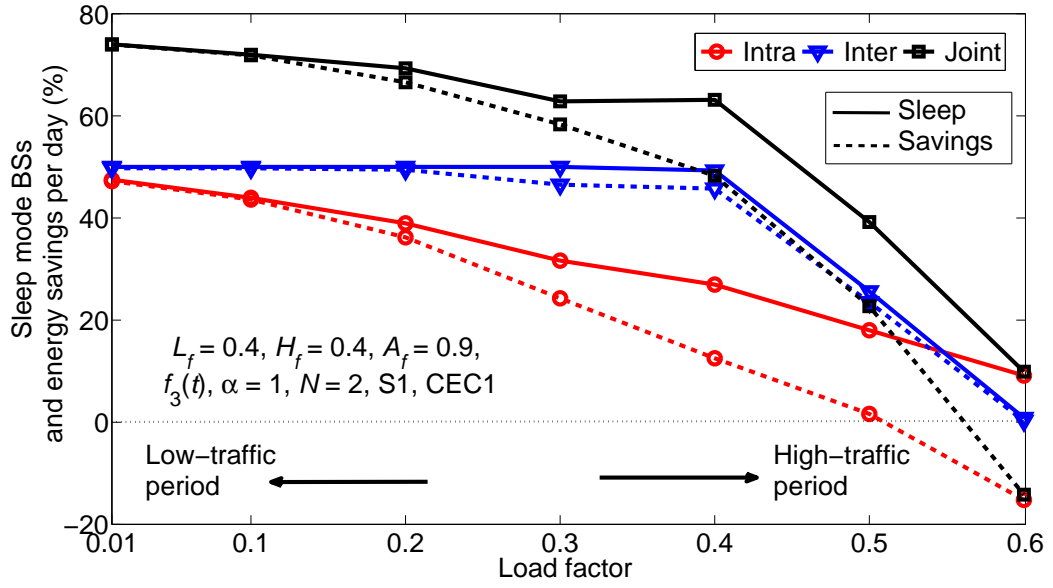
Figure 5.7: Daily energy savings under homogeneous traffic.

do not consume any energy in sleep mode, while the other two do. On the other hand, since BSs of NEP models are some extent optimized for efficient energy utilization, a network under the joint cooperation with the NEP BSs saves less than or close to that of having the CEC BSs.

Moreover, impact of the rate functions on the net energy savings can be realized from the two graphs in Fig. 5.6. Since a network with $f_2(t)$ corresponds to lower loading compared to that with $f_3(t)$, a higher number of BSs can switch into sleep mode in the former case. This results in much higher savings than that of a network with $f_3(t)$. Finally, traffic scenario can also drastically alter the degree of energy savings as evident from comparing Figs. 5.5(a) and 5.6(b). It can be noted that although a higher percentage of BSs sleeps under S2 than that of under S1, savings is much lower in case of S2. This is the direct consequence of the much higher additional transmit power in S2 as explained in Fig. 5.4.

5.4.3 Homogeneous Traffic Scenario

Net energy savings along with the percentage of sleep mode BSs under homogeneous traffic generation is evaluated and presented in Fig. 5.7. As seen, with the increase of traffic load in BSs, percentage of sleep mode BSs as well as the amount of energy savings drops steadily. This drop is slower in the lower range of traffic load (i.e., LF ≤ 0.4) becoming
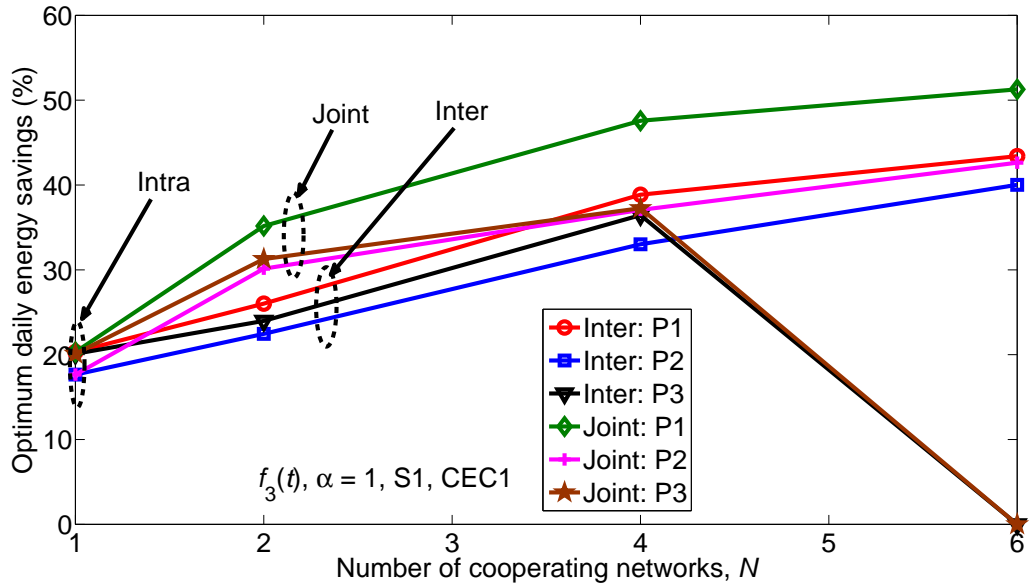
Figure 5.8: Optimal energy savings per day under scenario S1.

much faster for LF ¿ 0.4. In a low-traffic situation, much less additional transmit power is required resulting in savings close to the sleep mode BSs as observed for all the three cooperation techniques. However, as the traffic increases, additional power requirement increases significantly leading to a substantial reduction in savings. Energy savings can even be negative at higher loads (e.g., at LF $\geq$ 0.5, 0.55 and 0.6 for the intra-network, inter-network and the joint cooperation respectively).

5.4.4 Optimal Energy Savings

Using exhaustive search technique with a resolution of 0.1 for the thresholds, optimal energy savings per day under the three cooperation mechanisms is evaluated. Result corresponding to the CEC1 type BSs and inhomogeneous traffic with scenario S1 is demonstrated in Fig. 5.8. Session blocking threshold P_b^{th} equal to the original network and switching threshold $\mathcal{N}_{Sw}^{th} = 5\%$ are used for the optimizations.

Savings corresponding to $N = 1$ represents the savings from the intra-network cooperation. Thereafter, energy savings from the three optimization approaches is found increasing with N showing an exception for P3 objective. As the average number of switching also increases with the increase of N and eventually becomes greater than 5% for $N = 6$, no savings is achieved for P3. It can also be noted that up to $N = 4$, P1 optimization

realizes the highest savings, which has no restriction on the number of switching. On the other hand, P2 generates the lowest savings as it minimizes the number of switching as well. Whereas, savings from P3 varies between the savings from P1 and P2. For the sake of brevity, switching thresholds corresponding to optimal savings only for P1 optimization is presented in Table 5.5.

Table 5.5: Optimum switching thresholds for P1 optimization

Cooperation scheme	Threshold	$N = 1$	$N = 2$	$N = 4$	$N = 6$
	L_f	0.4	-	-	-
Intra-network	H_f	0.4	-	-	-
	A_f	0.8	-	-	-
	L_f	-	0.6	0.7	0.2
Inter-network	H_f	-	0.7	0.8	0.4
	A_f	-	0.9	0.9	0.8
	L_f	-	0.6	0.2	0.3
Joint	H_f	-	0.6	0.4	0.5
	A_f	-	0.8	0.9	0.7

The *cdf* of the sleep time per day of BSs under the joint cooperation is demonstrated in Fig. 5.9. Switching thresholds used for the simulations are determined from the P1 optimization having CEC1 type BSs. As expected, BSs under a higher number of cooperating networks sleep for longer durations. For example, for $\alpha = 1$, sleep times varies in the range of $[0.9, 15.6]$ hours, $[4.3, 16.7]$ hours and $[6.3, 17.4]$ hours for $N = 2, 4$ and 6 respectively. Also, the intersection of the *cdf* curves with the abscissa indicates that under the joint cooperation, all BSs in the cooperating networks have the chance to stay in sleep mode for a certain duration over a day for saving energy. With a lower traffic in the network, BSs can sleep for longer times as evident from the *cdf* curves corresponding to $\alpha \sim U[0.3, 0.8]$.

5.5   Chapter Summary

In this chapter, two alternative energy efficient distributed DSBS mechanisms by employing cooperation among multiple cellular RANs have been investigated. The formulated
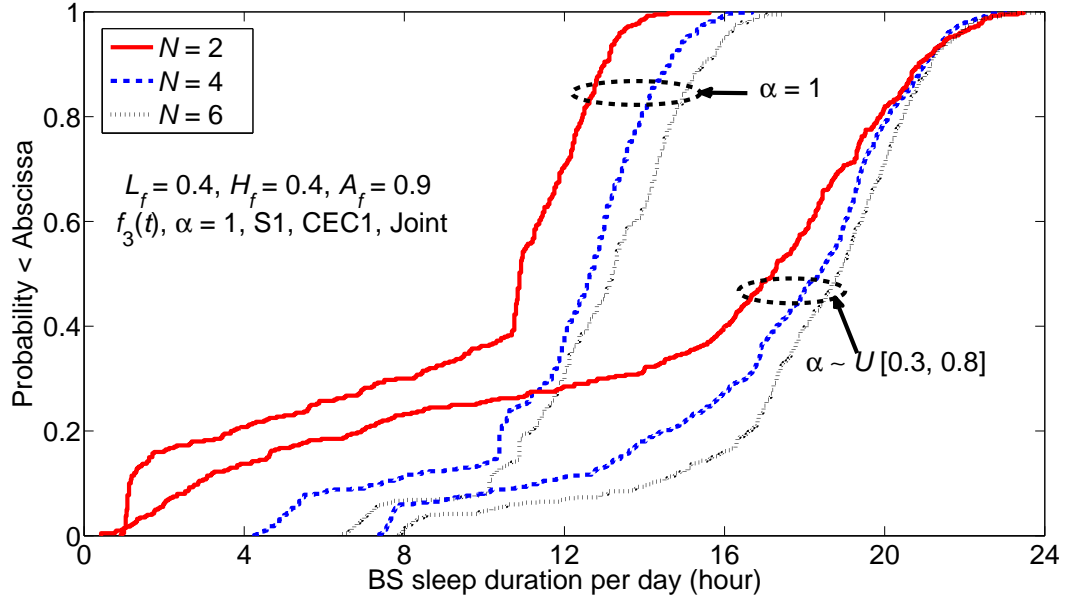
Figure 5.9: The *cdf* of sleep mode time of BSs per day under the joint cooperation in scenario S1.

cooperation mechanisms, named inter-network cooperation and joint cooperation, involve traffic-sensitive cooperation among BSs from different networks for dynamically reconfiguring the RANs with the reduced number of active BSs. It is identified that a network taking part in the joint cooperation can gain much higher savings than that of the intra-network and the inter-network cooperation only. Energy saving is found higher for higher number of cooperating networks. Another notable finding is that a higher number of BSs can switch to sleep mode in a network having traffic diversity in both time and space compared to that in a network with only temporal diversity. However, energy savings in the former scenario is much less than that of the second scenario due to much higher additional transmit power requirement. In addition, optimal energy savings and corresponding switching thresholds under various optimization objectives are evaluated. Furthermore, analytical results are found closely following the simulation results.

This chapter and the last one have explored the BS switching mechanisms for saving energy. In search of energy saving alternative techniques by dimensioning cellular RANs with a better granularity, the next chapter introduces the concept of dynamic switching of sectors in the underutilized BSs .

Chapter 6

Centralized Dynamic Sectorization and Base Station Switching

Despite the availability of many proposals on BS switching based energy saving cellular networks, its practical implementation has many challenging issues [5], [36], [43]. Frequent switching in BSs, potential creation of coverage holes, reduced battery life of UEs for increased uplink transmit power and highly dynamic interference from coverage adjustments are some of the greatest challenges. This implies the necessity of having highly intelligent, fast and stringent coordination among network entities. This chapter investigates for an alternate solution with less complexity, yet effective for saving energy. In light of this, this chapter proposes dynamic sectorization (DS) of BSs for reconfiguring BSs using fewer sectors. Qos requirements, namely, user data rates, service continuity and network coverage are also maintained. On the other hand, a centralized version of DSBS is also proposed in this chapter. Generalized energy saving optimization problems are formulated for the schemes, which are challenging combinatorial problems. Therefore, low complexity greedy style heuristic algorithms are presented. Performance of the schemes is evaluated using Monte Carlo simulations. Effectiveness of the proposed EWMA-based predictor in reducing the number of network reconfiguring events under these schemes is also presented. The content of this chapter has contributed to [163], [164] and [165].

6.1 Energy Efficient Dynamic Sectorization

This section presents the proposed traffic-aware energy saving DS technique in the context of LTE systems. System model, proposed algorithms and simulation results are also explained here below.

6.1.1 Network Layout

Proposed DS considers the downlink of a multi-cell cellular network having a set of BSs $\mathcal{B} = \{\mathcal{B}_1, \mathcal{B}_2, ..., \mathcal{B}_{|\mathcal{B}|}\}$ and covering an area $\mathcal{A} \subset \mathbb{R}^2$. Let $\mathcal{S}_i$ be the number of sectors in BS $\mathcal{B}_i$. Orthogonal frequency bands are assumed for all the $\mathcal{S}_i$ sectors of BS $\mathcal{B}_i, \forall i \in (1, 2, ..., |\mathcal{B}|)$. On the other hand, it is considered that the same frequency bands are reused among BSs.

6.1.2 System Model

In the conventional cellular networks, irrespective of traffic level, all the sectors in a BS are left in active mode for all time expecting that during the *worst-case* peak-traffic times, all of them would be required for supporting its UEs. Thus, during low traffic times, a substantial amount of energy is being wasted, which could be saved by switching some of the sectors into sleep mode. This is the core idea of the proposed DS scheme as demonstrated in Fig. 6.1. The patterns shown in the figure represent the coverage areas of sectors corresponding to the different orthogonal frequency bands.

In this particular example, it is assumed that the original network is provisioned to have $\mathcal{S}_i = 6, \forall i \in (1, 2, ..., |\mathcal{B}|)$ sectors. Hence, irrespective of traffic level, number of active sectors in all BSs remains $S_{i,ON}(t) = 6, \forall t \geq 0, \forall i \in (1, 2, ..., |\mathcal{B}|)$ as demonstrated in Fig. 6.1(a). Note that in practice, initial number of sectors may vary from BS to BS. On the other hand, under the proposed DS, with the variation of traffic generation, number of active sectors is adaptively adjusted for matching the instantaneous demand, i.e., $1 \leq S_{i,ON}(t) \leq \mathcal{S}_i, \forall i \in (1, 2, ..., |\mathcal{B}|)$. As illustrated in Fig. 6.1(b), most of the BSs at low-traffic times are operated with only few sectors keeping others in sleep mode and thus, energy savings is achieved.

Remarks: Remaining active sectors need to adjust (i.e., expand or shrink) their transmis-
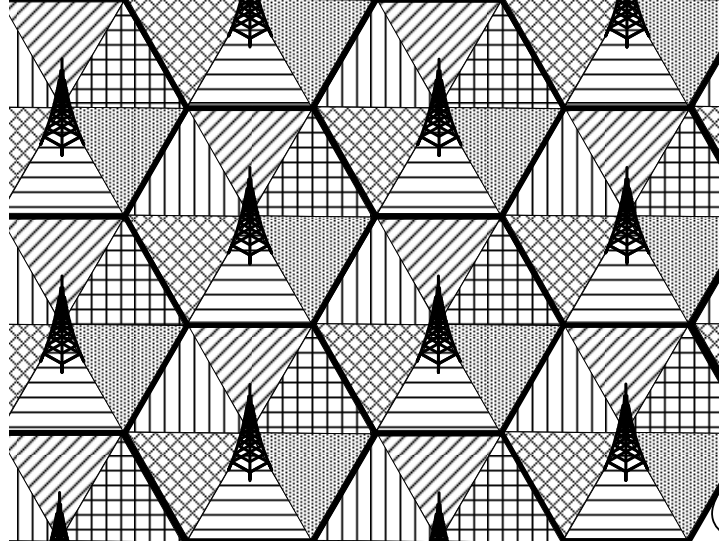
(a) Peak-traffic time. All the six sectors in each BS are in active mode.
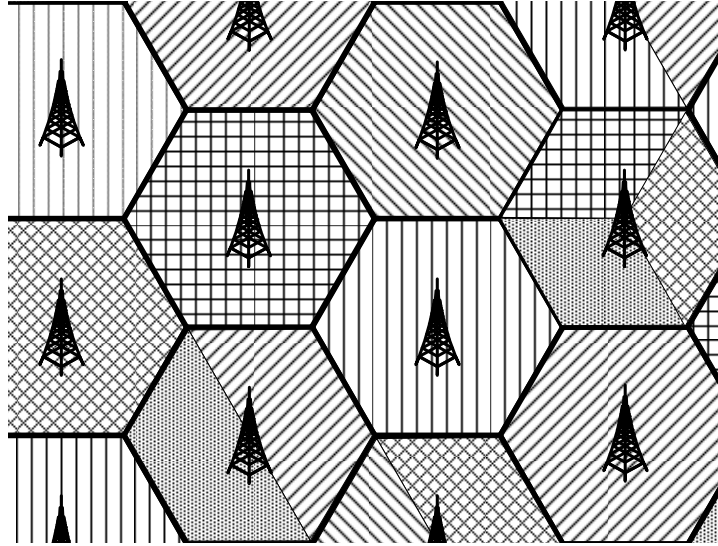
(b) Low-traffic time. Many BSs are reconfigured with fewer sectors.

Figure 6.1: Concept of the proposed dynamic sectorization scheme. Each pattern corresponds to a frequency band orthogonal to the others.

sion beamwidth for covering the entire area of a BS. Due to the utilization of the same amount of transmit power, this beamwidth adjustment will result in the change in the antenna gain as discussed later in Section 6.1.6. One of the simple and robust techniques for achieving this adjustment is to use adaptive smart antenna technology employing linear

antenna arrays [103]. Through the adjustment of the length and the spacing of the antenna array elements as well as the phase of their input currents, main beam of the array can be steered and shaped as desired and thus, it is possible to cover a sector of desired size. Alternatively, BSs can be equipped with multiple sets of antennas, where each set can correspond to a certain number of sectors. Based on the number of the required sectors, one of these sets can be activated, while others are left inactive. Moreover, recent development of reconfigurable beam antennas for BSs with beam fanning capability (discussed in Chapter 3) backs the proposed DS scheme as a practically implementable solution for energy savings [102].

6.1.3 Problem Formulation

The objective of the DS scheme is to employ the optimum set of sectors in all BSs $\mathbf{S}_{ON} = \{\mathbf{S}_1, \mathbf{S}_2, ..., \mathbf{S}_{|\mathcal{B}|}\}$ resulting a minimum operating power (i.e., maximum energy savings), while maintaining QoS. Here, $\mathbf{S}_i = \{s_1, s_2, ..., s_{S_{i,ON}}\}$ is the set of active sectors in $\mathcal{B}_i$. Following optimization problem can thus be formulated

$$\underset{\mathbf{S}_1, \mathbf{S}_2, ..., \mathbf{S}_{|\mathcal{B}|}}{\arg\min} \sum_{i=1}^{|\mathcal{B}|} \sum_{s \in \mathbf{S}_i} \left[(1 - \delta_i) L_f^{i,s}(t) P_{i,Op} + \delta_i P_{i,Op} \right] \tag{6.1}$$

$$s.t., \quad P_{i,b}(t) \leq P_b^{th}, i = 1, 2, ..., |\mathcal{B}|, \forall t \tag{6.2}$$

$$P_{i,out}(t) \leq P_{out}^{th}, i = 1, 2, ..., |\mathcal{B}|, \forall t \tag{6.3}$$

$$R_u^{(a)}(t) \geq R_u, u = 1, 2, ..., \sum_{i=1}^{|\mathcal{B}|} \sum_{s=1}^{\mathcal{S}_i} U_s(l_i, t), \forall t \tag{6.4}$$

$$\bigcup_{s \in \mathbf{S}_i} \mathcal{A}_{i,s}(t) = \mathcal{A}_i, i = 1, 2, ..., |\mathcal{B}|, \forall t \tag{6.5}$$

$$\sum_{u=1}^{U_s(l_i, t)} \beta_u^{i,s}(t) \leq \beta_{Tot}^{i,s}, i = 1, 2, ..., |\mathcal{B}|, \forall s \in \mathbf{S}_i, \forall t \tag{6.6}$$

$$\sum_{u=1}^{U_s(l_i, t)} P_u^{i,s}(t) \leq P_{i,Tx}, i = 1, 2, ..., |\mathcal{B}|, \forall s \in \mathbf{S}_i, \forall t \tag{6.7}$$

Here, l_i is the location of $\mathcal{B}_i$ and $L_f^{i,s}(t)$ is the LF of its sth sector, $P_{i,b}(t)$ and $P_{i,out}(t)$ are the session blocking and session outage probabilities respectively, P_b^{th} and P_{out}^{th} are the target blocking and outage probabilities respectively, $R_u^{(a)}(t)$ and R_u are the uth UE's achievable data rate and the required data rate respectively, $\mathcal{A}_i$ and $\mathcal{A}_{i,s}$ are the coverage

area of $\mathcal{B}_i$ and its sth sector respectively, $P_u^{i,s}(t)$ is the downlink transmit power for u^{th} UE, $P_{i,Op}$ and $P_{i,Tx}$ are the power profile parameters corresponding to a single sector, and $U_s(l_i,t)$ and $\beta_{Tot}^{i,s}$ are the total number of UEs and RBs in sector s of $\mathcal{B}_i$ respectively. Constraints (6.2), (6.3), (6.4) and (6.5) respectively guarantee the session blocking, session outage, UE data rates and the network coverage within acceptable limits. Finally, (6.6) and (6.7) imply that the required total number of RBs and total transmit power in BSs can not exceed their respective maximum limits.

6.1.4   DS Algorithm

The above optimization problem in (6.1) can be considered as a user association problem as it evaluates $L_f^{i,s}, \forall s \in (1,2,...\mathcal{S}_i), \forall i \in (1,2,...,|\mathcal{B}|)$ such that the optimal set of sectors $\mathbf{S}_{ON}$ is left active. Now, for a given $\mathbf{S}_{ON}$, the objective function in (6.1) is convex in $L_f^{i,s}, \forall s \in (1,2,...\mathcal{S}_i), \forall i \in (1,2,...,|\mathcal{B}|)$. However, for variable $\mathbf{S}_{ON}$, it becomes nonconvex. Thus, (6.1) is a challenging combinatorial problem with an exponentially increasing search space $\mathcal{O}(2^{\sum_{i=1}^{|\mathcal{B}|} \mathcal{S}_i})$. Therefore, a centralized greedy style heuristic algorithm with lower complexity is proposed here.

Proposed algorithm employs two-level triggering to initialize the traffic distribution process for associating UEs with the reduced number of sectors. First, if the predicted LF of the total network $\widehat{L}_{net}(t)$ at time t falls below a certain threshold L_{th}, a central coordinator initializes the event. Thereafter, each BS uses its own criterion for initializing the event for itself. The algorithm takes one BS at a time, say, $\mathcal{B}_i = \mathcal{B}_1$ and assumes that all $\mathcal{S}_i = \mathcal{S}_1$ sectors are active, i.e., $\mathbf{S}_i = \mathbf{S}_{i,all} = \{1,2,...,\mathcal{S}_i\}$. Let $L_i(t)$ be the actual LF of $\mathcal{B}_i$ at time t. Now, if $L_i(t) < (\mathcal{S}_i - 1)/\mathcal{S}_i$, traffic distribution by associating UEs with the reduced number of sectors is triggered. At first, $\mathcal{S}_i$ sectors of $\mathcal{B}_i$ are ordered in the ascending order of their LFs. Then the algorithm iteratively eliminates sectors from $\mathbf{S}_i$ one-by-one starting from the sector with the lowest LF. This policy of imposing the higher priority to the sectors with lower LFs in distributing traffic reduces the number of intra-cell handoffs. Each time the algorithm is successful in associating UEs of one sector (say, sector s), utility function $U_{i,DS}(t) = P_i^{(s-)}(t)/P_i^{(s+)}(t)$ is evaluated, where $P_i^{(s+)}$ and $P_i^{(s-)}$ are the operating power of $\mathcal{B}_i$ with and without sector s respectively. Now if (6.2)-(6.7) are met and $U_{i,DS}(t) < \eta_{DS}$ ($\eta_{DS} \in [0,1]$), then sector s is removed from $\mathbf{S}_i$. Here, $U_{i,DS}(t) < 1$ implies potential energy savings from switching of sector s into sleep mode.

Iteration continues as long as $L_i(t) < (n_i - 1)/\mathcal{S}_i$, where n_i is the number of active sectors from the last iteration. Sectors in the final $\mathbf{S}_i$ are kept active with essential beamwidth adjustments. Other sectors in $\mathbf{S}_{i,all} \setminus \mathbf{S}_i$ are switched into sleep mode. The algorithm then proceeds to the next BS $\mathcal{B}_{i+1}$, evaluates $\mathbf{S}_{i+1}$ and continues to the last BS. Pseudo code of the DS algorithm is presented in Table 6.1.

Computational complexity of the proposed algorithm is $\mathcal{O}(N_B N_S^2 N_U)$, while for the original optimal exhaustive search technique is $\mathcal{O}(N_U 2^{N_B N_S})$. Here, N_B, N_S and N_U are the number of BSs, sectors in each BS and UEs of the network respectively. On the other hand, signaling overhead of the algorithm in terms of the number of messages is $(N_U + 2N_B)$.

6.1.5 Interference Estimation

Let $\mathcal{I}_{u,intra}^{i,s}$ and $\mathcal{I}_{u,intra}^{i,s}$ be the intra-cell and inter-cell interference experienced by u^{th} UE located in s^{th} sector of $\mathcal{B}_i$. Due to the use of orthogonal frequency bands, $\mathcal{I}_{u,intra}^{i,s} = 0$. On the other hand, one way of estimating inter-cell interferenc $\mathcal{I}_{u,inter}^{i,s}$ is to keep track whether the same RB is simultaneously assigned in the interfering BS(s). Thus, the central coordinator needs to have the access to a RB allocation database maintained for each BS, which may create a large overhead on the system. Therefore, for reducing the overhead, inter-cell interference is evaluated using a RB collision based model [148], [166]. In the collision based model, only LF and frequency band information of each sector is required.

Let $L_f^{i,s}$ and $L_f^{j,c}$ be the LFs of two interfering sectors from $\mathcal{B}_i$ and $\mathcal{B}_j$ respectively. In this chapter, no coordination among BSs for multi-user scheduling to RBs is considered. Under such non-coordinated case, the indices of RBs allocated by a BS to its UEs appear as random to the neighboring BSs [166], [167]. Thus, it can be assumed that BSs select their RBs from the available pool in a random fashion [167]. Under such scenario, the upper bound of the probability of collision between two RBs becomes [166]

$$P_C(L_f^{i,s}, L_f^{j,c}) = L_f^{i,s} L_f^{j,c} \tag{6.8}$$

Total inter-cell interference $I_{u,inter}^{i,s}$ is then as follows

$$I_{u,inter}^{i,s} = \sum_{c=1}^{\mathcal{C}} P_C(L_f^{i,s}, L_f^{j,c}) P_{u,Rx}^{(c)} \tag{6.9}$$

Table 6.1: Centralized DS algorithm

1:	**If** $\widehat{L}_{net}(t) < L_{th}$
2:	**For** $i = 1$ to $|\mathcal{B}|$
3:	Initialize: $\mathbf{S}_i = \mathbf{S}_{i,all}, n_i = |\mathbf{S}_i|$
4:	**If** $L_i(t) < (n_i - 1)/\mathcal{S}_i$
5:	Find $\mathbf{S}_i^* = \{s_1^*, s_2^*, ..., s_{n_i}^*\}$ reordering $\mathbf{S}_i$, *s.t.*, $L_m^* \geq L_n^*, m > n$
6:	Set $q = 1$
7:	Associate all $U_{s_q^*}(l_i, t)$ UEs with the other sectors $\mathbf{S}_i \setminus \{s_q^*\}$ and calculate $U_{i,DS}(t)$
8:	**If** (6.2)-(6.7) are met and $U_{i,DS}(t) < \eta_{DS}$
9:	Set $\mathbf{S}_i = \mathbf{S}_i \setminus \{s_q^*\}$ and $n_i = n_i - 1$
10:	**Else** Set $q = q + 1$
11:	**If** $q <= n_i$, Go to Step 7, **End If**
12:	**End If**
13:	**If** $n_i > 1$, Go to Step 4
14:	**Else** Set $i = i + 1$, **End If**
15:	**End If**
16:	**End For**
17:	**End If**

where $\mathcal{C}$ is the number of colliding sectors from the neighboring BSs, which depends on the cell layout and the number of sectors in each BS; and $P_{u,Rx}^{(c)}$ is the received power at u^{th} UE in $\mathcal{B}_i$ from the colliding sector c.

6.1.6 Antenna Radiation Pattern

Antenna pattern is given by [142]

$$A(\theta) = -min\left\{12\left(\frac{\theta}{\theta_c}\right)^2, A_m\right\} \quad (6.10)$$

where $-180^0 \leq \theta \leq 180^0$, θ_c and A_m are the angle between the direction of interest and the antenna boresight, 3 dB beamwidth and the maximum attenuation respectively. Omnidirectional and 3-sector antennas are more popular in practice, and the more recent trend is in developing 6-sector antennas [102]. Nevertheless, for investigating various possible configurations, omnidirectional to 6-sector antennas are considered. Now, with the decrease of beamwidth by a factor of two, antenna gain roughly increases by 3 dB and vice versa [92], [168]. Thus, for the set of sectors $S = [2\ 3\ 4\ 5\ 6]$, antenna parameters can be approximated as follows: $\theta_c = [120\ 65\ 55\ 45\ 33]^0$, $A_m = [18\ 20\ 21\ 22\ 23]$ dB and antenna gain $= [13\ 15\ 16\ 17\ 18]$ dBi [92], [142], [168]. For omnidirectional antenna, $A(\theta) = 0$ dB [66] and antenna gain = 10 dBi [71] are taken.

6.1.7 Performance Evaluation

6.1.7.1 Simulation Setup

System performance is evaluated using Monte Carlo simulations. Simulated network covers an area served by 64 macrocell BSs deployed with hexagonal layout having an inter-site distance equal to $\sqrt{3} \times 500$ m, RBs per sector = 25 and transmit power per sector = 40 dBm. Other link budget parameters are taken same as those used in simulating the distributed DSBS scheme in Chapter 4. Antenna parameters are set according to the discussion in Section 6.1.6.

Three classes of real-time CBR services of data rates equal to 512 kbps, 768 kbps and 1024 kbps are considered. New sessions from all the classes arrives following a Poisson process with arrival rate λ and a constant session duration equal to 3 minutes. Variable number of RBs, calculated using (4.4)-(4.5), is allocated to the admitted sessions for maintaining their data rates, which remains dedicated for the session duration. No downlink power control is considered. On the other hand, for 6-sector BSs, four different sector switching patterns designated as R_{6-1}, R_{631}, R_{63} and R_{61} are investigated. R_{6-1} includes all possible combinations of sectors, while the other three allow only regular sector configurations. Thus, the set of configurable sectors under these schemes are $\{1, 2,...,6\}$, $\{1, 3, 6\}$, $\{3, 6\}$ and $\{1, 6\}$ respectively. Switching patterns for 3-sector BSs can be defined in the same way. Unless otherwise specified, traffic parameter $\alpha(l_i) = 1$, R_{6-1}, $P_b^{th} = 1\%, P_{out}^{th} = 1\%$, $\eta_{DS} = 1$, $L_{th} = 1$, $\delta_i = 0.7$, $\mathcal{S}_i = 6$, $p_{i,op}^s = 0$, $\{g_i = 21.45, h_i = 354.44\}$ [52], $\forall s \in (1, 2, ..., \mathcal{S}_i)$, $\forall i \in (1, 2, ..., |\mathcal{B}|)$, uniformly dis-

tributed UEs and homogeneous session generation are used for the presented results.

6.1.7.2   Sleep Mode Sectors and Energy Savings

Average percentage of sleep mode sectors and net energy savings with the session arrival rate λ are presented in Fig. 6.2. The 95% confidence intervals are also shown in the figures. With the increase of λ, higher number of sectors are required for serving UEs and hence, lower savings is achieved as evident from Fig. 6.2(b). The difference between the sleep node sectors and the net energy savings is due to $\delta_i = 0.7$. Here, $\delta_i = 0.7$ corresponds to the NEP type BSs in which the change in LFs of sectors due to reassociation of UEs is reflected in the operating power of BSs. If BSs were of CEC type (i.e., $\delta_i = 1$), then the sleep mode sectors and energy savings would have been equal. In addition, from the three points marked on the lines for 512 kbps, it can be identified that the difference is higher in the mid-range of λ and diminishing on both sides.

Besides, impact of single-cell and multi-cell scenarios, and UE data rates is also demonstrated in Fig. 6.2. In case of a multi-cell scenario, with the increase of λ and reduced number of sectors in BSs, increasingly higher amount of inter-cell interference is experienced by UEs leading to the requirement of higher number of RBs. Consequently, less number of sectors are allowed to switch into sleep mode and less savings is achieved. However, because of the absence of inter-cell interference in a single-cell case, a BS can afford a higher number of sleep mode sectors, while maintaining QoS. Furthermore, it is evident that a higher savings is possible for a network having UEs with a lower data rate requirement. For example, at $\lambda = 0.05$ of single-cell case, around 36%, 25% and 3% energy savings are achieved for 512 kbps, 768 kbps and 1024 kbps respectively. For higher data rates, higher number of RBs and thus, higher amount of transmit power are required. These two constraints together increase the session blocking and outage probabilities, and hence, more sectors are required to keep active for maintaining QoS resulting in reduced energy savings.

Impact of various switching patterns on the energy saving performance for 6-sector BSs under both homogeneous and inhomogeneous traffic scenario is presented in Figs. 6.3 and 6.4 respectively. From Fig. 6.3, R_{6-1} can be identified to achieve the highest energy savings as it can reconfigure BSs with any number of sectors between one to six. This is also confirmed from the daily savings illustrated in Fig. 6.4. It is also found that R_{61}
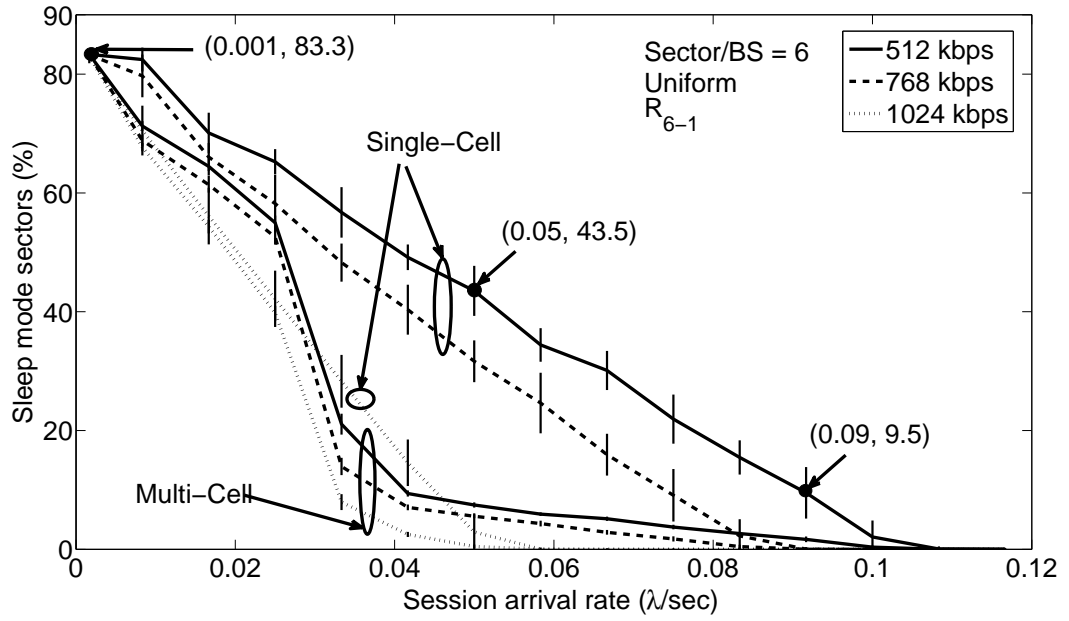
(a) Sleep mode sectors.
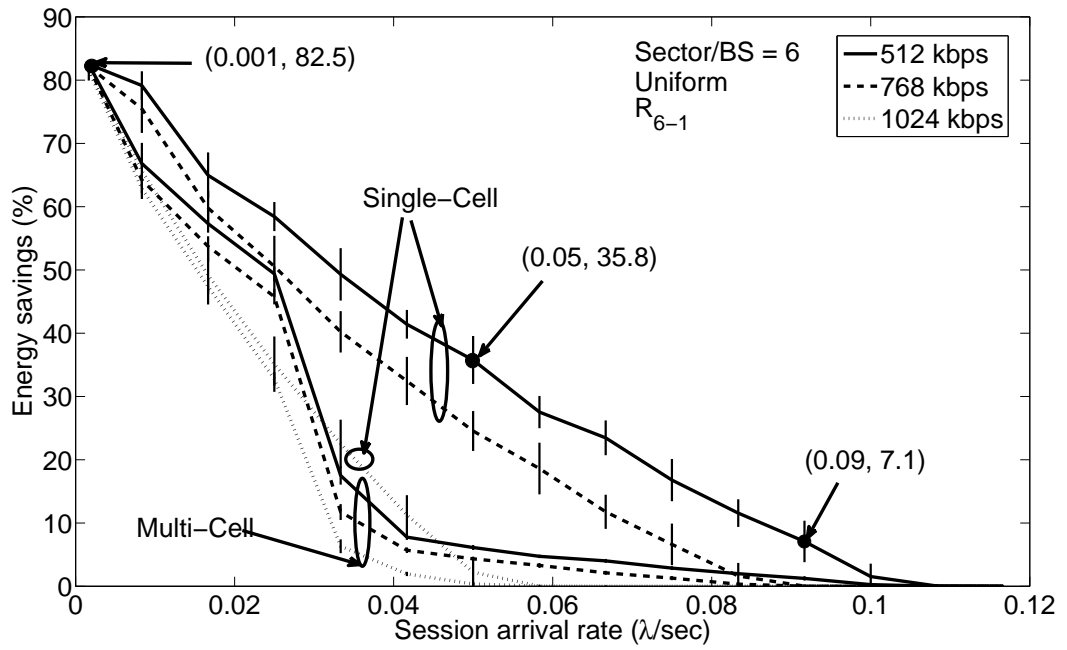
(b) Net energy savings.

Figure 6.2: Sleep mode sectors and net energy savings for single-cell and multi-cell scenarios under DS.
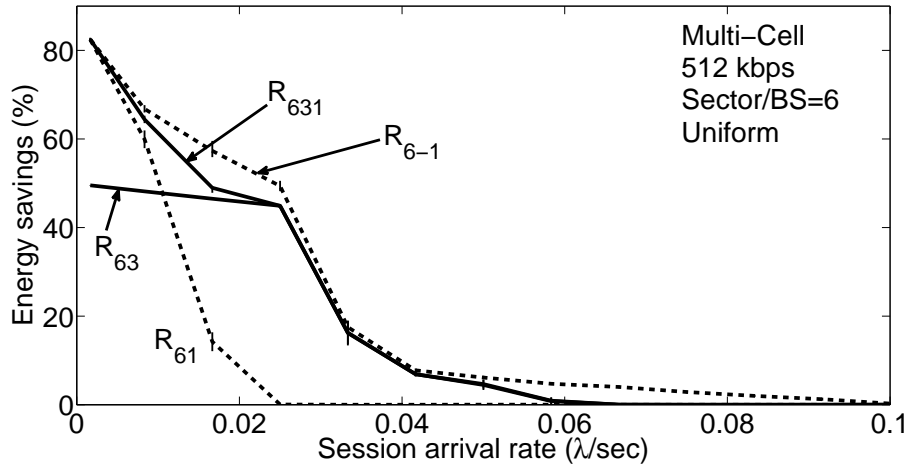
Figure 6.3: Energy savings under various switching patterns.
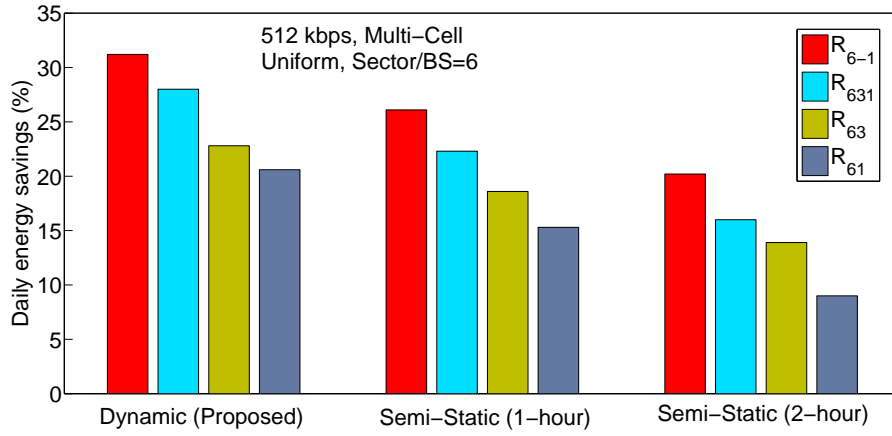
Figure 6.4: Comparison with the semi-static schemes.

achieves the lowest daily savings. Comparison of the proposed DS with the semi-static sector switching schemes is also included in Fig. 6.4. Under the semi-static schemes, sector switching decisions are made based on the hourly average peak traffic load, and the number of sectors is left unchanged for a longer time interval. As evident from the figure, the longer the sector switching interval, the lower is the energy savings.

Fig. 6.5 illustrates the impact of UE distributions and the number of sectors $\mathcal{S}_i$ on the energy savings. As shown, a network having Gaussian distributed UEs in BSs saves much more than that of having uniformly distributed UEs. In case of Gaussian distribution, a higher number of UEs are located near BSs experiencing a lower path loss. Therefore, many UEs require less number of RBs and thus, satisfactory QoS can be provided by
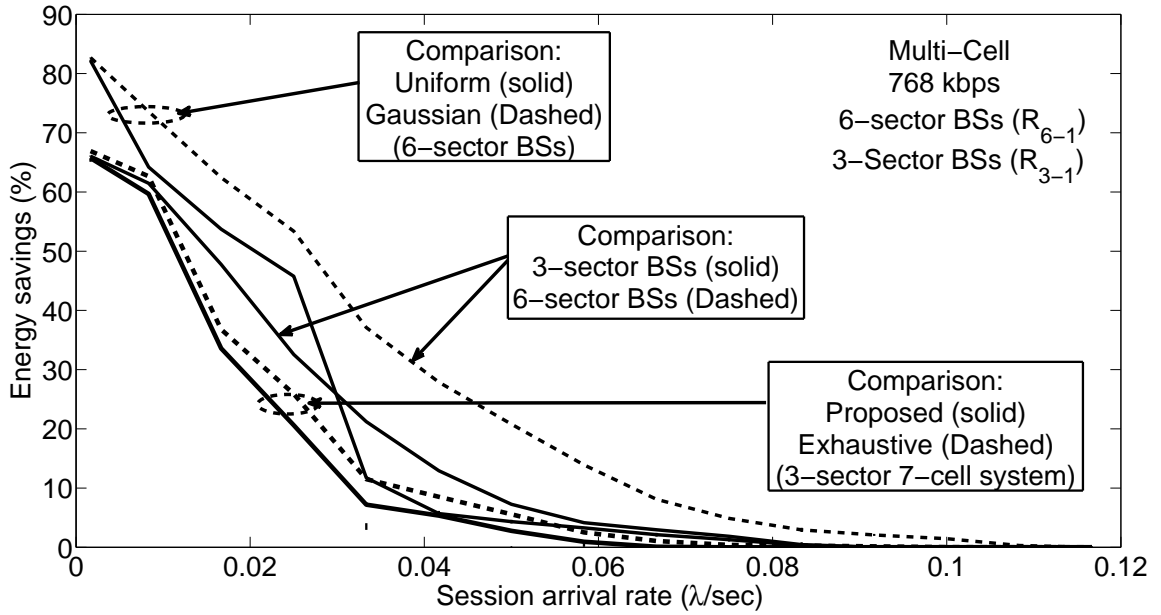
Figure 6.5: Impact of UE distribution and sector number on net energy savings under DS.

keeping fewer sectors active leading to higher savings. On the other hand, BSs with a higher number of sectors provide a higher number of options for associating UEs to the other sectors, which increases the sleeping probability of sectors as well as the energy savings. As seen in the figure, for the Gaussian distributed UEs, over 80% energy savings is possible from a network with 6-sector BSs, while it is around 65% for the case of 3-sector BSs.

Furthermore, for evaluating the performance gap of the proposed algorithm with that of the optimal exhaustive search, a small scale 7-cell system with 3-sector BSs is considered. Exhaustive search is then used for evaluating the optimal set of sectors out of the 2^{21} possible combinations of this system and the corresponding result is presented in Fig. 6.5. As evident from the figure, the performance gap between the proposed algorithm and the optimal exhaustive search is found less than 5%.

6.1.7.3 Spectral Efficiency and RB Utilization

The ratio of the achievable SE in the proposed scheme to that in the original network is illustrated in Fig. 6.6, whereas Fig. 6.7 demonstrates the ratio of the required RBs per UE. For smaller λ, many sectors are turned off, which results in lower antenna gains and higher inter-cell interference leading to lower SINR and hence, lower achievable SE than
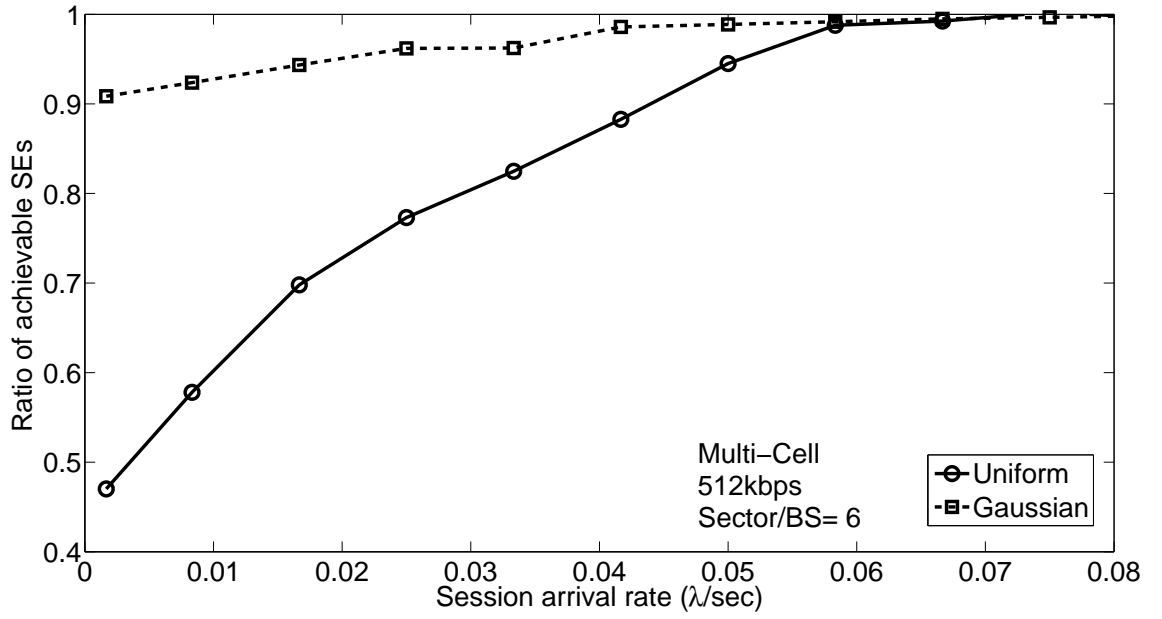
Figure 6.6: Impact on the achievable spectral efficiency under DS.
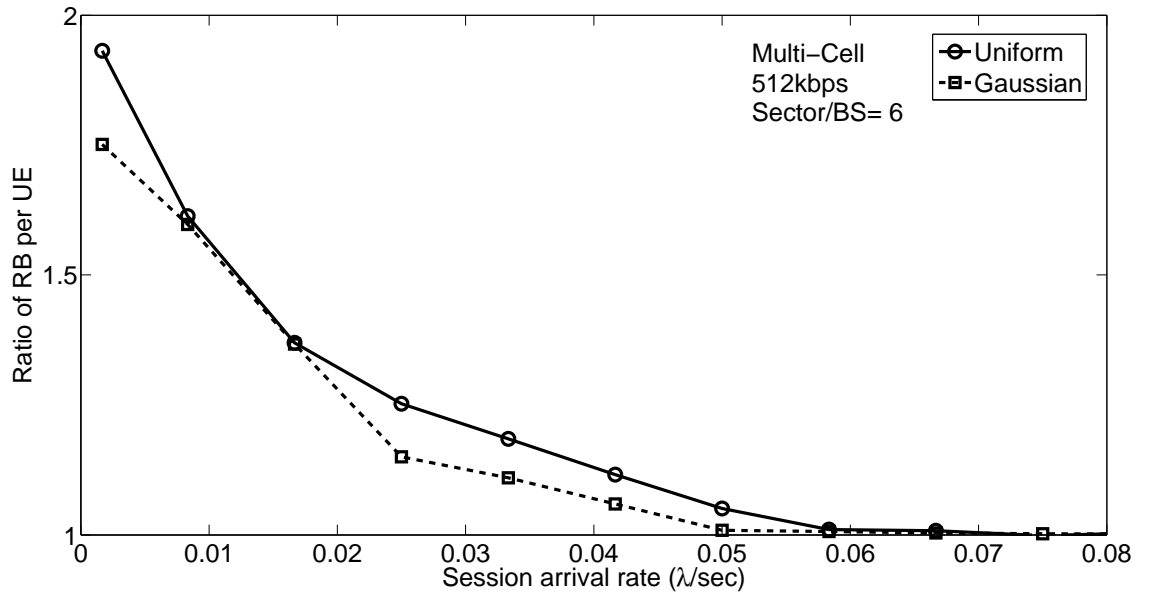
Figure 6.7: Impact on the RB requirement per UE under DS.

that in the original network. Consequently, a higher number of RBs per UE is required for maintaining user data rates. This leads to a SE ratio less than one and RB ratio greater than one in the lower range of λ. However, with the increase of λ, both the ratios approach to one due to the diminishing number of switched off sectors.

On the other hand, in case of Gaussian distribution, a higher number of UEs are located near BSs than that in uniformly distributed case. Thus, path loss for many UEs is relatively lower and consequently, the impact of decreasing antenna gain and increasing interference is not as dominant as in uniform case. Therefore, the reduction in SE as well as the increment in RB requirement per UE is much lower in the case of Gaussian distributed scenario, which is also evident from the Figs. 6.6 and 6.7.

6.1.8   An Algorithm for Distributed Implementation of DS

Here, an algorithm for distributed implementation of DS is presented. Under this distributed scheme, it is essential to have proper communications among neighboring BSs for exchanging information required for executing the algorithm, while a central coordinator is required for initializing the DS event. The algorithm is implemented in each BS requiring no assistance from the central coordinator. At each algorithm execution instance, the central coordinator initiates the DS procedure if $\widehat{L}_{net}(t)$ falls below L_{th}. After that, according to a pre-defined sequence, BSs sequentially evaluate their optimal sets of active sectors, $\mathbf{S}_i, \forall i \in (1, 2, ..., |\mathcal{B}|)$. Here, each BS initializes its algorithm assuming all of its sectors are in sleep mode, and then iteratively add sectors one-by-one until a BS finds the required set of sectors for supporting its UEs. Unlike the centralized DS algorithm, the sectors with the higher LFs are prioritized to be added in the optimal set with the same purpose of limiting the number of intra-cell handoffs. Once a BS evaluates its optimal set of sectors, information regarding its frequency bands and corresponding LFs are forwarded to the neighboring BSs for using in their optimal set calculations. Pseudo code of the algorithm is presented in Table 6.2.

Performance of the distributed DS can also be evaluated in a similar way of the centralized DS presented earlier. Considering a negligible energy requirement for signaling overhead, performance of both the schemes is found very close. Therefore, for the sake of brevity, no additional result is presented for this distributed DS scheme.

6.2   Centralized Dynamic Switching of Base Stations

DSBS scheme presented in Chapter 4 achieves dynamic switching of BSs by implementing distributed inter-BS cooperation. In this chapter, a centralized DSBS scheme is proposed, which is then jointly applied with the centralized DS in Chapter 7.

Table 6.2: Algorithm for distributed DS

1:	**If** $\widehat{L}_{net}(t) < L_{th}$
2:	**For** $i = 1$ to $|\mathcal{B}_i|$
3:	Initialize: $\mathbf{S}_i = \emptyset$
4:	Find $\mathbf{S}^*_{i,all} = \{s^*_1, s^*_2, ..., s^*_{\mathcal{S}_i}\}$ reordering $\mathbf{S}_{i,all}$, *s.t.*, $L^*_m \leq L^*_n, m > n$
5:	Set $q = 1$
6:	Set $\mathbf{S}_i = \{s^*_1, s^*_2, ..., s^*_q\}$
7:	Associate all $\sum_{s=1}^{\mathcal{S}_i} U_s(l_i, t)$ UEs of $\mathcal{B}_i$ with sectors in $\mathbf{S}_i$
8:	**If** Conditions (6.2)-(6.7) are met, Stop the algorithm
9:	**Else** Set $q = q + 1$
10:	**If** $q \leq \mathcal{S}_i - 1$, Go to Step 6
11:	**Else** Stop the algorithm, **End If**
12:	**End If**
13:	**End For**
14:	**End If**

6.2.1   System Model

Similar to the distributed DSBS scheme proposed in Chapter 4, a RAN under centralized DSBS is dynamically reconfigured by adaptively adjusting the number of active BSs for meeting the instantaneous traffic demand. However, for the centralized case, BSs do not need to interact with each other. Instead, a central coordinator evaluates the optimal set of active BSs. Other BSs are instructed to switch into sleep mode for saving energy. In addition, unlike DS, an active mode BS keeps all of its sectors in active mode.

6.2.2   Problem Formulation

As stated, under the centralized DSBS scheme, a central coordinator evaluates the optimum set of BSs $\mathcal{B}_{ON} = \{\mathcal{B}^*_1, \mathcal{B}^*_2, ..., \mathcal{B}^*_{|\mathcal{B}_{ON}|}\} \subseteq \mathcal{B}$, which have to be left in active mode consuming a minimum operating power. QoS is also guaranteed by the active BSs. The

optimization problem can then be formulated as below

$$\arg\min_{\{\mathcal{B}_1^*, \mathcal{B}_2^*, \ldots, \mathcal{B}_{|\mathcal{B}_{ON}|}^*\}} \sum_{i \in \mathcal{B}_{ON}} \sum_{s=1}^{\mathcal{S}_i} \left[(1 - \delta_i) L_f^{i,s}(t) P_{i,Op} + \delta_i P_{i,Op} \right] \tag{6.11}$$

$$s.t., \quad P_{i,b}(t) \leq P_b^{Th}, \forall i \in \mathcal{B}_{ON}, \forall t \tag{6.12}$$

$$P_{i,out}(t) \leq P_{out}^{Th}, \forall i \in \mathcal{B}_{ON}, \forall t \tag{6.13}$$

$$R_u^{(a)}(t) \geq R_u, u = 1, 2, \ldots, \sum_{i \in \mathcal{B}_{ON}} \sum_{s=1}^{\mathcal{S}_i} U_s(l_i, t), \forall t \tag{6.14}$$

$$\bigcup_{i \in \mathcal{B}_{ON}} \mathcal{A}_i(t) = \mathcal{A}, \forall t \tag{6.15}$$

$$\sum_{s=1}^{\mathcal{S}_i} \sum_{u=1}^{U_s(l_i,t)} \beta_u^{i,s}(t) \leq \sum_{s=1}^{\mathcal{S}_i} \beta_{Tot}^{i,s}, \forall i \in \mathcal{B}_{ON}, \forall t \tag{6.16}$$

$$\sum_{s=1}^{\mathcal{S}_i} \sum_{u=1}^{U_s(l_i,t)} P_u^{i,s}(t) \leq \sum_{s=1}^{\mathcal{S}_i} P_{i,Tx}, \forall i \in \mathcal{B}_{ON}, \forall t \tag{6.17}$$

Here again, QoS parameters session blocking, session outage, UE data rate and network coverage are guaranteed by (6.12), (6.13), (6.14) and (6.15) respectively. Also, (6.16) and (6.17) correspond to the limitations of available RBs and transmit power in each BS respectively.

6.2.3   Algorithm

The objective function in (6.11) is again nonconvex for a variable $\mathcal{B}_{ON}$. Thus the optimization becomes a combinatorial problem with a large search space $\mathcal{O}(2^{|\mathcal{B}_{ON}|})$. Therefore, we again propose a centralized greedy style heuristic algorithm. Similar to DS, proposed algorithm for the DSBS problem also uses a two-level triggering. Once again, if $\widehat{L}_{net}(t) < L_{th}$, the central coordinator itself triggers the network provisioning procedure followed by another triggering operation by each BS in its turn.

6.2.3.1   BS Switching Policy

For deciding on a BS whether to switch to sleep mode, proposed algorithm starts with the initialization $\mathcal{B}_{ON} = \mathcal{B}$. It then takes one BS at a time (say, $\mathcal{B}_i$) and checks its actual LF $L_i(t)$. If $L_i(t) <= L_{th}$, $\mathcal{B}_i$'s UE distribution process is triggered. Using one of the policies explained below in Section 6.2.3.2, all UEs of $\mathcal{B}_i$ is distributed by associating

Table 6.3: Demonstration of attempt order of neighbors for associating a UE of $\mathcal{B}_1$

Neighboring BS ID	$\mathcal{B}_2$	$\mathcal{B}_3$	$\mathcal{B}_4$	$\mathcal{B}_5$
δ_i	0.2	0.8	0.5	0.4
SINR (dB)	8	4	10	12
LH	I	IV	III	II
HL	IV	I	II	III
SS	I	II	III	IV
SBS	III	IV	II	I

them with the neighboring BSs. Following utility function is then evaluated

$$U_{i,BS}(t) = \sum_{l=1}^{\mathcal{L}} P_l^*(t) / \left\{ P_i(t) + \sum_{l=1}^{\mathcal{L}} P_l(t) \right\} \tag{6.18}$$

where $\mathcal{L}$ is the number of BSs to which UEs of $\mathcal{B}_i$ are to be associated, and $P_l(t)$ and $P_l^*(t)$ are the total operating power of lth neighbors before and after this association respectively. If utility $U_{i,BS}(t) < \eta_{BS}$ ($\eta_{BS} \in [0,1]$ is a constant) and (6.12)-(6.17) are met at the same time, then we set new $\mathcal{B}_{ON} = \mathcal{B}_{ON} \setminus \{\mathcal{B}_i\}$. For $U_{i,BS}(t) < 1$, energy savings can be achieved by switching $\mathcal{B}_i$ into sleep mode. The algorithm continues with the next BS, updates $\mathcal{B}_{ON}$ and so on. After finishing with all BSs, final $\mathcal{B}_{ON}$ provides the list of BSs, which are kept active mode and the other BSs in $\mathcal{B} \setminus \mathcal{B}_{ON}$ are switched into sleep mode.

6.2.3.2 UE Association Policy

Let $\mathbf{B}_{i,n} = \{\mathcal{B}_{i,1}^n, \mathcal{B}_{i,2}^n, ..., \mathcal{B}_{i,N_{i,b}}^n\}$ be the sequence of neighboring active BSs of $\mathcal{B}_i$ according to which the neighbors are approached for associating a UE located in $\mathcal{B}_i$. Here $N_{i,b}$ is the number of active neighbors of $\mathcal{B}_i$. By including only the active neighbors in $\mathbf{B}_{i,n}$, sleep mode BSs are allowed to sleep for longer times and the number of switching is reduced. In addition to the conventional SINR-based strategies [169], various new neighbor sequencing strategies are outlined here below. On the other hand, for selecting the sequence of BSs, $\mathbf{B}_{seq} = \{\mathcal{B}_1^*, \mathcal{B}_2^*, ..., \mathcal{B}_{|\mathcal{B}|}^*\}$ in which the algorithm proceeds from one BS to another for distributing their UEs, various alternative are considered. Thus, for accounting the level of received SINR at UEs and the possibility of the network having BSs with different energy proportionality (i.e., different values for ELPC $\delta_i, i = 1, 2, ..., |\mathcal{B}|$),

following four combinations are investigated.

a) Lower-to-Higher (LH): In this case, lower energy efficient BSs have the higher priority to distribute first. While, higher efficient neighbors are given the higher priority for accepting UEs from other BSs. That means, $\mathbf{B}_{seq} = \{\mathcal{B}_1^*, \mathcal{B}_2^*, ..., \mathcal{B}_{|\mathcal{B}|}^*\}$, $\delta_l^* \geq \delta_m^*, l < m$, and $\mathbf{B}_{i,n} = \{\mathcal{B}_{i,1}^n, \mathcal{B}_{i,2}^n, ..., \mathcal{B}_{i,N_{i,b}}^n\}$, $\delta_{i,p}^n \leq \delta_{i,q}^n, p < q$. Here, δ_l^* and $\delta_{i,p}^n$ are the ELPC of $\mathcal{B}_l^*$ and $\mathcal{B}_{i,p}^n$ respectively.

b) Higher-to-Lower (HL): This scheme is just the opposite of the *LH* scheme. Therefore, $\mathbf{B}_{seq} = \{\mathcal{B}_1^*, \mathcal{B}_2^*, ..., \mathcal{B}_{|\mathcal{B}|}^*\}$, $\delta_l^* \leq \delta_m^*, l < m$, and $\mathbf{B}_{i,n} = \{\mathcal{B}_{i,1}^n, \mathcal{B}_{i,2}^n, ..., \mathcal{B}_{i,N_{i,b}}^n\}$, $\delta_{i,p}^n \geq \delta_{i,q}^n, p < q$.

c) Sequential-Sequential (SS): Under this scheme, no reordering of BSs is done. The algorithm proceeds sequentially from one BS to another according to a predefined order. Thus, $\mathbf{B}_{seq} = \{\mathcal{B}_1, \mathcal{B}_2, ..., \mathcal{B}_{|\mathcal{B}|}\}$, $\mathcal{B}_l > \mathcal{B}_m, l > m$ and $\mathbf{B}_{i,n} = \{\mathcal{B}_{i,1}^n, \mathcal{B}_{i,2}^n, ..., \mathcal{B}_{i,N_{i,b}}^n\}$, $\mathcal{B}_{i,p}^n > \mathcal{B}_{i,q}^n, p > q$.

d) Sequential-to-Better-Signal (SBS): For this approach, $\mathbf{B}_{seq}$ is same as in the *SS* scheme. However, $\mathcal{B}_n$ is the set of neighbors sequenced according to the descending order of received SINR, i.e., $\mathbf{B}_{i,n} = \{\mathcal{B}_{i,1}^n, \mathcal{B}_{i,2}^n, ..., \mathcal{B}_{i,N_{i,b}}^n\}$, $SINR_{i,p}^n \geq SINR_{i,q}^n, p < q$. Here, $SINR_{i,p}^n$ is the received SINR at the UE from neighbor BS $\mathcal{B}_{i,p}^n$.

An example of the order of neighboring BSs at which they are approached for associating a UE of $\mathcal{B}_1$ under various schemes is demonstrated in Table 6.3. The values of δ_i and SINR for the example is chosen randomly.

Remarks: It is worth noting that in LTE, the primary synchronization channel (P-SCH) and the secondary synchronization channel (S-SCH) signals are used by a UE to carry out cell search for detecting its own BS ID as well as the neighbor BSs' IDs [170]. Here, it is assumed that a UE is capable to detect its own BS and its adjacent BSs, and feedback this information to the central coordinator via its own BS. Many cell searching algorithms are available for LTE and WiMAX [171], which can be adopted in the proposed system. On the other hand, as mentioned above, using the channel state information (CSI) feedback supported in both LTE [172] and WiMAX [107], SINR at UEs can also be collected.

Pseudo code of the algorithm is presented in Table 6.4. Proposed algorithm has a computational complexity $\mathcal{O}(N_B N_U)$ in place of $\mathcal{O}(N_U 2^{N_B})$ of exhaustive search. On the

Table 6.4: Centralized DSBS algorithm

1:	**If** $\widehat{L}_{net}(t) < L_{th}$
2:	Initialize: $\mathcal{B}_{ON} = \mathcal{B}, i = 1$
3:	**If** $L_i(t) < L_{th}$
4:	Associate all UEs of $\mathcal{B}_i^*$ with BSs in $\mathbf{B}_{i,n}$
5:	Calculate $U_{i,BS}(t)$ for $\mathcal{B}_i^*$
6:	**If** (6.12)-(6.17) are met and $U_{i,BS}(t) < \eta_{BS}$
7:	Set $\mathcal{B}_{ON} = \mathcal{B}_{ON} \setminus \{\mathcal{B}_i^*\}$ and $i = i + 1$
8:	**Else** Set $i = i + 1$, **End If**
9:	**If** $i \leq |\mathcal{B}|$, Go to Step 3
10:	**Else** Stop the algorithm, **End If**
11:	**End If**
12:	**End If**

other hand, signaling overhead of the algorithm is same as that of the centralized DS, i.e., $(N_U + 2N_B)$.

6.2.4 Performance Evaluation

6.2.4.1 Simulation Setup

Simulation settings are same as those used for the DS scheme presented in this chapter other than two exceptions made for the sake of computational tractability. Firstly, inter-cell interference is once again approximated by Gaussian-like noise and dealt in the same way as explained in Chapter 4. Secondly, instead of calculating $A(\theta)$ for each UE, an average value equal to 3 dB, calculated from (6.1.6), is used for all UEs.

6.2.4.2 Sleep Mode BSs and Energy Savings

Percentage of sleep mode BSs with the 95% confidence intervals under the outlined four UE association policies is illustrated in Fig. 6.8. For all of these schemes, values of δ_i for BSs are drawn from a uniform distribution $U(0.4, 1.0)$. An additional case of the
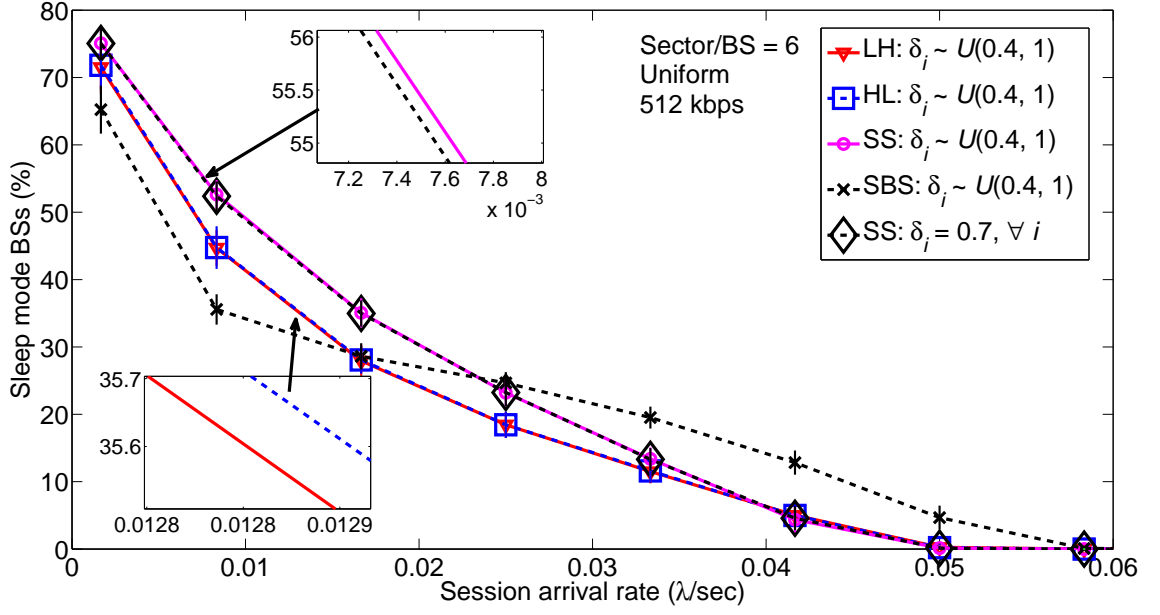
Figure 6.8: Percentage of sleep mode BSs under DSBS.

SS scheme with $\delta_i = 0.7, \forall i$ (i.e., all BSs are equally energy efficient) is also included in the figure. As expected, with the increase of session arrival, number of sleep mode BSs decreases. For this particular parameter settings, higher number of BSs switch into sleep mode under the *SS* scheme compared to that in both the *LH* and the *HL* schemes. However, approximately equal number of BSs sleep under the *LH* and the *HL* schemes. This is due to drawing δ_i from a uniform distribution $U(0.4, 1.0)$. Since the average of $U(0.4, 1.0)$ is equal to 0.7, for the two cases of the *SS* scheme with $\delta_i \sim U(0.4, 1.0)$ and $\delta_i = 0.7, \forall i$, almost equal number of BSs stays in sleep mode. On the other hand, under the *SBS* scheme, in the lower traffic scenario, lower number of BSs sleeps compared to the other four schemes. However, the *SBS* scheme outperforms the others in the higher traffic scenario. Since the *SBS* scheme associates users to BSs corresponding to higher SINR, UEs require less number of RBs and less transmit power. Consequently, active BSs are lightly loaded compared to the other cases. Thus, even in a higher traffic case, a higher number of BSs can switch to sleep mode.

Fig. 6.9 presents the energy savings achieved under the same schemes explained in Fig. 6.8. As seen, although equal number of BSs sleep in the *LH* and the *HL* schemes, energy savings is much higher in the *LH* scheme. This is because, unlike the *HL* scheme, the *LH* scheme prioritizes lower energy efficient BSs to switch to sleep mode by distributing
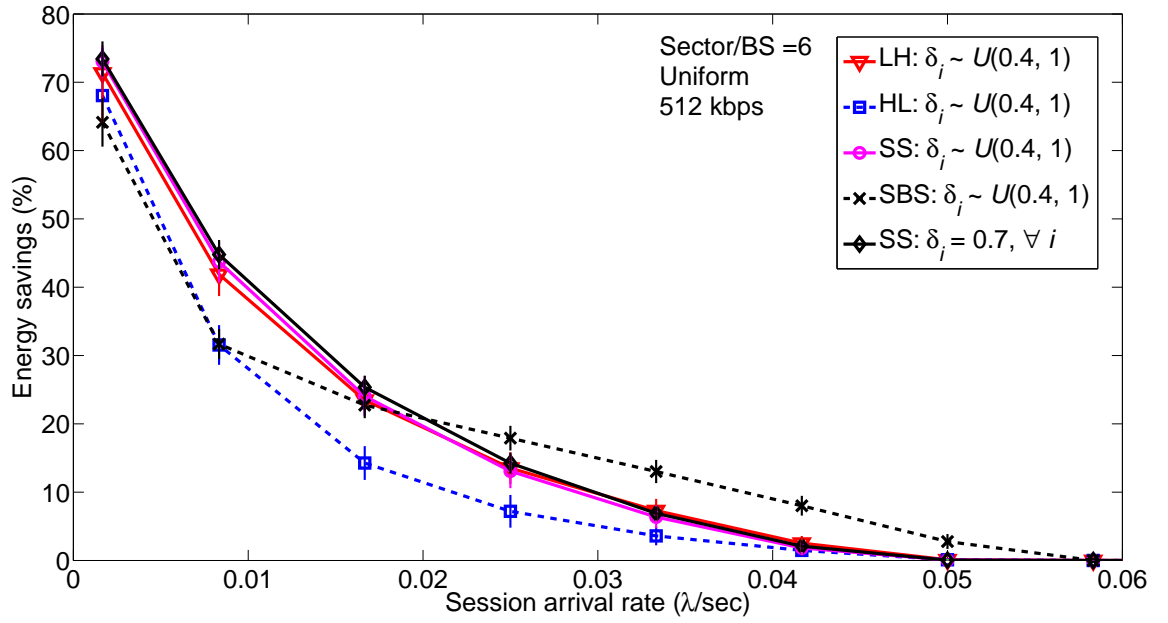
Figure 6.9: Energy saving performance of the centralized DSBS mechanism.

its traffic to the higher energy efficient BSs. Thus the network is reconfigured keeping relatively higher energy efficient BSs active leading to higher savings. Furthermore, for the same reasons explained in Fig. 6.8, the *SBS* scheme outperforms the others in terms of energy savings in the higher traffic region.

6.2.4.3 Spectral Efficiency and RB Utilization

The ratio of the achievable SEs as well as the ratio of the required RBs per UE under the centralized DSBS mechanism to the corresponding parameters in the original network is demonstrated in Figs. 6.10 and 6.11 respectively. Similar to the DS scheme, for smaller λ, many BSs are switched to sleep mode and their UEs are associated with the other active BSs located at a longer distance than that of their original serving BSs. This results in higher path loss and lower SINR, and hence, the achievable SE is decreased making the ratio lower than one. For the same reason, a higher number of RBs per UE is required for maintaining user data rates.

On the other hand, under the *SBS* scheme, UEs of the sleep mode BSs are associated with BSs providing higher SINR. Therefore, decrease in SE is much lower in the *SBS* scheme compared to the other schemes as evident from Fig. 6.10. Consequently, as shown in
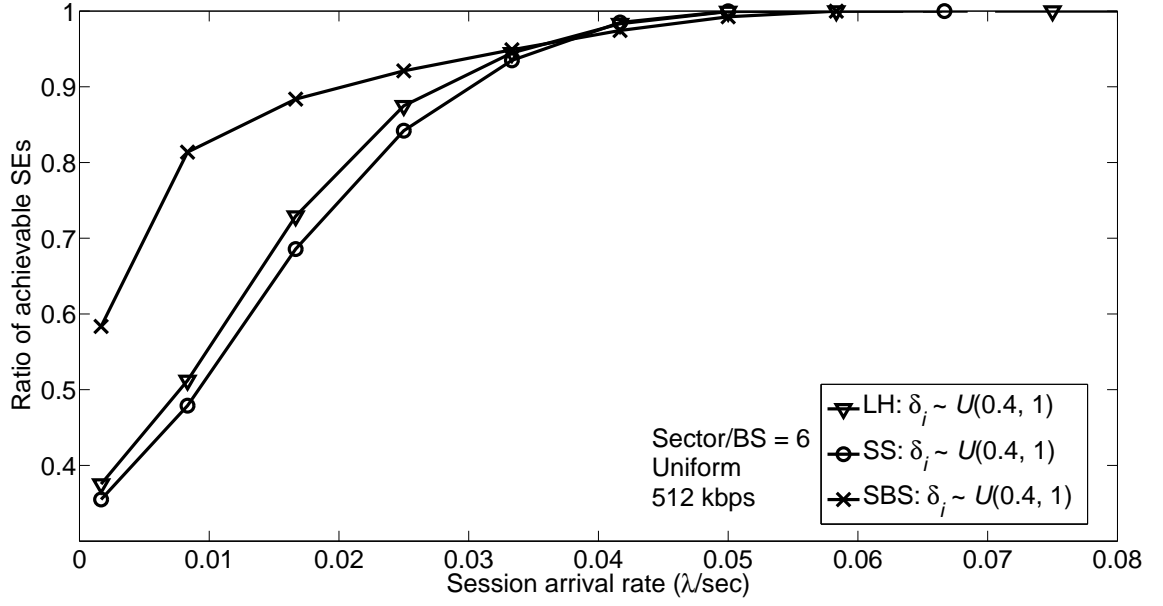
Figure 6.10: Impact on the achievable spectral efficiency under the centralized DSBS mechanism.
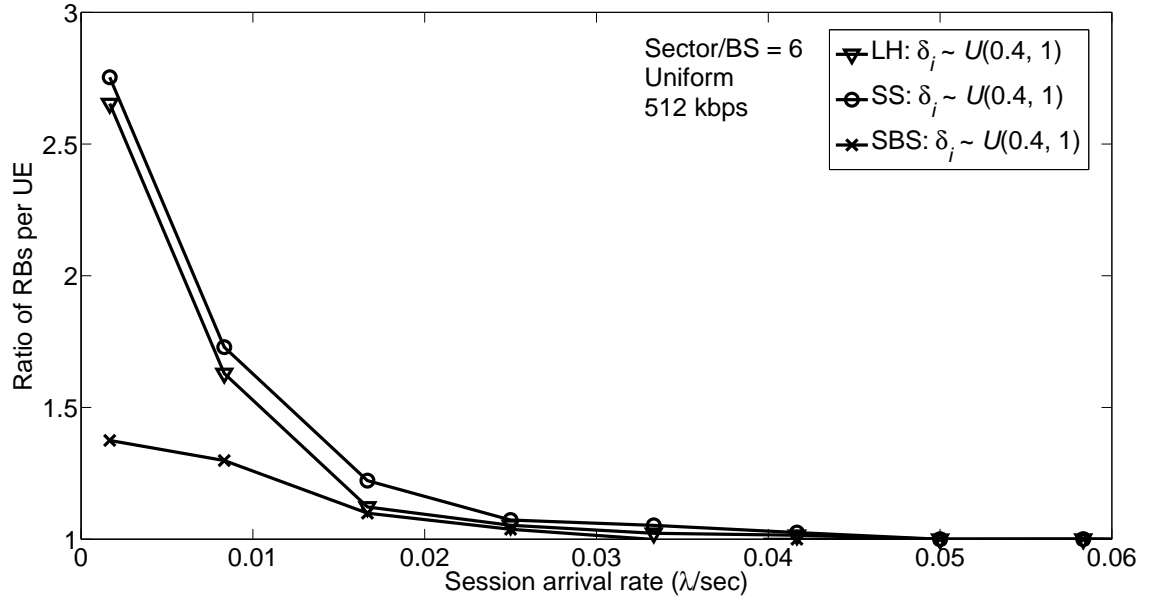
Figure 6.11: Impact on the RB requirement per UE under the centralized DSBS mechanism.

Fig. 6.11, increase in the required number of RBs per UE is lower under the *SBS* scheme compared to the other two.

6.3   Network Reconfiguring Events

Effectiveness of employing the proposed EWMA-based LF predictor and the LF threshold L_{th} in reducing the network reconfiguring events under both the DS and the DSBS schemes is demonstrated in Fig. 6.12. From Fig. 6.12(a), it is clear that use of a higher value for L_{th} results in a higher number of network reconfiguring events. On the other hand, daily energy savings is found to exhibit an increasing trend with L_{th} as demonstrated in Figs. 6.12(b) and 6.12(c).

Comparing these two groups of curves, optimal values of L_{th} are evaluated for both the schemes. The minimum value of L_{th} for the maximum energy savings is defined as the optimal value of L_{th}. This value is found equal to around 0.8 and 0.5 for the DS and the DSBS mechanisms respectively for all the rate functions. At these optimal settings, for example, energy savings per day under the DS technique become 38%, 52% and 41% for $f_1(t)$, $f_2(t)$ and $f_3(t)$ respectively. Corresponding reductions in network reconfiguring events are found 26%, 20% and 31% respectively, which in turn reduce the amount of feedback to the central coordinator. From the figure, it is also evident that with the tradeoff of small amount of energy saving performance, these events can be further reduced by a significant percentage.

6.4   Chapter Summary

This chapter has proposed both the centralized and the distributed traffic-sensitive DS techniques for energy savings in OFDMA-based cellular access networks. In addition, a DSBS mechanism for centralized implementation has also been presented. Various BS switching and UE association policies are also explored. Generalized optimization problems are formulated for the schemes and because of their challenging nature, low complexity greedy style heuristic algorithms are proposed. Simulation results have demonstrated the potential of the techniques in substantially reducing the total energy consumption. User data rates, user distributions, UE association policies and original network configurations have shown large impact on the achievable energy savings. Impact of the
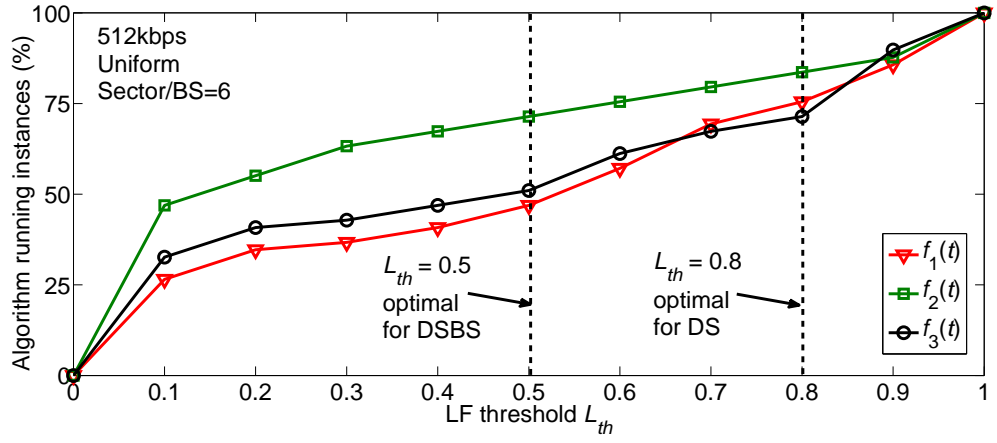
(a) Percentage of instances at which network reconfiguration occurs.
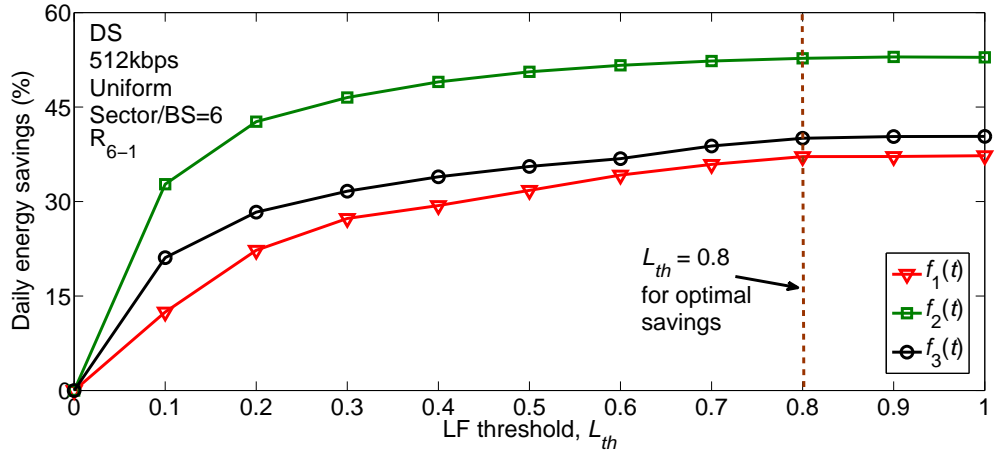
(b) Daily savings under the DS mechanism.
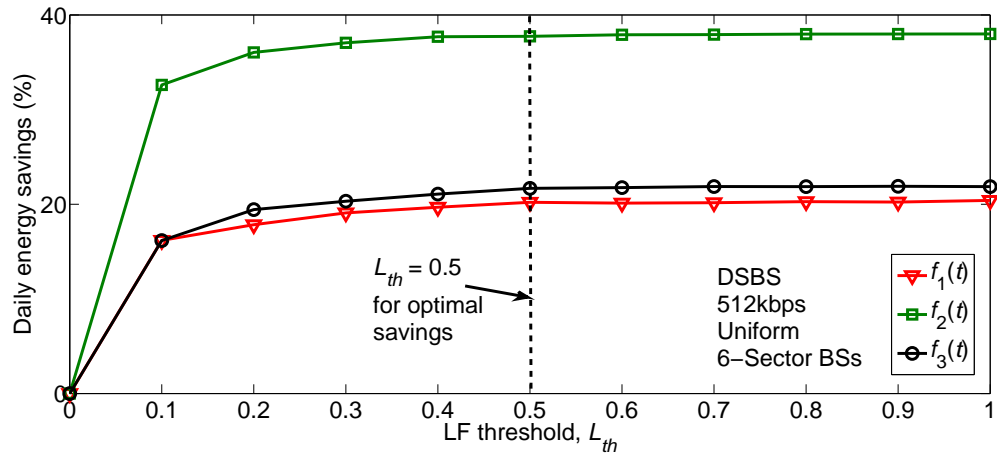
(c) Daily savings under the DSBS mechanism.

Figure 6.12: System performance under the proposed EWMA-based LF predictor.

schemes on the SE and RBs requirement per UE are also investigated thoroughly. It is also demonstrated that the use of the proposed EWMA-based LF predictor in conjunction with the schemes can significantly reduce the number of network reconfiguring events without sacrificing any energy saving performance.

To this end, the prospect of dynamic BS switching and dynamic sectorization techniques for saving energy have been investigated by applying them separately. Therefore, the next chapter concentrates on exploring the potential of energy savings through joint applications of these two schemes.

Chapter 7

Joint Dynamic Sectorization and Base Station Switching

This chapter proposes a traffic-aware energy saving framework for cellular access networks by employing network reconfiguring operation in two different dimensions. Proposed framework is termed joint dynamic sectorization and switching of base station (JDSBS) under which both DS and DSBS mechanisms are jointly applied for maximizing potential energy savings. For the sake of ease implementation, the two dimensions, i.e., DS and DSBS operations are decoupled into time domain and applied one after another. Based on the sequence of applications of DS and DSBS techniques, two different variants of the JDSBS scheme are investigated. System performance is evaluated using extensive simulations, which demonstrates the potential of a large scale energy savings. Superiority of the JDSBS is also demonstrated by comparing with the individual applications of DS and DSBS. The contribution of this chapter has been presented in [165].

7.1 System Model

The proposed JDSBS framework utilizes a two-dimensional dynamic network provisioning technique, which implements network wide DSBS as well as DS in each BS jointly. More precisely, under this scheme, under-loaded BSs are dynamically switched into sleep mode, while each of the remaining active BSs are configured with fewer sectors as well.
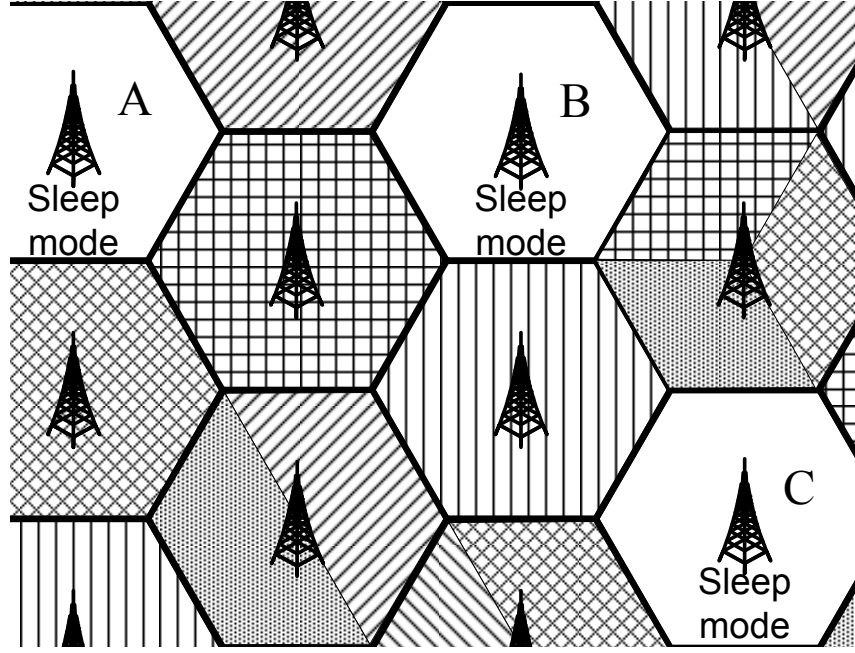
Figure 7.1: A sample view of the network under the proposed JDSBS framework at a low-traffic instance. Some BSs (e.g., A, B and C) and some sectors in the remaining active BSs are in sleep mode. Each pattern in the figure corresponds to the coverage area of a sector.

Thus, the achievable energy savings is maximized, while QoS is guaranteed. A snapshot of the network under this scheme at a random low-traffic instance is illustrated in Fig. 7.1. In the original network, all BSs as well as all the sectors (for this example, six sectors per BS) are always left in active mode. However, as shown in the figure, several BSs (e.g., A, B and C) as well as many sectors in the active mode BSs are switched into sleep mode during a low-traffic period for saving energy.

7.1.1 Problem Formulation

Once again, the downlink of an OFDMA-based cellular network served by a set of multi-sector BSs $\mathcal{B} = \{\mathcal{B}_1, \mathcal{B}_2, ..., \mathcal{B}_{|\mathcal{B}|}\}$ is considered. The goal of JDSBS is to maximize the energy savings by minimizing both the number of active BSs and the number of sectors in these BSs. Therefore, the objective is to evaluate the following two optimal sets: the set of active BSs $\mathcal{B}_{ON} = \{\mathcal{B}_1^*, \mathcal{B}_2^*, ..., \mathcal{B}_{|\mathcal{B}_{ON}|}^*\} \subseteq \mathcal{B}$ and the set of active sectors $\mathbf{S}_{ON} = \{\mathbf{S}_1, \mathbf{S}_2, ..., \mathbf{S}_{|\mathcal{B}_{ON}|}\}$. Here, $\mathbf{S}_i = \{s_1, s_2, ..., s_{|\mathbf{S}_i|}\} \subseteq \mathbf{S}_{i,all} = \{1, 2, ..., \mathcal{S}_i\}$ and $\mathcal{S}_i$ are the

set of active sectors and the total number of sectors in $\mathcal{B}_i$ respectively. Thus the following optimization problem can be formulated

$$\underset{\substack{\{\mathcal{B}_1^*,\mathcal{B}_2^*,....,\mathcal{B}_{|\mathcal{B}_{ON}|}^*\} \\ \{\mathbf{S}_1,\mathbf{S}_2,.....,\mathbf{S}_{|\mathcal{B}_{ON}|}\}}}{\arg\min} \sum_{i\in\mathcal{B}_{ON}} \sum_{s\in\mathbf{S}_i} \left[(1-\delta_i)L_f^{i,s}(t)P_{i,Op} + \delta_i P_{i,Op} \right] \tag{7.1}$$

$$s.t., \quad P_{i,b}(t) \leq P_b^{Th}, \forall i \in \mathcal{B}_{ON}, \forall t \tag{7.2}$$

$$P_{i,out}(t) \leq P_{out}^{Th}, \forall i \in \mathcal{B}_{ON}, \forall t \tag{7.3}$$

$$R_u^{(a)}(t) \geq R_u, u = 1,2,...,\sum_{i=1}^{|\mathcal{B}|}\sum_{s=1}^{\mathcal{S}_i} U_s(l_i,t), \forall t \tag{7.4}$$

$$\bigcup_{i\in\mathcal{B}_{ON}}\bigcup_{s\in\mathbf{S}_i} \mathcal{A}_{i,s}(t) = \mathcal{A}, \forall t \tag{7.5}$$

$$\sum_{s\in\mathbf{S}_i}\sum_{u=1}^{U_s(l_i,t)} \beta_u^{i,s}(t) \leq \sum_{s\in\mathbf{S}_i} \beta_{Tot}^{i,s}, \forall i \in \mathcal{B}_{ON}, \forall t \tag{7.6}$$

$$\sum_{s\in\mathbf{S}_i}\sum_{u=1}^{U_s(l_i,t)} P_u^{i,s}(t) \leq \sum_{s\in\mathbf{S}_i} P_{i,Tx}, \forall i \in \mathcal{B}_{ON}, \forall t \tag{7.7}$$

The notations utilized in (7.1) - (7.7) have the same meanings as discussed in Chapter 6, which are repeated here for the convenience of the readers. Here, $l_i \in \mathbb{R}^2$ is the location of $\mathcal{B}_i$ and the LF of its sth sector is denoted by $L_f^{i,s}(t)$, the session blocking and the session outage probabilities are given by $P_{i,b}(t)$ and $P_{i,out}(t)$ respectively, P_b^{th} and P_{out}^{th} are the target blocking and outage probabilities respectively, $R_u^{(a)}(t)$ and R_u are the uth UE's achievable data rate and the required data rate respectively, $\mathcal{A}$ is the coverage area of the network, $\mathcal{A}_i$ and $\mathcal{A}_{i,s}$ are the coverage area provided by $\mathcal{B}_i$ and its sth sector respectively, $P_u^{i,s}(t)$ is the downlink transmit power for u^{th} UE, $P_{i,Op}$ and $P_{i,Tx}$ are the power profile parameters corresponding to a single sector, and $U_s(l_i,t)$ and $\beta_{Tot}^{i,s}$ are the total number of UEs and RBs in sector s of $\mathcal{B}_i$ respectively.

7.1.2 Solution Approach

Network reconfiguring procedure under the proposed JDSBS mechanism is carried out periodically in every T_d time units. Now, since both $\mathcal{B}_{ON}$ and $\mathbf{S}_{ON}$ are variable, optimization problem in (7.1) is nonconvex and highly challenging as well with $\mathcal{O}(2^{\sum_{i=1}^{\mathcal{B}_i}\mathcal{S}_i})$ possible cases. For reducing the complexity, the JDSBS problem is first divided into two sub-problems by decoupling DS and DSBS in time domain. This implies that at every

Table 7.1: Algorithmic framework for JDSBS

1: Set $\mathcal{B}_{ON} = \mathcal{B}$ and $\mathbf{S}_{ON} = \left\{ \mathcal{S}_{1,all}, \mathcal{S}_{2,all}, ..., \mathcal{S}_{|\mathcal{B}|,all} \right\}$
2: **For JDSBS-I scheme:**
3:     Perform DSBS $\forall \mathcal{B}_i \in \mathcal{B}$ and update $\mathcal{B}_{ON}$
4:     Perform DS $\forall \mathcal{B}_i \in \mathcal{B}_{ON}$ and update $\mathbf{S}_{ON}$
5: **For JDSBS-II scheme:**
6:     Perform DS $\forall \mathcal{B}_i \in \mathcal{B}$ and update $\mathbf{S}_{ON}$
7:     Perform DSBS $\forall \mathcal{B}_i \in \mathcal{B}$ and update $\mathcal{B}_{ON}$

instance of network reconfiguration, either of these DS and DSBS is carried out first for the entire network followed by the other. Secondly, heuristically guided greedy style algorithms are employed for DS and DSBS. Centralized algorithms for DS and DSBS schemes presented in Chapter 6 are adopted here in the proposed JDSBS scheme. Based on the sequence in which DS and DSBS are applied, following two variants of the JDSBS are investigated.

a. JDSBS-I: At every instance when the network is reconfigured, first DSBS is applied to reconfigure the network using reduced number of BSs. Following this, DS is employed for switching several sectors in each under-utilized BSs into sleep mode.

b. JDSBS-II: The order of applying DSBS and DS is opposite to that in the JDSBS-I. That means, first DS is employed followed by DSBS.

The algorithmic framework for the JDSBS scheme is presented in Table 7.1. Computational complexity and the signaling overhead of the proposed algorithm are same as those of the centralized DS presented in Chapter 6, i.e., $\mathcal{O}(N_B N_S^2 N_U)$ and $(N_U + 2N_B)$ respectively.

Remarks: Instead of this sequential approach of implementation, an integrated approach can also be used. In this alternative approach, both DS and DSBS have to be executed first for a BS. Then, the same procedure has to be repeated for the next BS until the last one. Investigation of the integrated approach has been left for future works.
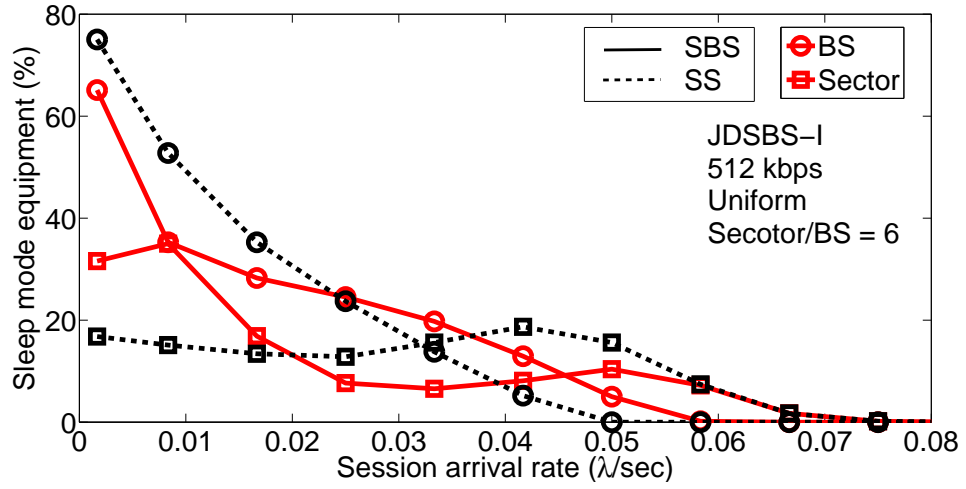
Figure 7.2: Sleep mode equipment under user association policies.
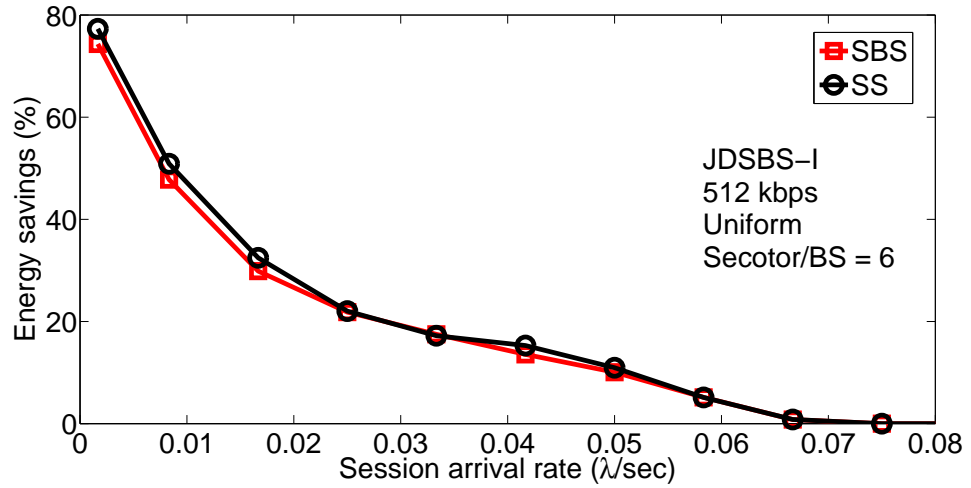
Figure 7.3: Energy saving performance under user association policies.

7.2   Performance Evaluation

Simulation settings are exactly same as that used for the centralized DSBS scheme presented in Chapter 6. BSs are considered equally energy proportional, i.e., $\delta_i = \delta, \forall i$. Additionally, unless otherwise specified, the sector switching pattern R_{6-1} and the *SBS* UE association policy are used for the simulations.

7.2.1   Impact of UE Association Policies

First, the impact of the UE association policies on the system performance is evaluated. Fig. 7.2 presents the percentage of sleep mode BSs and sectors under the JDSBS-I scheme. It is identified that in the low traffic region (e.g., $\lambda < 0.025$), lower number of BSs can switch to sleep mode in the *SBS* policy than that in the *SS* policy, while vice versa for the case of sleep mode sectors. This can be explained as below: the *SBS* policy has the higher probability in associating UEs with all the surrounding BSs resulting in reduced chance for many of the neighbors to switch into sleep mode. On the other hand, the *SS* policy associates UEs based on the neighbor ID. Therefore, it has the higher probability to associate UEs to a smaller subset of neighbors leading to a higher probability for the other neighbors in switching into sleep mode. However, for the higher traffic region, this subset of neighboring BS to which UEs are associated under the *SS* policy becomes same as that of the *SBS* policy. Correspondingly, the difference between the two policies diminishes with the increase of λ. In contrast, for higher λ regions, the *SBS* policy is benefited from the fact that for a higher received SINR, a lower number of RBs (and hence a lower transmit power) is required for supporting UEs leading to the requirement of fewer active BSs, i.e., a higher number of BSs in sleep mode.

In the JDSBS-I, DSBS is carried out first leading to the increase of traffic in the remaining active BSs. Therefore, the opportunity to switch sectors into sleep mode from the subsequent application of DS is reduced. Thus, the higher the number of sleep mode BSs, the lower the number of sleep mode sectors, which is also evident from the figure. Notably, a slight increase in the sleep mode sectors is observed in the higher traffic region followed by a slow drop to zero. This is due to the fact that during high-traffic times, fewer BSs can switch into sleep mode leaving slightly higher unused capacity, which is used by DS for switching more sectors into sleep mode.

Despite the large disparity between the two UE association policies in terms of sleep mode BSs and sectors over the entire range of λ, overall energy savings from both these policies are very close as shown in Fig. 7.3. From Fig. 7.2, it is clearly seen that for both the policies, a lower number of sleep mode sectors is compensated by a higher number of sleep mode BSs and vice versa. Consequently, the two policies generate almost equal energy savings.
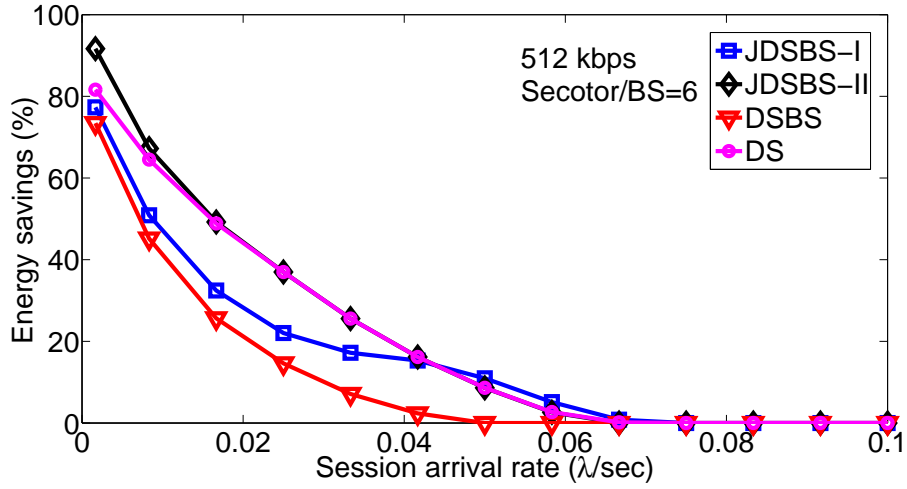
(a) Uniform distribution.
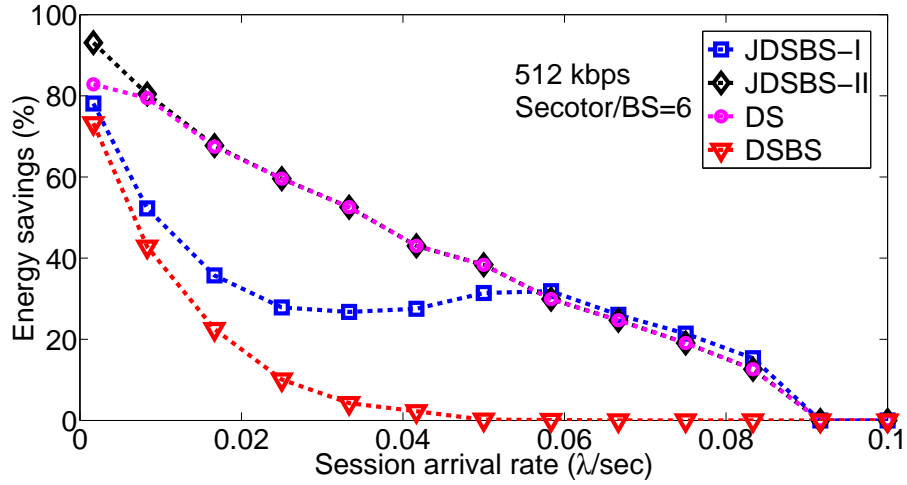
(b) Gaussian distribution.

Figure 7.4: Energy saving performance with user distributions.

7.2.2 Impact of UE Distribution and Data Rates

Energy saving performance of the system with both the uniform and the Gaussian dis-
tributed UEs is illustrated in Fig. 7.4. For the convenience of explanation, energy savings
by the DS and the DSBS alone are also included in the figure. First of all, it is found
that except the DSBS scheme, other three schemes can extract higher savings having the
Gaussian distributed UEs than that with uniformly distributed. Since many UEs are closer
to BSs in a Gaussian distribution scenario, they can achieve higher SINR resulting from
lower path loss. This leads to the requirement of fewer RBs and less transmit power,
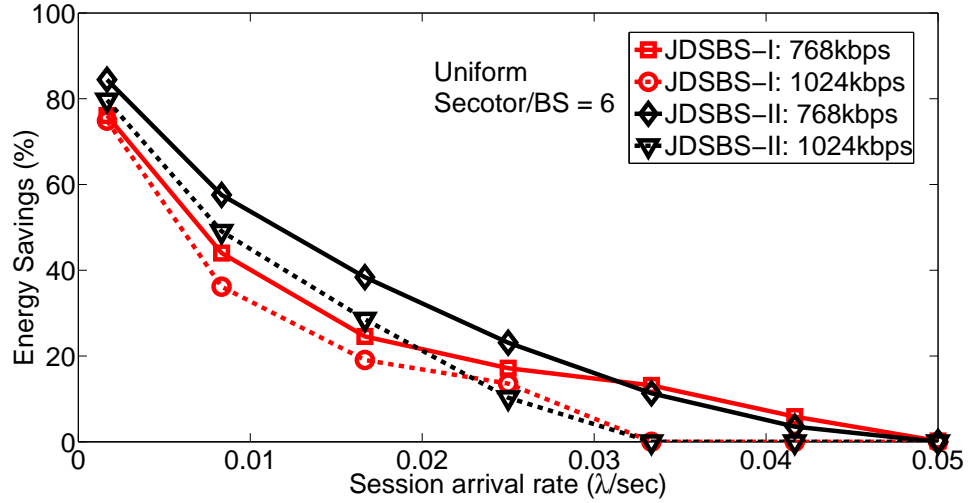
Figure 7.5: Energy saving performance with data rates.

which allows more sectors in sleep mode and generates higher energy savings under the DS scheme. However, for the DSBS scheme, UEs of the switched off BSs are associated with BSs located further than the original serving BSs. Thus, a higher number of RBs as well as a higher amount of transmit power is required, which is more evident in a Gaussian scenario as more UEs are concentrated near BSs. The consequence is the reduced number of sleep mode BSs and less energy savings. Despite these two opposing facts, because of the dominance of DS over DSBS, the proposed JDSBS mechanism generates higher savings under a Gaussian distributed case.

Secondly, diminishing energy savings with the rise of λ is observed in all the cases except the JDSBS-I scheme. The slight increase of energy savings in the higher traffic region for the JDSBS-I is due to the increase in the number of sleep mode sectors as explained in Fig. 7.2. It can be identified that DS can achieve nearly equal savings of the JDSBS-II except in the very low-traffic region. This is because, in JDSBS-II, DS is carried out first and thus, the remaining active sectors become nearly fully loaded for $\lambda \geq 0.015$, beyond which almost no BS can switch into sleep mode. It is also evident that the proposed JDSBS-II mechanism can outperform the separate applications of DS and DSBS schemes.

Fig. 7.5 demonstrates the impact of UE data rates on the achievable energy savings, which clearly identifies a higher savings for a network with lower data rate UEs. As explained in Chapter 6, this is due to the combined effect of the requirement of a higher number of RBs and a higher amount of transmit power as well for serving a UE with a higher data
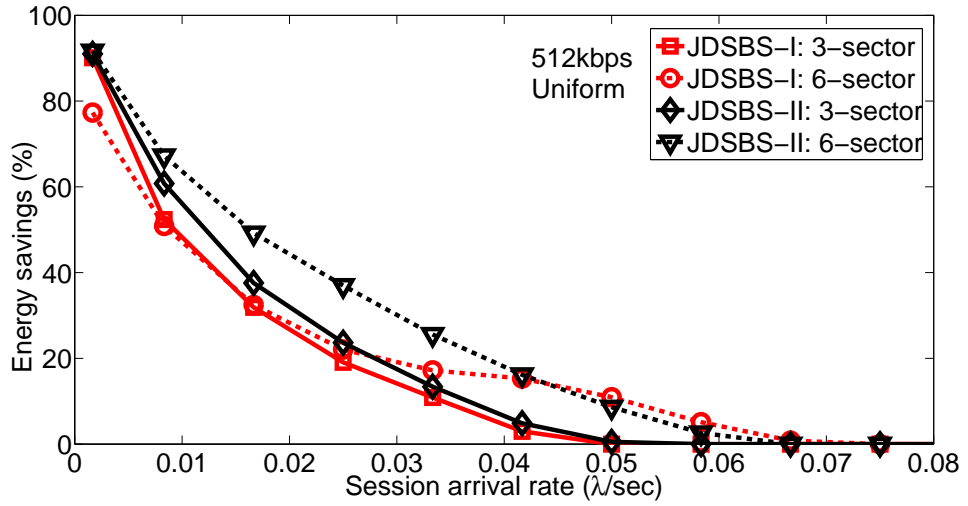
Figure 7.6: Energy saving performance with the number of sectors.
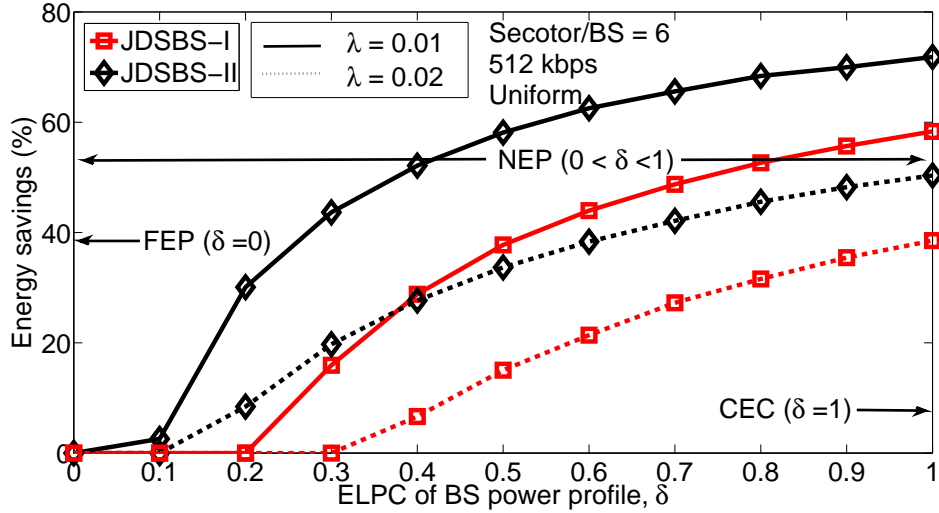
Figure 7.7: Energy saving performance with BS power profile parameter δ.

rate requirement. Consequently, fewer number of BSs as well as fewer sectors can switch to sleep mode and less savings is achieved.

7.2.3 Impact of the Number of Sectors and Power Profile of BSs

Energy saving performance for a network having 3-sector BSs is presented in Fig. 7.6. For the convenience of visualizing the impact of the number of sectors per BS, energy savings from 6-sector BSs is also repeated in this figure. Higher number of sectors provides higher
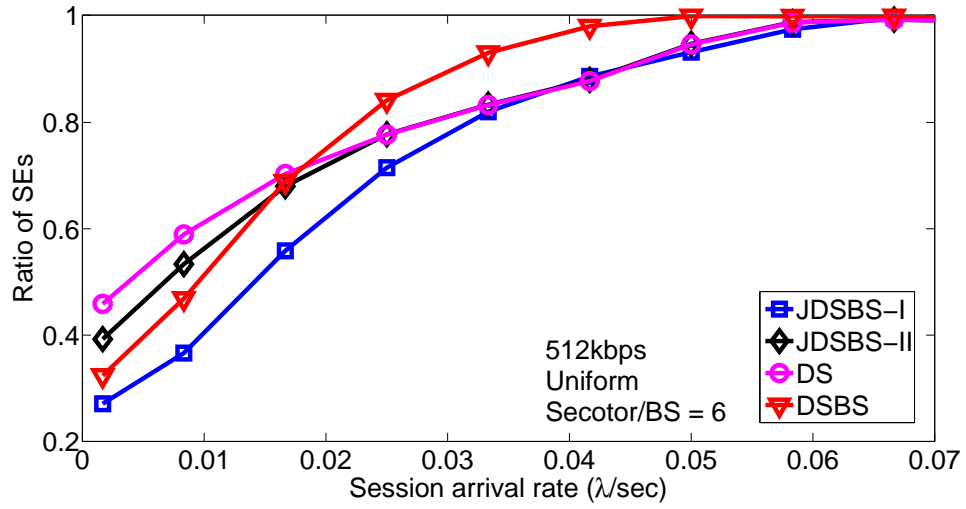
Figure 7.8: Ratio of achievable spectral efficiency under the proposed scheme to that of the original network.
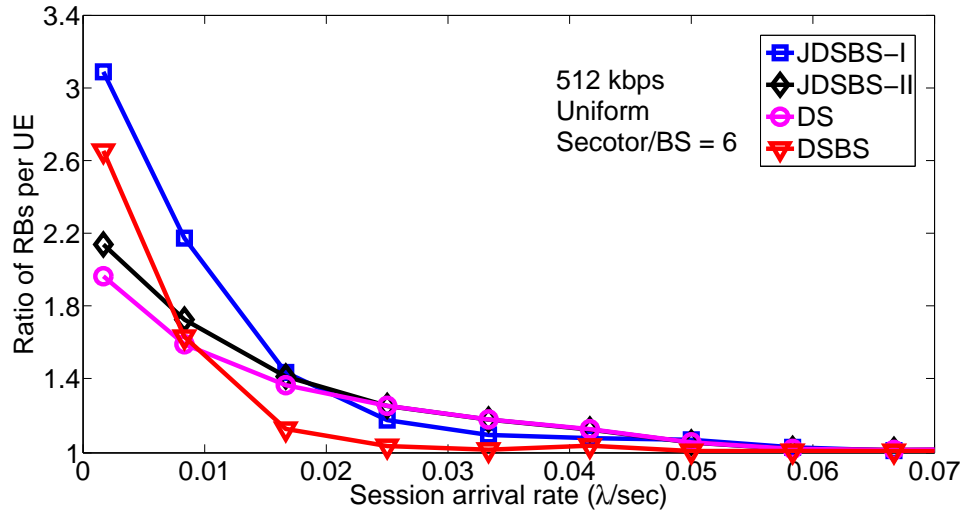
Figure 7.9: Ratio of required RBs per UE under the proposed scheme to that of the original network.

number of options for associating UEs to the other sectors and BSs, which increases the probability of switching sectors as well as BSs into sleep mode. Thus, with the increase of number of sectors per BSs, energy savings increases. For instance, at $\lambda = 0.02$, energy saving from JDSBS-II is equal to 32% and 44% for 3-sector and 6-sector BSs respectively.

On the other hand, impact of BS ELPC δ on the net energy savings for two different

settings of λ is depicted in Fig. 7.7. Parameter $\delta = 1$ corresponds to the CEC BSs in which the highest wastage occurs and hence, the proposed JDSBS achieves the highest energy savings as illustrated in the figure. With the decrease of δ, increasingly reduced wastage of energy occurs causing decreased energy savings. For example, with $\lambda = 0.02$, savings from JDSBS-II decreases from 50% at $\delta = 1$ to 0% for $\delta \leq 0.1$. In addition, with the increase of λ (i.e., network loading), drop in energy savings as well as rise in the value of δ below which no savings is feasible are identified from the figure.

7.2.4   Impact on Spectral Efficiency and RB Utilization

Fig. 7.8 presents the ratio of the achievable SE in the proposed JDSBS scheme to that in the original network. Due to combined effect of decreasing SE by both the DS and the DSBS schemes, achievable SE under the JDSBS scheme is less than that in the original network, which is evident from the ratio being smaller than one. Highest reduction is found under the JDSBS-II scheme. With the increase of network load, reduced number of BSs and sectors are switched to sleep mode, and consequently, the ratio approaches to one for higher λ.

On the other hand, due to the reduced SE, a higher number of RBs per UE is required for guaranteeing the required data rate as evident in Fig. 7.9. Consequently, the number of utilized RBs for the same number of UEs is higher under the proposal. It is to be noted that if these RBs were not utilized by the JDSBS scheme, they would have been left in idle.

7.3   Performance under the EWMA-based LF Predictor

Fig. 7.10 illustrates the incentives of integrating the EWMA-based LF predictor and the threshold L_{th} into the JDSBS-II scheme. Similar to the DS and the DSBS schemes presented in Chapter 6, it is again evident that with the increase of L_{th}, energy savings increases steadily becoming almost constant above a certain value. Optimal value of L_{th} is also evaluated around $0.6 \sim 0.7$ and $0.5 \sim 0.6$ for $f_1(t)$ and $f_2(t)$ respectively. At these settings, extracted energy savings per day amounts around 35% and 50% for $f_1(t)$ and $f_2(t)$ respectively, while the network reconfiguring events are reduced by 43% and 29% respectively.
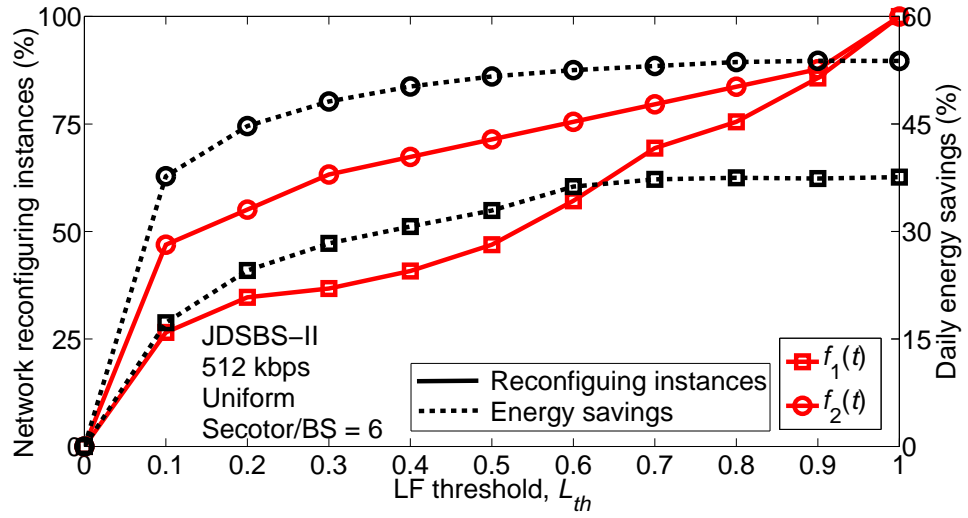
Figure 7.10: Daily energy savings and the percentage of instances at which network reconfiguration occurs.

7.4 Chapter Summary

A novel traffic-sensitive two-dimensional network reconfiguring mechanism called JDSBS for energy efficiency in cellular access networks has been proposed in this chapter. The proposed JDSBS mechanism performs dynamic network provisioning by adjusting the number of active BSs as well as the number of sectors in each active BS. For avoiding the high computational complexity of generalized optimization problem, the JDSBS problem is decomposed into DS and DSBS sub-problems in time-domain. Centralized low complexity greedy style heuristic algorithms are developed for both the sub-problems, which are sequentially applied. Simulation results have demonstrated a substantial energy savings amounting over 90% at very low traffic times. The impact of the sequence of DS and DSBS implementations, user association policies, BS power profiles, data rates, user distributions and original network configurations have been thoroughly analyzed. Reduction in SE leading to the requirement of higher number of RBs per user for maintaining the data rates than that in the original network is also identified. Moreover, the EWMA-based LF predictor has also been effectively used in substantially reducing the network reconfiguring events, while achieving significant energy savings.

Chapter 8

Conclusions and Future Works

8.1 Conclusions

This thesis has proposed and investigated various novel distributed as well as centralized traffic-driven dynamic operation mechanisms for energy efficiency in cellular networks. More specifically, the goal was to minimize energy utilization in cellular RANs by leveraging the natural temporal-spatial traffic diversity in adaptively switching RAN equipment between a high power active mode and a low power sleep mode, while maintaining service quality. Devised network operations were of a self-organizing nature requiring no human intervention, and thus, compatible with the future SONs.

SONs are envisaged to minimize human involvement in network operation and management leading to reduced cost and complexity. On the other hand, the ecosystem on Earth can be regarded as one of the best examples of a self-sustainable system with extreme intelligence and no visible controller. The self-organization feature of the ecosystem is playing a major role behind this self-sustainability. In light of this, by establishing an analogy between the HWNs and the ecosystem through a one-to-one mapping, Chapter 3 introduced a new notion of eco-inspired design by integrating ecological principles into cellular networks. With the aim of demonstrating the applicability of ecological principles in cellular networks, an ecological MSMRC-based RRM scheme was proposed. First, the intense competition among multi-class services for multiple radio resources was analytically modeled, which demonstrated that the service-classes requiring a higher amount of

radio resources were eventually completely excluded. The proposed RRM scheme was then imposed for regulating this competition by eliminating any chance of competitive exclusion of any service class. Thorough investigation verified the capability of the RRM scheme in shaping the unfair competition to a sustainable one, which guaranteed the co-existence of diverse service classes under extreme competitive scenarios.

Non-load-proportional energy consumption in BSs and the conventional approach of keeping all BSs active irrespective of traffic demand lead to a significant amount of energy wastage in the existing networks. Therefore, Chapter 4 proposed a distributed inter-BS cooperation assisted DSBS scheme for energy efficiency in cellular RANs. Under the proposal, neighboring BSs were made to mutually cooperate for dynamically swapping traffic and adjusting the number of active BSs, while meeting the instantaneous traffic demand. The proposed distributed cooperation, called intra-network cooperation, was developed following the principle of ecological self-organization and the degree of cooperation was governed by the designed LF thresholds. Various selection schemes for regulating the search space to choose the best BSs for offloading traffic were also explored. Measures were integrated into the algorithm for reducing the number of communications among BSs. An EWMA-based technique was also proposed for forecasting the LF in advance from the historical data, which was then used for initiating the cooperation procedure. Furthermore, an analytical model was also formulated for modeling the BS switching dynamics.

Thorough investigation of the proposed DSBS mechanism was conducted over a wide range of switching thresholds, BS selection schemes, BS power models, UE data rates and traffic scenarios. LF thresholds were found to have significant impact on the energy savings. Higher energy savings as well as higher switching in BSs were identified for the selection schemes with a larger search space. A network with lower data rate users showed the potential of higher energy savings. Furthermore, a steady rise in energy savings was observed with the increase of non-proportionality in power consumption of BSs being the highest for the CEC BSs, while the lowest for the FEP BSs. Moreover, BSs with a higher sleep mode power produced significantly less savings. Finally, analytical results were found in close agreement with the simulation results.

Many cities around the world are under the coverage of multiple cellular networks. Therefore, Chapter 5 focused on exploring this multi-RAN scenario for developing energy

saving DSBS mechanisms by implementing cooperation among these colocated RANs. Two alternative traffic-sensitive distributed multi-RAN cooperation mechanisms, namely, inter-network cooperation and joint cooperation, were developed in this chapter. Under the inter-network cooperation, according to an agreed upon policy among the network operators, colocated BSs that belong to different networks redistributed traffic among themselves allowing some of the BSs to switch into sleep mode for saving energy. In this case, no intra-network cooperation (as in Chapter 4) was implemented. Finally, both the intra-network cooperation and the inter-network cooperation were applied in combination under the joint cooperation. Analytical models for a 2-RAN scenario were also formulated for both the cooperation mechanisms.

Investigations identified longer sleep durations for BSs under the joint cooperation resulting in the highest energy savings, while the lowest savings was generated by the intra-network cooperation. An increasing trend in energy savings with a higher number of cooperating networks was also identified. On the other, achievable energy savings in a network having both temporal and spatial traffic diversities was found much less than in a network with temporal traffic diversity only. In addition, optimal energy savings and corresponding LF thresholds under various optimization constraints were also evaluated. The highest optimal savings was found for the case with no restriction on the number of switching in BSs, while the savings became the lowest when minimizing the switching in BSs was considered as well. Once again, analytical results were fairly close to the simulation results.

Considering various high-level complexities in practical implementations of BS switching based schemes, energy-aware DS mechanism having less complexity and effective as well was proposed in Chapter 6. Under the DS scheme, each BS was adaptively reconfigured with fewer sectors for matching with the traffic demand and saving energy. For avoiding the high computational complexity of the optimal exhaustive search technique, low complexity heuristically guided greedy style algorithms for both the centralized and distributed implementations were proposed. Various regular and irregular sector switching patterns were explored. Due to the absence of inter-cell interference, higher savings was achieved in a single-cell case compared to that in a multi-cell scenario. Savings was also identified higher in a Gaussian distributed user scenario than in a uniformly distributed case. Rise in energy savings was found with the increase of the number of sectors in BSs as well as with the decrease of user data rate requirement. Moreover, energy savings of the

proposed dynamic algorithm was found higher than that of the counterpart semi-dynamic schemes, while the performance gap was within 5% of the optimal exhaustive search. On the other hand, reduction in achievable SEs under the proposed network from those in the original network was observed resulting in the requirement of a higher number of RBs per user. A significant reduction in network reconfiguring events was also achieved from the utilization of the EWMA-based LF predictor.

Chapter 6 also proposed a centralized version of the DSBS scheme for a single-RAN scenario. Once again a greedy style heuristic algorithm was proposed for evaluating the optimal set of active BSs. Various UE association policies, namely, BS's energy efficiency based *LH* and *HL*, SINR-based *SBS* and the sequence-based *SS* schemes, were investigated. Simulation results demonstrated that although a nearly equal number of BSs slept under the *LH* and the *HL* schemes, much higher energy savings was achieved with the *LH* scheme. On the other hand, due to the preference of BSs with higher SINR for associating UEs, the centralized DSBS scheme with the *SBS* scheme outperformed all others in the higher traffic region. SEs, RBs requirement and the reduction in network dimensioning events followed similar trends as those observed under the DS scheme.

Chapter 7 proposed a novel traffic-aware two-dimensional centralized dynamic network provisioning mechanism named JDSBS for saving energy in cellular RANs. Under the JDSBS scheme, both the DS and the DSBS presented in Chapter 6 were jointly applied for maximizing the potential energy savings by adaptively switching several BSs as well as some of the sectors in the remaining under-utilized active BS into sleep mode. Based on the sequence of applications of DS and DSBS, two variants of the JDSBS scheme, designated JDSBS-I and JDSBS-II, were outlined. Impact of the UE association policies, BS power profiles, user data rates, user distributions and original network configurations was thoroughly investigated. JDSBS-I and JDSBS-II were identified to outperform each other in the higher and lower traffic regions respectively. Furthermore, the JDSBS-II showed the potential of achieving higher savings than that under the individual applications of DS and DSBS. The proposed LF predictor was once again effectively used in reducing the network provisioning events.

8.2   Future Research Directions

At the current stage of the proposed research, developed dynamic network operation mechanisms have much room for being improved and extended in several interesting directions. Some of these potential research openings are summarized below.

• The proposed mechanisms were developed aiming to reduce energy consumption in BSs and thus, only the downlink direction was considered. However, these dynamic switching of network equipment may increase the energy consumption in UEs leading to reduced battery life. Impact on UE power consumption can be more apparent under the DSBS schemes as a UE located in a sleep mode BS is served by a distant BS. Therefore, it is vital to take into account both uplink and downlink directions jointly for developing effective energy efficient dynamic network operation mechanisms. On the other hand, for compensating this probable increased energy utilization in UEs, relay stations can be introduced into the network. Then, the relays located around the sleep mode BSs can be dynamically activated for connecting their (BSs) users to distant neighboring BSs, which can be considered as a future focus for thorough study.

• The system models were developed and investigated for CBR services. However, the relaxed bit rate requirements of non-CBR services can be exploited for achieving higher energy savings. Therefore, it would be really interesting to extend the proposed schemes to various cases of multi-class services with diverse QoS requirements, such as CBR and non-CBR (e.g., GBR and best effort) traffic, symmetric and asymmetric data rates, real-time and non-real time applications and different delay constraints. Furthermore, for computational tractability, like majority of the existing works, this thesis adopted conservative strategies for modeling the highly dynamic interference, especially under the DSBS schemes. If the interference could be accurately modeled, evaluated energy savings could be higher. Therefore, accurate modeling of the inter-cell interference under the proposed dynamic schemes can be considered for future works, which can have a broader significance in developing dynamic interference management techniques.

• Under the proposed schemes, BSs mutually cooperate with each other in an unselfish manner, i.e., they cooperate for maximizing the total energy savings without being concerned about their individual benefit. However, it would be interesting to evaluate the energy saving performance with BSs aware of their own payback. This is particularly more

important for the case of the proposed multi-RAN DSBS schemes in which a pre-ranked sequence of RANs was assumed for redistributing traffic among them. In practice, network operators are competitor of each other and eager to optimize their respective profits. Therefore, it is essential to develop cooperative business models for traffic redistribution as well as profit sharing among the operators. For instance, a game-theoretic approach or an ecological coopetition (i.e., both cooperation and competition together) based model can be used for this kind of strategy formulation.

• For overcoming several performance limitations of the conventional macrocell networks, the notion of multi-tier networks employing a blend of macro, micro, femto and pico cells for cellular networks has gained universal recognition. This thesis proposed and investigated the energy saving mechanisms for homogeneous cellular networks having macrocells only. Therefore, there is a large research prospect in extending the proposed mechanisms and the algorithms to the complex scenarios of multi-tier networks. Developing advanced traffic-aware joint dynamic macro-micro-femto-pico BSs switching mechanisms by offloading traffic from one another for achieving energy savings can be of fundamental importance. In addition to the utilization of ideal circular shape cell coverage, stochastic geometry based network models can also be integrated into the analysis for achieving a more realistic system design.

• CoMP transmission/reception integrated in the 3GPP LTE-A is a promising candidate for efficient interference management through inter-cell interference coordination (ICIC), achieving higher throughput, better radio resource utilization and so on. Under the downlink JT-CoMP technique, multiple BSs in a cooperative and coordinated way can simultaneously transmit to a single UE resulting in reduced interference and higher SINR [86]. Therefore, incorporation of the downlink JT-CoMP technique in the proposed schemes may result in reduced downlink transmit power and RB requirement in each BS. Consequently, a higher number of BSs and sectors might be switched into sleep mode leading to higher energy savings. In addition, the proposed schemes with other CoMP techniques [86], such as the downlink CS/CB, and the uplink multipoint reception (MR) with IRC and CS may achieve higher energy savings, which can be an attractive subject matter of investigation.

• Utilization of green energy, such as sustainable biofuels, solar, wind and marine energy for powering up BSs can considerably decrease the on-grid energy consumption resulting

in reduced CO_2 footprint. BS manufacturers Ericsson and Nokia Siemens Networks have already developed such types of green BSs. On the other hand, climate conditions and consequently, green energy generation can vary from location to location. Furthermore, due to the variation in traffic intensity, effective sunlight duration, wind velocity, etc., available green energy among BSs may differ significantly. Under such cases, it might be possible to run a BS from green energy for a fraction of the day, while the rest of the day by the on-grid energy. Moreover, by keeping the green powered BSs active for a longer duration and switching the on-grid powered BSs into sleep mode, energy savings can be further enhanced. Additional energy savings would be possible by serving more traffic by BSs having higher green energy. Therefore, for such a scenario of combined on-grid energy and green energy supply, development of joint energy sources scheduling and equipment switching strategies for minimizing the on-grid energy usage can be of immense importance.

Appendix A

Derivation of Probabilities in Chapter 4 and Chapter 5

Let us consider a scenario of N RANs each having N_T BSs serving Q classes of services. Without losing the generality, it is assumed that all the sessions generated from the qth class in the ith network are of equal duration denoted by $h_{i,q}, \forall i \in (1, 2, ..., N), \forall q \in (1, 2, ..., Q)$, and require equal number of RBs denoted by $\eta_{i,q}, \forall i \in (1, 2, ..., N), \forall q \in (1, 2, ..., Q)$, as well. Instantaneous LF at time t in BS $\mathcal{B}_{i,j}$ can then be given by

$$L_{i,j}(t) = \frac{\alpha(l_{i,j}) f_{i,j}(t)}{\beta_{i,j}} \sum_{q=1}^{Q} \rho_{i,j}^{(q)} h_{i,q} \eta_{i,q}, \forall i, \forall j \tag{A.1}$$

where $f_{i,j}(t)$, $\beta_{i,j}$ and $l_{i,j}$ are the rate function, total number of RBs and the location of $\mathcal{B}_{i,j}$ respectively. $\rho_{i,j}^{(q)}$ is a Poisson RV with parameter $\lambda_{i,j}^{(q)}$. Assuming $\alpha(l_{i,j}) \geq 0, \forall i, \forall j$ are independent identically distributed uniform RVs over a range $[a, b]$, we can replace $\alpha(l_{i,j})$ by $\alpha, \forall i, \forall j$ and write as below

$$Pr\left\{ \sum_{i=1}^{N} K_{i,j} L_{i,j}(t) < \Theta|_\alpha \right\} = Pr\left\{ \sum_{i=1}^{N} \sum_{q=1}^{Q} \frac{K_{i,j} \rho_{i,j}^{(q)} f_{i,j}(t) h_{i,q} \eta_{i,q}}{\beta_{i,j}} < \frac{\Theta}{\alpha}|_\alpha \right\}$$

$$= Pr\left\{ Z_{N,j} < \frac{\frac{\Theta}{\alpha} - \mu_{z_{N,j}}}{\sqrt{\sigma_{z_{N,j}}^2}}|_\alpha \right\} = 1 - Q\left(\frac{\frac{\Theta}{\alpha} - \mu_{z_{N,j}}}{\sqrt{\sigma_{z_{N,j}}^2}} \right), \forall j \tag{A.2}$$

where $Z_{N,j}$ is a Normal RV with zero mean and unit variance, and Θ and $K_{i,j}, \forall i, \forall j$ are constants. The assumption that a Poisson RV with large rate parameter λ can be

approximated by a Normal RV with both mean and variance equal to λ has been used in deriving (A.2). Here, $\mu_{z_{N,j}}$ and $\sigma^2_{z_{N,j}}$ are given by

$$\mu_{z_{N,j}} = \sum_{i=1}^{N} \sum_{q=1}^{Q} \frac{K_{i,j} \lambda_{i,j}^{(q)} f_{i,j}(t) h_{i,q} \eta_{i,q}}{\beta_{i,j}}, \forall j \qquad (A.3)$$

$$\sigma^2_{z_{N,j}} = \sum_{i=1}^{N} \sum_{q=1}^{Q} \frac{K_{i,j}^2 \lambda_{i,j}^{(q)} f_{i,j}^2(t) h_{i,q}^2 \eta_{i,q}^2}{\beta_{i,j}^2}, \forall j \qquad (A.4)$$

By removing the summation over N, and setting $K_{i,j} = 1$ and appropriate value for Θ in (A.2), we can evaluate the following probabilities for a particular BS $\mathcal{B}_{i,j}$

$$Pr\left\{L_{i,j}(t) < L_f|\alpha\right\} = Pr\left\{\sum_{q=1}^{Q} \rho_{i,j}^{(q)} h_{i,q} \eta_{i,q} < \frac{\beta_{i,j} L_f}{\alpha f_{i,j}(t)}|\alpha\right\} = 1 - Q\left(\frac{\frac{\beta_{i,j} L_f}{\alpha f_{i,j}(t)} - \mu_{x_{i,j}}}{\sqrt{\sigma^2_{x_{i,j}}}}\right) \qquad (A.5)$$

where $\mu_{x_{i,j}} = \sum_{q=1}^{Q} \lambda_{i,j}^{(q)} h_{i,q} \eta_{i,q}$ and $\sigma^2_{x_{i,j}} = \sum_{q=1}^{Q} \lambda_{i,j}^{(q)} h_{i,q}^2 \eta_{i,q}^2$. Similarly, we can write

$$Pr\left\{L_{i,j}(t) \geq H_f|\alpha\right\} = 1 - Pr\left\{L_{i,j}(t) < H_f|\alpha\right\} = Q\left(\frac{\frac{\beta_{i,j} H_f}{\alpha f_{i,j}(t)} - \mu_{x_{i,j}}}{\sqrt{\sigma^2_{x_{i,j}}}}\right) \qquad (A.6)$$

$$Pr\left\{L_f \leq L_{i,j}(t) < H_f|\alpha\right\} = Q\left(\frac{\frac{\beta_{i,j} L_f}{\alpha f_{i,j}(t)} - \mu_{x_{i,j}}}{\sqrt{\sigma^2_{x_{i,j}}}}\right) - Q\left(\frac{\frac{\beta_{i,j} H_f}{\alpha f_{i,j}(t)} - \mu_{x_{i,j}}}{\sqrt{\sigma^2_{x_{i,j}}}}\right) \qquad (A.7)$$

Again, $Pr\left\{(A_f - L_{i,j}^{n,k}(t) > \psi_{i,j}^{n,k} L_{i,j}(t)|\alpha\right\} = Pr\left\{\psi_{i,j}^{n,k} L_{i,j}(t) + L_{i,j}^{n,k}(t) < A_f|\alpha\right\}$

$$= Pr\left\{\frac{\alpha \psi_{i,j}^{n,k} f_{i,j}(t)}{\beta_{i,j}} \sum_{q=1}^{Q} \rho_{i,j}^{(q)} h_{i,q} \eta_{i,q} + \frac{\alpha f_{i,j}^{n,k}(t)}{\beta_{i,j}^{n,k}} \sum_{q=1}^{Q} \rho_{i,j}^{n,k(q)} h_{i,q} \eta_{i,q} < A_f|\alpha\right\}$$

$$= Pr\left\{Y_{i,j} < \frac{A_f - \mu_{y_{i,j}}}{\sqrt{\sigma^2_{y_{i,j}}}}\right\} = 1 - Q\left(\frac{A_f - \mu_{y_{i,j}}}{\sqrt{\sigma^2_{y_{i,j}}}}\right) \qquad (A.8)$$

where $f_{i,j}^{n,k}$, $L_{i,j}^{n,k}$, $\beta_{i,j}^{n,k}$ and $\lambda_{i,j}^{n,k(q)}$ are respectively the rate function, LF, total RBs and the qth class Poisson rate parameter in the candidate BS $C_{i,j}^{n,k}$ of $\mathcal{B}_{i,j}$. Whereas, $Y_{i,j}$ is a Normal RV with zero mean and unit variance, and $\mu_{y_{i,j}}$ and $\sigma^2_{y_{i,j}}$ are given by

$$\mu_{y_{i,j}} = \frac{\alpha \psi_{i,j}^{n,k} f_{i,j}(t)}{\beta_{i,j}} \sum_{q=1}^{Q} \lambda_{i,j}^{(q)} h_{i,q} \eta_{i,q} + \frac{\alpha f_{i,j}^{n,k}(t)}{\beta_{i,j}^{n,k}} \sum_{q=1}^{Q} \lambda_{i,j}^{n,k(q)} h_{i,q} \eta_{i,q} \qquad (A.9)$$

$$\sigma^2_{y_{i,j}} = \frac{\alpha^2 (\psi_{i,j}^{n,k})^2 f_{i,j}^2(t)}{\beta_{i,j}^2} \sum_{q=1}^{Q} \lambda_{i,j}^{(q)} h_{i,q}^2 \eta_{i,q}^2 + \frac{\alpha^2 (f_{i,j}^{n,k}(t))^2}{(\beta_{i,j}^{n,k})^2} \sum_{q=1}^{Q} \lambda_{i,j}^{n,k(q)} h_{i,q}^2 \eta_{i,q}^2 \qquad (A.10)$$

Appendix B

Multi-Dimensional Erlang-B Formula

Let i^{th} cellular network has N_T BSs and serves Q classes of services. A state of its jth BS $\mathcal{B}_{i,j}$ can be given as, $\overline{\boldsymbol{\gamma}}_{i,j} = \left(\gamma_{i,j}^{(1)}, \gamma_{i,j}^{(2)}, ..., \gamma_{i,j}^{(Q)} \right)$, where $\gamma_{i,j}^{(q)}$ is the number of active sessions from class q. We can also write, $\overline{\boldsymbol{\eta}}_{i,j} = \left(\eta_{i,j}^{(1)}, \eta_{i,j}^{(2)}, ..., \eta_{i,j}^{(Q)} \right)$, where $\eta_{i,j}^{(q)}$ denotes the number of channels (e.g., RBs in LTE) required for a session from q^{th} class.

Thus, the state space of $\mathcal{B}_{i,j}$ becomes, $\boldsymbol{\Omega}_{i,j} = \left\{ \overline{\boldsymbol{\gamma}}_{i,j} : \overline{\boldsymbol{\gamma}}_{i,j}(\overline{\boldsymbol{\eta}}_{i,j})^T \leq \Upsilon_{i,j}, \gamma_{i,j}^{(q)} \geq 0, \forall q \right\}$, where $\Upsilon_{i,j}$ is the total number of channels in $\mathcal{B}_{i,j}$.

Let $\boldsymbol{\Omega}_{i,j}^{(q)} = \left\{ \overline{\boldsymbol{\gamma}}_{i,j} : \Upsilon_{i,j} - \overline{\boldsymbol{\gamma}}_{i,j}(\overline{\boldsymbol{\eta}}_{i,j})^T < \eta_{i,j}^{(q)}, \gamma_{i,j}^{(q)} \geq 0, \forall q \right\} \subseteq \boldsymbol{\Omega}_{i,j}$ and $a_{i,j}^{(q)} = \lambda_{i,j}^{(q)} h_{i,j}^{(q)}$. Here, $\lambda_{i,j}^{(q)}$ and $h_{i,j}^{(q)}$ are the average session arrival rate and the session duration of class q respectively. Then, the session blocking probability of class q in $\mathcal{B}_{i,j}$ can be given by

$$P_{i,j}^{q,b} = \frac{G\left(\boldsymbol{\Omega}_{i,j}^{(q)}\right)}{G\left(\boldsymbol{\Omega}_{i,j}\right)} \tag{B.1}$$

where

$$G\left(\boldsymbol{\Omega}_{i,j}\right) = \sum_{\overline{\boldsymbol{\gamma}}_{i,j} \in \boldsymbol{\Omega}_{i,j}} \prod_{q=1}^{Q} \frac{\left(a_{i,j}^{(q)}\right)^{\gamma_{i,j}^{(q)}}}{\gamma_{i,j}^{(q)}}, \quad G\left(\boldsymbol{\Omega}_{i,j}^{(q)}\right) = \sum_{\overline{\boldsymbol{\gamma}}_{i,j} \in \boldsymbol{\Omega}_{i,j}^{(q)}} \prod_{q=1}^{Q} \frac{\left(a_{i,j}^{(q)}\right)^{\gamma_{i,j}^{(q)}}}{\gamma_{i,j}^{(q)}} \tag{B.2}$$

Thus, the average session blocking probability in i^{th} network can be written as

$$P_{i,b} = \frac{\sum_{j=1}^{N_T} \sum_{q=1}^{Q} \lambda_{i,j}^{(q)} P_{i,j}^{q,b}}{\sum_{j=1}^{N_T} \sum_{q=1}^{Q} \lambda_{i,j}^{(q)}} \tag{B.3}$$

Bibliography

[1] T. Edler and S. Lundberg, "Energy Efficiency Enhancements in Radio Access Networks," *Ericsson Review*, 2004.

[2] "Improving Energy Efficiency, Lower CO_2 Emission and TCO," *Huawei White Paper*, pp. 1–16, 2011.

[3] S. Mongay, "Green IT: The New Industry Shockwave," *Presentation Gartner Symposium /ITXPO*, Apr 2007. [Online]. Available: http://www.ictliteracy.info/rf.pdf/Gartner_on_Green_IT.pdf

[4] J. Malmodin, A. Moberg, D. Lunden, G. Finnveden, and N. Lovehagen, "Greenhouse Gas Emissions and Operational Electricity Use in the ICT and Entertainment & Media Sectors," *Journal of Industrial Ecology*, vol. 14, no. 5, pp. 770–790, 2010.

[5] Z. Hasan, H. Boostanimehr, and V. Bhargava, "Green Cellular Networks: A Survey, Some Research Issues and Challenges," *IEEE Communications Surveys & Tutorials*, vol. 13, no. 4, pp. 524–540, 2011.

[6] "Smart 2020: Enabling the Low Carbon Economy in the Information Age," *Study Report, The Climate Group, Global e-Sustainability Initiative (GeSI)*, pp. 1–85, 2008. [Online]. Available: http://www.smart2020.org/

[7] "Understanding the Environmental Impact of Communication Systems," *Ofcom Study Report*, pp. 1–85, Apr 2009. [Online]. Available: http://www.ofcom.org.uk/research/technology/research/sectorstudies/environment/

[8] A. Fehske, G. Fettweis, J. Malmodin, and G. Biczok, "The Global Footprint of Mobile Communications: The Ecological and Economic Perspective," *IEEE Communications Magazine*, vol. 49, no. 8, pp. 55–62, Aug 2011.

[9] E. Oh, K. Son, and B. Krishnamachari, "Dynamic Base Station Switching-On/Off Strategies for Green Cellular Networks," *IEEE Transactions on Wireless Communications*, vol. 12, no. 5, pp. 2126–2136, May 2013.

[10] R. Bolla, R. Bruschi, F. Davoli, and F. Cucchietti, "Energy Efficiency in the Future Internet: A Survey of Existing Approaches and Trends in Energy-Aware Fixed Network Infrastructures," *IEEE Communications Surveys & Tutorials*, vol. 13, no. 2, pp. 223–244, 2011.

[11] K. Son, H. Kim, Y. Yi, and B. Krishnamachari, "Base Station Operation and User Association Mechanisms for Energy-Delay Tradeoffs in Green Cellular Networks," *IEEE Journal on Selected Areas in Communications*, vol. 29, no. 8, pp. 1525–1536, Sep 2011.

[12] C. Peng, S. B. Lee, S. Lu, H. Luo, and H. Li, "Traffic-Driven Power Saving in Operational 3G Cellular Networks," in *ACM International Conference on Mobile Computing and Networking (MobiCom)*, Sep 2011, pp. 121–132.

[13] C. Han, T. Harrold, S. Armour, I. Krikidis, S. Videv, P. M. Grant, H. Haas, J. Thompson, I. Ku, C.-X. Wang, T. A. Le, M. Nakhai, J. Zhang, and L. Hanzo, "Green Radio: Radio Techniques to Enable Energy-Efficient Wireless Networks," *IEEE Communications Magazine*, vol. 49, no. 6, pp. 46–54, June 2011.

[14] X. Ge, C. Cao, M. Jo, M. Chen, J. Hu, and I. Humar, "Energy Efficiency Modelling and Analyzing Based on Multi-cell and Multi-antenna Cellular Networks," in *KSII Transactions on Internet and Information Systems*, vol. 4, no. 4, Aug 2010, pp. 560–574.

[15] C. Desset, B. Debaillie, V. Giannini, A. Fehske, G. Auer, H. Holtkamp, W. Wajda, D. Sabella, F. Richter, M. Gonzalez, H. Klessig, I. Godor, M. Olsson, M. Imran, A. Ambrosy, and O. Blume, "Flexible Power Modeling of LTE Base Stations," in *IEEE Wireless Communications and Networking Conference (WCNC)*, Apr 2012, pp. 2858–2862.

[16] O. Arnold, F. Richter, G. Fettweis, and O. Blume, "Power Consumption Modeling of Different Base Station Types in Heterogeneous Cellular Networks," in *Future Network and Mobile Summit*, June 2010, pp. 1–8.

[17] L. Correia, D. Zeller, O. Blume, D. Ferling, Y. Jading, I. Godor, G. Auer, and L. Van Der Perre, "Challenges and Enabling Technologies for Energy Aware Mobile Radio Networks," *IEEE Communications Magazine*, vol. 48, no. 11, pp. 66–72, Nov 2010.

[18] G. Auer, V. Giannini, C. Desset, I. Godor, P. Skillermark, M. Olsson, M. A. Imran, D. Sabella, M. J. Gonzalez, O. Blume, and A. Fehske, "How Much Energy is Needed to Run a Wireless Network?" *IEEE Wireless Communications*, vol. 18, no. 5, pp. 40–49, Oct 2011.

[19] L. Xiang, X. Ge, C. Wang, F. Li, and F. Reichert, "Energy Efficiency Evaluation of Cellular Networks Based on Spatial Distributions of Traffic Load and Power Consumption," *IEEE Transactions on Wireless Communications*, vol. 12, no. 3, pp. 961–973, Mar 2013.

[20] U. Paul, A. Subramanian, M. Buddhikot, and S. Das, "Understanding Traffic Dynamics in Cellular Data Networks," in *IEEE International Conference on Computer Communications (INFOCOM)*, Apr 2011, pp. 882–890.

[21] M. Z. Shafiq, L. Ji, A. X. Liu, and J. Wang, "Characterizing and Modeling Internet Traffic Dynamics of Cellular Devices," in *ACM SIGMETRICS*, June 2011, pp. 305–316.

[22] S. McLaughlin, P. M. Grant, J. Thompson, H. Haas, D. Laurenson, C. Khirallah, Y. Hou, and R. Wang, "Techniques for Improving Cellular Radio Base Station Energy Efficiency," *IEEE Wireless Communications*, vol. 18, no. 5, pp. 10–17, Oct 2011.

[23] O. Sallent, J. Perez-Romero, J. Sanchez-Gonzalez, R. Agusti, M. Diaz-guerra, D. Henche, and D. Paul, "A Roadmap from UMTS Optimization to LTE Self-Optimization," *IEEE Communications Magazine*, vol. 49, no. 6, pp. 172–182, June 2011.

[24] C. Prehofer and C. Bettstetter, "Self-Organization in Communication Networks: Principles and Design Paradigms," *IEEE Communications Magazine*, vol. 43, no. 7, pp. 78–85, July 2005.

[25] C. Kappler, P. Poyhonen, M. Johnsson, and S. Schmid, "Dynamic Network Composition for Beyond 3G Networks: a 3GPP Viewpoint," *IEEE Network*, vol. 21, no. 1, pp. 47–52, Jan-Feb 2007.

[26] H. Hu, J. Zhang, X. Zheng, Y. Yang, and P. Wu, "Self-Configuration and Self-Optimization for LTE Networks," *IEEE Communications Magazine*, vol. 48, no. 2, pp. 94–100, Feb 2010.

[27] "NGMN Use Cases Related to Self Organizing Network, Overall Description," *NGMN Alliance Deliverable*, pp. 1–18, May 2007.

[28] 3GPP, "Technical Specification Group Services and System Aspects; Telecommunication Management; Self-Organizing Networks (SON); Concepts and requirements," *Technical Specification, 3GPP TS 32.500 V11.1.0*, Dec 2011.

[29] "Architecture, Detailed Protocols and Procedures: Self-Organizing Networks," *WiMAX Forum Network Architecture, WMF-T33-120-R016v01*, June 2010.

[30] J. Rao and A. Fapojuwo, "A Survey of Energy Efficient Resource Management Techniques for Multicell Cellular Networks," *IEEE Communications Surveys & Tutorials*, vol. PP, no. 99, pp. 1–27, May 2013.

[31] 3GPP, "Evolved Universal Terrestrial Radio Access Network (E-UTRAN); Self-Configuring and Self-Optimizing Network (SON): Use Cases and Solutions," *Technical Report, 3GPP TR 36.902 ver. 9.3.1 Rel. 9*, Apr 2011.

[32] M. Marsan, L. Chiaraviglio, D. Ciullo, and M. Meo, "Optimal Energy Savings in Cellular Access Networks," in *IEEE International Conference on Communications (ICC) Workshops*, June 2009, pp. 1–5.

[33] F. Han, Z. Safar, W. S. Lin, Y. Chen, and K. J. R. Liu, "Energy Efficient Cellular Network Operation via Base Station Cooperation," in *IEEE International Conference on Communications (ICC)*, June 2012, pp. 5885–5889.

[34] M. Marsan, L. Chiaraviglio, D. Ciullo, and M. Meo, "Multiple Daily Base Station Switch-offs in Cellular Networks," in *International Conference on Communications and Electronics (ICCE)*, Aug 2012, pp. 245–250.

[35] L. Chiaraviglio, D. Ciullo, M. Meo, and M. Marsan, "Energy-Efficient Management of UMTS Access Networks," in *IEEE INternational Teletraffic Congress (ITC)*, Sep 2009, pp. 1–8.

[36] E. Oh, B. Krishnamachari, X. Liu, and Z. Niu, "Toward Dynamic Energy-Efficient Operation of Cellular Network Infrastructure," *IEEE Communications Magazine*, vol. 49, no. 6, pp. 56–61, Jun 2011.

[37] E. Oh and B. Krishnamachari, "Energy Savings Through Dynamic Base Station Switching in Cellular Wireless Access Networks," in *IEEE Global Communications Conference (GLOBECOM)*, Dec 2010, pp. 1–5.

[38] S. Zhou, G. J, Z. Yang, Z. Niu, and P. Yang, "Green Mobile Access Network with Dynamic Base Station Energy Saving," in *ACM International Conference on Mobile Computing and Networking (MobiCom)*, Sep 2009, pp. 1–3.

[39] R. Li, Z. Zhao, X. Chen, and H. Zhang, "Energy Saving through a Learning Framework in Greener Cellular Radio Access Networks," in *IEEE Global Communications Conference (GLOBECOM)*, Dec 2012, pp. 1574–1579.

[40] L. G. Hevizi and I. Godor, "Power Savings in Mobile Networks by Dynamic Base Station Sectorization," in *IEEE International Symposium on Personal, Indoor and Mobile Radio Communications (PIMRC)*, Sep 2011, pp. 2415–2417.

[41] G. Micallef, P. Mogensen, and H. O. Scheck, "Cell Size Breathing and Possibilities to Introduce Cell Sleep Mode," in *IEEE European Wireless Conference (EW)*, Apr 2010, pp. 111–115.

[42] Y. Qi, M. A. Imran, and R. Tafazolli, "Energy-Aware Adaptive Sectorisation in LTE Systems," in *IEEE International Symposium on Personal, Indoor and Mobile Radio Communications (PIMRC)*, Sep 2011, pp. 2402–2406.

[43] Z. Niu, Y. Wu, J. Gong, and Z. Yang, "Cell Zooming for Cost-Efficient Green Cellular Networks," *IEEE Communications Magazine*, vol. 48, no. 11, pp. 74–79, Nov 2010.

[44] Y. S. Soh, T. Q. Quek, M. Kountouris, and H. Shin, "Energy Efficient Heterogeneous Cellular Networks," *IEEE Journal on Selected Areas in Communications*, vol. 31, no. 5, pp. 840–850, May 2013.

[45] H. Elsawy, E. Hossain, and D. I. Kim, "HetNets with Cognitive Small Cells: User Offloading and Distributed Channel Access Techniques," *IEEE Communications Magazine*, vol. 51, no. 6, pp. 28–36, June 2013.

[46] I. Ashraf, F. Boccardi, and L. Ho, "SLEEP Mode Techniques for Small Cell Deployments," *IEEE Communications Magazine*, vol. 49, no. 8, pp. 72–79, Aug 2011.

[47] D. Willkomm, S. Machiraju, J. Bolot, and A. Wolisz, "Primary User Behavior in Cellular Networks and Implications for Dynamic Spectrum Access," *IEEE Communications Magazine*, vol. 47, no. 3, pp. 88–95, Mar 2009.

[48] M. A. Marsan and M. Meo, "Energy Efficient Management of Two Cellular Access Networks," in *GreenMetrics Workshop in Conjunction with ACM SIGMETRICS*, June 2009, pp. 1–5.

[49] Ericsson, "Mobile Data Traffic Surpasses Voice," *Ericsson Press Release*, pp. 1–2, Mar 2010. [Online]. Available: http://hugin.info/1061/R/1396928/353017.pdf

[50] CISCO, "Cisco Visual Networking Index: Global Mobile Data Traffic Forecast Update, 2012-2017," *CISCO White Paper*, pp. 1–34, Mar 2013. [Online]. Available: http://www.cisco.com/en/US/solutions/collateral/ns341/ns525/ns537/ns705/ns827/white_paper_c11-520862.pdf

[51] A. J. Fehske, F. Richter, and G. P. Fettweis, "Energy Efficiency Improvements Through Micro Sites in Cellular Mobile Radio Networks," in *IEEE Global Communications Conference (GLOBECOM) Workshop*, Dec 2009, pp. 1–5.

[52] F. Richter, A. Fehske, and G. Fettweis, "Energy Efficiency Aspects of Base Station Deployment Strategies for Cellular Networks," in *IEEE Vehicular Networking Conference (VTC)*, Sep 2009, pp. 1–5.

[53] R. Litjens and L. Jorguseski, "Potential of Energy-Oriented Network Optimisation: Switching OFF Over-Capacity in Off-Peak Hours," in *IEEE International Symposium on Personal, Indoor and Mobile Radio Communications (PIMRC)*, Sep 2010, pp. 1660–1664.

[54] K. Son, E. Oh, and B. Krishnamachari, "Energy-Aware Hierarchical Cell Configuration: From Deployment to Operation," in *IEEE International Conference on Computer Communications (INFOCOM) Workshops*, Apr 2011, pp. 289–294.

[55] M. Deruyck, E. Tanghe, W. Joseph, and L. Martens, "Modelling and Optimization of power consumption in wireless access networks," *Elsevier Journal of Computer Communications*, vol. 34, no. 17, pp. 2036 – 2046, Nov 2011.

[56] A. Shafiul Alam, L. Dooley, and A. Poulton, "Energy Efficient Relay-Assisted Cellular Network Model Using Base Station Switching," in *IEEE Global Communications Conference (GLOBECOM) Workshops*, Dec 2012, pp. 1155–1160.

[57] V. Mancuso and S. Alouf, "Reducing Costs and Pollution in Cellular Networks," *IEEE Communications Magazine*, vol. 49, no. 8, pp. 63–71, Aug 2011.

[58] T. Chen, Y. Yang, H. Zhang, H. Kim, and K. Horneman, "Network Energy Saving Technologies for Green Wireless Access Networks," *IEEE Wireless Communications*, vol. 18, no. 5, pp. 30–38, Oct 2011.

[59] B. Debaillie, B. Bougard, G. Lenoir, G. Vandersteen, and F. Catthoor, "Energy-Scalable OFDM Transmitter Design and Control," in *ACM/IEEE Design Automation Conference*, 2006, pp. 536–541.

[60] Z. Niu, S. Zhou, , Y. Hua, Q. Zhang, and D. Cao, "Energy-Aware Network Planning for Wireless Cellular System with Inter-Cell Cooperation," *IEEE Transactions on Wireless Communications*, vol. 11, no. 4, pp. 1412–1423, Apr 2012.

[61] D. Cao, S. Zhou, C. Zhang, and Z. Niu, "Energy Saving Performance Comparison of Coordinated Multi-Point Transmission and Wireless Relaying," in *IEEE Global Communications Conference (GLOBECOM)*, Dec 2010, pp. 1–5.

[62] H. Chen, Y. Jiang, J. Xu, and H. Hu, "Energy-Efficient Coordinated Scheduling Mechanism for Cellular Communication Systems with Multiple Component Carriers," *IEEE Journal on Selected Areas in Communications*, vol. 31, no. 5, pp. 959–968, May 2013.

[63] B. Badic, T. O'Farrrell, P. Loskot, and J. He, "Energy Efficient Radio Access Architectures for Green Radio: Large versus Small Cell Size Deployment," in *IEEE Vehicular Technology Conference (VTC)*, Sep 2009, pp. 1–5.

[64] H. Leem, S. Y. Baek, and D. K. Sung, "The Effects of Cell Size on Energy Saving, System Capacity, and Per-Energy Capacity," in *IEEE Wireless Communications and Networking Conference (WCNC)*, Apr 2010, pp. 1–6.

[65] I. Humar, X. Ge, L. Xiang, M. Jo, M. Chen, and J. Zhang, "Rethinking Energy Efficiency Models of Cellular Networks with Embodied Energy," *IEEE Network*, vol. 25, no. 2, pp. 40–49, Mar-Apr 2011.

[66] K. Dufkova, M. Popovic, R. Khalili, L. Boudec, J. Yves, M. Bjelica, and L. Kencl, "Energy Consumption Comparison Between Macro-Micro and Public Femto Deployment in a Plausible LTE Network," in *ACM International Conference on Energy-Efficient Computing and Networking (e-Energy)*, May-June 2011, pp. 67–76.

[67] D. Lee, S. Zhou, and Z. Niu, "Spatial Modeling of Scalable Spatially-Correlated Log-normal Distributed Traffic Inhomogeneity and Energy-Efficient Network Planning," in *IEEE Wireless Communications and Networking Conference (WCNC)*, 2013, pp. 1285–1290.

[68] Y. S. Soh, T. Q. Quek, M. Kountouris, and H. Shin, "Energy efficient heterogeneous cellular networks," *IEEE Journal on Selected Areas in Communications*, vol. 31, no. 5, pp. 840–850, 2013.

[69] D. Cao, S. Zhou, and Z. Niu, "Optimal Base Station Density for Energy-Efficient Heterogeneous Cellular Networks," in *IEEE International Conference on Communications (ICC)*, June 2012, pp. 1–5.

[70] Z. Niu, "TANGO: Traffic-Aware Network Planning and Green Operation," *IEEE Wireless Communications*, vol. 18, no. 5, pp. 25–29, Oct 2011.

[71] T. Han and N. Ansari, "On Optimizing Green Energy Utilization for Cellular Networks with Hybrid Energy Supplies," *IEEE Transactions on Wireless Communications*, vol. 12, no. 8, pp. 3872–3882, Aug 2013.

[72] J. Louhi, "Energy Efficiency of Modern Cellular Base Stations," in *International Telecommunications Energy Conference (INTELEC)*, Sep-Oct 2007, pp. 475–476.

[73] T. Han and N. Ansari, "Optimizing Cell Size for Energy Saving in Cellular Networks with Hybrid Energy Supplies," in *IEEE Global Communications Conference (GLOBECOM)*, Dec 2012, pp. 5411–5415.

[74] X. Zhang and P. Wang, "Optimal Trade-Off Between Power Saving and QoS Provisioning for Multicell Cooperation Networks," *IEEE Wireless Communications*, vol. 20, no. 1, pp. 90–96, Feb 2013.

[75] T. Han and N. Ansari, "On Greening Cellular Networks via Multicell Cooperation," *IEEE Wireless Communications*, vol. 20, no. 1, pp. 82–89, Feb 2013.

[76] M. Ismail and W. Zhuang, "Network Cooperation for Energy Saving in Green Radio Communications," *IEEE Wireless Communications*, vol. 18, no. 5, pp. 76–81, Oct 2011.

[77] D. Tipper, A. Rezgui, P. Krishnamurthy, and P. Pacharintanakul, "Dimming Cellular Networks," in *IEEE Global Communications Conference (GLOBECOM)*, Dec 2010, pp. 1–6.

[78] S. Bhaumik, G. Narlikar, S. Chattopadhyay, and S. Kanugovi, "Breathe to Stay Cool: Adjusting Cell Sizes to Reduce Energy Consumption," in *ACM SIGCOMM workshop on Green networking*, Aug 2010, pp. 41–46.

[79] W. Guo and T. O'Farrell, "Dynamic Cell Expansion: Traffic Aware Low Energy Cellular Network," in *IEEE Vehicular Technology Conference (VTC)*, 2012, pp. 1–5.

[80] Y. S. Soh, T. Q. S. Quek, and M. Kountouris, "Dynamic Sleep Mode Strategies in Energy Efficient Cellular Networks," in *IEEE International Conference on Communications (ICC)*, June 2013, pp. 1724–1729.

[81] K. Son, S. Nagaraj, M. Sarkar, and S. Dey, "QoS-Aware Dynamic Cell Reconfiguration for Energy Conservation in Cellular Networks," in *IEEE Wireless Communications and Networking Conference (WCNC)*, June 2013, pp. 2022–2027.

[82] J. Wu, S. Zhou, and Z. Niu, "Traffic-Aware Base Station Sleeping Control and Power Matching for Energy-Delay Tradeoffs in Green Cellular Networks," *IEEE Transactions on Wireless Communications (accepted for publication)*, pp. 1–14, 2013.

[83] Z. Niu, J. Zhang, X. Guo, and S. Zhou, "On Energy-Delay Tradeoff in Base Station Sleep Mode Operation," in *IEEE International Conference on Communication Systems (ICCS)*, Nov 2012, pp. 235–239.

[84] H.-S. Jung, H.-T. Roh, and J.-W. Lee, "Energy and Traffic Aware Dynamic Topology Management for Wireless Cellular Networks," in *IEEE International Conference on Communication Systems (ICCS)*, Nov 2012, pp. 205–209.

[85] K. Adachi and S. Sun, "Power-Efficient Dynamic BS Muting in Clustered Cellular System," in *IEEE International Symposium on Personal, Indoor and Mobile Radio Communications (PIMRC)*, Apr 2012, pp. 1149–1154.

[86] M. Sawahashi, Y. Kishiyama, A. Morimoto, D. Nishikawa, and M. Tanno, "Coordinated Multipoint Transmission/Reception Techniques for LTE-Advanced," *IEEE Wireless Communications*, vol. 17, no. 3, pp. 26–34, 2010.

[87] S. Han, C. Yang, G. Wang, and M. Lei, "On the Energy Efficiency of Base Station Sleeping with Multicell Cooperative Transmission," in *IEEE International Symposium on Personal, Indoor and Mobile Radio Communications (PIMRC)*, Sep 2011, pp. 1536–1540.

[88] S. Han, C. Yang, , and A. F. Molisch, "Spectrum and Energy Efficient Cooperative Base Station Doze," *IEEE Journal of Selected Areas in Communications*, vol. 32, no. 12, pp. 1–12, 2014.

[89] M. A. Marsan and M. Meo, "Energy Efficient Wireless Internet Access with Cooperative Cellular Networks," *Elsevier Journal of Computer Networks*, vol. 55, no. 2, pp. 386–398, Feb 2011.

[90] A. Conte, A. Feki, L. Chiaraviglio, D. Ciullo, M. Meo, and M. Marsan, "Cell Wilting and Blossoming for Energy Efficiency," *IEEE Wireless Communications*, vol. 18, no. 5, pp. 50–57, Oct 2011.

[91] J. Christoffersson, "Energy Efficiency by Cell Reconfiguration: MIMO to Non-MIMO and 3-Cell Sites to Omni," in *IEEE Vehicular Networking Conference (VTC)*, May 2011, pp. 1–5.

[92] R. Stegen, "The Gain-Beamwidth Product of an Antenna," *IEEE Transactions on Antennas and Propagation*, vol. 12, no. 4, pp. 505– 506, July 1964.

[93] R. Gupta, "Collaborative Heterogeneity for Energy Efficient Systems," in *IEEE Global Communications Conference (GLOBECOM) Workshop (Keynote Talk)*, Nov-Dec 2009, pp. 1–44.

[94] M. A. Marsan, L. Chiaraviglio, D. Ciullo, and M. Meo, "A Simple Analytical Model for the Energy Efficient Activation of Access Points in Dense WLANs," in *ACM International Conference on Energy-Efficient Computing and Networking (e-Energy)*, Apr 2010, pp. 159–168.

[95] N. Pletcher, S. Gambini, and J. Rabaey, "A 52μW Wake-Up Receiver With 72 dBm Sensitivity Using an Uncertain-IF Architecture," *IEEE Journal of Solid-State Circuits*, vol. 44, no. 1, pp. 269–280, Jan 2009.

[96] E. Nilsson and C. Svensson, "Ultra Low Power Wake-Up Radio Using Envelope Detector and Transmission Line Voltage Transformer," *IEEE Journal on Emerging and Selected Topics in Circuits and Systems*, vol. 3, no. 1, pp. 5–12, Mar 2013.

[97] R. Cohen and B. Kapchits, "An Optimal Wake-up Scheduling Algorithm for Minimizing Energy Consumption while Limiting Maximum Delay in a Mesh Sensor Network," *IEEE/ACM Transactiona on Networking*, vol. 17, no. 2, pp. 570–581, Apr 2009.

[98] F.-J. Wu and Y.-C. Tseng, "Distributed Wake-up Scheduling for Data Collection in Tree-Based Wireless Sensor Networks," *IEEE Communications Letters*, vol. 13, no. 11, pp. 850–852, Nov 2009.

[99] H. Imaizumi, T. Nagata, G. Kunito, K. Yamazaki, and H. Morikawa, "Power Saving Mechanism Based on Simple Moving Average for 802.3ad Link Aggregation," in *IEEE Global Communications Conference (GLOBECOM) Workshops*, Nov-Dec 2009, pp. 1–6.

[100] E. Shih, P. Bahl, and M. J. Sinclair, "Wake on Wireless: An Event Driven Energy Saving Strategy for Battery Operated Devices," in *ACM International Conference on Mobile Computing and Networking (MobiCom)*, Sep 2002, pp. 1–12.

[101] N. P. Le, T. Morohashi, H. Imaizumi, and H. Morikawa, "A Performance Evaluation of Energy Efficient Schemes for Green Office Networks," in *IEEE Green Technologies Conference (GreenTech)*, Apr 2010, pp. 1–9.

[102] "MIMO and Smart Antennas for Mobile Broadband Systems," *4G Americas*, pp. 1–138, Oct 2012.

[103] Z. Zhang, M. Iskander, Z. Yun, and A. Host-Madsen, "Hybrid Smart Antenna System Using Directional Elements - Performance Analysis in Flat Rayleigh Fading," *IEEE Transactions on Antennas and Propagation*, vol. 51, no. 10, pp. 2926–2935, Oct 2003.

[104] F. Athley and M. Johansson, "Impact of Electrical and Mechanical Antenna Tilt on LTE Downlink System Performance," in *IEEE Vehicular Networking Conference (VTC)*, May 2010, pp. 1–5.

[105] H. Burchardt and H. Haas, "Multicell Cooperation: Evolution of Coordination and Cooperation in Large-Scale Networks," *IEEE Wireless Communications*, vol. 20, no. 1, pp. 19–26, Mar 2013.

[106] 3GPP, "Technical Specification Group Radio Access Network; Evolved Universal Terrestrial Radio Access (E-UTRA) and Evolved Universal Terrestrial Radio Access Network (E-UTRAN); Overall description; Stage 2," *Technical Report, 3GPP TS 36.300 V11.3.0*, Sep 2012.

[107] "Architecture Tenets, Reference Model and Reference Points: Base Specifications," *WiMAX Forum Network Architecture, WMF-T32-001-R021v02*, Mar 2013.

[108] R. Srinivasan and S. Hamiti, "IEEE 802.16m-09/0034r4: IEEE 802.16m System Description Document (SDD)," *IEEE Standard 802.16m*, Dec 2010.

[109] F. Dressler and O. B. Akan, "A survey on Bio-Inspired Networking," *Computer Networks*, vol. 54, no. 6, pp. 881 – 900, Apr 2010.

[110] S. Camazine, J. Deneubourg, N. R. Franks, J. Sneyd, G. Theraula, and E. Bonabeau, *Self-Organization in Biological Systems*.   New Jersey, USA: Princeton Press, 2002.

[111] P. H. Longstaff, "Competition and Cooperation: From Biology to Business Regulation," *Centre for Information Policy Research, Harvard University*, pp. 1–57, Oct 1998.

[112] W. R. Engels, "Evolution of Altruistic Behaviour by Kin Selection: An Alternative Aproach," in *National Academy of Sciences*, Jan 1983, pp. 515–518.

[113] I. Carreras, I. Chlamtac, F. De Pellegrini, and D. Miorandi, "BIONETS: Bio-Inspired Networking for Pervasive Communication Environments," *IEEE Transactions on Vehicular Technology*, vol. 56, no. 1, pp. 218–229, Jan 2007.

[114] K. Ramachandran and B. Sikdar, "A Population Based Approach to Model the Lifetime and Energy Distribution in Battery Constrained Wireless Sensor Networks," *IEEE Journal of Selected Areas in Communications*, vol. 28, no. 4, pp. 576–586, May 2010.

[115] M. Dorigo, V. Maniezzo, and A. Colorni, "Ant System: Optimization by a Colony of Cooperating Agents," *IEEE Transactions on Systems, Man, and Cybernetics, Part B: Cybernetics*, vol. 26, no. 1, pp. 29–41, 1996.

[116] M. Farooq, *Bee-Inspired Protocol Engineering: From Nature to Networks*. Springer, 2009.

[117] F. Bai, K. Munasinghe, and A. Jamalipour, "An Ecologically Inspired Intelligent Agent Assisted Wireless Sensor Network for Data Reconstruction," in *IEEE International Conference on Communications (ICC)*, May 2010, pp. 1–5.

[118] A. Tyrrell, G. Auer, and C. Bettstetter, "Fireflies as Role Models for Synchronization in Ad Hoc Networks," in *Bio-Inspired Models of Network, Information and Computing Systems*, Dec 2006, pp. 1–7.

[119] B. Atakan and O. Akan, "Immune System Based Distributed Node and Rate Selection in Wireless Sensor Networks," in *Bio-Inspired Models of Network, Information and Computing Systems*, Dec 2006, pp. 1–8.

[120] M. F. Hossain, K. S. Munasinghe, and A. Jamalipour, "Ecological Competition Based Resource Control for Sustainable Heterogeneous Wireless Networks," in *IEEE International Symposium on Personal, Indoor and Mobile Radio Communications (PIMRC)*, Sep 2011, pp. 1361–1365.

[121] D. Niyato and E. Hossain, "A Noncooperative Game-Theoretic Framework for Radio Resource Management in 4G Heterogeneous Wireless Access Networks," *IEEE Transactions on Mobile Computing*, vol. 7, no. 3, pp. 332–345, Jan 2008.

[122] K. Piamrat, A. Ksentini, J.-M. Bonnin, and C. Viho, "Radio Resource Management in Emerging Heterogeneous Wireless Networks," *Elsevier Journal of Computer Communications*, vol. 34, no. 9, pp. 1066 – 1076, Feb 2011.

[123] E. Tragos, G. Tsiropoulos, G. Karetsos, and S. Kyriazakos, "Admission Control for QoS Support in Heterogeneous 4G Wireless Networks," *IEEE Network*, vol. 22, no. 3, pp. 30–37, May/Jun 2008.

[124] A. Hasib and A. Fapojuwo, "Analysis of Common Radio Resource Management Scheme for End-to-End QoS Support in Multiservice Heterogeneous Wireless Networks," *IEEE Transactions on Vehicular Technology*, vol. 57, no. 4, pp. 2426–2439, July 2008.

[125] X. Liu, V.-K. Li, and P. Zhang, "NXG04-4: Joint Radio Resource Management through Vertical Handoffs in 4G Networks," in *IEEE Global Communications Conference (GLOBECOM)*, Nov 2006, pp. 1–5.

[126] Y. Choi, H. Kim, S. wook Han, and Y. Han, "Joint Resource Allocation for Parallel Multi-Radio Access in Heterogeneous Wireless Networks," *IEEE Transactions on Wireless Communications*, vol. 9, no. 11, pp. 3324–3329, Nov 2010.

[127] A. L. Wilson, A. Lenaghan, and R. Malyan, "Optimising Wireless Access Network Selection to Maintain QoS in Heterogeneous Wireless Environments," in *International Symposium on Wireless Personal Multimedia Communications (WPMC)*, 2005.

[128] X. Pei, T. Jiang, D. Qu, G. Zhu, and J. Liu, "Radio-Resource Management and Access-Control Mechanism Based on a Novel Economic Model in Heterogeneous Wireless Networks," *IEEE Transactions on Vehicular Technology*, vol. 59, no. 6, pp. 3047–3056, Apr 2010.

[129] Y. Guang, C. Jie, Y. Kai, Z. Ping, and V.-K. Li, "Joint Radio Resource Management Based on the Species Competition Model," in *IEEE Wireless Communications and Networking Conference (WCNC)*, Apr 2006.

[130] A. Jamalipour, F. Javadi, and K. S. Munasinghe, "Resource Competition in a Converged Heterogeneous Networking Ecosystem," *Elsevier Journal of Computer Networks*, vol. 55, no. 7, pp. 1549 – 1559, May 2011.

[131] J. A. Leon and D. B. Tumpson, "Competition Between Two Species for Two Complementary or Substitutable Resources," *Journal of Theoretical Biology*, vol. 50, no. 1, pp. 185–201, 1975.

[132] S. C. Chapra and R. P. Canale, *Numerical Methods for Engineers*. Boston, MA, USA: McGraw-Hill Higher Education, 2010.

[133] M. Deruyck, W. Vereecken, E. Tanghe, W. Joseph, M. Pickavet, L. Martens, and P. Demeester, "Power Consumption in Wireless Access Network," in *IEEE European Wireless Conference (EW)*, April 2010, pp. 924–931.

[134] M. F. Hossain, K. Munasinghe, and A. Jamalipour, "A Protocooperation-Based Sleep-Wake Architecture for Next Generation Green Cellular Access Networks," in *IEEE International Conference on Signal Processing and Communication Systems (ICSPCS)*, Dec 2010.

[135] M. F. Hossain, K. S. Munasinghe, and A. Jamalipour, "An Eco-Inspired Energy Efficient Access Network Architecture for Next Generation Cellular Systems," in *IEEE Wireless Communications and Networking Conference (WCNC)*, Mar 2011, pp. 992–997.

[136] M. F. Hossain, K. Munasinghe, and A. Jamalipour, "On the Energy Efficiency of Self-Organizing LTE Cellular Access Networks," in *IEEE Global Communications Conference (GLOBECOM)*, Dec 2012, pp. 5314–5319.

[137] M. F. Hossain, K. S. Munasinghe, and A. Jamalipour, "Distributed Inter-BS Cooperation Aided Energy Efficient Load Balancing for Cellular Networks," *IEEE Transactions on Wireless Communications (in press)*, pp. 1–11, Aug 2013.

[138] K. Son, S. Chong, and G. Veciana, "Dynamic Association for Load Balancing and Interference Avoidance in Multi-Cell Networks," *IEEE Transactions on Wireless Communications*, vol. 8, no. 7, pp. 3566–3576, July 2009.

[139] W. Song, W. Zhuang, and Y. Cheng, "Load Balancing for Cellular/WLAN Integrated Networks," *IEEE Network*, vol. 21, no. 1, pp. 27–33, Jan-Feb 2007.

[140] H. Wang, L. Ding, P. Wu, Z. Pan, N. Liu, and X. You, "Dynamic Load Balancing and Throughput Optimization in 3GPP LTE Networks," in *ACM International*

Wireless Communications and Mobile Computing (IWCMC), June-July 2010, pp. 939–943.

[141] A. Lobinger, S. Stefanski, T. Jansen, and I. Balan, "Load Balancing in Downlink LTE Self-Optimizing Networks," in *IEEE Vehicular Networking Conference (VTC)*, May 2010, pp. 1–5.

[142] 3GPP, "Technical Specification Group Radio Access Network; Evolved Universal Terrestrial Radio Access (E-UTRA); Radio Frequency (RF) system scenarios," *Technical Report, 3GPP TR 36.942 Ver. 11.0.0 Rel. 11*, Sep 2012.

[143] M. Rupp, C. Mehlfuhrer, and S. Caban, "Cellular System Physical Layer Throughput: How Far off are We from the Shannon Bound?" *IEEE Wireless Communications*, vol. 18, no. 6, pp. 54–63, Dec 2011.

[144] Z. Xu, G. Y. Li, and C. Yang, "Optimal Threshold Design for FFR Schemes in Multi-Cell OFDMA Networks," in *IEEE International Conference on Communications (ICC)*, June 2011, pp. 1–5.

[145] C. Seol and K. Cheun, "A statistical Inter-Cell Interference Model for Downlink Cellular OFDMA Networks Under Log-Normal Shadowing and Multipath Rayleigh Fading," *IEEE Transactions on Communications*, vol. 57, no. 10, pp. 3069–3077, Oct 2009.

[146] S. Shamai and A. Wyner, "Information-Theoretic Considerations for Symmetric, Cellular, Multiple-Access Fading Channels. I," *IEEE Transactions on Information Theory*, Nov 1997.

[147] T. Novlan, R. Ganti, A. Ghosh, and J. Andrews, "Analytical Evaluation of Fractional Frequency Reuse for OFDMA Cellular Networks," *IEEE Transactions on Wireless Communications*, vol. 10, no. 12, pp. 4294–4305, Dec 2011.

[148] S.-E. Elayoubi, O. Ben Haddada, and B. Fourestie, "Performance Evaluation of Frequency Planning Schemes in OFDMA-Based Networks," *IEEE Transactions on Wireless Communications*, vol. 7, no. 5, pp. 1623–1633, May 2008.

[149] R. Bosisio and U. Spagnolini, "Interference Coordination vs. Interference Randomization in Multicell 3GPP LTE System," in *IEEE Wireless Communications and Networking Conference (WCNC)*, Mar-Apr 2008, pp. 824–829.

[150] Y. Qiang, G. Vivier, J. Yang, and N. Xu, "Inter-Cell Interference Modeling for OFDMA Systems with Beamforming," in *IEEE Vehicular Technology Conference (VTC)*, Sep 2008, pp. 1–5.

[151] S. Chung and Y. Chen, "Performance Analysis of Call Admission Control in SFR-Based LTE Systems," *IEEE Communications Letters*, vol. 16, no. 7, pp. 1014–1017, July 2012.

[152] H. Holma and A. Toskala, *LTE for UMTS - OFDMA and SC-FDMA Based Radio Access.* United Kingdom: John Wiley and Sons Ltd., 2009.

[153] W. S. Cleveland, "Robust Locally Weighted Regression and Smoothing Scatterplots," *Journal of the American Statistical Association*, vol. 74, no. 368, p. 829836, Dec 1979.

[154] J. S. Hunter, "The Exponentially Weighted Moving Average," *Journal of Quality Technology*, vol. 18, no. 4, pp. 203–207, 1986.

[155] "D5.3: WINNER+ Final Channel Models," *Wireless World Initiative New Radio WINNER+*, June 2010.

[156] "IEEE 802.16m-08/004r5: IEEE 802.16m Evaluation Methodology Document (EMD)," *IEEE Standard 802.16m*, Jan 2009.

[157] A. V. Krishnamoorthy and et. al., "Progress in Low-Power Switched Optical Interconnects," *IEEE Journal of Selected Topics in Quantum Electronics*, vol. 17, no. 2, pp. 357–376, Mar-Apr 2011.

[158] M. F. Hossain, K. S. Munasinghe, and A. Jamalipour, "A Self-Organizing Cooperative Heterogeneous Cellular Access Network for Energy Conservation," in *IEEE International Conference on Communications (ICC)*, June 2012, pp. 5316–5320.

[159] M. F. Hossain, K. Munasinghe, and A. Jamalipour, "Two Level Cooperation for Energy Efficiency in Multi-RAN Cellular Network Environment," in *IEEE Wireless Communications and Networking Conference (WCNC)*, Apr 2012, pp. 2493–2497.

[160] M. F. Hossain, K. S. Munasinghe, and A. Jamalipour, "On the eNB-Based Energy-Saving Cooperation Techniques for LTE Access Networks," *Wireless Communications and Mobile Computing (in press)*, pp. 1–20, Jan 2013.

[161] 3GPP, "Technical Specification Group Services and System Aspects; Architecture enhancements for non-3GPP accesses," *Technical Specification, 3GPP 3GPP TS 23.402 V12.0.0 Rel. 12*, Mar 2013.

[162] F. Han, Z. Safar, and K. Liu, "Energy-Efficient Base-Station Cooperative Operation with Guaranteed QoS," pp. 1–13, 2013.

[163] M. F. Hossain, K. S. Munasinghe, and A. Jamalipour, "Toward Self-Organizing Sectorization of LTE eNBs for Energy Efficient Network Operation Under QoS Constraints," in *IEEE Wireless Communications and Networking Conference (WCNC)*, Apr 2013, pp. 1297–1302.

[164] M. F. Hossain, K. Munasinghe, and A. Jamalipour, "Energy-Aware Dynamic Sectorization of Base Stations in Multi-Cell OFDMA Networks," *IEEE Wireless Communications Letters (in press)*, pp. 1–4, Aug 2013.

[165] M. F. Hossain, K. S. Munasinghe, and A. Jamalipour, "Traffic-Aware Two-Dimensional Dynamic Network Provisioning for Energy-Efficient Cellular Systems," *Transactions on Emerging Telecommunications Technologies (under review)*, pp. 1–13, June 2013.

[166] S. Yarkan, K. H. Teob, H. Arslan, J. Zhangb, and K. A. Qaraqed, "Upper and Lower Bounds on Subcarrier Collision for Inter-Cell Interference Scheduler in OFDMA-Based Systems: Voice traffic," *Elsevier Journal of Physical Communications*, vol. 3, no. 4, pp. 265–275, Dec 2010.

[167] R. Kwan and C. Leung, "On Collision Probabilities in Frequency-Domain Scheduling for LTE Cellular Networks," *IEEE Communications Letters*, vol. 15, no. 9, pp. 965–967, Sep 2011.

[168] 3GPP, "Evolved Universal Terrestrial Radio Access (E-UTRA); Spatial Channel Model for Multiple Input Multiple Output (MIMO) Simulations," *Technical Report, 3GPP TR 25.996, v.11.0.0 Rel. 11*, Sep 2012.

[169] D. Amzallag, R. B. Yehuda, D. Raz, and G. Scalosub, "Cell Selection in 4G Cellular Networks," *IEEE Transactions on Mobile Computing*, vol. 12, no. 7, pp. 1443–1455, July 2013.

[170] 3GPP, "Technical Specification Group Radio Access Network; Physical Layer Aspects for Evolved Universal Terrestrial Radio Access (UTRA)," *Technical Report, 3GPP TR 25.814 V.7.1.0 Rel. 7*, Sep 2006.

[171] Y. Shen, T. Luo, and M. Z. Win, "Neighboring Cell Search for LTE Systems," *IEEE Transactions on Wireless Communications*, vol. 11, no. 3, pp. 908–919, Mar 2012.

[172] 3GPP, "Technical Specification Group Radio Access Network; Evolved Universal Terrestrial Radio Access (E-UTRA); Physical Layer Procedures," *Technical Report, 3GPP TS 36.213 V11.1.0 Rel 11*, Dec 2012.